NOTICE

The quality of this microform is heavily dependent upon the quality of the original thesis submitted for microfilming. Every effort has been made to ensure the highest quality of reproduction possible.

If pages are missing, contact the university which granted the degree.

Some pages may have indistinct print especially if the original pages were typed with a poor typewriter ribbon or if the university sent us an inferior photocopy.

Reproduction in full or in part of this microform is governed by the Canadian Copyright Act, R.S.C. 1970, c. C-30, and subsequent amendments.

AVIS

La qualité de cette microforme dépend grandement de la qualité de la thèse soumise au microfilmage. Nous avons tout fait pour assurer une qualité supérieure de reproduction.

S'il manque des pages, veuillez communiquer avec l'université qui a conféré le grade.

La qualité d'impression de certaines pages peut laisser à désirer, surtout si les pages originales ont été dactylographiées à l'aide d'un ruban usé ou si l'université nous a fait parvenir une photocopie de qualité inférieure.

La reproduction, même partielle, de cette microforme est soumise à la Loi canadienne sur le droit d'auteur, SRC 1970, c. C-30, et ses amendements subséquents.

Canada

SEISMIC ANALYSIS OF PRECAST CONCRETE LARGE PANEL SHEAR WALLS

Denis Hum

A Thesis

in

The Department

of

Civil Engineering

Presented in Partial Fulfillment of the Requirements
for the Degree of Master of Engineering at

Concordia University
Montréal, Québec, Canada

June 1989

ISBN 0-315-51349-7

ABSTRACT

SEISMIC ANALYSIS OF PRECAST CONCRETE
LARGE PANEL SHEAR WALLS

Denis Hum

The seismic response of precast concrete large panel (LP) shear walls is investigated. Nonlinear inelastic horizontal and vertical joint behaviour is examined. Two prototype wall models are employed in this thesis: a 12-story multi-panel shear wall with welded headed stud mechanical connectors along vertical joints, and a 10-story coupled shear wall with previously proposed friction-type mechanical connectors along vertical joints. Horizontal platform type joints are used.

A finite element procedure is employed in nonlinear time-history analyses of the walls. Panels are represented by plane stress rectangular finite elements having linear elastic behaviour, and horizontal and vertical joints are represented by discrete orthogonal spring elements having nonlinear inelastic behaviour. Elastic truss elements are used to model the horizontal and vertical ties.

A parametric study is performed for the 12-story wall. The influences of horizontal joint coefficient of friction, vertical continuity using distributed vertical reinforcement or post-tensioned ties, and mechanical connector strength and hysteretic shear behaviour

are studied. The effectiveness of friction-type connectors along vertical joints to improve seismic response of the 10-story wall is investigated. The relative role of these connectors and gap-friction action in the horizontal joints is examined. Deformations in the horizontal joints are evaluated in terms of its relation to structural integrity; vertical reinforcement detailing and base isolation are studied. The design slip load at which optimum response occurs is determined. Integrity of both walls is examined.

ACKNOWLEDGEMENTS

The author wishes to express his sincere gratitude to his supervisor Dr. O.A. Pekau for his guidance, judgement and valuable criticism during the course of this research. His encouragement and contribution to the writing of the thesis are greatly appreciated.

The financial support for this research was provided by the National Sciences and Engineering Research Council of Canada (NSERC) under grant No. A8258 and La Formation de Chercheurs et d'Action Consertée du Québec (FCAR). The use of the computing facilities of Concordia University's Civil Engineering Department are also gratefully acknowledged. Thanks are also extended to Dr. Armin Wulf for his work in the programming of original versions of the joint element subroutines while at the University of California at Berkeley.

Eternal gratitude to all my fellow researchers for their support; special and heartfelt thanks to V.B. and R.G. for the encouragement and friendship. Extended thanks to all Civil Engineering staff; thanks C.E. for the help.

The moral support of the author's family, and in particular his parents, is greatly appreciated. To my friends from the Group, the author gratefully acknowledges their unyielding incomprehension of the work. And finally, to a very special person, the author would like to extend his deepest thanks for her continuous source of inspiration and friendship throughout the course of his work.

TABLE OF CONTENTS

PAGE

LIST OF FIGURES

LIST OF TABLES

NOMENCLATURE

E	modulus of elasticity
f'_c	compressive strength of platform horizontal joint
f_y	elastic strength of reinforcing steel
F_a	axial (normal) force in joint element
F_c	compressive force in joint element
F_u	axial force corresponding to f'_c
F_s	shear force in joint element
F_y	shear connector strength
F_r	axial force ratio F_c/F_u in horizontal joint
F_{sb}	slip load of LSB connectors
F_t	tension force in joint
k_1	elastic compressive stiffness of horizontal joint element
k_2	first yield compressive stiffness of horizontal joint element
k_3	compressive stiffness of horizontal joints following crushing at displacement u_2
k_b	bearing stiffness of LSB connector element
k_c	elastic compressive stiffness of vertical joint element
k_r	shear stiffness in horizontal joint due to reinforcement
k_s	shear stiffness of horizontal or vertical joint element

r	parameter controlling hysteretic shear behaviour of reinforced horizontal joint element
u	joint displacement
u_1	yield displacement for compressive behaviour of horizontal joint element
u_2	displacement corresponding to horizontal joint element compressive crushing at force F_u and displacement u_2
u_b	limited slip distance for LSB connector
u_c	relative compressive displacement in joint element
u_{max}	maximum shear displacement in vertical shear connector
u_s	relative shear displacement in joint element
u_t	relative tensile displacement in joint element
u_y	yield displacement of vertical shear connector element
α	parameter for vertical joint stiffness degrading shear behaviour
μ	ductility factor of vertical shear connectors, equal to u_{max}/u_y
μ_f	horizontal joint coefficient of friction
ν	Poisson's ratio

CHAPTER I

INTRODUCTION

1.1 BACKGROUND

Large panel (LP) buildings, of the form where story-height precast concrete wall units comprise the main structural supports and lateral force resisting members, were developed in Europe in the 1960s. Ease of erection combined with good quality control over the panel units have offered immediate advantages over conventional building systems. The load-bearing shear walls are commonly used as partitions between apartments, with floors consisting of one-way precast, prestressed planks spanning between the walls. Such a 'cross-wall' plan characterizes precast systems favoured by the North American precast concrete industry. LP construction is popular for hotels and office blocks up to about nine stories but, despite widespread use of such structural systems in earthquake regions of Japan and Eastern Europe, enjoys only limited deployment in seismic areas of North America and is seldom used for high-rise construction[1].

Earthquake ground motions cause structures to respond in proportion to the amount of the seismic input energy. Efficient control and dissipation of this energy is necessary to ensure that buildings escape serious damage. In modern philosophy of earthquake resistance, ductility has been accepted as the prime design criterion. However, the limited inherent ductility of precast concrete LP structures has led to doubts concerning their capacity for energy dissipation. Furthermore, the generally higher stiffness associated with such buildings over conventional framed systems invites higher

inertial forces, thereby placing even greater demands on strength and ductility.

The only location of ductile behaviour in panelized systems exists in the interpanel connections, consisting of horizontal joints, which behave primarily in compression, and vertical joints acting predominantly in shear, although in the former gap opening and shear slip are also critical factors. Under high intensity ground shaking, these joints can be expected to enter the inelastic range of behaviour, while the panels themselves remain elastic. Opinion has been divided as to whether these joints, through such inelastic action during seismic activity, can provide the energy dissipation necessary for adequate seismic response. Moreover, failure of precast panel wall systems during severe earthquake excitation can occur as a result of damage to the joints when inelastic deformations become large. Reduced stiffness and strength of the joints in comparison to the panels create locations of weaknesses and lack of continuity in LP walls.

1.1.1 1977 Romanian and 1988 Armenian Earthquakes

The ability of precast concrete panel buildings to resist seismic forces has been demonstrated dramatically from investigations following two severe earthquakes in Eastern Europe. On March 4, 1977 an earthquake of magnitude 7.2 on the Richter scale struck Romania. The capital city of Bucharest, located 165 km from the epicenter, suffered 35 building collapses and 1500 deaths. Thirty-two of the collapsed structures were built prior to World War II when seismic code criteria had not yet been established. Of the three modern

structures that collapsed only one was precast, and its failure was directly attributed to poor construction methods and inferior quality concrete. Precast concrete buildings of various configurations and large panel buildings designed for earthquake resistance were otherwise able to survive with minimum distress, and thus for the first time provided evidence of the earthquake resistance of such structures[2].

Soviet Armenia was devastated by a Richter magnitude 6.9 earthquake on December 7, 1988 resulting in up to 50,000 deaths and the virtual destruction of entire towns and cities. A major aftershock of magnitude 5.8 occuring 3 to 4 minutes after the first collapsed most buildings still standing. Unlike the Romanian earthuake, hundreds of precast concrete frame buildings as well as unreinforced masonry buildings collapsed. A report[3] by a visiting U.S. team of experts noted that improperly detailed connections and poor construction led to the failure of many of the precast buildings. In the city of Leninaken, less than a dozen of fifty 9-story precast concrete frame structures comprising beams, columns and floor planks remained standing. Brittle failure of connections, lack of proper strength concrete and insufficient reinforcement were reported. However, 9-story precast concrete buildings consisting of panels connecting directly to one another performed remarkably well, and 14 of these buildings were noted to survive with only "hairline cracks".

1.2 PREVIOUS STUDIES

Findings from the Romanian and Armenian earthquakes have shown that precast panel structures perform well under seismic loading. The

importance of developing proper ductility in panel wall joints was dramatically demonstrated from the collapse of precast buildings where improper detailing caused brittle connection failure. A number of studies focusing on joint behaviour have been carried out on precast panel walls subjected to seismic loads.

1.2.1 Experimental Studies

Oliva and Sharooz[4] tested one-third size scale models of 3-story precast panel wall segments, designed and loaded to simulate conditions near the middle of a 15-story structure. The models employed horizontal joints of the wet type, with block keys inserted at the panel corners for slip control. The shaking table experiments revealed that behaviour was dominated by rocking of the panels, causing stretching of the vertical reinforcement in the joints and precipitating additional damage to the walls. This damage consisted primarily of corner crushing when the panel ends opened and closed. Joint slip was effectively controlled by the block key insertions, although it was noted that the wall gained a limited slip distance along the joint crack once crushing commenced. However, the experiments showed that the dominant rocking behaviour also served to limit the level of moment and story shear force in the wall. No signs of instability in the wall segments were suggested by the tests.

Harris and Caccese[5] tested 1/32 scale models of 5-story simple (ie. vertical stack of solid panels with only horizontal joints) walls with wet horizontal joints. The tests determined the static and dynamic properties of the structure, in addition to its response to seismic forces. Softening of the model was noted as the horizontal joints became damaged. Failure mechanisms of the system were shown to

involve slip and crushing of the panel corners as a result of panel rocking. However, it was noted that the structure remained standing even after intensified loading, this being attributed to the large amount of energy absorbed from inelastic slip of the horizontal joint at the first level. The reduced structural frequency in the wall due to joint damage and general seismic behaviour of the model compared well with results obtained in an earlier analytical study of the structure by Becker and Llorente[6].

Zhang and Na[7] tested 1/15 scale models of 3 precast concrete coupled large panel buildings constructed according to Chinese practice, comprising wet horizontal joints and welded reinforcement vertical joints with grouting. As with the tests conducted by Harris and Caccese[5], softening of the structure was noted as loosening of the joints commenced. Although slip action was observed, rocking dominated horizontal joint behaviour once increased loading caused cracking in the joint. Rocking and shear slip was confined mainly to the lower wall regions, and damage in the upper joints of the structure was minimal. A mathematical modelling procedure was proposed, with the observation that vertical joints acted with primarily elasto-plastic yielding in shear, while opening and closing of the joint governed horizontal joint deformations.

1.2.2 Analytical Studies

The seismic behaviour of simple and composite coupled walls has been studied extensively by Becker, Mueller et al in a number of computer-based works focusing on the role of joint connections.

The influence of horizontal joints on seismic response was investigated through analyses of a 10-story simple wall[6,8]. Wall

panels were modeled as linear elastic substructures while horizontal joints were represented by 4-noded rectangular interface or contact elements with nonlinear elastic behaviour in compression and elasto-plastic behaviour in shear. A Coulomb friction shear transfer mechanism was employed for the shear modeling, thus coupling axial and shear behaviour. Elasto-plastic truss elements modeled the effects of vertical reinforcement.

Rocking dominated behaviour of the simple wall, introducing progressive softening of the structure and a lengthening of the apparent period. This led to either an increase or decrease in the seismic forces, depending on the earthquake characteristics. Local shear slip occured with gap opening at the joint edges; stress concentrations also developed at the joint edges from rocking and slip. Global slip (ie. movement between entire panels) occured only in limited situations such as when low joint coefficient of friction was used or at the upper levels of non-tensioned walls. The possibility of hysteretic damping through such slip was shown. However, since global slip represented an 'unconfined yield mechanism', the risk to overall stability was raised.

Related work on a 10-story composite U-shaped wall was also performed[9,10]. Orthogonal spring elements with stiffness and strength degradation in shear were included to represent the vertical connectors, and flange walls were statically reduced to elastic line stiffnesses coupled to the web wall. Finite element procedures for the web wall followed those in the simple wall study[6,8]. Results revealed decreased response when inelastic yielding of the vertical connectors and rocking of the web wall occured. It was opined that

the cumulative effects of the two actions could contribute to improved seismic response. However, it was noted also that loss of strength and stiffness with continued loading could override the otherwise beneficial hysteretic damping associated with such inelastic connector behaviour.

A study of a 10-story I-shaped wall coupled by mechanical connectors was conducted[11,12]. A simplified frame analogy model was employed in the computer study, where walls and horizontal joints remained elastic and inelastic action was confined to the vertical joints. Elasto-plastic and strength and stiffness degrading shear hysteretic models were used for the connectors, and properties kept constant over the wall height.

It was found that vertical coupling stiffness was optimized at the threshold value required for monolithic wall stiffness, above which changes in the coupling stiffness had little effect on overall response and stiffness. The vertical connector yield strength was the most important factor for seismic response; an optimum yield level minimizing response was demonstrated, which was significantly lower than the maximum force found with elastic coupling. Elasto-plastic behaviour was shown to provide excellent energy dissipating characteristics. Although stiffness degrading introduced to the elasto-plastic shear behaviour of the connectors had little effect on response, it was noted that strength degradation and shear pinching adversely affected response.

A weak vertical bre concept was thus proposed, where inelastic action is confined to the vertical joints and the vulnerable load-bearing horizontal joints thus protected from inelastic action.

This design was demonstrated also to be beneficial in the case of inelastic wall behaviour, where a plastic hinge was formed at the composite wall base at excitation levels sufficient to induce the maximum base moment found in the elastic wall. The optimum yield load for the vertical joint connectors was shown to be approximately the same for both inelastic and elastic wall behaviour, and further to be relatively independent of earthquake selection.

Pall, Marsh, and Fazio[13] performed seismic computer analyses on coupled LP shear walls of 5, 10, 15 and 20 stories. The studies investigated the effectiveness of employing limited slip bolted (LSB) friction-type vertical joint connectors as coupling elements. Tests confirmed essentially elasto-plastic energy dissipating characteristics in the hysteretic behaviour of the connectors. The wall model also idealized the coupled wall as an equivalent wide column frame; vertical panel walls were considered as continuous elastic cantilevers without horizontal joints. Vertical connectors were modeled using modified truss elements. Since slip was allowed in the connectors once the shear load acting upon them reached the design slip load, energy dissipation through vertical joint slip could be accomplished without damage to the connecting elements. A building could thus be 'tuned' for optimum response by adjusting the slip load to yield minimum response. It was demonstrated that vertical joints are ideally suited for energy absorbtion, and that the proposed slip-type vertical joint connectors can, in effect, behave as safety valves and structural dampers.

Shricker and Powell[14] conducted analytical studies on the seismic behaviour of simple 10-story panel walls with continuous nonlinear

inelastic behaving horizontal joints. The influence of design and analysis assumptions on response was investigated with particular consideration of slip and gap opening of the horizontal joints. Parameters such as horizontal joint coefficient of friction, joint keys and stops, various joint behaviour models, and vertical post-tensioning, was studied. Reduction in forces induced in the panels of the large panel system were shown to occur as a result of slip and gap opening in the horizontal joints. The reduction was considered to be due to a 'base isolation' effect and hysteretic energy absorbtion in the nonlinear behaviour of the joints during seismic activity. However, it was noted that concentrations of deformation in some horizontal joint locations can be undesirable if the joint is designed such that shear strength in the joint diminishes with increasing slip.

More recently, Kianoush and Scanlon[15,16,17] performed seismic analyses of coupled 10-story large panel shear walls. The analytical model considered nonlinear inelastic action in both the horizontal joints and vertical joint coupling elements. Two basic types of coupling elements were considered: slender beams, with relatively high ductility, and deep beams, with very limited ductility. The results suggested that coupling beams can be used to improve seismic behaviour of LP systems. In addition, the level of coupling beam strength can also have a significant effect on seismic response, including the reduction of rocking motion in the individual walls. Improvements over seismic response in simple uncoupled walls was found when post-tensioning bars were used as vertical continuity, although horizontal joint shear slip increased. Reinforced walls were also able

to sustain intense loads satisfactorily, and without increasing slip. The results showed generally poor agreement with code design forces, and suggested that design of precast wall systems be based upon inelastic dynamic analysis.

1.3 SCOPE AND OBJECTIVE OF THE PRESENT STUDY

The objective of the present study is to examine the seismic behaviour of precast concrete large panel shear wall structures, and in particular the response of horizontal joints and vertical joint connectors. Analyses are conducted upon a 12-story multi-panel wall and a 10-story LSB (limited slip bolted)[13] coupled wall. Nonlinear inelastic joint behaviour is assumed in the finite element representations of the wall models. The scope of the work is limited to identifying the influences of various structural parameters on the seismic response of the 12-story wall, and to evaluating the performance of the 10-story coupled wall considering both strong rigid horizontal joints and nonlinear behaving horizontal joints. Whereas the parametric investigation of the 12-story precast wall is concerned mainly with recognizing the relative effects of the basic LP system parameters on response, the latter studies on the 10-story wall include determination of structural integrity and damage in the joints. Introduced are proposals to redress the potential of such damage through the provision of vertical continuity and base isolation.

The present study of a 10-story LSB-coupled shear wall is based partially on earlier work by Pall et al[13] and also follows related studies by Becker and Mueller[11,12]. The effects of horizontal joint

behaviour, in particular gap opening and shear slip, are included herein. Full finite element modeling of the panels is utilized to allow for this horizontal joint action; the frame analogies employed in Refs.[11-13] assumed continuous elastic wall and joint behaviour.

Studies on simple walls in Refs. [6,8,9,10] included nonlinear elastic horizontal joints. Introduced in this work is the possibility of compressive failure in the horizontal joints when the joint strength is reached. This is modelled by allowing inelastic axial compressive behaviour for the horizontal joint elements, where zero compressive stiffness develops once the ultimate strain has been reached. Thus, nonlinear inelastic horizontal joint action is developed. The effect of vertical reinforcement on the shear behaviour of the horizontal joints is also incorporated, based upon the model described by Kianoush and Scanlon[15,16,17] which also used nonlinear inelastic compressive joint behaviour. Both contribution to tensile stiffness from the reinforcement and zero gap stiffness is used. Instead of the 4-noded interface or contact finite elements used in the other works, the current work employs 2-noded orthogonal spring elements to represent the horizontal joints.

LSB friction-type vertical joint connectors are modelled by elements with elasto-plastic hysteretic behaviour in shear and a return of elastic stiffness when the limited slip length is reached. Since the present model includes the effects of axial stiffness in the connectors, 4-DOF orthogonal spring elements (similar to the horizontal joint elements but with different orientation) are used instead of the modified truss elements of Ref.[13]. Other works included bolted mechanical connectors[10,11,12] and coupling beams[15,16,17]

along the vertical joint. In Chapter II, a stiffness degrading model with constant strength envelopes in addition to an elasto-plastic model is developed for shear behaviour of bolted mechanical connectors; Refs.[11,12] included also degrading strength envelopes for these type of connectors. The axial stiffness effects of transverse ties and vertical joint grout are included in the vertical connector elements. Other aspects of the 12-story wall of Chapter II are otherwise similar to that of the 10-story wall.

1.4 ORGANIZATION OF THESIS

Work concerning the study of LP shear walls is organized into three distinct chapters. Each chapter represents a different phase of the research and is presented as relatively independent of each other. To such an end, and to avoid ambiguity and imcompleteness in the text of Chapters II to IV, selected passages are carried over from chapter to chapter.

The parametric investigation of the 12-story multi-panel wall is described in Chapter 1. Modeling and behaviour of the horizontal and vertical joint orthogonal spring elements are detailed herein. The system parameters studied include the horizontal joint coefficient of friction, vertical continuity employing either vertical ties or reinforcement, and vertical joint connector yield strength and behaviour. Structural integrity of the wall is examined for various parameters.

Chapter III introduces study of the 10-story LSB-coupled shear wall. The effectiveness of slip-type vertical joint connectors in reducing seismic response is examined, particularly in relation to

either rigidly behaving or nonlinear behaving gap-friction horizontal joints. As with the multi-panel wall of Chapter II, plane-stress finite elements are used to model the panels, rather than the wide column analogy employed earlier by Pall[13] . Description of the joint elements is also included herein for completeness.

Finally, Chapter IV focuses attention on behaviour of the 10-story wall model with nonlinear behaving horizontal joints used in Chapter III. Response of both horizontal and vertical joints is detailed. Addressed is the problem of controlling seismic damage in the vulnerable horizontal joints, particularly with respect to axial compressive failure and gap opening. Introduced are the beneficial aspects of vertical continuity and seismic base isolation.

CHAPTER II

SEISMIC RESPONSE OF MULTI-PANEL PRECAST WALLS: PARAMETRIC STUDY

2.1 INTRODUCTION

In this chapter, an analytical model is developed to study the seismic behaviour of a prototype 12-story multi-panel precast concrete shear wall, part of a typical LP building of the cross-wall type. Horizontal joints consist of wet platform, or "American", type continuous joints, whereas vertical joints consist of dry mechanical connectors, each comprised of two welded headed-stud anchors. The model used is three panels wide and 12 panels in height, and is generally similar to a model used in earlier studies by Pekau et al[18,19]. Nonlinear inelastic action is assumed in both the horizontal and vertical joints, while the panels and vertical ties are assumed to remain elastic. Effects of varying selected structural parameters on seismic response are studied. Horizontal joint coefficient of friction, vertical continuity employing either vertical ties or vertical reinforcement, and vertical joint connector strength and behaviour are examined.

As with any study involving computer analyses, caution must be taken in interpreting results. In particular, it should be noted that this work involves a particular structure subjected to a specific ground motion record. Emphasis is placed upon anticipated differences in response due to the variation of parameters. Nevertheless, the modelled behaviour is similar to that observed in tests, and hence it is believed that, while numerical results may not be applied in a

general sense, overall response is qualitatively close to the expected actual response. Experimental data on similar structures, required to verify the values predicted in this work are, however, lacking at this time and future experimental verification is an obvious necessity.

2.2 PROTOTYPE STRUCTURE

Fig. 2.1(a) shows the 12-story precast shear wall selected for this study. This multi-panel assembly, measuring three panels in width and twelve panels in height, is part of a typical 12-story precast building of the cross wall type, as shown in Fig. 2.1(b), consisting of one of the interior walls. Panels are one story in height (2970 mm), panel width is 3670 mm, and panel thickness 200 mm. Floor loads are based on an 8460 mm width of tributary floor area. An allowance for a 250 mm concrete slab and partitions leads to a uniformly distributed dead load of 36 kN per meter-width at all floor levels, excluding the weight of the panels. A uniformly distributed dead load of 14 kN per meter-width of panel is added as a result of the panels' self-weight. Table 2.1(a) summarizes the panels' material properties and the wall's loading.

The 12-story shear wall performs as a multi-panel assembly, with continuous platform type horizontal joints in which gap opening and shear slip may occur. Based upon tests of full-scale horizontal joint assemblies by Harris and Iyengar[20] and CPCI design formulae[21], the strength f'_c of the composite horizontal joints is taken to be approximately half that of the joint grout strength itself (29 MPa), or 14.5 MPa, while the corresponding elastic modulus of the joint, 13 800 MPa, is also assumed to be half that of the grout value (27 600

MPa). Vertical connections between adjacent panel stacks consist of headed-stud mechanical connectors slotted to transfer shear only, with two such connectors per panel height. Two 12.7 X 155 mm headed stud anchors per connector are employed with a design strength of 104 kN[22,23]. To compensate for possible compressive stress concentrations in the area, and following PCA design recommendations[24], dry-packing of the lower region of the vertical joints is performed over a length equal to 1/4 of the panel height. Figs. 2.2(a) and 2.2(b) show details of the horizontal and vertical joints.

Tension forces developed across the vertical joints are carried by horizontal, or transverse, ties, provided at the floor levels and passing through the horizontal joints (Fig. 2.2(a)). The ties chosen follow PCA design recommendations[24], consisting of 12.7 and 9.5 mm (1/2 and 3/8 in) diameter strands without prestressing, at the roof and floor levels, respectively. Vertical ties, introduced separately in the structure following study of behaviour without its use, consist of high strength steel bars of 17.5 mm (11/16 in) diameter. Fig. 2.1(a) shows the location of the bars, placed two per panel and through the panel edges. The vertical ties are anchored to the base and roof levels, and coupling at the floor levels assures full continuity of the ties over the wall height. The PCA design strengths of the horizontal ties selected are 142 and 80 kN for the roof and floor level ties, respectively, while the vertical ties have a design strength of 224 kN.

2.3 STRUCTURAL IDEALIZATION

Idealization of the prototype structure for computer analysis utilizes the following elements: (1) plane-stress 4-node finite

elements; (2) discrete 2-node orthogonal spring elements; and, with the introduction of vertical ties, (3) uniaxial bar, or truss, elements.

Panels in the multi-panel wall structure are modelled as an assemblage of linear elastic plane-stress finite elements and, as shown in Fig. 2.3, a mesh consisting of three story-height elements are employed per panel. Horizontal and vertical joints are established by discrete 2-node spring elements, possessing two degrees-of-freedom per node. The joint elements consist, as shown in Fig. 2.4, of a spring placed parallel and normal to the joint surfaces, with properties representing the shear and axial behaviour of the joint. The springs are defined across the joints using the same nodes as the plane stress elements (Fig. 2.3), with each individual horizontal panel joint comprising 4 such spring elements, whereas the vertical joints consist of 2 spring elements per panel placed at the floor levels.

Truss elements are introduced to model the vertical ties along the panel edges. The elements are placed as shown in Fig. 2.1(a), and possess tensile axial stiffness only. Six truss elements, anchored from base to roof, are employed.

2.4 IDEALIZED BEHAVIOUR OF HORIZONTAL AND VERTICAL JOINTS

2.4.1 Horizontal Joint Axial Behaviour

Axial behaviour of the horizontal joint spring elements is intended to model the behaviour of platform-type continuous joints. A force-displacement relation for the joint is determined from the joint strength and modulus of elasticity, based upon the stress-strain curve

proposed by Desayi and Krishan[25] for concrete, and a joint height and thickness of 250 and 200 mm, respectively. For the base joint, strength and stiffness values are doubled to represent a stronger joint, and the force-displacement curve is based on a 50 mm joint height.

For computer analysis, the force-displacement relation is approximated by a trilinear constitutive monotonic path. As shown in Fig. 2.5(a), behaviour is elastic until displacement u_1 is reached, after which the stiffness reduces to k_2. At displacement u_2, the ultimate strength F_u is reached. To maintain numerical stability, a positive stiffness close to zero is used for k_3 to approximate the force-displacement curve following joint "crushing" at displacement u_2. Unloading at any instant follows the initial elastic stiffness k_1. When tensile forces develop at the joint, stiffness is reduced to k_t, approximately zero and thus allowing gap opening at the joint.

2.4.2 Horizontal Joint Shear Behaviour

Tests on panel joints[26,27,28,29] show that shear force along the joints is carried mainly by aggregate interlock, surface shear transfer and dowel action of the vertical reinforcement. With little vertical reinforcement, the results indicate that the contribution of dowel action is relatively minor, and shear along the joint is governed primarily by friction. Fig. 2.5(b) shows the elasto-plastic constitutive model chosen for the horizontal joint shear springs, which allows for the expected variation of normal force in the joint during earthquake loading. Thus, slip will occur when the shear force reaches the available frictional resistance $\mu_f F_c$, where μ_f is the

horizontal joint coefficient of friction and F_c (see Fig. 2.5(a)) the normal compressive force at that instant. The corresponding elastic shear stiffness k_s is determined from the modulus of elasticity E for axial behaviour assuming a Poisson's ratio of $\nu = 0.2$, and from test results by Verbic and Terzic[27].

When reinforcement across the horizontal joints is such that dowel action becomes significant, the modified elasto-plastic model shown in Fig. 2.5(c) is used. Following shear slip, tension forces are developed in the reinforcing bars, providing clamping action across the joint and increasing both the friction and aggregate interlock effects, with the result that shear resistance against slip is restored. Prior to the horizontal joint reaching the yield level $\mu_f F_c$, the model assumes that the reinforcing bars contribute little to the shear stiffness, so that the initial stiffness is equal to k_s. When shear force F_s reaches the yield level, the joint develops shear stiffness k_r due to dowel action of the reinforcing bars, where the ratio k_r/k_s is taken to be 0.1.

Unloading thereafter takes place with elastic stiffness k_s; when the shear strength $\mu_f F_c$ is again reached, the reinforcement does not immediately provide the necessary clamping action to provide shear resistance against slip. Only at some point along the hysteresis loop does the reinforcement again provide the tension force required to develop the shear stiffness k_r. This point, as shown in Fig. 2.5(c), is controlled by parameter r, the value for which is taken as 0.15. The remaining hysteresis loops are modelled in the same way. Parameter r and stiffness ratio k_r/k_s are assumed to be unaffected by the amount of reinforcing steel employed. This model for shear

behaviour of the horizontal joint elements is based on that employed by Kianoush and Scanlon[16].

For axial behaviour of the joint with reinforcement, the model shown in Fig. 2.5(a) is also employed, except that the tensile stiffness k_t, previously close to zero, assumes a value based upon an amount of steel distributed uniformly over the joint area. Reinforcement equal to 0.5 per cent of the gross concrete area at the joint is used, satisfying the CPCA minimum distributed reinforcement ratio requirement of 0.25 per cent for seismic design of ductile flexural walls[31]. Tensile stiffness is based approximately on monotonic load tests[20] on reinforcing bars anchored in grouted concrete masonry. A stiffness equivalent to an assumed ungrouted reinforcement length of 850 mm for each reinforcing bar is thus employed. Behaviour of the reinforcement is assumed to remain linear elastic.

2.4.3 Vertical Joint Axial Behaviour

Earlier studies[32] showed that, compared to the stiffness in shear, stiffness normal to the vertical joint is of little importance to the integrity of panelized systems. Vertical joint minimum axial stiffness of only 0.1% of the panel stiffness in shear is found to ensure against appreciable loss of structural stiffness due to transverse flexibility of the joints. Hence, the linear elastic constitutive model shown in Fig. 2.6(a) is adopted for axial behaviour of the vertical joint elements. The tensile stiffness k_t represents the equivalent tensile stiffness of the horizontal ties, based on a debonding length of 60 tie diameters. At the floor levels, this tie stiffness is divided between the two vertical joint elements, whereas

the roof tie is represented by the single vertical spring element at the roof level. For the elements located at the panel bottoms, where dry-packing of the joint is performed, the compressive stiffness k_c approximates the estimated behaviour of the joint grout. Properties equivalent to the horizontal joint assembly are used, assuming a vertical joint gap of 20 mm and an effective grout length of 1/10 the panel height. For the elements at the panel tops, where there is no dry-packing, the compressive stiffness estimates the stiffness of the steel connecting plates.

2.4.4 Vertical Joint Shear Behaviour

Cyclic load tests by Spencer and Neille[22] on welded headed stud connectors produced load shear-deflection hysteresis loops of the 'pinched' type. It was found that for loads above a certain stability level, successive loops exhibited a monotonically decreasing yield envelope. This strength degradation was shown to be characteristic of the shear behaviour of the stud connectors subjected to cyclic loads. A measure of the amount of energy absorbed in the connectors during such cyclic loading is from the ductility factor μ, where:

$$\mu = u_{max}/u_y$$

which defines the ductility demand in the vertical joint, where u_{max} is the maximum shear deformation of the connector and u_y the elastic yield point. Based approximately upon the tests by Neille[22] (and also from an empirical formula[23] for connectors under monotonically increasing load and at approximately 100 per cent of the ultimate strength), u_{max} = 12.8 mm. Assuming an elastic limit of u_y = 0.36 mm[22], this corresponds to a maximum ductility capacity of μ = 36 for the stud

connectors.

Fig. 2.6(b) shows an elasto-plastic constitutive model for shear behaviour of the vertical connectors. The model is a simplification of observed test behaviour of shear connectors in the tests by Spencer and Neille[22], displaying important aspects of the experimental results, including the exhibition of large ductility prior to failure.

The material law assumed for the vertical joint elements in shear shown in Fig. 2.6(c) is an attempt to better reflect the behaviour of the connectors observed in tests[22]; the stiffness degradation exhibited by the model appears to be suitable for the vertical connectors. Strength degradation could easily be incorporated by introducing monotonically decreasing strength envelopes. Earlier studies[11,12] incorporated such stiffness and strength degradation behaviour in the vertical joint mechanical connectors. The present model, however, assumes a constant strength envelope with only degrading of stiffness.

Progressive deterioration of the element as a result of plastic action is controlled by the parameter α, where $0 < \alpha < 1$. Following initial loading of the element, only subsequent unloading occurs at the elastic stiffness. Yielding in one direction of the loading cycle will cause the yield point of the load-displacement curve to advance in the opposite direction with load reversal in proportion to the value of α; the result is that further reloading occurs along a path leading from the intercept of the horizontal axis to the updated yield pint. With continued yielding of the element, the stiffness defined by this path decreases and stiffness degradation becomes apparent. For $\alpha = 0$, yielding commences when the previous maximum slip is reached, whereas for $\alpha = 1$, yielding occurs only when the mirror image

of the last reversal point is reached. Fig. 2.6(c) indicates these mirror image points by primed letters.

When reversal occurs along a path leading to the anticipated yield point, small amplitude cyclic behaviour of the vertical connectors occurs, as shown in Fig. 2.6(d) (for $\alpha = 0$). Following large positive and negative yield excursions, the figure shows the behaviour for small amplitude load reversals. The basic governing laws are: (1) unloading, as previously, occurs at the elastic stiffness (path a-b); (2) instead of a path leading to the previous peak, as with path b-c, reloading now occurs along a path leading from the intercept of the horizontal axis to the previous point of reversal (path d-a); and (3) beyond the previous point of reversal, the path leads to the most recent point of reversal for large amplitude yielding in the current direction. An exception to this behaviour occurs when the previous point of reversal of (2) represents a displacement small in absolute magnitude, in which case the path leads directly to the previous large amplitude reversal point of (3), as for the behaviour of Fig. 2.6(c). This model is analogous to the moment-rotation relationship for reinforced concrete beams developed by Takeda[33].

Shear stiffness and strength of the connectors are based on experimental data[22,23] as well as CPCI design formulae[21], assuming two 12.7 x 155 mm headed- stud anchors per connector. Tables 2.1(b) and 2.1(c) contain the respective properties of the horizontal and vertical joint elements.

2.5 COMPUTER IMPLEMENTATION

Nonlinear time-history dynamic analysis of the structural model was performed using a modified version of the nonlinear finite element program ANSR-I[34]. Panels and vertical ties were modelled using the available isoparametric plane-stress elements and truss elements, whereas subroutines for the joint elements were developed separately and added to ANSR-I. Further changes to the program were required for its use as a micro-computer package implemented on the SUN computer system in the Civil Engineering Department of Concordia University, Montreal. This included the accommodation of a number of post-processing programs for time-history output analyses and graphics applications.

Rayleigh damping corresponding to 5 per cent of critical damping in the first and second modes was assumed; damping coefficients proportional to the mass and tangent stiffness were used as input parameters for the program to define the structure damping matrix, derived from the first two periods of vibration. These periods were estimated from a modal analysis of the wall using the program SAP-4[35], where rigid horizontal panel joints were assumed. Periods of vibration corresponding to the first and second modes were found to be 0.53 and 0.13 seconds, respectively.

Structural masses were assigned as nodal lumped masses at the floor levels, and assumed to be proportional to the wall's gravity loads; masses in both the lateral and vertical directions were the same. Floor masses were divided equally between nodes above and below the horizontal joints, and exterior nodes (those on the panel edges) were assigned masses and loads equal to half those assigned to

interior nodes. A mass of 56 000 kg per story was employed.

An integration time-step of 0.001 seconds was used for all computer analyses, utilizing the Newton-Raphson iterative procedure with stiffness reformation at every time-step for dynamic solution. The north-south component of the El Centro 1940 earthquake record (Fig. 2.7) was used for input ground motion. Analyses was conducted for a duration of 5 seconds, which included the most severe earthquake motion and peak acceleration (0.32 g).

2.6 PARAMETRIC INVESTIGATION

A parametric study of the prototype structure is conducted to examine the seismic behaviour of large panel systems. The parameters consist of the following:

1. The coefficient of friction μ_f in the horizontal joints can determine to a large extent the level of slipping action and thus energy dissipation in the horizontal joints. As noted in earlier experimental and analytical studies[4,5,8,14], slip of the horizontal joints can have a significant effect on the response of precast panel walls. Individual tests have each shown a wide range of values, from 0.2 to 1.8[36]. The present study employs four values, 0.2, 0.4, 0.8 and 1.2, with an assumed design value of 0.4.

2. Structural integrity and response during seismic activity may be improved through the use of post-tensioned vertical ties[17]. Steel bars of 17.5 mm diameter placed through the panel edges and anchored from base to roof, with coupling at floor levels for continuity, are introduced (Fig. 2.1(a)). A post-tensioning force equal to 60 per cent of the tie design strengtn is employed.

3. Vertical joint shear connectors employing two headed-stud anchors of size 12.7 x 155 mm correspond to the design strength of F_y = 104 kN. Results employing vertical joint connectors of strength F_y = 60 kN (9.5 mm diameter studs) and F_y = 146 kN (15.9 mm diameter studs) are compared with those for the design connectors (12.7 mm diameter studes and F_y = 104 kN) to examine the influence of strength F_y on structural response.

4. Vertical connector shear behaviour is of particular importance to the energy dissipation capacity of the panelized system. The use of a stiffness degrading model for shear behaviour of the vertical joints is compared with results obtained employing the design elasto-plastic model to determine the effect of vertical joint hysteretic shear behaviour on overall response.

5. Reinforcement across the horizontal joints provides resistance against slip when shear forces reach the frictional shear capacity of the joint. In addition, tensile stiffness is developed by the reinforcing bars. The importance to seismic behaviour of the resulting 'clamping' action and tensile stiffness is studied through a comparison to the prototype wall with only mild reinforcement. As well, the individual contributions due to the two effects (provision of shear resistance due to the dowel action, and introduction of tensile stiffness) are examined.

Results of the parametric study are presented in the form of envelopes of maximum dynamic response over the 12 stories of the wall. Four response parameters describe the behaviour of horizontal joints: slip, accumulated slip, gap opening, and axial force ratio F_r. Maximum horizontal joint slip indicates the largest absolute magnitude of slip

length attained, whereas accumulated horizontal joint slip measures the absolute sum of slip that occurs over the seismic duration. Gap opening occurs when tensile forces in the joint cause separation of the joint interface. Axial force ratio F_r is defined as:

$$F_r = F_c / F_u$$

where F_c is the compressive force in the joint and F_u the ultimate joint strength (see Fig. 2.5 (a)). Note that due to variations in axial force, both gap opening and F_r vary across the horizontal joints at any moment. When $F_c = F_u$, an axial force ratio F_r = 1.0 implies crushing in the joint.

Vertical joint behaviour is described by the ductility factor μ in the mechanical shear connectors, where a maximum ductility factor at any level indicates the greatest value of μ at that level between the four connectors there (see Fig. 2.1(a)). Envelopes of maximum story shear, lateral floor displacement, and horizontal tie force demonstrate the overall response in the prototype wall. Maximum response values for the range of μ_f used are summarized in Table 2.2, while maximum response values for the other parameters are shown in Table 3.

2.7 DISCUSSION OF RESULTS

2.7.1 Coefficient of Friction of Horizontal Joints

Influence of the horizontal joint coefficient of friction μ_f on overall seismic behaviour of the prototype wall is shown in Figs. 2.8 and 2.9, respectively depicting overall response envelopes and peak response values as a function of μ_f.

Fig. 2.8(a) demonstrates substantially lower story shears at all

levels with μ_f = 0.2, while lateral displacement and axial force ratio shown in Figs. 2.8(b) and 2.8(c) also show noticeable reductions over the wall height for low μ_f. Peak response values shown in Fig. 2.9 demonstrate the marked decrease in response with low μ_f. For axial force ratio F_r of the horizontal joints, crushing at joint level one shown in Fig. 2.8(c) yields a peak ratio F_r = 1.0 for all μ_f values. Lower values of F_r are noted for the upper levels at μ_f = 0.2.

The elastic strength capacity of 142 kN for the roof horizontal ties is exceeded at all μ_f values, while the 80 kN capacity of the floor ties is also exceeded at most of the upper levels, as indicated by Fig. 2.8(d). Fig. 2.9(d) also shows minimum tie force at the roof level for μ_f = 0.2, although this is not true at most other levels. Selection of the ties based on the PCA procedure previously noted are, hence, inappropriate for the seismic forces incurred herein, and ties of greater strength are required to limit their behaviour to the elastic range.

Envelopes of maximum horizontal joint response are shown in Fig. 2.10 for μ_f = 0.2, 0.4 and 0.8, while peak joint response values are plotted in Fig. 2.11 as a function of μ_f. Fig. 2.10(b) shows that for μ_f = 0.2, accumulated slip of the horizontal joints is considerably higher than that for both μ_f = 0.4 and 0.8. For the latter two values of μ_f, accumulated slip is essentially the same up to level 6. However, maximum slip length attained during such slip action is noted to be actually lower for μ_f = 0.2 than either 0.4 or 0.8, as evidenced by Fig. 2.10(a). Maximum values over the wall height shown in Figs. 2.11(a) and 2.11(b) reveal conflicting trends between maximum and accumulated slip. Table 2.2 summarizes the maximum magnitudes of

response for μ_f = 0.2, 0.4, 0.8 and also 1.2, including both overall and joint response.

Energy dissipation through slip of the horizontal joints is thus much more pronounced for μ_f = 0.2 than at higher μ_f, since slip action is more evident and hence a decrease in overall response follows. Gap opening also is minimized at low μ_f, although without reinforcement through the joint, this in itself is not critical. Gap opening *is* important in that reduced gap opening implies reduced levels of rocking in the wall; this latter phenomena is characterized by alternate opening and closing of the joint which can cause high degrees of stress in the joint edges.

Increased horizontal joint slip at μ_f = 0.2 also eliminates the need for inelastic action in the vertical joint to dissipate seismic energy, preventing the vertical joint connectors from reaching their maximum ductility. As shown in Fig. 2.10(d), ductility requirements are reduced over the entire wall height at μ_f = 0.2 with a maximum ductility factor of less than 10, while a factor of nearly 25 is obtained at μ_f = 0.8 (see Table 2.2).

2.7.2 Introduction of Vertical Ties

To investigate the effectiveness of employing vertical ties in the precast panel structure, 17.5 mm high-strength steel bars are introduced and placed two per panel, as shown by the dashed lines in Fig. 2.1(a). Maximum envelopes of overall response are shown in Fig. 2.12 while envelopes of maximum joint response are shown in Fig. 2.13, both for a wall with no vertical ties and with ties post-tensioned to 60% of tis design strength of 224 kN. Ties without post-tensioning

were seen to have little effect on the seismic behaviour of the precast wall and thus are omitted from the figures.

More dramatic results are achieved when the vertical ties are post-tensioned. Fig. 2.12 shows slightly increased response with respect to story shear, lateral displacement and axial force ratio with post-tensioned ties. Of note, however, is the considerable reduction in horizontal tie forces as a result of the introduction of the post-tensioned vertical ties (Fig. 2.12 (d)). The PCA design strength of 80 kN for the floor level horizontal ties are now satisfied at all floor levels, and the roof level tie force of 142 kN is coincident with the PCA design strength of 142 kN for the roof ties.

Figs. 2.13(a) and 2.13(b) demonstrate how post-tensioned vertical ties serve to enhance structural integrity of the structure; reductions in slip and accumulated slip of the horizontal joints from levels 3 upwards indicates considerable success in restraining overall joint movement. Maximum slip length in the horizontal joints is limited to a peak magnitude of under 8 mm at level 4, whereas in the structure without ties or with non-tensioned ties, slip is greater than 12 mm at the top joint. The improved integrity through the employment of post-tensioned ties is further illustrated in Fig. 2.13(c), where the vertical clamping effect of the post-tensioned ties on the upper panels is seen to limit gap opening of the horizontal joints to under 2 mm from levels 2 upwards. However, the effect of post-tensioned ties on gap opening of the lower stories is negligible. The effect of post-tensioning the vertical ties on ductility demand in the vertical joints is also minimal; Fig. 2.13(d) shows only a slight

decrease in vertical joint connector ductility factor over the structure height.

It should be added, however, that an earlier study[18] noted that, in the event of local panel failure, the additional loads induced in the upper panels from post-tensioned ties can cause failure of the vertical shear connectors. Considerable attention must be given to the vertical joint connectors when post-tensioned vertical ties are employed.

2.7.3 Vertical Joint Connector Shear Strength Fy

The influence of vertical joint connector shear strength F_y on structural response is shown in Figs. 2.14 and 2.15, where results for F_y = 60 kN and F_y = 146 kN are compared with those for the connector design strength of 104 kN. Fig. 2.15(d) shows the immediate effects of variations in the connector shear strength F_y; since F_y determines the yield point of the connectors, it is obvious that low F_y means larger plastic deformation in the connectors and thus ductility factor μ.

For the stronger connectors (F_y = 146 kN), a 60% reduction to a maximum ductility factor of 9.4 (from 22) is realized over the design strength of 104 kN. Use of weaker connectors (F_y = 60 kN) results in a substantially increased ductility demand for the vertical joints; values of μ exceed the design (F_y = 104 kN) maximum from levels 3 upwards, and exceed the expected capacity of 36 from levels 6 upwards. The maximum value of μ for F_y = 60 kN is more than twice that of the design strength connectors. Of interest is the observation that the

maximum ductility factor occurs at higher levels for decreasing connector strength; for F_y = 60, 104 and 146 kN, the maximum ductility factors occur at levels 10, 6 and 2, respectively.

Fig. 2.14(a) shows a general increase of story shear force with F_y, while the displacements over the wall height shown in Fig. 2.14(b) appear to show an optimum F_y of 104 kN for lateral vibration. Fig. 2.14(c) shows that horizontal joint crushing is eliminated at level 1 when F_y = 60 kN, with joint axial forces reduced substantially up to level 5. At F_y = 146 kN, crushing also occurs at level 2, while an axial force ratio F_r = 0.98 at the base is close to the crushing point. Horizontal tie forces are reduced to magnitudes below the PCA specified strengths at all levels with F_y = 60 kN, as shown in Fig. 2.14(d). In general, tie forces are shown to increase with F_y.

Figs. 2.15(a) and 2.15(b) show the effect of F_y on horizontal joint behaviour. The tendency towards increased inelastic horizontal joint action with increasing F_y is demonstrated; at F_y = 60 kN, slip in the horizontal joints is practically eliminated, with under 5 mm of accumulated slip up to level 9. At F_y = 146 kN, accumulated slip increases dramatically from F_y = 104 kN, with nearly 100 mm of total slip at the upper 5 levels. Fig. 2.15(c) indicates that high magnitudes of gap opening at levels 1 and 11 are found at the higher connector strengths (104 and 146 kN), but not for F_y = 60 kN, where gap opening is under 2 mm at all levels.

The energy dissipation potential of the vertical joints in a large panel system is demonstrated. By reducing the strength F_y of the vertical joint elements, increased energy dissipation through plastic yielding of the vertical joints is realized, as indicated by the rise

in the ductility demand of the connectors (Fig. 2.15(d)). Figs. 2.14 and 2.15 demonstrate a decided advantage to employing weak vertical joints; inelastic horizontal joint action is greatly reduced, and overall structural integrity is thus improved. Tie forces decrease to levels satisfying PCA design forces, and horizontal joint crushing is eliminated. Use of weaker vertical connectors to obtain F_y = 60 kN, however, must necessarily be accompanied by proper detailing so as to prevent failure of the vertical joints, since the increased ductility demand encountered exceeds the expected capacity of 36 from levels 6 upwards.

The procedure of allowing inelastic action to occur in the vertical joints, as opposed to allowing slipping of the horizontal joints has the advantage of confining inelastic action largely to elements that are not part of the primary load bearing system. In addition, as noted in an earlier study by Pall[13], energy dissipation through vertical joint action allows for softening of the structure to occur while retaining its elasticity and resilience, with little or no evidence of the permanent set that is associated with horizontal joint deformations. Thus, while it was shown that allowing slip to occur in the horizontal joints can be beneficial in terms of energy dissipation (Figs. 2.8 and 2.9), the vertical joints appear to possess a more advantageous location for energy dissipation.

Control of the strength parameter F_y in the vertical joints to improve response was also noted in earlier studies[11], and is similar to the use of slip loads studied by Pall[13] . The use of strong elements (F_y = 146 kN), while clearly reducing the ductility demand, results in poor seismic response. Since the expected capacity of the

connectors is 36, the larger stud size (15.9 mm diameter and F_y = 146 kN) fails to exploit the energy dissipating potential of the joint fully. With the smaller size studs (9.5 mm diameter and F_y = 60 kN), while seismic response is greatly improved and the energy dissipation capabilities of the vertical joints are fully realized, the drawback exists to the fact that ductility demand is excessive.

2.7.4 Vertical Joint Shear Behaviour

Accurate modelling of the vertical joint elements for shear behaviour must reflect the anticipated cyclic response of the mechanical connectors to seismic loading. Tests by Spencer and Neille[22] on headed-stud connectors produced load shear-deflection hysteresis loops that can be approximated by an elasto-plastic model (Fig. 2.6(b)). Figs. 2.16 and 2.17 compare results for the structure using vertical joint elements modelled by the stiffness-degrading shear model (Figs. 2.6(c) and 2.6(d)) to that of the design model assuming elasto-plastic behaviour.

Fig. 2.16 illustrates the variations noted in the overall response parameters due to the different shear behaviour models. Differences here are small in terms of story shear, lateral displacement and axial force ratio, with the exception that horizontal tie forces are reduced by about 25 per cent at all levels, but still above PCA design strength at roof level and the upper floors.

Fig. 2.17(d) shows a slight change in the magnitude of ductility demand for the vertical joint elements as a result of using the stiffness-degrading model; while no differences are exhibited up to level 3, reductions of approximately 10 per cent are encountered

elsewhere. The effect on horizontal joint behaviour is shown in Figs. 2.17(a), and 2.17(c). Maximum slip decreases by as much as 30 per cent at level 4, but shows no significant changes from levels 7 upwards. Accumulated slip, however, decreases at all levels, to a maximum reduction of over 25 per cent at the uppermost joint. Gap opening indicates noticeable differences from levels 7 upwards, with as much as a 60 per cent reduction at level 9 and an approximately 25 per cent decrease from the peak magnitude at the top joint.

While these numerical comparisons show apparently large differences, the diagrams also reveal that no noticeable shifts in actual patterns of behaviour are formed when the vertical joint shear behaviour is changed. Moreover, the numerical differences, as a whole, are not outstanding; only at certain levels are the disparities drastic, and in general, less than 10 per cent differences are encountered. Thus, stiffness degrading instead of elasto-plastic hysteretic behaviour, as evidenced in Fig. 2.15, does not introduce significant variations in overall seismic response. However, it has been noted[12] that stiffness degradation, when combined also with connector strength loss, can lead to detrimental response.

2.7.5 Horizontal Joint Reinforcement

Vertical reinforcement perpendicular to the horizontal joints provides resistance against slip when the shear capacity $\mu_f F_c$ of the joints is reached while also allowing for tensile stiffness to develop in the horizontal joints. The modified shear-slip model for the reinforced joints is shown in Fig. 2.5(c); unreinforced horizontal joints used in the prototype wall possess the shear-slip behaviour

shown in Fig. 2.5(b).

Figs. 2.18 and 2.19 illustrate the combined effects of such modified shear and axial behaviour in the horizontal joint elements on seismic response of the wall. Added shear resistance provided by the reinforcing bars invites higher shear forces at the floor levels, as demonstrated in Fig. 2.18(a); base shear increases by over 20 per cent to 1660 kN. Lateral vibration is compromised as well, with higher maximum floor displacements at all levels (Fig. 2.18(b)) with an increase of 41 per cent to 78 mm at roof level. Fig. 2.18(c), however, shows axial forces in the horizontal joints reduced at nearly every level; crushing at the joint edges enccuntered with unreinforced horizontal joints also occurs with reinforced joints at level 1. Reductions in horizontal tie forces are more significant; Fig. 2.18(d) indicates forces at all levels reduced to values satisfying PCA strength requirements for elastic design. Except for the 67 kN force for the roof tie, all forces in the horizontal ties due to the reinforcement are under 20 kN.

As Figs. 2.19(a) and 2.19(b) reveal, shear slip in the horizontal joints is dramatically reduced with the addition of vertical reinforcement; maximum joint slip is less than 1 mm and total slip accumulated at any level does not exceed 5 mm. Reinforcement presents substantial decreases in gap opening at the upper 4 levels, as shown in Fig. 2.19(c). The influence of reinforced horizontal joints on vertical joint connector ductility demand, shown in Fig. 2.19(d), also reveals changes. Ductility demand is reduced slightly up to level 6, and then increases from levels 7 upwards, to an increase of 25 per cent at the top. The peak magnitude of ductility

factor in the connectors shifts from level 6 to level 10 for the reinforced wall, from 22 to 23.

The diagrams have demonstrated the importance of reinforced horizontal joints on seismic response of panelized systems. Continuity provided by the reinforcing bars across the horizontal joints serves to greatly improve the integrity of a structure; as seen in Figs. 2.19(a), (b) and (c), the behaviour of the separate panel wall stacks in the 3-bay modified prototype, described by its limited shear slip and gap opening in the reinforced horizontal joints, approaches that of individual continuous elastic cantilevers. Joint deformations are limited essentially to the vertical joints, as Fig. 2.19(d) indicates, and then varies only marginally with that of the vertical joint deformations in the unreinforced wall. The restriction on horizontal joint deformations imposed by the reinforcing bars, however, removes the potential for energy dissipation through slip in the horizontal joints. While the forces found in the horizontal ties are greatly improved through the addition of reinforcement, both story shear and structural displacement show noticeable increases (Figs. 2.18(a) and 2.18(b)).

Nevertheless, the design of horizontal joints with vertical reinforcement is of particular value. Continuity across the horizontal connections is provided, and structural integrity is substantially improved. Ties remain elastic throughout, and the effect on the ductility demand in the vertical joint connectors is not remarkable and generally similar to that of unreinforced horizontal joints. While the story shears and lateral displacements are increased, the magnitudes are not excessive; thus, the advantages to

be gained from vertically reinforced horizontal joints are decisive.

The relative contributions provided by the horizontal joint reinforcement on behaviour of the connecting elements - i.e. shear-slip and axial - are shown in Figs. 2.20 and 2.21. Results for full action (as depicted in Figs. 2.18 and 2.19) are compared with responses assuming only shear-slip behaviour (no tensile stiffness), and responses assuming only the addition of an axial tensile stiffness (no shear stiffness due to reinforcement). Figs. 2.21(a) and 2.21(b) indicate that the reductions in slip of the horizontal joints are due almost entirely to the shear resistance provided by the reinforcement, and very little by the tensile stiffness produced by the steel bars. Fig. 2.21(c), however, shows that the reductions in gap opening due to the reinforcement occurs primarily as a result of the tensile stiffness developed by the bars. Thus, neither of the changes to the horizontal joint element model taken by itself effectively eliminates horizontal joint deformations; however, when taken together to represent the expected behaviour of the vertical reinforcement, deformations in the horizontal joints are reduced substantially.

The other figures from Figs. 2.20 and 2.21 representing the remaining response parameters indicate that the shear influence of the reinforcement model dominates; with horizontal tie forces, however, the added effects of the shear and axial behaviour are utilized to bring forces in the ties to the low magnitudes observed in Fig. 2.18(d).

2.7.6 Structural Integrity

Greater understanding concerning the level of structural

integrity in the prototype structure during seismic loading is rendered by Figs. 2.22 and 2.23, which show the deformed shapes of the wall model, considering separately: (a) the prototype structure with design properties, assuming no vertical reinforcement through the horizontal joints nor vertical ties, and a strength F_y = 104 kN for the vertical joint elements; (b) vertical ties introduced to the wall, and post-tensioned at 150 kN per tie; (c) strength F_y of vertical joint connectors lowered to 60 kN; and (d) horizontal joints containing vertical reinforcement. The deformed configurations correspond to a time of 2.0 seconds after seismic initiation, illustrating horizontal joint slip and gap opening, in Figs. 2.22 and 2.23, respectively. This time coincides approximately with the instant of maximum magnitudes for most of the response parameters considered. Joint deformations are exaggerated and adjusted for clarity, and discretization of the joint elements reduces joint thicknesses to zero.

The integrity of a building structure subjected to seismic loading has been demonstrated to be significantly influenced by a number of design parameters. As previously observed in Figs. 2.10(a) and 2.10(b), the design prototype structure allows for substantial horizontal joint movement, regardless of the horizontal joint coefficient of friction. This is graphically verified by Fig. 2.22(a), where slip is evident at all levels, and particularly at the upper levels. Opening of the horizontal joints is shown in Fig. 2.23(a); at t = 2.0 seconds, gap opening in the joints is limited to the lower levels, with the exception that the maximum magnitude over the seismic duration noted in Fig. 2.10(c) at the uppermost joint is

evident even here. The lack of continuity provided in the horizontal joints allows for considerable uplift to occur in the uppermost joint, as the panel above tilts with the leftward oscillating wall, demonstrated in Fig. 2.23(a). Vertical post-tensioned ties introduces vertical continuity to the wall assembly serving to clamp the panels together. Large gap opening that may appear in the top joints is thus restrained, as Fig. 2.23(b) displays. A tendency for less slip to occur due to the post-tensioned ties is also illustrated in Fig. 2.22(b), where the two panel stacks on the left side of the leftward leaning wall exhibit limited slip, with only significant slip on the rightmost stack. Overall, as earlier noted by Figs. 2.13(a) and 2.13(b), slip is reduced, and the importance of the vertical ties to structural integrity is seen.

Fig. 2.22(c) demonstrates the influence of vertical joint connector strength F_y on structural behaviour. Employing a weaker connector strength of F_y = 60 kN allows for increased deformations in the vertical joints, thus reducing the degree of horizontal joint movement. The diagram indicates only marginal slip at the upper joints of the rightmost panel stack, and virtually none at the lower floor levels and leading stacks of the leftward leaning structure. Fig. 2.22(d) shows even less slip in the horizontal joints at t = 2.0 seconds, as a result of vertical reinforcement through the horizontal joints. As detailed in Figs. 2.19(a) and 2.19(b), slip action in the horizontal joints is effectively eliminated through the introduction of the reinforcement. Overall behaviour more closely resembles that of three continuous cantilevers, coupled at the vertical joints by connector elements. Gap opening at t = 2.0 seconds shown in Figs.

2.23(c) and 2.23(d) for the lower F_y and horizontal reinforcement models confirms the elimination of the high magnitude of gap opening at the uppermost joint associated with the design prototype; as noted earlier, gap opening is higher at lower levels.

Large magnitudes of deformation in the horizontal joints are generally undesirable due to the lack of corrective elastic forces there to straighten the wall, and thus a permanent set in the building can result. Moreover, while slip can be beneficial to the extent that the resulting dissipation of energy can improve structural response, the lack of continuity in the horizontal joints can threaten overall stability. Continuity provided by vertical post-tensioning ties improves structural integrity substantially, while even better results are obtained for the wall containing vertical reinforcement through the horizontal joints. In either case, the loss of energy dissipation through horizontal joint slip had only minor adverse effects on seismic response. Lowering the strength of the vertical joints allows for increased energy dissipation there, and the horizontal joints show substantially reduced slip as a result.

2.8 CONCLUSIONS

A model is developed for the analytical study of a prototype multi-panel wall, consisting of one of the interior crosswalls of the typical 12-story precast panel building shown in Fig. 2.1(b). A parametric study is performed on the structure to determine its response to seismic loading. The following conclusions are noted:

1. The coefficient of shear friction μ_f in the horizontal joints assumes an important role in the wall's seismic behaviour. A low

coefficient dissipates more energy through joint slip, thus improving structural response. However, maximum slip length in the joints is seen to increase with high μ_f.

2. Horizontal ties designed according to PCA recommendations yield at the upper levels for all values of μ_f, while ductility demand in the vertical joint connectors are well below the capacity of 36 for all cases; crushing of the horizontal joint corners occurs at the first level. These initial observations, however, are for the prototype structure, having no vertical ties and horizontal joints without reinforcement.

3. Introduction of un-stressed vertical ties to the wall has little effect on seismic response. Post-tensioned ties, however, improve upon the integrity of the panelized system considerably at the upper levels. In addition, horizontal ties designed according to PCA recommendations remain elastic at all levels.

4. Vertical joint shear strength F_y can be varied by specifying different size stud anchors for the vertical connectors. Considerable energy dissipation can be realized by allowing high ductility demand to occur in the vertical planes with weak connectors. With a relatively small stud size (9.6 mm diameter), horizontal joint movement is reduced considerably, while crushing is eliminated entirely. Reductions in shear force and horizontal tie force are also seen, with forces in the ties reduced to levels below the PCA design recommended elastic strengths. The subsequent increase in ductility demand, however, exceeds the expected capacity of 36 for the connectors, from levels 6 upwards. As well, the design strength connectors produce lower floor displacements. Optimization of

vertical joint design through the shear strength F_y is demonstrated.

5. As verified by tests[22], shear behaviour of the vertical joint connectors can be approximated by an elasto-plastic hysteretic loop. A stiffness- degrading model, similar to the elasto-plastic model, more closely follows behaviour noted in the tests. However, general response in the prototype wall does not change perceptibly with the introduction of stiffness degradation.

6. Provision of vertical reinforcement perpendicular to the horizontal joints improves the structural integrity of the panel wall. Horizontal joint shear deformations are virtually eliminated, and gap opening reduced considerably. Behaviour of the individual walls approaches that of separate continuous elastic cantilevers. As well, horizontal ties designed according to PCA recommendations remain elastic. Increases to maximum shear forces and lateral floor displacements occur.

TABLE 2.1 - Properties of prototype wall.

Description	Value
(a) Panels and loading	
Panel thickness (mm)	200
Modulus of elasticity (MPa)	27.6 x 1000
Poisson's ratio	0.17
Compressive strength (MPa)	34
Unit weight of concrete (kg/m^3)	2400
Distributed floor load/story (kN/m)	36.0 (*)
Distributed panel load/story (kN/m)	14.0
(*) not including panel weight	

	floors	base
(b) Horizontal joints		
Thickness (mm)	250	50
Modulus of elasticity (MPa)	13.8 x 1000	27.6 x 1000
Compressive strength (MPa)	14.5	29
Axial parameters:		
k_1 (kN/mm/mm)	10.52	105.20
k_2 (kN/mm/mm)	1.91	19.19
k_3 (kN/mm/mm)	0.01	0.01
k_t (kN/mm/mm)	0.01	0.01 (#)
u_1 (mm)	0.220	0.044
u_2 (mm)	0.525	0 105
Shear parameters		
k_s (kN/mm/mm)	4.60	46.00
k_r (kN/mm/mm)	0.46	4.6
r	0.15	0.1
μ_f	0.4	0.4 ($)

- k_t = 0.25 kN/mm/mm if joint is reinforced
$ - design value

(cont.)

(cont.) **TABLE 2.1** - Properties of prototype wall.

(c) Vertical joints

	grouted	ungrouted
Axial parameters:		
k_c (kN/mm)	19530	1953
k_t-roof (kN/mm)	24.4	24.4
k_t-floors (kN/mm)	9.05	9.05
Shear parameters		
k_s (kN/mm)	294	294
F_y (kN)	104	104 ($)

$ - design value

TABLE 2.2 - Maximum Responses of Wall for Different μ_f Values

	μ_f	shear slip (mm)	total slip (mm)	gap opening (mm)	ductility demand μ
(a)	0.2	11.2	96.9	1.5	7.9
(b)	0.4	12.6	56.4	5.9	21.6
(c)	0.8	12.7	40.2	4.2	23.8
(d)	1.2	13.7	26.9	8.9	22.7

	μ_f	axial force ratio F_r	tie force (kN)	shear force (kN)	floor displacement (mm)
(e)	0.2	1.0	183	1325	49.7
(f)	0.4	1.0	257	1342	54.5
(g)	0.8	1.0	210	1510	60.1
(h)	1.2	1.0	246	1561	69.2

TABLE 2.3 - Maximum responses of wall.

	description	shear slip (mm)	total slip (mm)	gap opening (mm)	ductility demand
1.	design	12.6	56.4	5.9	21.6
2.	vertical ties	12.1	58.1	6.4	21.6
	vertical ties (PT)	7.2	12.6	2.4	19.7
3.	stiffness-degrading	12.9	41.0	4.6	20.2
4.	F_y = 60 kN	4.4	13.0	2.0	43.7
	= 146 kN	17.2	99.7	5.1	9.4
5.	reinforcement	0.6	3.1	1.9	23.3

		axial force ratio F_r	tie force (kN)	shear force (kN)	floor displacement (mm)
1.	design	1.0	257	1342	54.5
2.	vertical ties	1.0	256	1332	54.4
	vertical ties (PT)	1.0	142	1533	62.5
3.	stiffness-degrading	1.0	208	1414	59.9
4.	F_y = 60 kN	0.9	65	1148	70.9
	= 146 kN	1.0	253	1515	89.2
5.	reinforcement	1.0	67	1651	78.0

1. Design prototype wall contains no vertical reinforcement through the horizontal joints, nor vertical ties. An elasto-plastic model is assumed for shear behaviour in the vertical joint elements, with shear strength F_y = 104 kN.
2. Post-tensioned vertical ties (PT) tensioned to 150 kN, or 60 per cent of design strength.
3. Stiffness-degrading model assumed for shear behaviour of the vertical joint elements.
4. Shear strength F_y of the vertical joint elements varied.
5. Vertical reinforcement through the horizontal joints introduced, allowing for added shear resistance against slip and tensile stiffness against joint opening.

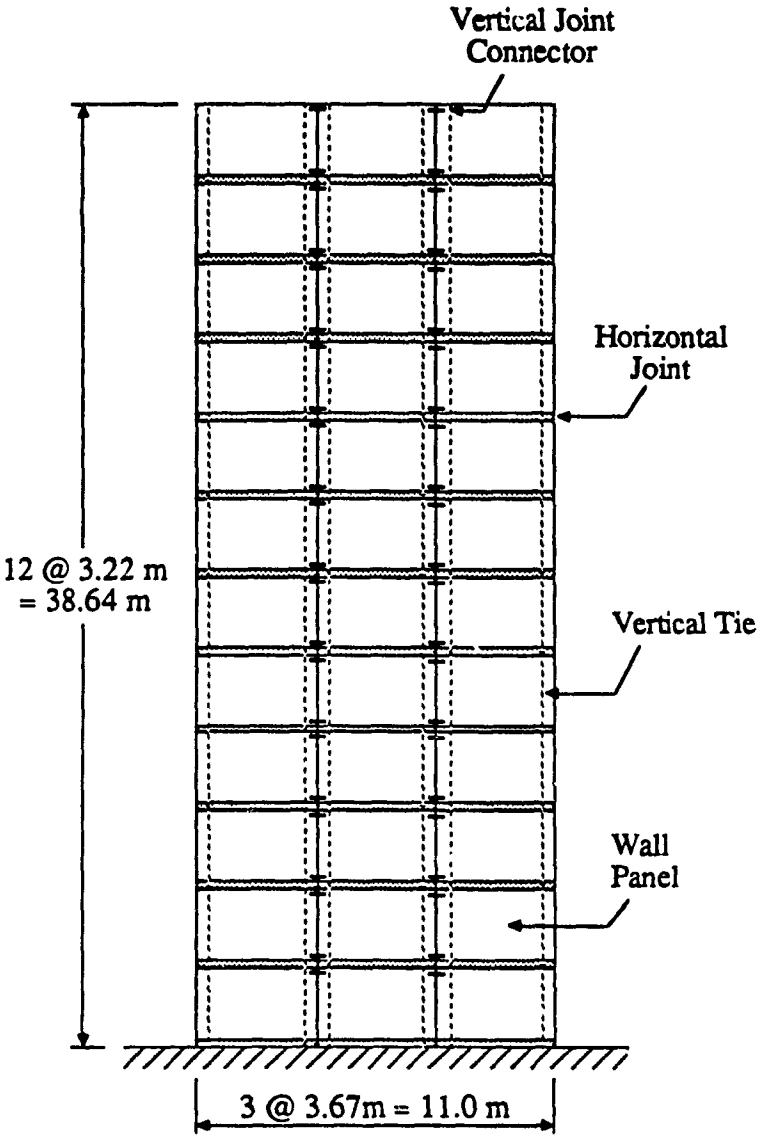

Figure 2.1(a) Typical precast multi-panel interior wall.

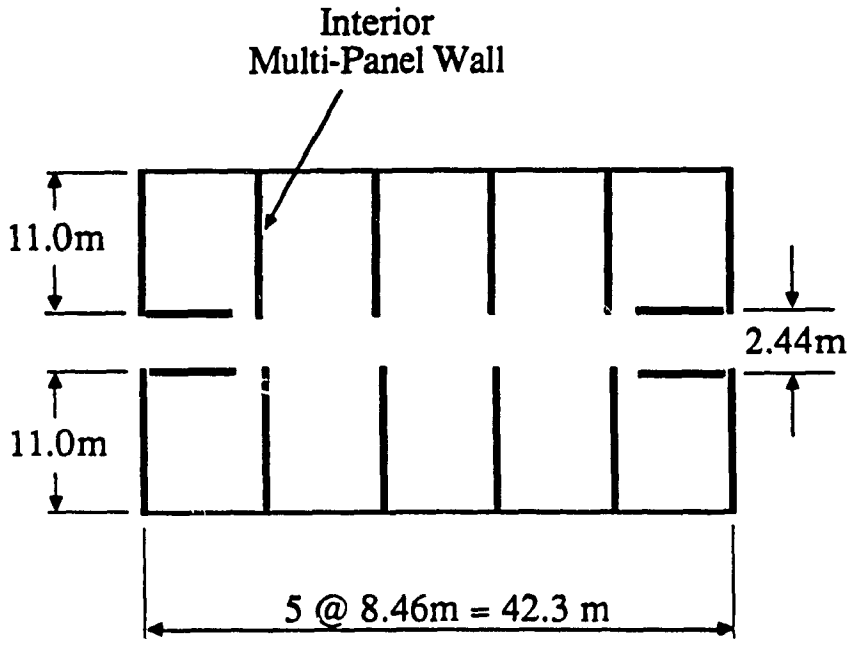

Figure 2.1(b) Floor plan of prototype structure.

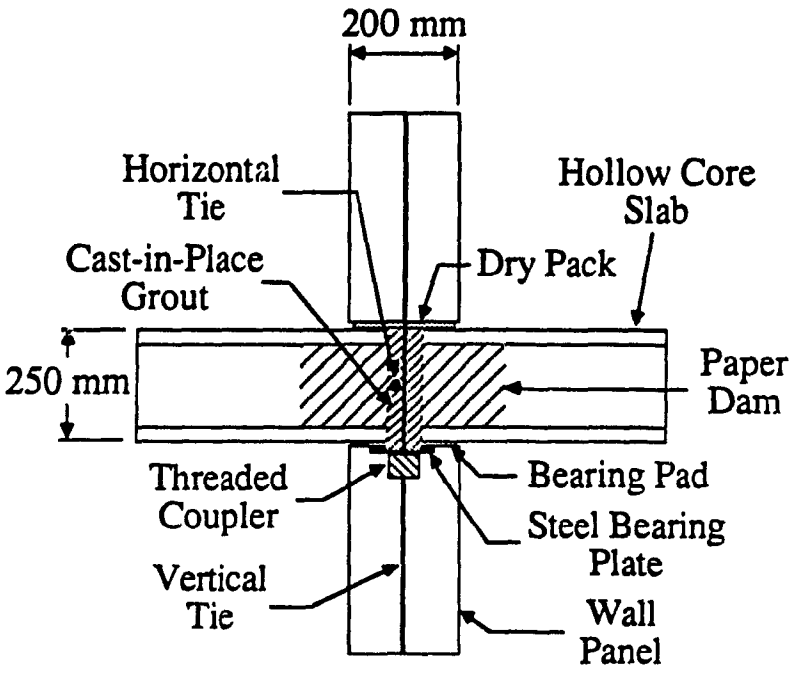

Figure 2.2(a) Typical horizontal platform joint.

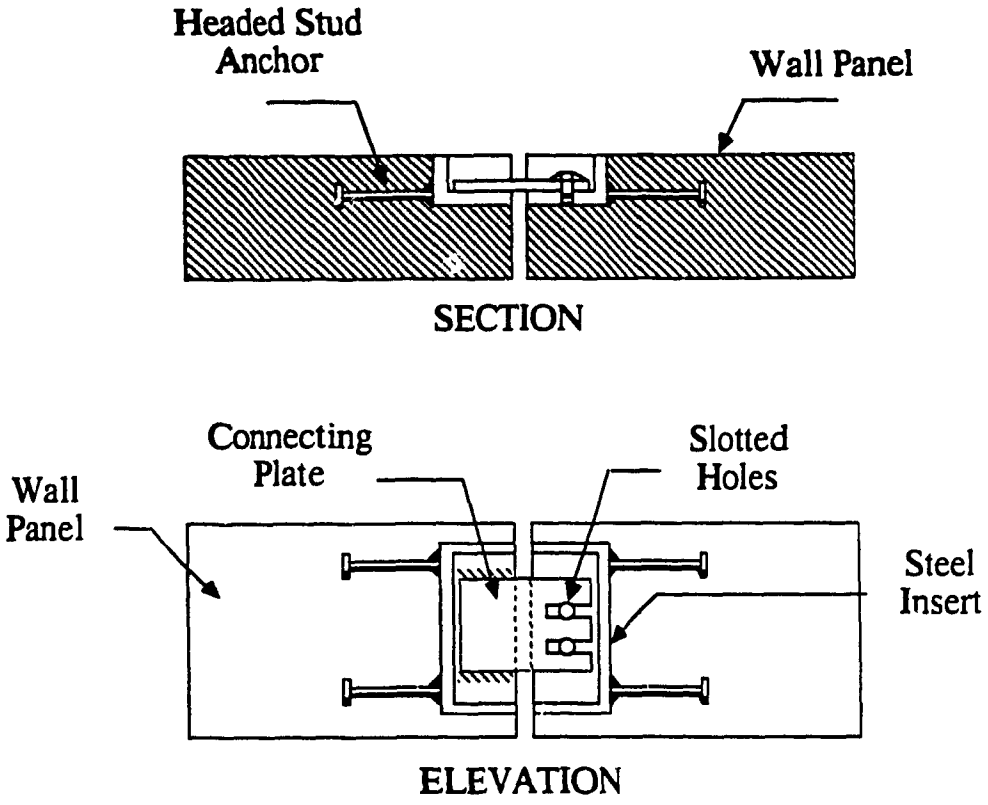

Figure 2.2 (b) Vertical shear connector.

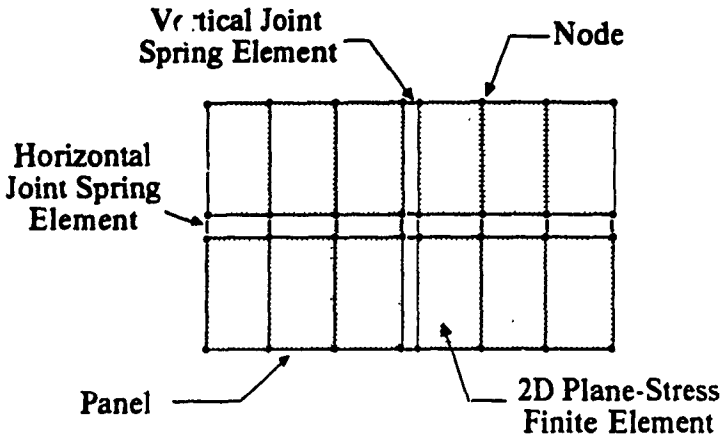

Figure 2.3 Finite element discretization of wall.

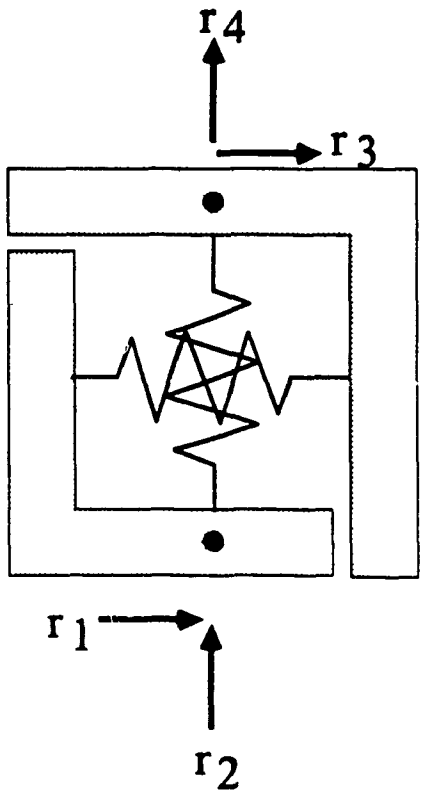

Figure 2.4 Model of 2-noded orthogonal joint spring element with degrees-of-freedrom r_1 - r_4.

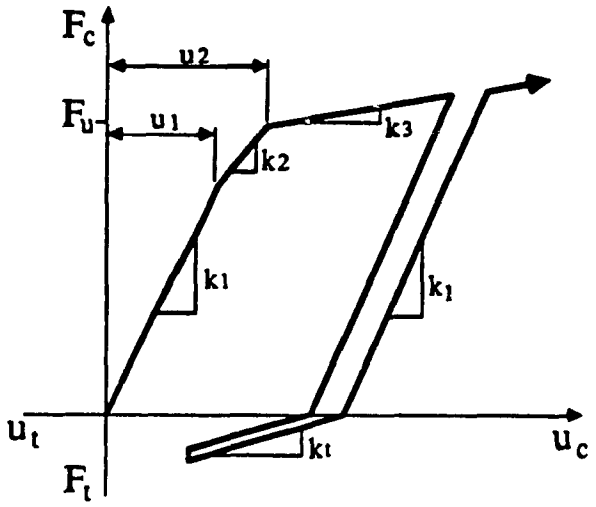

(a) Compression and Tension

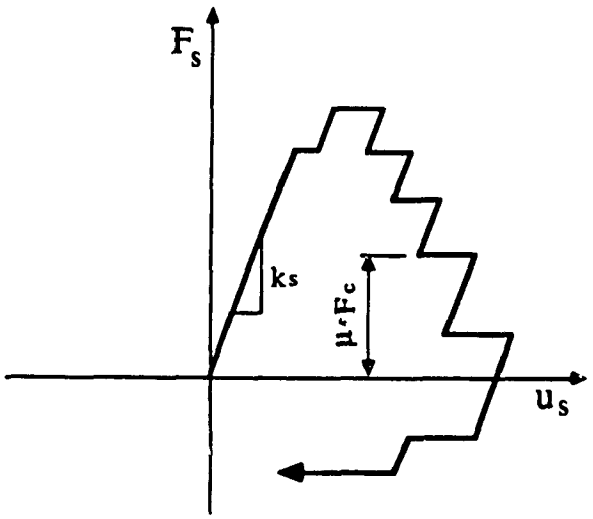

(b) Shear (unreinforced)

Figure 2.5 Force-deformation relations for horizontal joints.

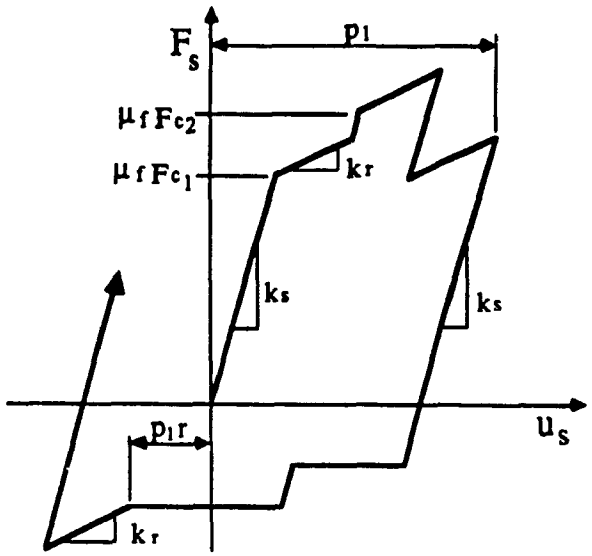

(c) Shear (reinforced)

Figure 2.5 Force-deformation relations for horizontal joints.

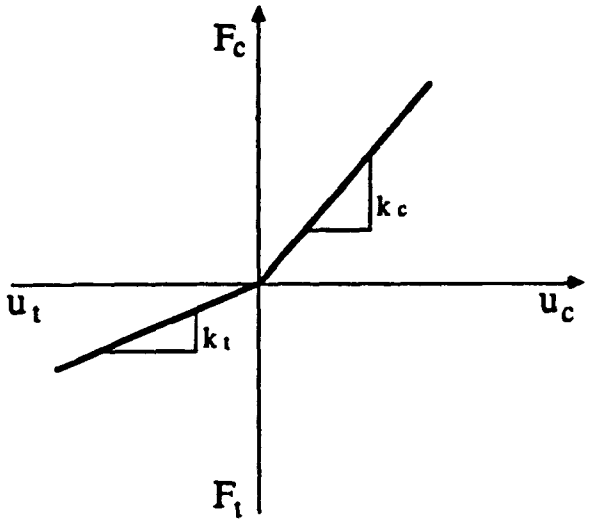

(a) Compression and Tension

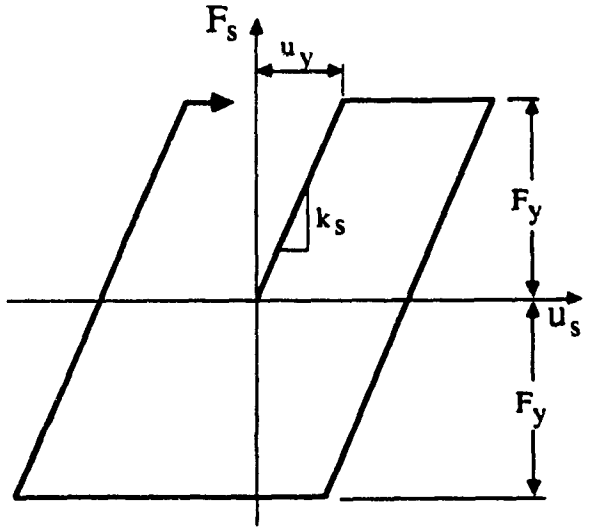

(b) Shear (elastoplastic)

Figure 2.6 Force-deformation relations for vertical joint connectors.

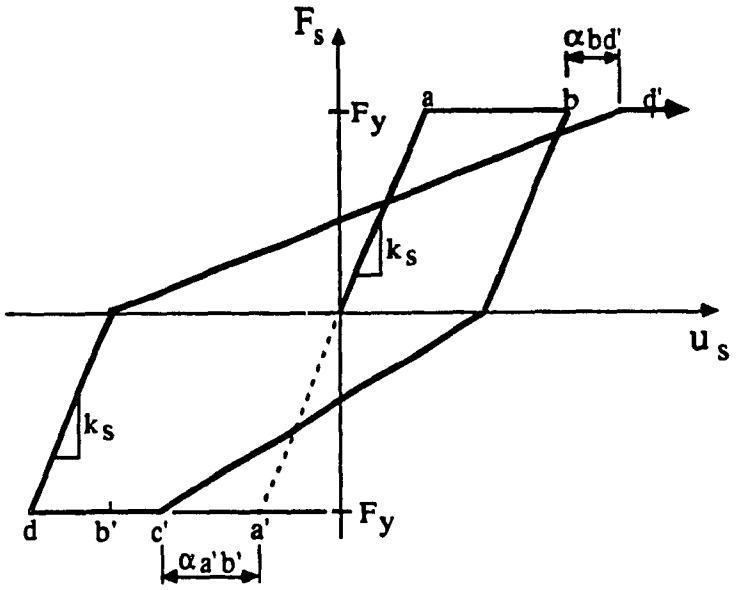

(c) Shear (stiffness degrading: $0 < \alpha < 1$)

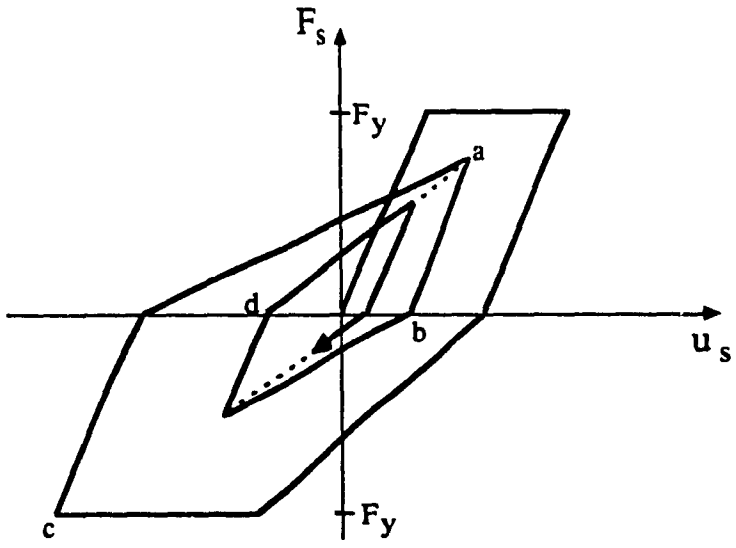

(d) Small Amplitude Shear Behaviour ($\alpha = 0$)

Figure 2.6 Force-deformation relations for vertical joint connectors.

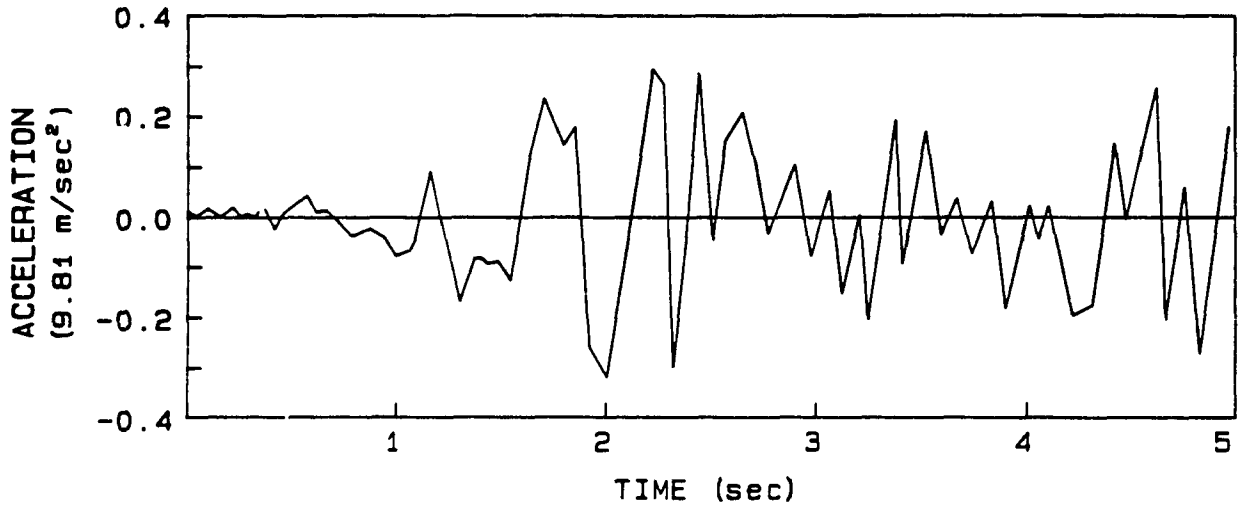

Figure 2.7 1940 El Centro NS earthquake excitation used for study.

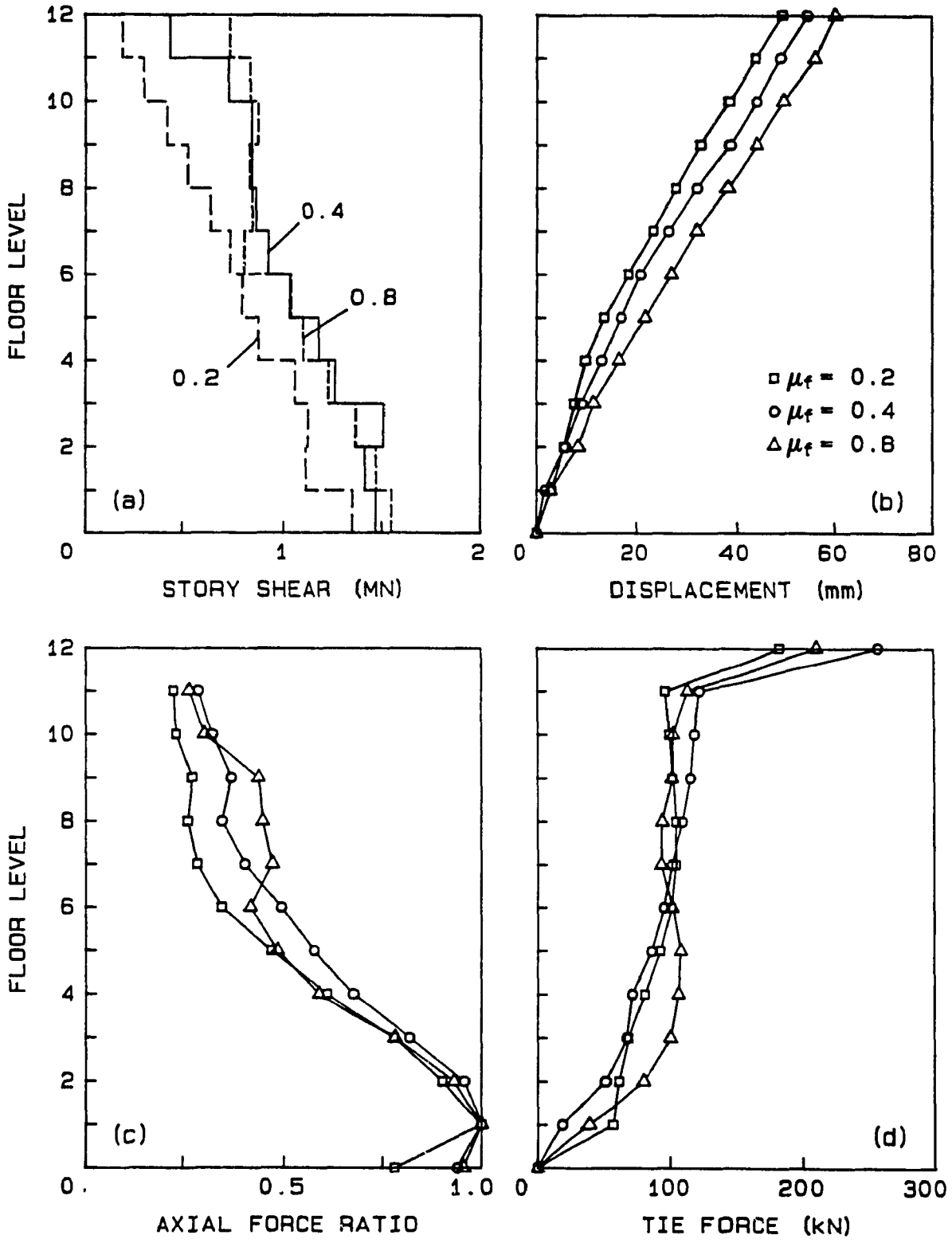

Figure 2.8 Comparison of envelopes of maximum overall response for μ_f = 0.2, 0.4 and 0.8.

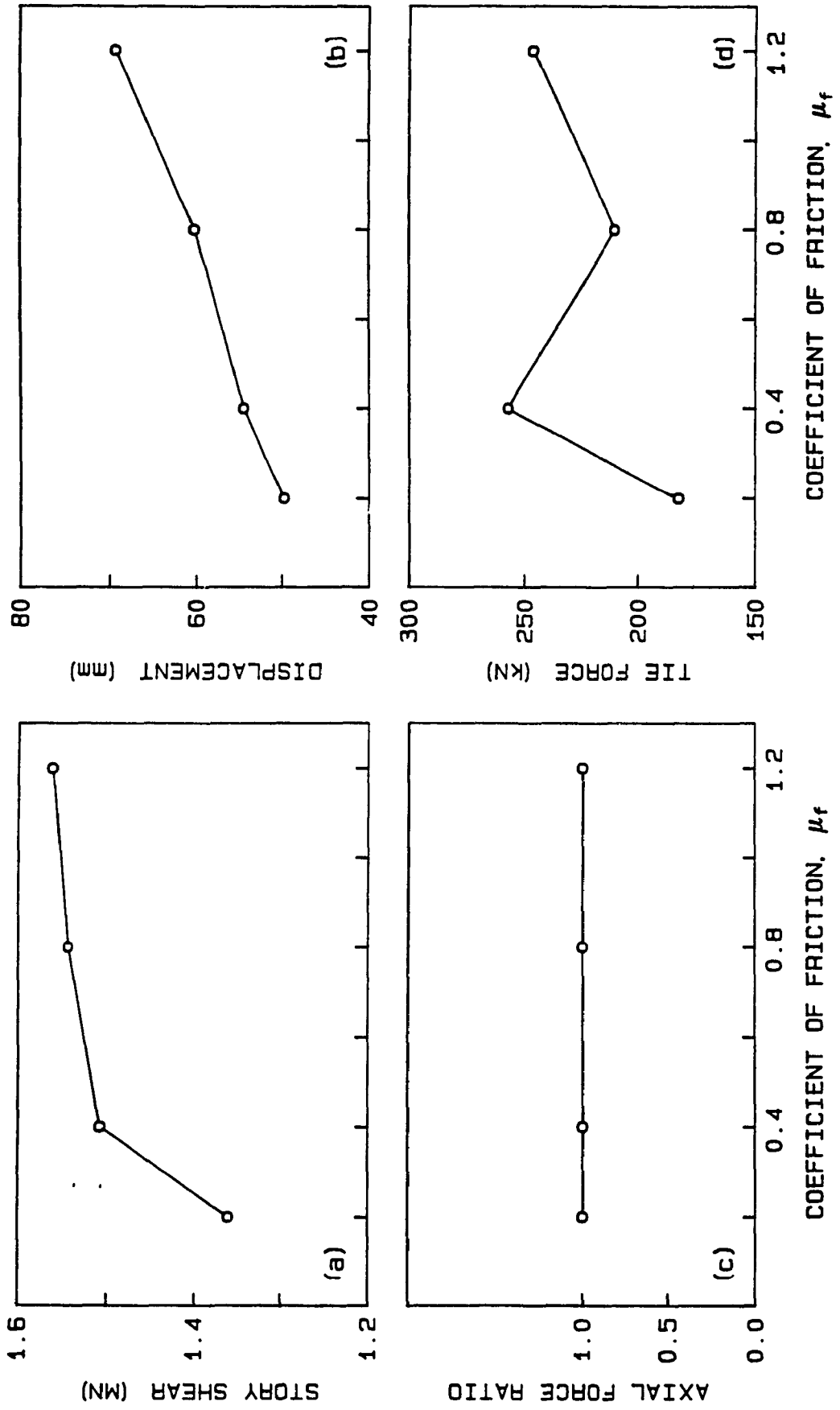

Figure 2.9 Effect of horizontal joint coefficient μ_f on peak overall response.

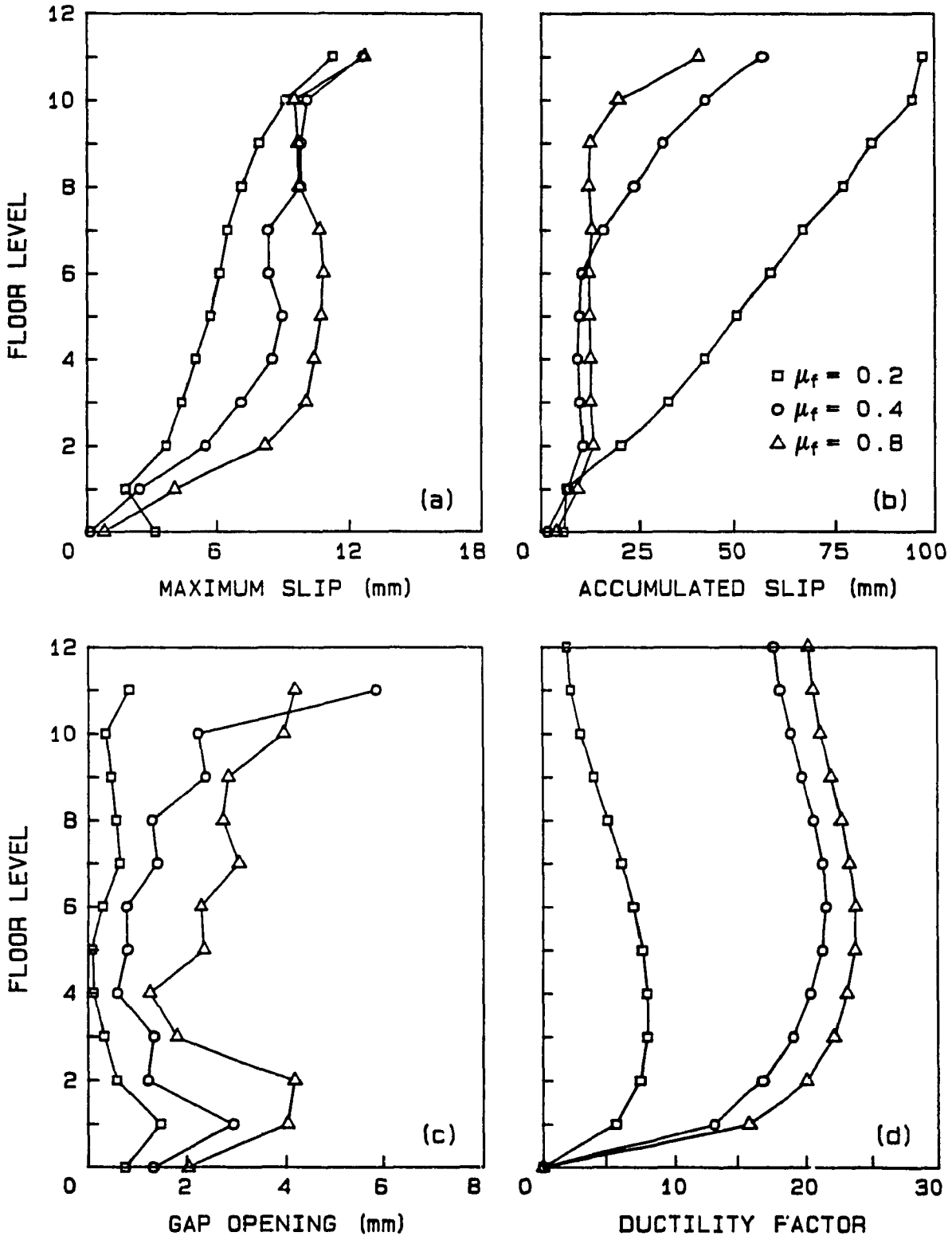

Figure 2.10 Comparison of envelopes of maximum joint response for μ_f = 0.2, 0.4 and 0.8.

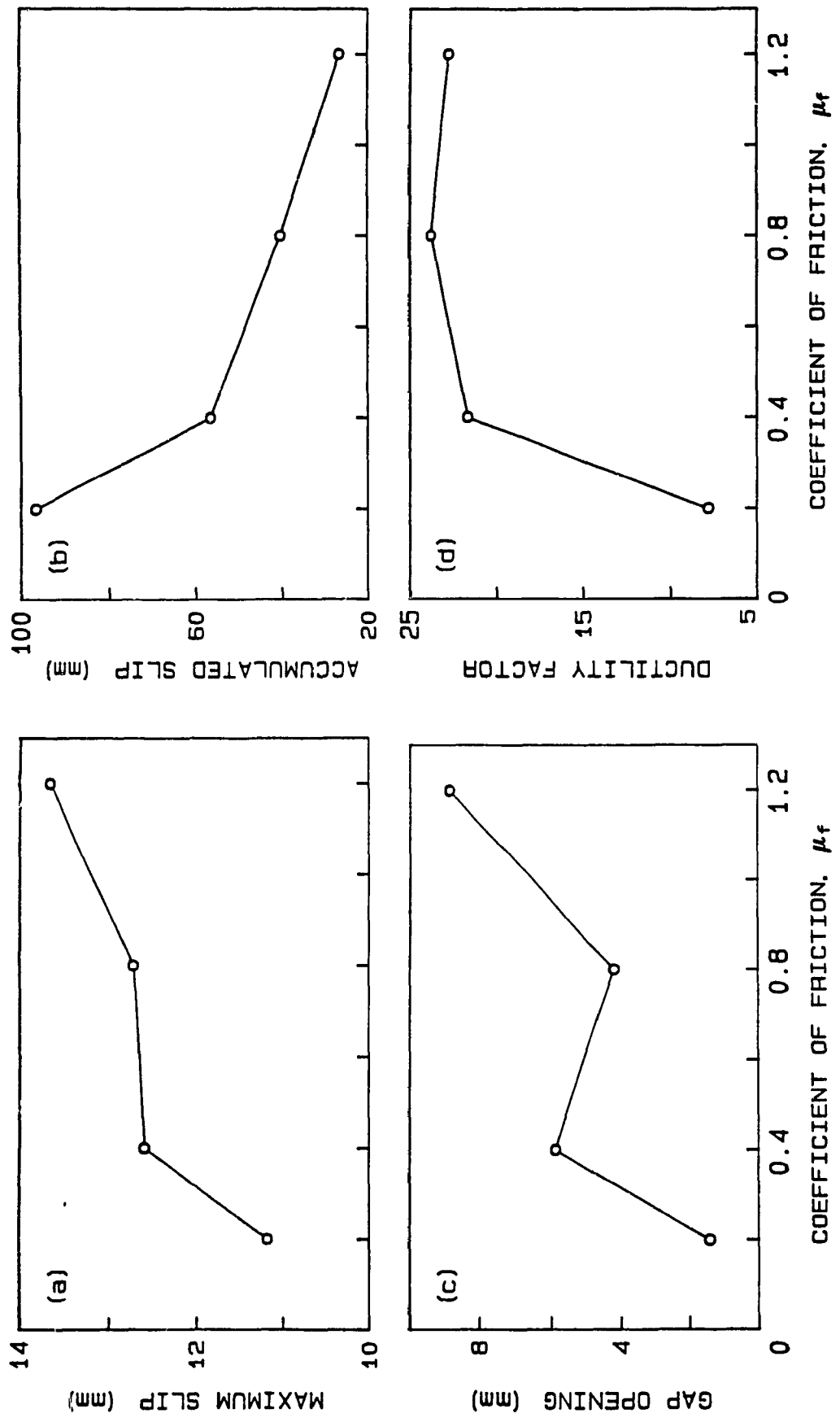

Figure 2.11 Effect of horizontal joint coefficient μ_f on peak joint response.

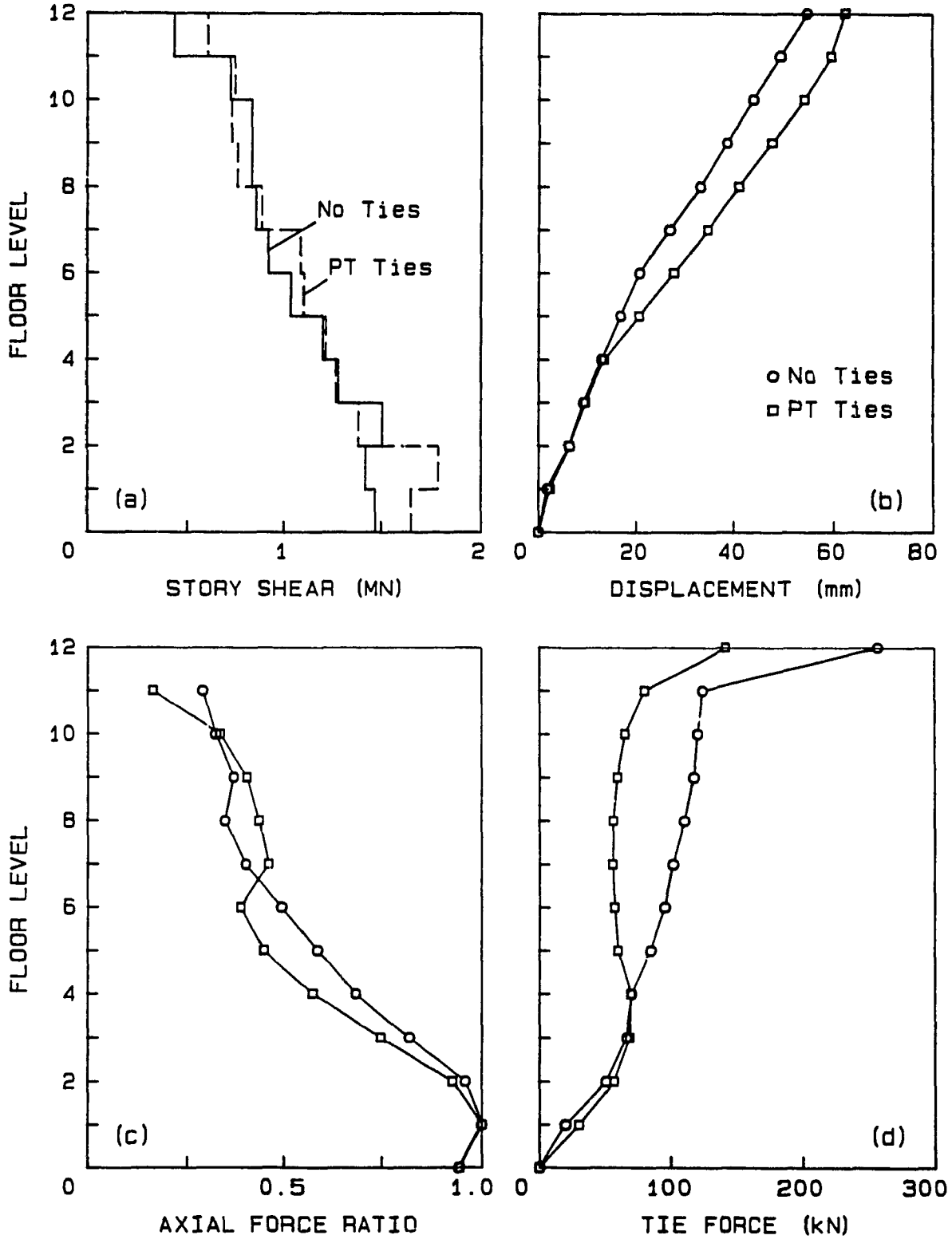

Figure 2.12 Effect of post-tensioned vertical ties on envelopes of maximum overall response.

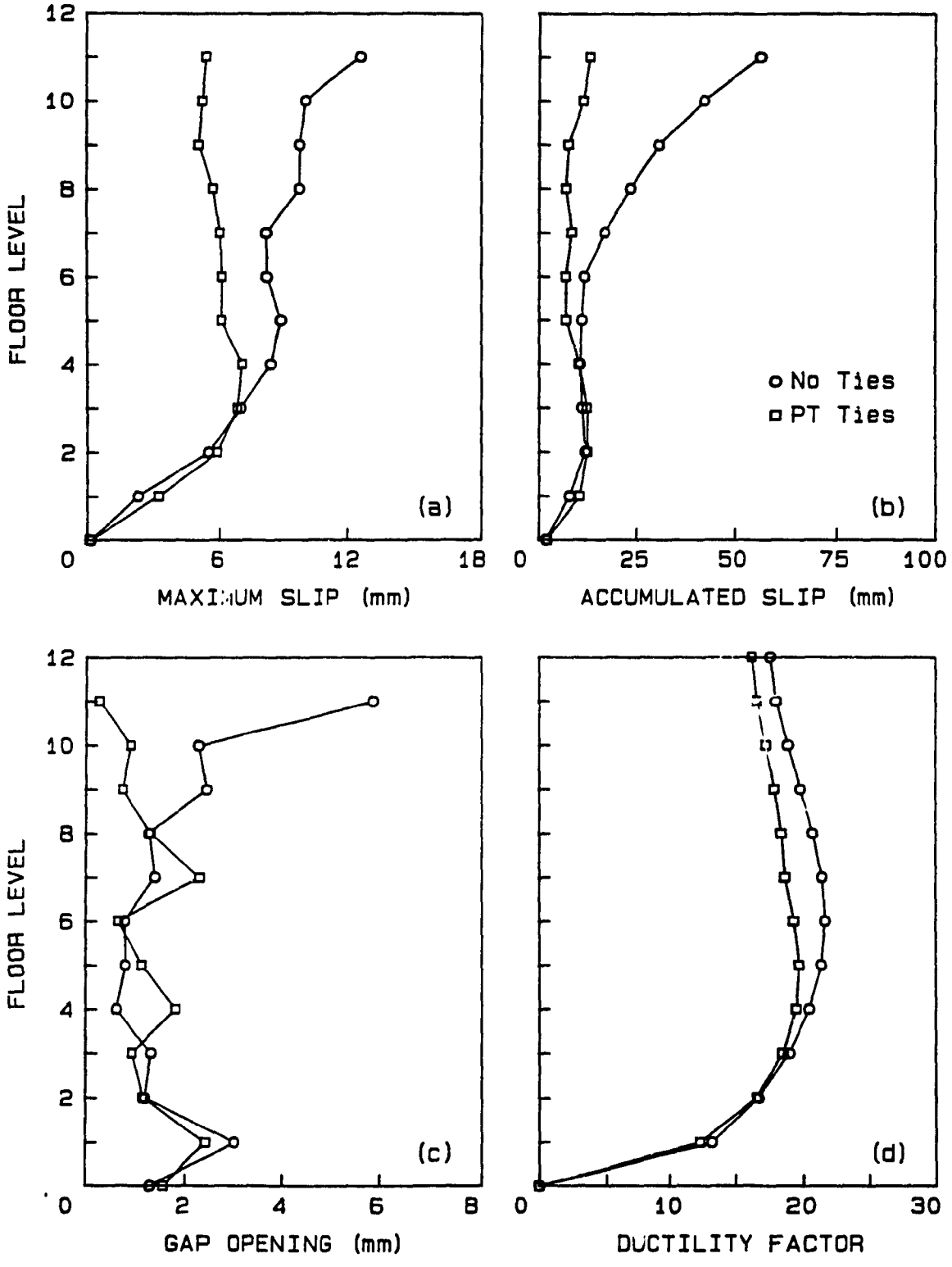

Figure 2.13 Effect of post-tensioned vertical ties on envelopes of maximum joint response.

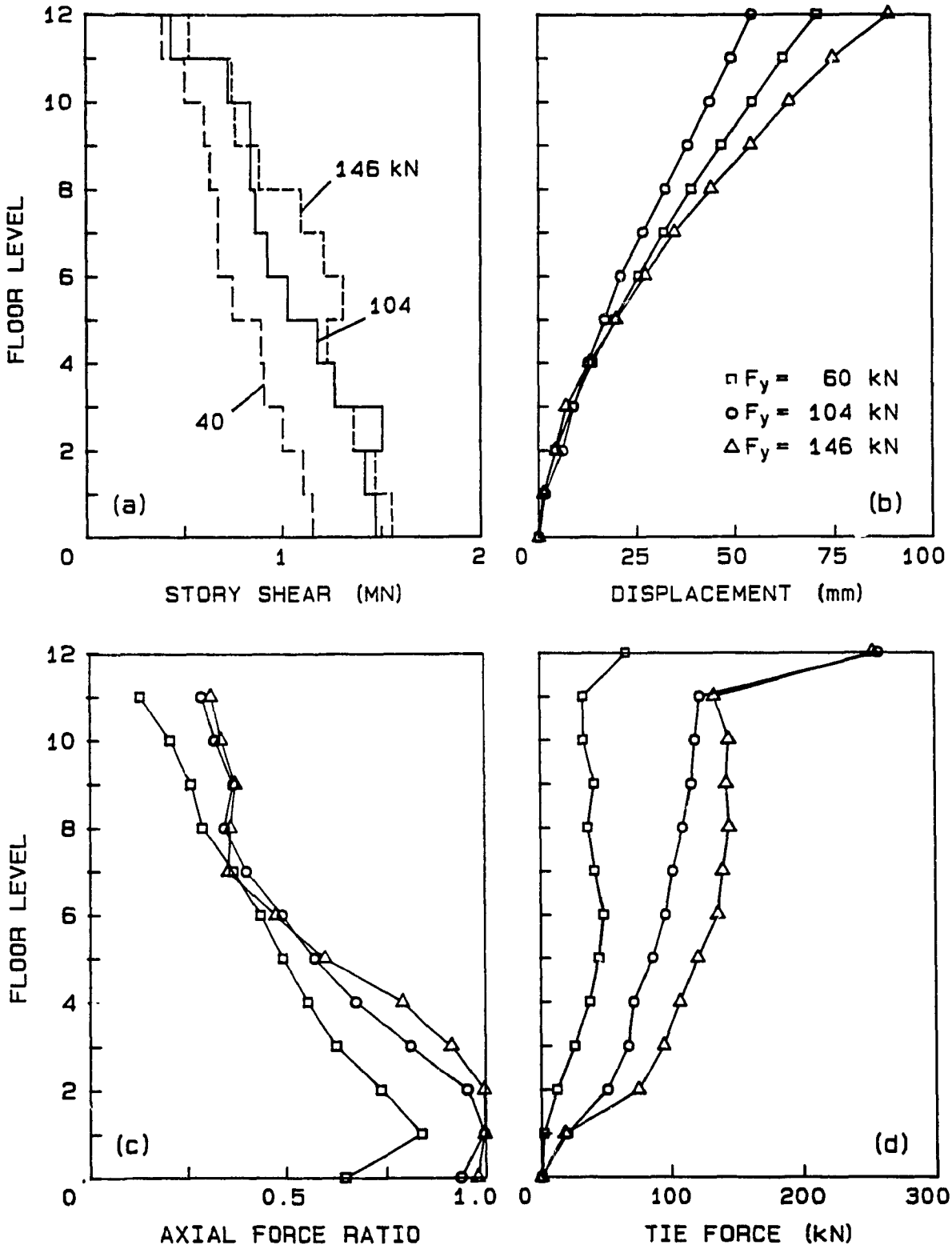

Figure 2.14 Comparison of envelopes of maximum overall response for vertical connector strength F_y = 80, 104 and 146 kN.

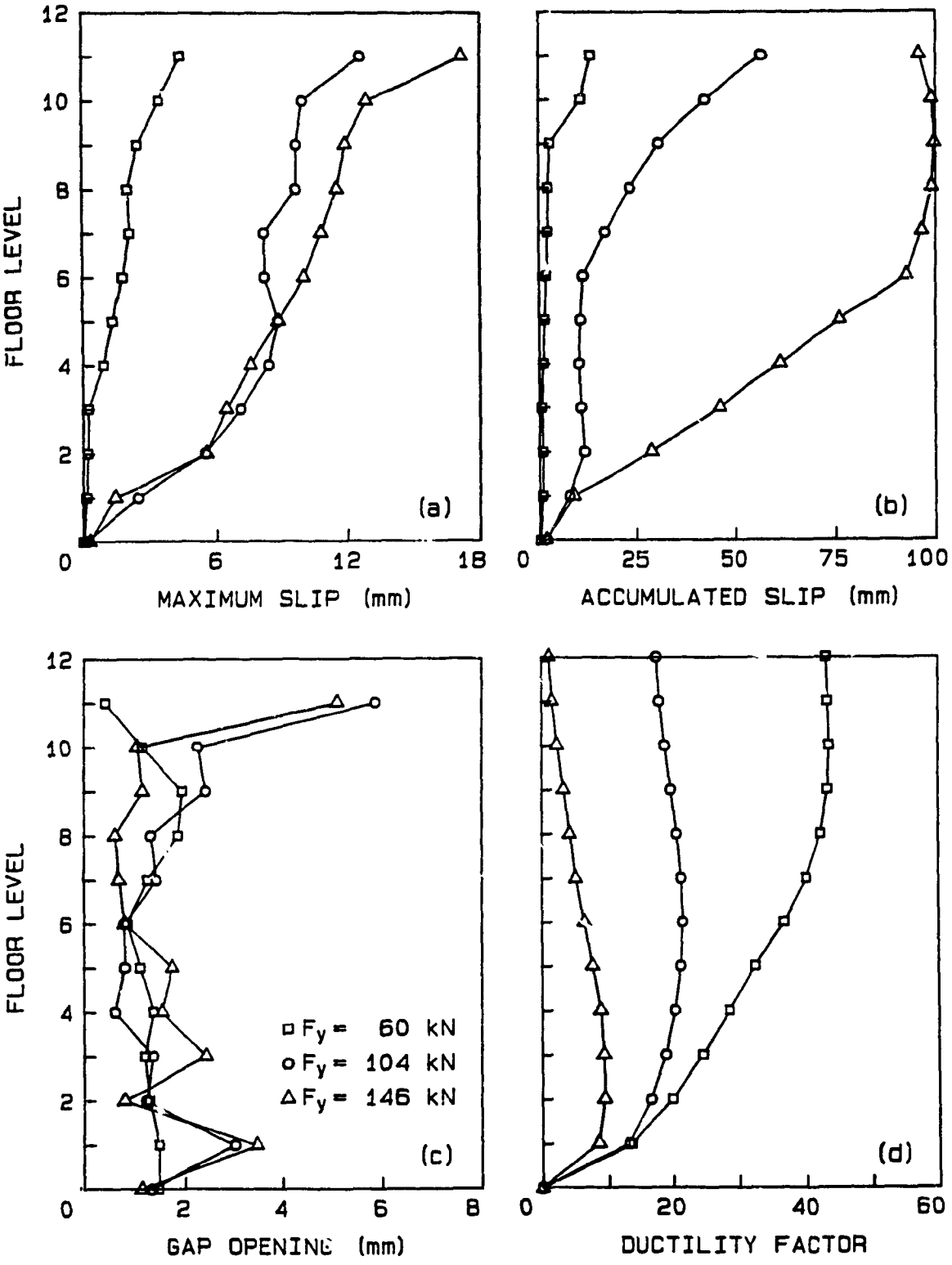

Figure 2.15 Comparison of envelopes of maximum joint response for vertical connector strength F_y = 80, 104 and 146 kN.

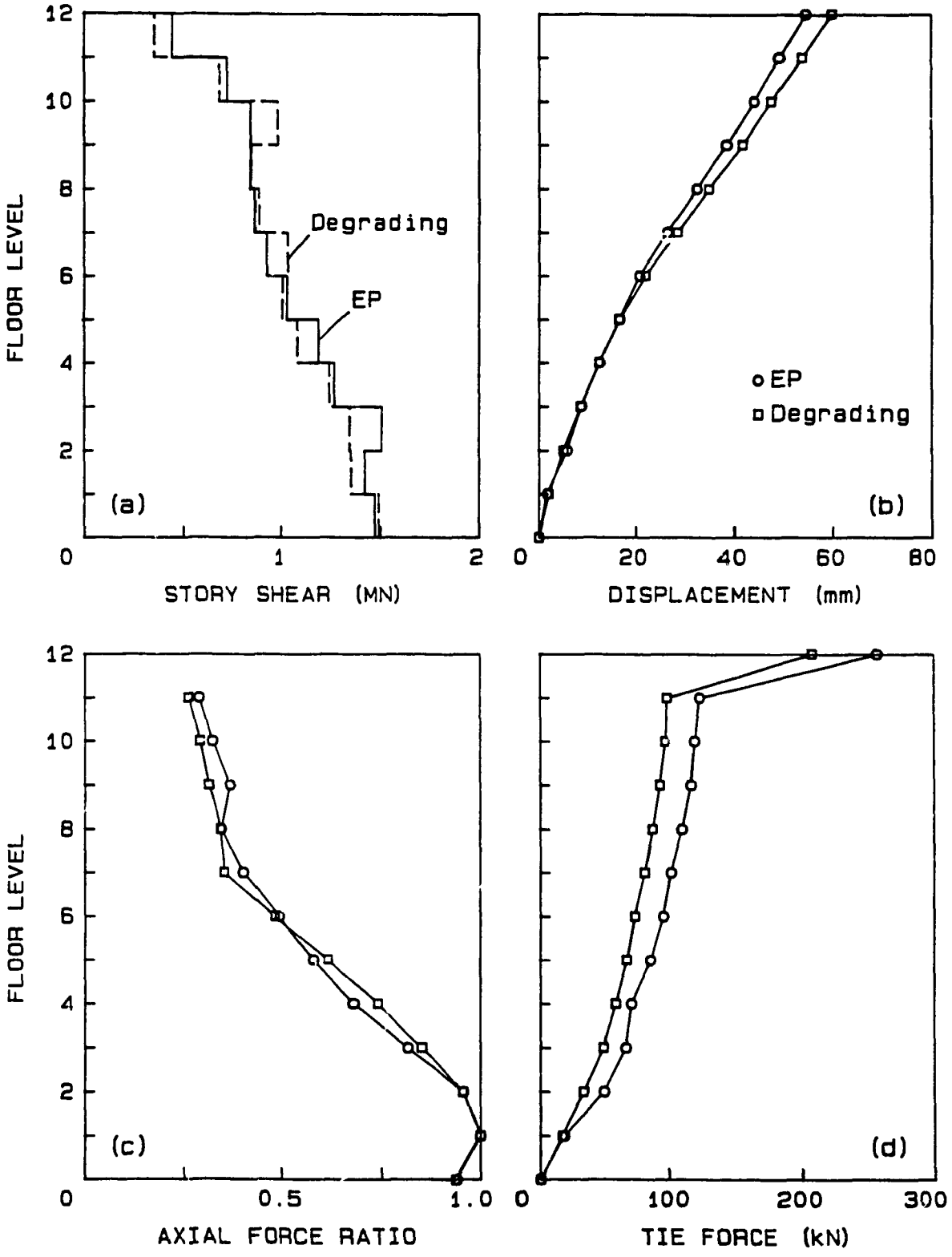

Figure 2.16 Effect of vertical connector shear behavior on envelopes of maximum overall response.

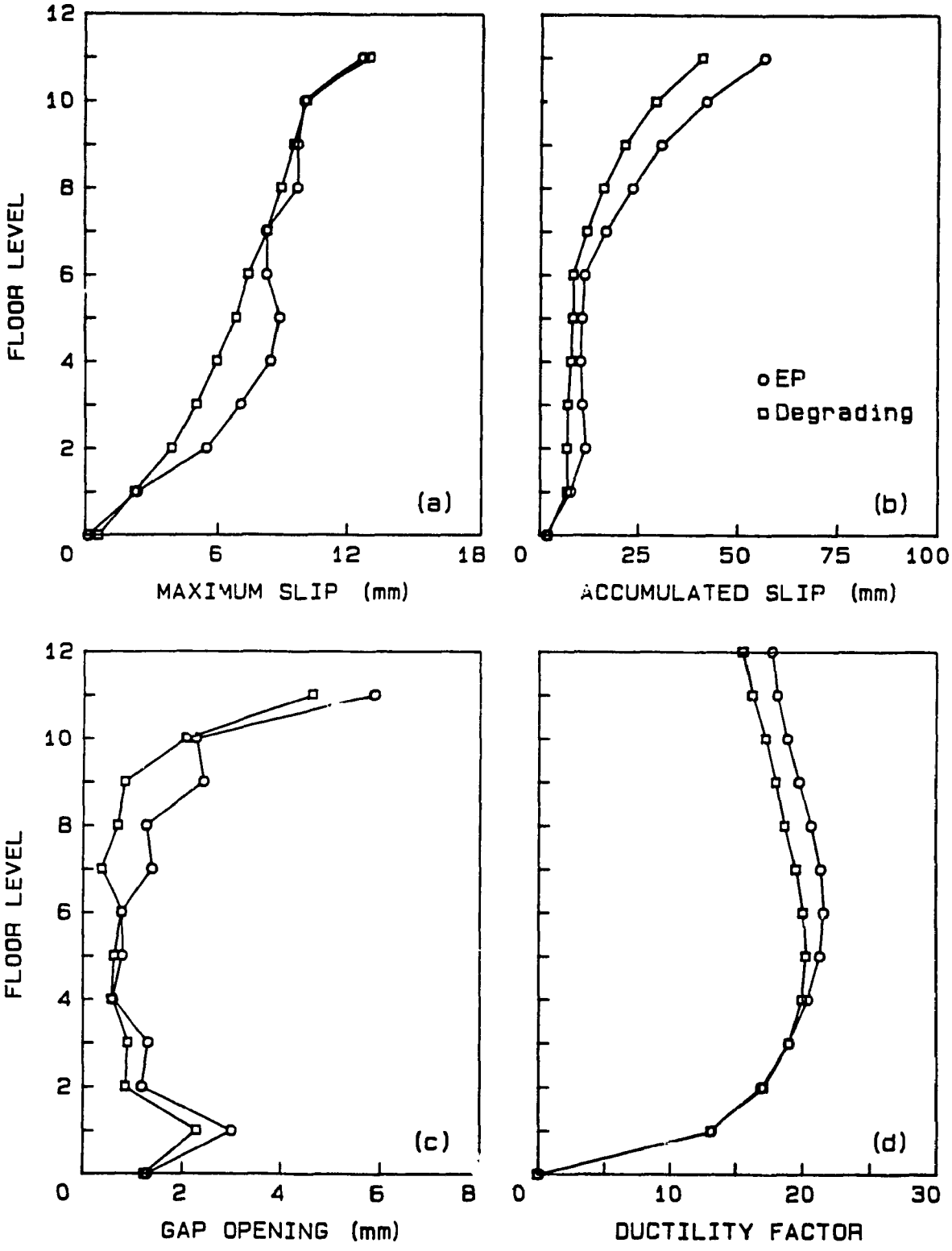

Figure 2.17 Effect of vertical connector shear behaviour on envelopes of maximum joint response.

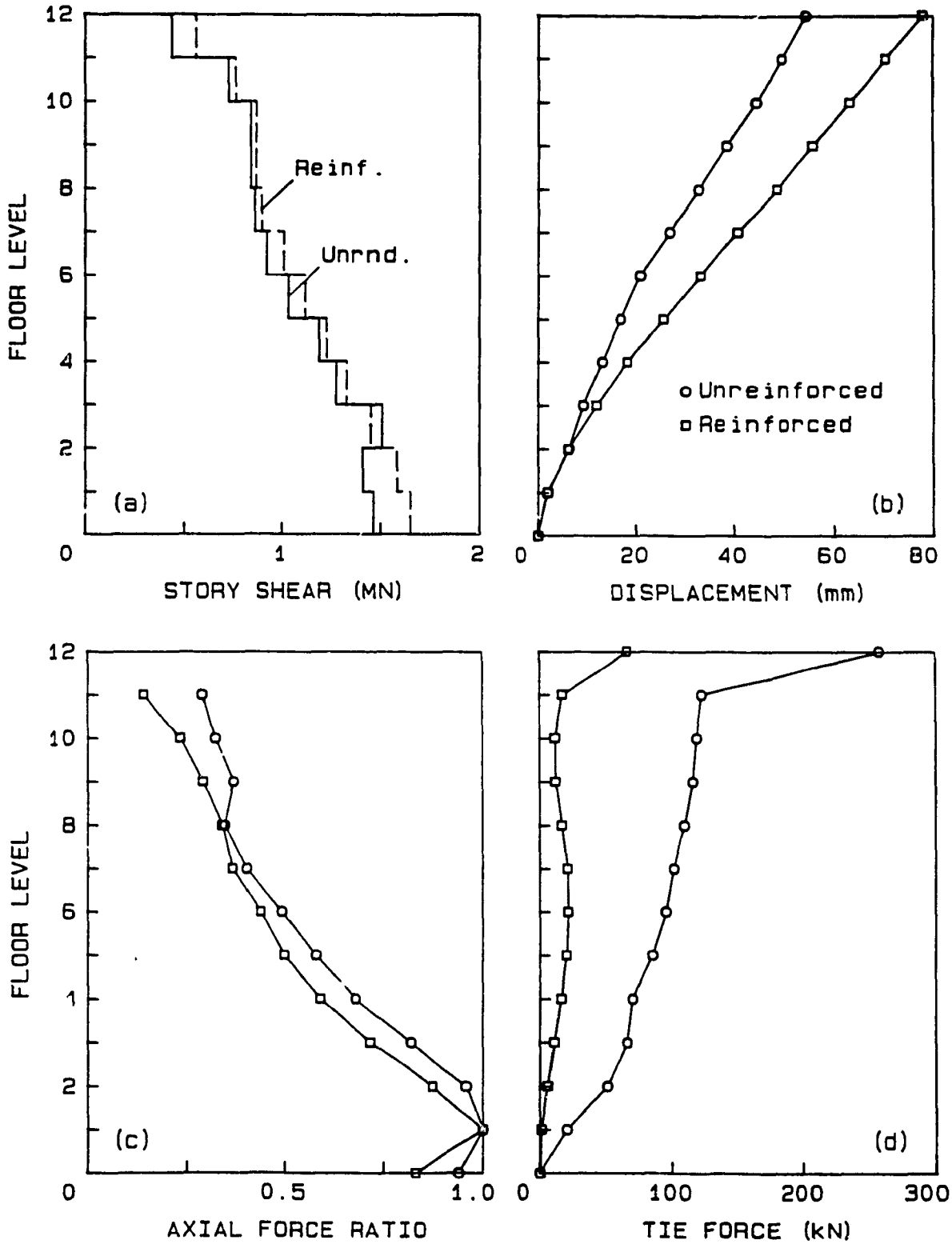

Figure 2.18 Effect of horizontal joint reinforcement on envelopes of maximum overall response.

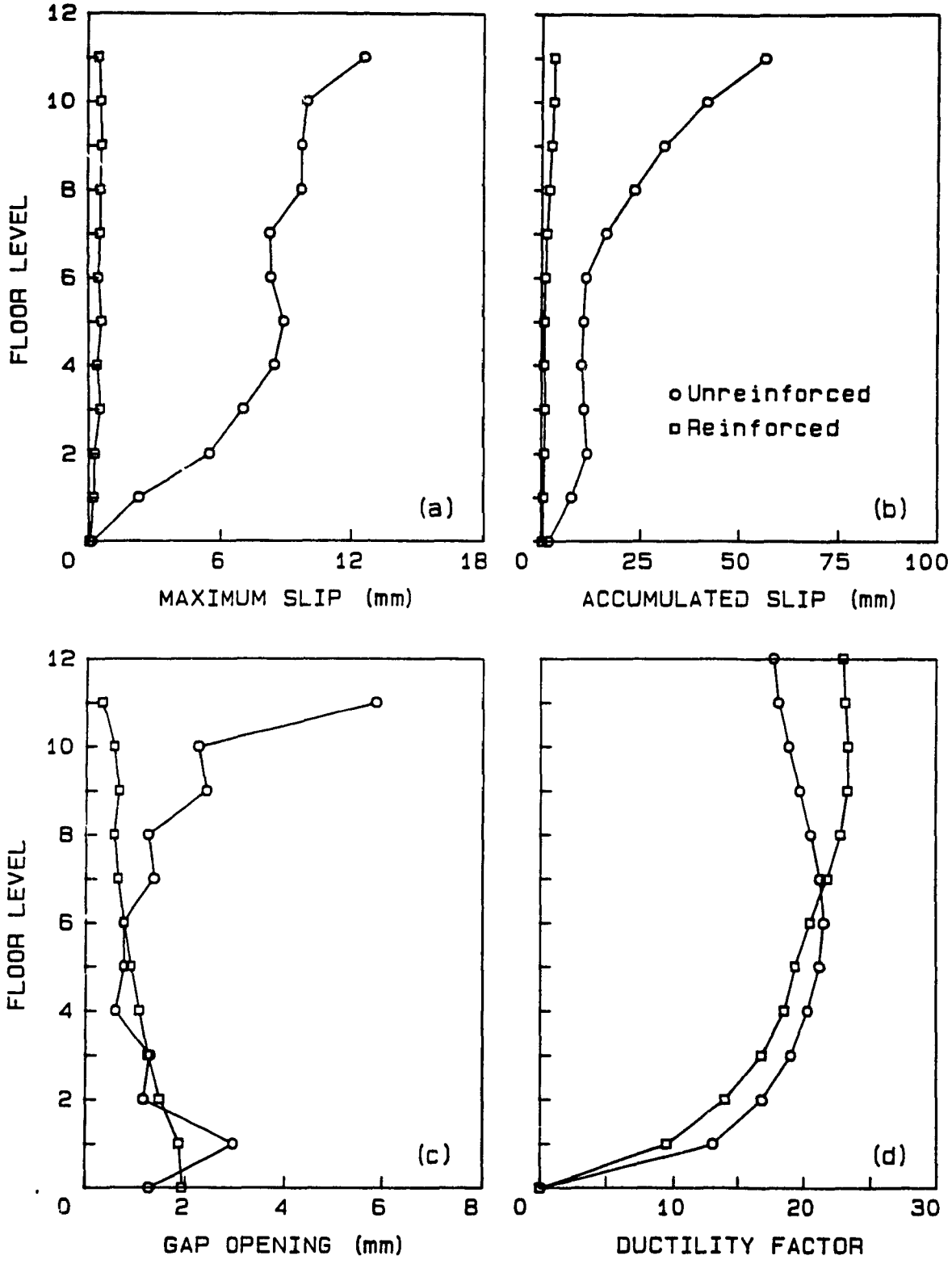

Figure 2.19 Effect of horizontal joint reinforcement on envelopes of maximum joint response.

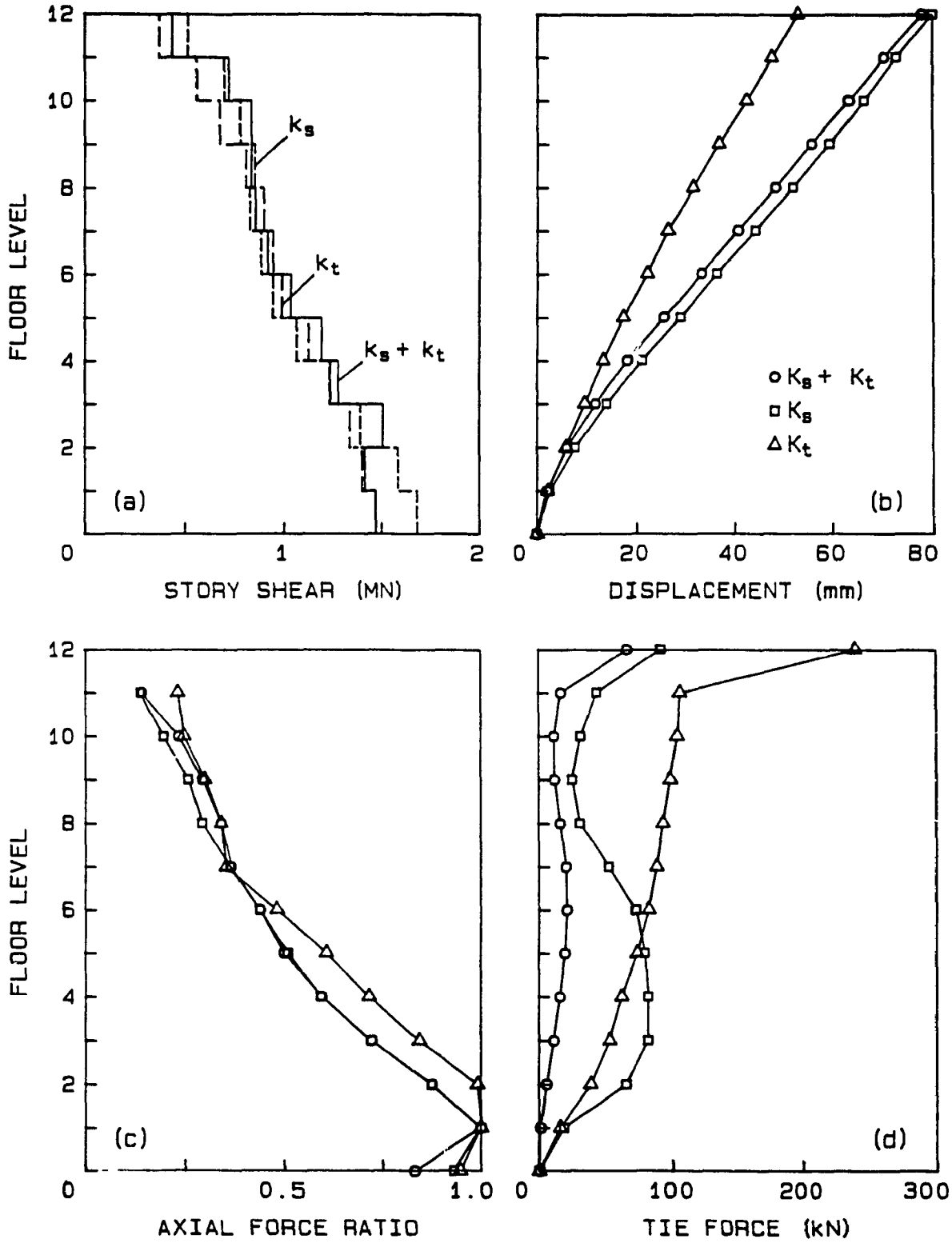

Figure 2.20 Contribution of shear and axial behaviour of horizontal joint reinforcement on envelopes of maximum overall response.

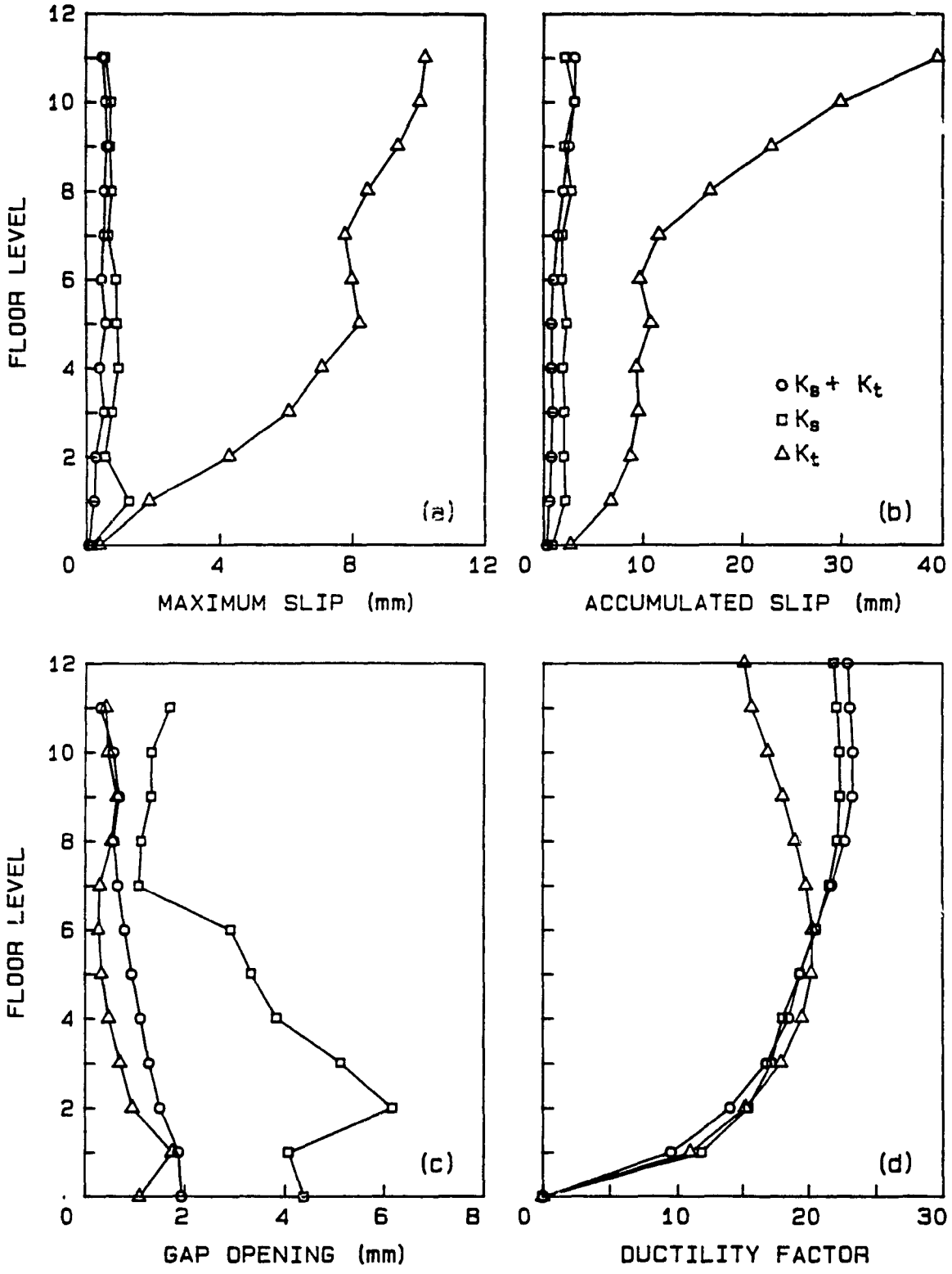

Figure 2.21 Contribution of shear and axial behaviour of horizontal joint reinforcement on envelopes of maximum joint response.

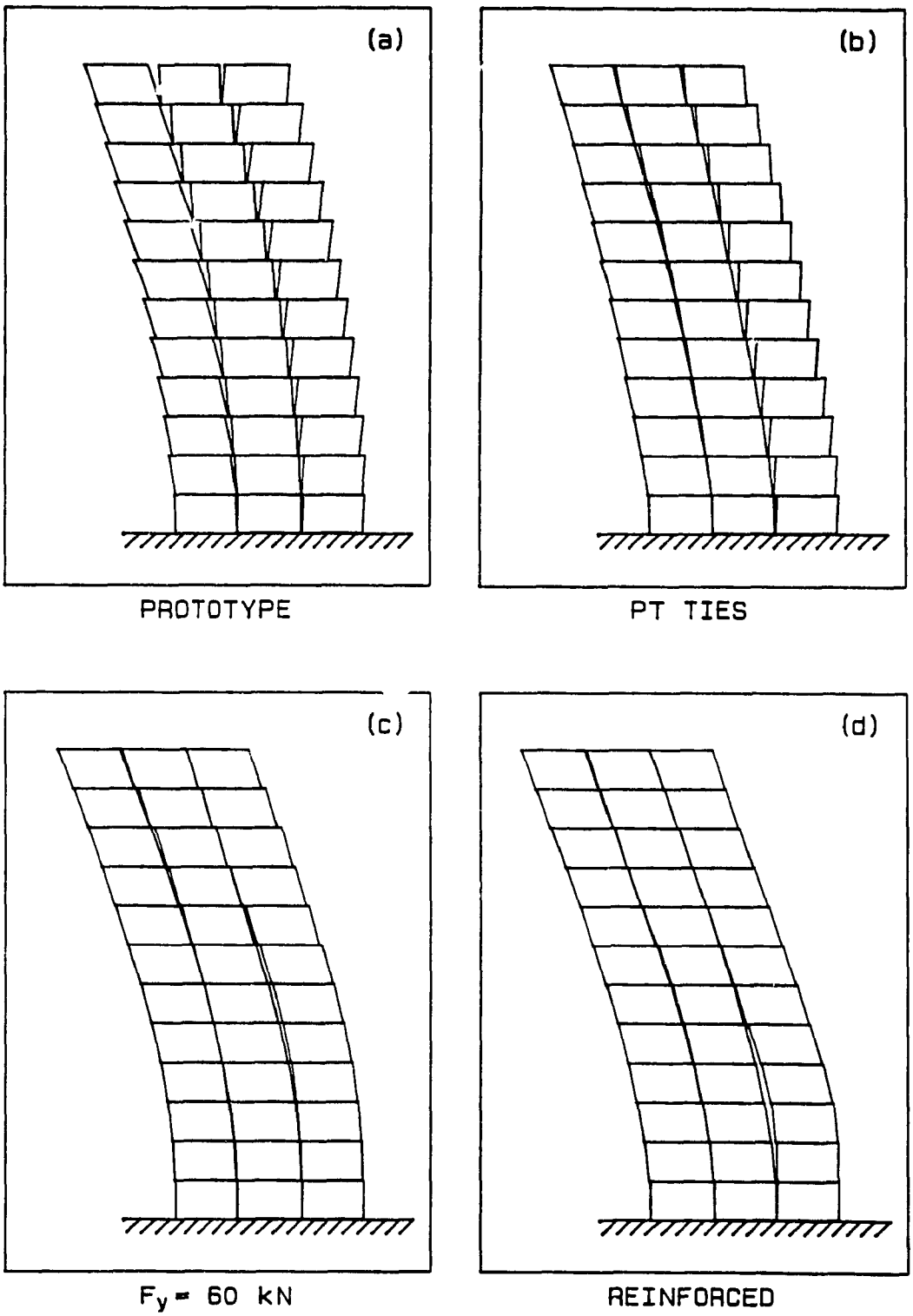

Figure 2.22 Deformed wall configurations at 2.0 seconds showing horizontal joint shear slip.

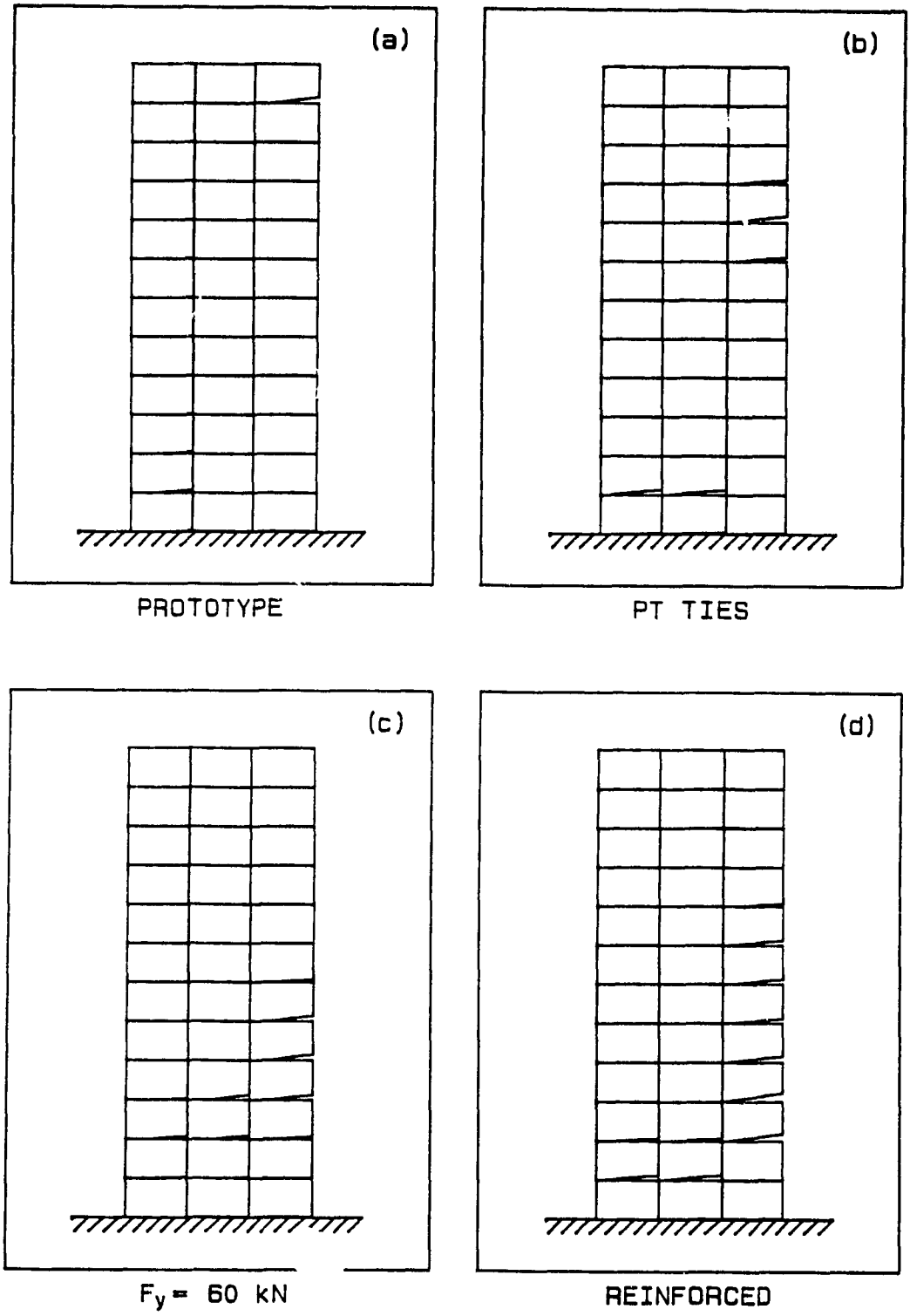

Figure 2.23 Deformed wall configurations at 2.0 seconds showing horizontal joint gap opening.

CHAPTER III

SEISMIC RESPONSE OF FRICTION JOINTED PRECAST PANEL SHEAR WALLS

3.1 INTRODUCTION

In 1980, Pall et al[13] introduced the concept of friction joints in order to improve the seismic behaviour of precast panel structures. Analytical studies were performed on coupled large panel (LP) shear walls of varying height to determine the effectiveness of employing limited slip bolted (LSB) friction-type mechanical connectors located along the vertical joints. It was demonstrated that walls coupled through such LSB connectors could be "tuned" to provide optimum response by varying the connector shear slip load. Thus, the LSB connectors were shown to act both as "safety valves" in releasing load on the vertical connections and as "dampers" to reduce the overall response of the structure.

The study assumed that the precast walls of the LP system act as two coupled continuous elastic cantilevers; hence, no horizontal joint action was considered and nonlinear behaviour in the structure was confined to the vertical joint only. Full vertical continuity was therefore assumed to exist either because of post-tensioning or due to large gravity load sufficient to prevent shear slip and gap opening in the horizontal joints. This idealized situation may not, however, often be encountered in practice since gravity load on shear walls is seldom adequate to prevent action of the horizontal joints and economic considerations may preclude the use of fully post-tensioned construction.

Shear slip and rocking, associated with such horizontal joint action, can affect the behaviour of a precast panel system considerably. Analytical studies by Becker and Llorente[6,8], Shricker and Powell[14], and Kianoush and Scanlon[17] confirmed the influence of horizontal joint action on seismic response, while experimental work conducted by Oliva and Sharooz[4] as well as Harris and Caccese[5] also revealed the importance of the energy absorbing mechanism related to the horizontal joints.

In an attempt to develop a more realistic approach toward the anticipated behaviour of precast shear walls equipped with LSB connectors, the present study examines the importance of action in the horizontal joints. Rather than modelling the precast shear wall as two continuous cantilever walls coupled along the vertical joint by LSB connectors, wet platform-type horizontal joints commonly used in North American LP practice are incorporated and assigned properties based on available experimental data. In place of the simplified wide-column frame analogy of Ref. 13, a finite element idealization of the structure is employed. The latter comprises: (1) panel elements possessing linear elastic behaviour; (2) horizontal joint elements exhibiting gap opening and shear slip; and (3) limited slip bolted (LSB) connectors along the vertical joints acting primarily in shear.

3.2 PROTOTYPE STRUCTURE

The prototype wall chosen for this study consists of one of the end walls of a typical 10-story precast LP building of the crosswall type, for which the plan layout is shown Fig. 3.1(a). The greater

lateral stiffness of the end walls, as compared to the interior walls which generally carry higher gravity loads, warrants the former's selection for study in view of the severe lateral forces attracted during seismic activity. As well, whereas the two halves of each end wall are coupled along the vertical joint by employing two LSB connectors per story height, only one LSB connector would be used for the interior walls to couple the connecting lintel.

Fig. 3.1(b) shows the end wall prototype. Dimensions and loading follow the original model developed by Pall et al[13], with minor changes due to the revised nature of the model. Each individual panel measures 2.45 m in height and 7.30 m in width. Allowing for a 200 mm thickness of the horizontal joints, each story attains a height of 2.65 m, for a total height of 26.50 m. The individual walls of 7.30 m width are coupled at the vertical joint; the resulting gap is not generally greater than 30 mm, and thus a total wall width of 14.60 m is assumed. A uniformly distributed gravity load of 22 kN per meter width of wall is assigned to each level, including the roof. The contribution due to the panel self-weight adds an additional 11.6 kN/m at each floor level, and 5.8 kN/m at the roof. This corresponds to a total gravity load of 490 kN at all floor levels, and 406 kN at the roof. Whereas the vertical masses correspond to these gravity loads, the mass associated with lateral motion is considerably higher, at 128 metric tons (128,000 kg) per story. Table 3.1(a) summarizes the wall's properties and loading.

Two types of horizontal joints are employed in this study. To model the continuous walls of the previous study[13] which allowed no horizontal joint action, the strong Type A "open" joints shown in Fig.

3.2(a) are adopted; gap opening and shear slip are assumed to be prevented by vertical post-tensioning bars. Weaker platform, or "American", Type B horizontal joints are used in the model allowing nonlinear behaviour of the joints, as illustrated in Fig. 3.2(b); a composite strength of 14.5 MPa and elastic modulus of 13,800 MPa are assumed, based on CPCI[21] design formulae and data as well as on the results of tests of full-scale horizontal joints by Harris and Iyengar[20]. Vertical reinforcement through the horizontal joints equal to 0.5 per cent of the gross cross-sectional area of the joint is provided in this Type B prototype LP wall. Detailing allows for shear slip and gap opening to occur. A total thickness of 200 mm, which includes the hollow core floor slabs, grout, and bearing pads, is allowed for the horizontal joints.

The vertical joint between wall panels comprises LSB mechanical connectors, provided two per panel at the edges; Fig. 3.2(c) illustrates the basic components of these connectors, which are described in greater detail in Reference (13). Each connector consists of a steel plate with slotted holes that is bolted on-site to inserts anchored into the concrete panels. The slotted bolt holes allow for normal fabrication and erection tolerances as well as clearance for the expected slip. Brake lining pads are inserted between the steel connecting plates and the inserts, assuming tight clean mill scale surface treatment. Two A325 M22 bolts and two 155 mm long, 19.1 mm diameter headed stud anchors are employed per side for the prototype LSB connectors of the Type B structure.

Depending on the level of pre-stress of the bolts, the LSB connectors allow for a variable shear slip resistance, the "so-called"

slip load F_{sb}, and an ultimate shear capacity of 254 kN if bearing occurs following slip[37]. However, the elastic shear strength of the anchorage in the prototype connection is only 160 kN[21,22] and, thus, while yielding of the anchor studs is avoided at the anticipated optimum slip load (F_{sb} = 80 kN), anchorage yielding would occur prior to shear failure of the bolts. The pullout capacity of the stud anchors is 325 kN[21]; however, the tensile capacity of the connector is governed by the shear capacity of the bolts and is thus equal to 254 kN also.

As Fig. 3.2(c) demonstrates, the LSB connector allows slip to occur only in the vertical direction, with rotation prevented by welding one side of the plate to the insert.

3.3 STRUCTURAL IDEALIZATION

The analysis of the prototype wall is accomplished through a finite element representation of the coupled wall structure. The earlier study[13] employed a simplified approach toward modelling the structure by idealizing the coupled walls as an equivalent wide column frame, coupled by modified truss elements to represent the LSB connectors. However, with the introduction of horizontal joint action, the wide column analogy can no longer be employed. Instead, the panels are modelled as an assemblage of linear elastic plane-stress finite elements, and discrete two-node four-degree-of-freedom orthogonal spring elements are used to model both the continuous horizontal joints and the LSB vertical joint connectors. The elements are defined across the interpanel joints using the plane-stress element nodes, and possess properties in both the normal

and shear directions. Nonlinear, inelastic action and coupled shear-axial behaviour is possible. For the Type A horizontal joints, rigid material behaviour is assumed for the joint elements in both the normal and shear directions. A single spring element suffices to model the behaviour of each LSB connection, whereas five such elements are used to approximate the behaviour of each continuous horizontal joint between panels.

3.4 IDEALIZED BEHAVIOUR OF HORIZONTAL AND VERTICAL JOINTS

3.4.1 Horizontal Joint Axial Behaviour

Fig. 3.3(a) shows the force-displacement relationship assumed for behaviour normal to the horizontal joints and intended to model the expected behaviour of platform type, or "American", continuous joints (Type B). The trilinear curve is a simplification over that obtained from a stress-strain equation for concrete proposed by Desayi and Krishan[25], based upon the concrete strength f'_c and elastic modulus E. Values of 14.5 MPa and 13,800 MPa for the two concrete parameters, respectively, are employed.

As shown in Fig. 3.3(a), compressive behaviour in the horizontal joints remains within the linear elastic k_1 region until displacement u_1 is reached; inelastic behaviour commences with stiffness k_2, and at displacement u_2 the joint element is assumed to have reached the ultimate strength. Region k_3, following the point u_2, is given a small, positive stiffness for reasons of numerical stability and simplicity, although the curve as proposed by Desayi and Krishan[25] actually begins to "dip" following the point u_2.

When tensile force develops in the joint element, stiffness is reduced to k_t, representing the effect of the vertical reinforcing bars crossing the joint. The magnitude of this stiffness is based upon an area of steel equal to 0.5 per cent of the gross concrete area in the joint, and an effective bar length equal to the horizontal joint thickness plus a 300 mm debonded bar length on each side of the joint. Gap opening occurs when compressive contact stress reduces to zero, occurring typically first at the panel edges. In the analysis, no yielding is assumed to take place in the vertical reinforcement.

Type A horizontal joint elements employ the same force-displacement relationship, except that high magnitudes of k_1 and u_1 are used to model rigid behaviour.

3.4.2 Horizontal Joint Shear Behaviour

Based upon tests of horizontal joints[26,27,36,38], the modified elasto-plastic shear-friction model shown in Fig. 3.3(b) is used to represent shear behaviour in the horizontal joints. Elastic shear stiffness k_s is determined from the modulus of elasticity E for compression of the joint, assuming Poisson's ratio $\nu = 0.2$, and also based approximately upon the tests by Verbic and Terzic[27] of horizontal joints. Shear slip occurs in the joint when the shear force reaches the available resistance $\mu_f F_c$, where μ_f is the horizontal joint coefficient of friction and F_c is the normal compressive force at that instant; a value of 0.4 is assumed for μ_f in this study. The steel reinforcing bars, however, develop tension force once such slip commences, providing clamping action across the joint and increasing both the friction and aggregate interlock effects; the result is that

some shear resistance against further slip is restored. The stiffness k_r that develops is assigned a value equal to 0.10 of the initial shear stiffness k_s. Development of stiffness k_r in subsequent hysteretic excursions is controlled by the parameter r shown in Fig. 3.3(b), which is taken to be 0.15 based on tests. Unloading takes place with elastic stiffness k_s. For unreinforced horizontal joints, k_r is set to zero. This model for shear behaviour of the horizontal joints is based on that developed by Kianoush and Scanlon[16].

Type A horizontal joint behaviour is represented by the same model, except that both k_r and k_s are given high values, and slip of the element in shear is prevented by adding a large constant to the available shear resistance $\mu_f F_c$ at all times. Thus, rigid shear behaviour is assured.

3.4.3 Vertical Joint Axial Behaviour

Since the primary function of the LSB connectors is to dissipate seismic energy through shear slip, its behaviour normal to the vertical joint does not assume as important a role in the overall response of the structure as does its shear behaviour. The study conducted on LSB jointed walls by Pall et al[13] did not consider such stiffness in the vertical coupling elements, assigning only shear properties to the LSB connector elements. Moreover, earlier studies[32] indicate that stiffness normal to the vertical joint does not have a significant influence on the integrity of panelized systems. Nevertheless, provision of properties for the elements in this direction, however simplified, is necessary to examine fully the behaviour of the LSB connections themselves, in particular the

magnitude of pullout forces incurred in the connection anchors during seismic activity.

The elastic constitutive model shown in Fig. 3.3(c) is adopted for behaviour in the normal direction of the LSB connections, which assumes that the vertical LSB joint elements do not yield in this direction. Compressive stiffness k_c is based approximately on the stiffness of the steel connecting plates (see Fig. 3.2(c)), assuming an elastic effective plate length of 200 mm between bolt lines on each side of the connector. For the tensile stiffness k_t, a value equal to 1/4 of the compressive stiffness is employed.

3.4.4 Vertical Joint Shear Behaviour

From tests[13], the LSB connectors have been shown to follow essentially elasto-plastic hysteretic behaviour, with negligible degradation. This is accomplished with the insertion of the brake lining pads under the steel connecting plates, possessing either a mill scale or sand blasted surface. Fig. 3.3(d) depicts the shear behaviour adopted for the vertical joint elements. The LSB connections slip, or exhibit plastic behaviour, when the slip load F_{sb} is reached, prior to which the load-deformation relationship is elastic with stiffness k_s. During slip, the bolts move within the slotted holes; when the end of the slot is reached at slip distance u_b, the bolt begins to bear against the slot edge and stiffness k_b restores elastic behaviour. In the analysis, however, the possibility of bearing of the bolts is reserved for comparison only, and slot lengths are otherwise assumed to be sufficient to allow unrestricted slip.

Anchorage into the panel concrete with the headed studs is

assumed to remain elastic, with selection of studs such that the strength is adequate to prevent yielding of the anchors at force below the slip load of the connection. Thus, plastic behaviour in the connections is always associated with slipping of the bolts in the slotted holes and not yielding of the anchor studs.

Table 3.1(b) and 3.1(c) summarizes the stiffness and strength properties for the horizontal and vertical joint elements respectively.

3.5 PARAMETRIC STUDY

This study was accomplished using an expanded version of the Fortran program ANSR-I (Analysis of Nonlinear Structural Response)[34], implemented on the SUN micro-computer system in the Department of Civil Engineering, Concordia University. Subroutines for the horizontal and vertical joint elements were developed separately and attached to the main program, whereas the panel plane-stress elements utilized existing subroutines. Changes to the original prcgram were necessary to accommodate ANSR-I for the SUN computer system, and further additions include pre- and post-processing programs to allow for expanded time-history output analyses as well as extensive graphics capabilities.

Structural masses were lumped at floor levels, and distributed equally to nodes above and below the horizontal joints. Vertical mass components correspond to the applied gravity loading on the wall at each level, whereas the masses associated with lateral inertia forces were distributed to the end wall from the total building floor mass in proportion to the wall's lateral stiffness. Rayleigh damping

corresponding to 5 per cent of critical in the first and second modes was assumed. Dynamic properties for the structure, specifically the periods of vibration, were determined through a modal analysis of a similar wall model using the finite element program SAP-4[35], modified to include the joint subroutines. Mass and tangent stiffness proportional damping coefficients, derived from the first two periods, are required for the ANSR-I program to define the system damping matrix.

An integration time-step of 0.001 sec was used for the time-history analysis, employing the Newton-Raphson iterative procedure with stiffness reformation at every step as the dynamic solution scheme. Six seconds of the north-south component of the 1940 El Centro earthquake were used as the seismic input, followed by one second of relaxation, for a total of seven seconds of analysis for the prototype wall.

The results discussed below are based on the following variation of parameters:

(a) For each of the structural models (Type A and Type B horizontal joints), the slip load F_{sb} of the LSB connectors is varied. Slip loads of 0, 40, 80, 160, 320, and 640 kN are considered, with proposed design slip loads of 160 and 80 kN for the A and B systems, respectively.

(b) Comparison of response in Type B walls is examined for reinforced and unreinforced horizontal joints (i.e. with and without vertical steel), at slip load F_{sb} = 80 kN.

(c) For all cases, the slot length provided is assumed to be sufficient to prevent bearing of the bolts against the slot edges.

Restriction of the slot length in practice, however, may be unavoidable due to dimensional considerations. For the design slip load of 80 kN for the Type B wall, the effect of a restricted slot length equal to 75 per cent of the maximum required is also examined.

3.6 RESULTS AND DISCUSSION

Seismic response in the prototype wall is examined assuming both strong (rigid) Type A and nonlinear behaving horizontal joints, the latter allowing both gap opening and shear slip as well Type B as nonlinear deformation. The influence of LSB connector slip load F_{sb} on response in the walls is studied, with particular focus on the proposed design slip load of 80 kN, chosen based on results indicating optimization of the structural response in the Type B wall at this magnitude of F_{sb}. The maximum slip load of 640 kN represents a practical upper limit to the strength of the connector anchorages, when failure of the anchors cannot realistically be prevented prior to bolt slip. Moreover, the results reveal that, at F_{sb} = 640 kN, the wall is essentially an elastically coupled shear wall, as no slip in the vertical joints is observed. An isolated or uncoupled shear wall is represented by F_{sb} = 0.

Two forms of Type B horizontal joints are considered. Reinforced, Type B joints allow dowel action of the vertical steel which develops shear resistance once slip is initiated, thereby reducing the level of shear slip induced in the horizontal joints. In the unreinforced joints, on the other hand, a simple gap-friction element models behaviour, possessing no tensile stiffness across the joint but where shear resistance is based only on the normal force and

coefficient of friction μ_f.

3.6.1 Comparison of Behaviour for Types A and B Horizontal Joints

Fig. 3.4 illustrates the differences in selected structural responses for the two joints types with slip load varied over the range F_{sb} = 0 - 640 kN. Maximum values of compressive panel stress, total base shear, and top lateral displacement for seven seconds of analysis are shown.

The data demonstrate improved behaviour for Type B horizontal joints with respect to maximum panel stress and base shear, while maximum top displacement of the wall increases for Type B joints. However, lateral displacement alone is not critical, provided that accommodation of such increased displacement is possible at an acceptable level of damage to nonstructural components, and also that the displacement is not excessive so as to invite instability. With a maximum top displacement of 64 mm in the Type B walls for F_{sb} = 80 kN, the drift index (ratio of maximum top displacement to overall building height) for the 10-story building is under 1/400, and falls well within the acceptable range[39].

With the exception of panel stresses in Type B walls, significant reductions in response magnitudes are noted over both uncoupled (F_{sb} = 0) and fully coupled elastic (F_{sb} = 640 kN) walls, employing LSB connectors with appropriate slip load. Walls with Type A horizontal joints show definite optimum response at F_{sb} = 160 kN. (Although F_{sb} = 160 kN is taken herein as providing optimum response, only small changes are noted in the magnitudes of base shear and top displacement

with the use of F_{sb} = 320 kN)$^{+}$.

Type B horizontal joint behaviour, on the other hand, does not allow an as well defined optimum slip load. In contrast to Type A walls, maximum panel stress is not affected by F_{sb}, showing less than 5 per cent difference between any two values of F_{sb}. Base shear is minimized at F_{sb} = 40 kN, while top displacement is least at F_{sb} = 320 kN. A compromise choice of 80 kN is more satisfactory, reducing base shear by 35 per cent from that for elastically coupled walls and decreasing top displacement by 38 per cent from that for uncoupled walls. Thus, the LSB jointed Type B wall exhibits the best features of the two alternatives, namely a base shear 15 per cent less than the low base shear of uncoupled walls and a top displacement only 13 per cent greater than for fully coupled walls. Based on the above observations related to Fig. 3.4, it is evident that LSB jointed walls (with or without the action of horizontal joints) exhibit optimized seismic response.

Corresponding envelopes of maximum response over the height of the structure are presented in Fig. 3.5 for the same response parameters as Fig. 3.4; included also is the LSB connector slip. Presented is the response for Types A and B horizontal joints at their respective optimum slip loads, i.e. F_{sb} = 160 kN and 80 kN, respectively. As predicted by the peak response values of Fig. 3.4, the Type B jointed walls show considerably improved behaviour in terms of story shears at all levels (Fig. 3.5(a)), although this is accompanied by the increased lateral displacements of Fig. 3.5(b). Maximum panel stresses are quite similar in magnitude except at the base, as seen in Fig. 3.5(c). As expected for cantilever structures,

these stresses increase down the structure but are noted to remain well below the panel compressive strength f'_c = 34 MPa, thus confirming the validity of assuming elastic behaviour of the panels. For Type B behaviour, the horizontal joint compressive strength f'_c = 14.5 Mpa limits the stress in the panels, and the lowermost level shows that the strength of the Type B joints is indeed reached.

Considerably higher magnitudes of LSB connector shear slip over the wall height are shown in Fig. 3.5(d) for Type B walls, indicating a maximum slip of 20 mm in the uppermost connector. However, since the friction-type LSB connectors are designed to slip without yielding of materials, greater slip permits higher levels of energy dissipation in the vertical joint without accompanying permanent damage. In both wall types, this process is seen to act over most of the wall height. Detailing of the vertical joint to accommodate the differential movement of the walls, and the provision of a slot length sufficient to permit unrestrained bolt slip, ensure efficient LSB connector action.

Table 3.2 summarizes peak dynamic magnitudes of response for Types A and B horizontal joints.

3.6.2 Effect of Vertical Reinforcement in Type B Joints

Type B horizontal joints have thus far been assumed to contain vertical reinforcement sufficient to develop dowel action and thus restrict shear slip in the joints. The influence of such reinforcement is now examined by comparing the behaviour of the Type B prototype structure with and without vertical steel.

Comparison of structural response for Type A horizontal joints

and unreinforced, Type B horizontal joints is shown in Fig. 3.6, for F_{sb} = 160 kN and 80 kN, respectively. As for reinforced Type B horizontal joints, story shears exhibit large reductions over the height of the wall when unreinforced Type B horizontal joints are used; Fig. 3.6(a) shows a reduction in maximum base shear of over 50 per cent. Whereas Fig. 3.5(c) showed similar panel stresses associated with Type A and reinforced Type B horizontal joint behaviour, Fig. 3.6(c) indicates that panel stresses are substantially reduced if vertical reinforcement is not employed.

Instead of the increase in lateral displacements for reinforced Type B walls observed in Fig. 3.5(b), unreinforced horizontal joints reduce displacements to the same level as for Type A walls as evident in Fig. 3.6(b). The most dramatic effect of lack of vertical steel, however, is shown in Fig. 3.6(d), which shows that slip in the LSB vertical joint connectors is nearly eliminated, with less than 3 mm of slip at all levels.

Fig. 3.7 compares the responses of the two Type B horizontal joints (reinforced and unreinforced), for F_{sb} = 80 kN. While differences in shear are significant at all storeys, panel stresses are noticeably reduced when no reinforcement is employed. The displacement profile shown in Fig. 3.7(b) for the unreinforced case reflects the fact that shear slip is the principal cause of lateral deflection, as opposed to the reinforced wall where flexural deformation dominates.

The above-implied increase in horizontal joint slip for unreinforced, Type B joints is evident in Figs. 3.8(a) and 3.8(b), where envelopes of maximum slip and accumulated slip in the horizontal

joints are presented. While less than 1 mm of maximum slip is noted at all levels for the reinforced wall, maximum slip of 3 - 5 mm is incurred from levels 1 to 7 in the unreinforced wall, peaking at 11 mm at the uppermost level. Similar increases are observed for accumulated slip, measuring the amount of energy dissipated by this mechanism.

Although the increase in slip is more dramatic in the uppermost horizontal joint, story shears are higher near the base and thus energy dissipation as a result of horizontal joint slippage assumes greater significance at the lower levels. Accumulated slip for unreinforced walls is 300 - 400 per cent greater at levels 1 - 3 than for fully reinforced walls. The apparent conflict between the lack of energy dissipation due to virtual elimination of vertical joint slip as noted in Fig. 3.7(d) and the observation that overall structural responses such as story shears and panel stresses are nonetheless improved upon (Figs. 3.7(a) and 3.7(c)) is thus resolved by the foregoing compensation in energy absorption in the horizontal joints.

Although effective and therefore attractive, allowing large slip in the horizontal joints to increase seismic energy dissipation, as opposed to vertical joint slip, introduces a number of problems, however. Panelized wall systems, in particular those employing platform-type horizontal joints, are apt to suffer permanent damage as a direct consequence of the large magnitude of slip in these joints. Elastic corrective forces which would otherwise restore the wall to its original position following vertical joint slip are not available during lateral panel slippage; in addition, the in-plane slip of the horizontal joints is liable to cause out-of-plane displacement of the

wall panels. Tests by Mattock[26] have shown that cyclic loading at large amplitude of slip precipitates deterioration of the joint interfaces; thus, the subsequent loss of joint shear strength can seriously compromise both the serviceability and integrity of LP walls. The analyses performed herein showed only 6 load reversals in shear across the level 1 reinforced horizontal joint, whereas over 18 cycles were noted in the unreinforced joint. Combined with the larger amplitude of slip, degradation of the horizontal joints is therefore substantially more pronounced in the unreinforced walls.

Envelopes of gap opening in the horizontal joints are shown in Fig. 3.8(c), indicating significantly higher values for reinforced Type B horizontal joints than for unreinforced Type B joints. Magnitudes of joint opening are under 0.6 mm at all levels for the unreinforced wall, whereas a maximum of 4.2 mm at the base is observed for the reinforced wall. Experimental tests[4] have shown that forces in panelized wall systems can be reduced by such horizontal joint opening, through a base isolation effect even though accompanied by very little energy dissipation. The high level of gap opening for the reinforced wall thus contributes to the reduction in storey shears shown in Fig. 3.5(a) where the continuous, rigidly jointed Type A wall without joint opening experiences higher magnitudes of induced force.

Comparisons of peak response in the reinforced and unreinforced Type B walls are shown in Table 3.2.

3.6.3 Bolt Bearing and Tensile Loads in LSB Connectors

Fig. 3.5(d) and Table 3.2 indicate a maximum slip of 20 mm in the LSB connectors for Type B behaviour at F_{sh} = 80 kN, and thus a slot

length of 65 mm (for M22 bolts) is sufficient to accommodate the expected shear slip. The effect of limiting the slip distance in the connectors and consequently permitting bearing of the bolts is shown in Fig. 3.9, where a maximum slip length of 15 mm, or 75 per cent of the expected unrestricted maximum, is imposed on the LSB connectors.

Although data are not presented herein, overall response due to such limited slip was noted not to be adversely affected; only story shears and horizontal joint slip exhibit noticeable changes. Figs. 3.9(a) and 3.9(b) show base shear to increase by 17 per cent, and base slip to increase by 64 per cent. The direct effect of the limited slot length is, of course, to limit the slip in the connectors to 15 mm, as Fig. 3.9(c) shows; this maximum slip is reached from levels 5 to 10, where bearing of the bolts against the slot edges occurs. The expected result is a dramatic increase in the shear load on the LSB connectors, as the design slip load of 80 kN is exceeded. Fig. 3.9(d) shows load levels above 160 kN, the yield strength of the connector anchorages, at all levels where bearing occurs, and permanent damage to the vertical joint due to yielding is to be expected.

Supplying more and/or larger stud anchors, with shear strength greater than 220 kN, avoids material yielding when bearing occurs. However, the results obtained herein assume unlimited elastic strength of the anchors. As Fig. 3.9(d) shows, the shear load, which would otherwise be limited to 160 kN if the LSB connector anchorages yield, is approximately 210 kN at levels 6 and 7, but below the 254 kN shear strength of the two M22 bolts provided. The predicted yielding of the anchorage prior to shear failure of the bolts is a desirable feature since the otherwise sequential "unbuttoning" along the vertical joint

accompanying bolt failure would invite the increased response associated with vertically uncoupled walls. Table 3.2 shows relative responses for the bearing and non-bearing cases for reinforced, Type B walls.

The tensile capacity of the LSB connectors is also governed by failure in shear of the two M22 bolts provided, which at 254 kN is less than the concrete pullout capacity of 325 kN for the anchor studs. Fig. 3.10(a) shows maximum tensile force in the connectors incurred for differing slip load F_{sb}. Whereas vertically continuous Type A walls exhibit zero tensile forces, it is evident that the connector tensile capacity becomes an important design consideration for precast walls with Type B horizontal joints. For the optimum slip load F_{sb} = 80 kN, Fig. 3.10(b) shows that accidental bearing in the LSB connectors results in only slight increase in the tensile loads on the connectors. Equally important, the tensile loads incurred in the LSB connectors are well below the failure strength at all levels. The peak tensile load, induced in the uppermost connector, is observed to be 65 per cent of the failure capacity of 254kN.

3.6.4 Overall Structural Integrity

Structural integrity of precast walls is important to their serviceability and stability following seismic loading. Control of overall structural responses such as panel stresses and lateral shear forces, ensure against collapse of the building; however, minimizing damage to the panel joints is equally important when considering future performance of the structure. The use of LSB connectors is an immediate advantage in this regard, as deformation in the vertical

joint is controlled and material yielding is avoided. Damage to the horizontal joints is consequently the remaining principal factor affecting the structural integrity of panelized walls.

The time histories of top displacement for Types A and B (reinforced) walls, shown in Fig. 3.11(a), indicate higher amplitude of vibration for Type B walls, with maximum response occurring at approximately 2 seconds (thus confirming use of 7 seconds of excitation as appropriate). Drift in displacement, an indication of potential instability during the seismic loading, is absent. In both cases, the walls are seen to return almost to the original position, and no permanent set which may harm future performance of the walls is observed. The time histories of base shear, shown in Fig. 3.11(b), reveal similar trends in behaviour.

Fig. 3.12 shows the time histories of both the LSB connector shear slip and force at the uppermost level for both wall types. Although a maximum slip of 20 mm is observed for the Type B structure, with at least 8 reversals in slip displacement, damage to the vertical joint is controlled by the design of the LSB connectors. By allowing slip at the predetermined load F_{sb}, a ceiling on the maximum shear load on the connectors is imposed, so that this a priori knowledge allows anchorages to be designed not to yield before bolt slip occurs. Fig. 3.12(b) shows that the respective slip loads of 160 kN and 80 kN are not exceeded, although some residual forces remain at the end of the earthquake. However, as indicated by Pall[13], such residual forces do not affect the future performance of the LSB connectors.

Fig. 3.13 presents graphically exaggerated deformed shapes of the coupled walls for the three cases of horizontal joints considered:

namely, Type A (F_{sb} = 160 kN); reinforced Type B (F_{sb} = 80 kN); and Type B unreinforced (F_{sb} = 80 kN). For comparison purposes, times corresponding to the representations are not identical for the three cases but are, instead, selected based on the times when maximum absolute lateral displacements of the three structures are reached.

Fig. 3.13(a) illustrates the continuous nature of the Type A walls, with the predominant deformation limited to the vertical joint. Integrity of the wall is excellent here, as elastic corrective forces in the panels correct the slip in the vertical plane following the earthquake, with no resulting damage. Fig. 3.13(b) shows the dominant role played by the rocking response mechanism which led to the large reduction in story shears noted earlier for Type B reinforced walls. Also evident is the increased shear slip in the LSB connectors, indicating the enhanced level of energy dissipation along the vertical joint.

Fig. 3.13(c), depicting the deformation of the unreinforced Type B wall, confirms that the lateral displacements are caused primarily by shear slip in the horizontal joints. With negligible vertical joint shear, energy dissipation is thus confined to the horizontal joints. However, as noted previously, large accumulated slip accompanied by an increased number of load reversals compared to reinforced Type B walls, invites deterioration of these joints and thus compromises the structural integrity of this system.

Fig. 3.14 depicts the deformed shapes of the coupled walls for the three cases at 6.75 seconds, or 0.75 seconds following termination of the earthquake excitation. As shown in Fig. 3.14(a), elastic corrective forces in the wall panels are sufficient to return the Type

A jointed wall to what is essentially its original undeformed shape; only a slight permanent displacement along the vertical joint is observed, approximately 2 mm at the topmost LSB connector (see Fig. 3.12 (a) for time history). The residual lateral displacement of the wall is negligible.

The reinforced type B jointed wall allows for a similar final shape, with the LSB connectors returning almost to their original positions also (Fig. 3.14(b)). As also the for the Type A wall, this is in contrast to various times during the earthquake when slip in the mechanical connectors can be considerable (as in Figs. 3.13(a) and 3.13(b)). Thus the effectiveness of the LSB connectors to dissipate energy through inelastic joint action, while not incurring damage and at the same time allowing the joint to return almost to its original position, becomes apparent. However, unlike the strong Type A jointed wall, Fig. 3.14(b) also shows that the weaker inelastic joints of the Type B wall exhibit some residual compressive deformation at the lowermost level. This deformation is the expected result of rocking and is therefore a localized effect; it is confined to the two edges of the wall at the base and thus does not imply distress of the joint as a whole. Furthermore, for F_{sb} = 80 kN the maximum compressive deformation is only 48 and 36 per cent, respectively, compared to that for uncoupled (F_{sb} = 0) and elastically coupled (F_{sb} = 640 kN) walls. Thus, while some damage is to be expected in the lowermost horizontal joint, the reduced level is not expected to affect seriously the otherwise enhanced structural integrity of the "tuned" type B wall.

Fig. 3.14(c), representing the final deformed shape of the unreinforced Type B jointed wall, shows no permanent vertical joint

deformation which is as expected, since virtually no slip occurs there. However, relatively large permanent horizontal joint slip is noted at nearly all floor levels, with the most pronounced residual deformation induced at the top of the structure.

3.7 DESIGN IMPLICATIONS

The earthquake performance of three different types of 10-storey prototype precast panel structures equipped with LSB mechanical connectors along the vertical joint to improve seismic response has been studied, namely: (1) Type A - no horizontal joint action; (2) Reinforced Type B - includes action of vertically reinforced platform horizontal joints; and (3) Unreinforced Type B - no vertical reinforcing in the platform joints. Based on the foregoing discussion of the results, the following observations related to the seismic design of such friction-jointed precast structures are noted:

1. For precast walls which are fully post-tensioned and possess strong open (Type A) horizontal joints, limited-slip bolted (LSB) connections optimize response effectively at a relatively well-defined optimum slip load (F_{sb} = 160 kN for the prototype structure).

2. For walls with weaker but vertically reinforced platform (Type B) joints, on the other hand, the optimum slip load is less well defined and depends on the particular response parameter. Nevertheless, the structure can still be "tuned" to provide overall optimum response at a connector slip load less than for Type A joints (F_{sb} = 80 kN for the prototype structure).

3. Over the full range of LSB connector slip load examined, considerably lower panel stresses and story shears are noted for Type

B jointed walls, although these are accompanied by larger (but easily acceptable) displacements.

4. Unreinforced Type B horizontal joints exhibit large energy absorption capacity through shear slip, thus eliminating both the effectiveness and need for LSB connections along the vertical joints. Dramatic reductions in story shears, panel stresses and gap opening arise from this source of energy dissipation. As expected, however, these are accompanied by relatively large increases in maximum and accumulated slip, as well as the number of slip reversals.

5. A design slot length of 65 mm is adequate for both Type A and B horizontally jointed structures. Inadequate length resulting in bearing of the bolts against the connector plates has no major effect on overall response in general. The primary effects are large-relative increases in horizontal shear slip in the lowermost joints and, most importantly, a dramatic increase in the load on the LSB connectors. The latter is sufficient to indicate yielding of the prototype connector anchorages but failure of the LSB connector bolts is not anticipated. Based on the data presented, anchorage and bolt-shear capacities should be designed for approximately three times the optimum slip load F_{sb} to prevent these modes of failure if the required slot length is not provided.

6. In terms of structural integrity, both during and following the earthquake, Type A jointed walls are characterized by excellent performance, returning to the undeformed configuration with virtually no permanent deformation. Reinforced Type B jointed walls show pronounced rocking at the time of peak response and some permanent, though not large, deformation along the vertical joint. By

comparison, unreinforced Type B jointed walls respond primarily in non-corrective horizontal shear slip, with insignificant participation of the vertical joint connectors.

7. The tensile capacity of the LSB connectors is also an important design consideration. For a "tuned" structure this capacity will generally be governed by the shear strength of the LSB connector bolts when headed stud anchors are employed. Here also, three times the optimum LSB slip load will avoid this mode of failure.

Whereas the preceding observations have been obtained from an investigation wherein it was attempted to model the precast system in a realistic manner, it nevertheless needs to be remembered that the numerical results are applicable only to 10-storey structures of similar properties. Actual design recommendations must await additional studies of structures possessing different characteristics.

3.8 CONCLUSION

The results of this study indicate that limited-slip bolted (LSB) connectors placed along the vertical joints of precast large panel structures are an effective means of improving seismic response. First demonstrated in Reference (13) for idealized structures, the study has shown that such friction joints can have equally positive effect on more realistic models of precast structures. While the present study has considered only 10-storey prototype structures, the idealized cases of Reference 1 encompass the range of 5 - 20 stories, thus predicting optimization of seismic response for the more realistic horizontally jointed structures of the present study over this range also.

Since a more direct procedure is not available, inelastic dynamic analysis such as employed herein can be used to determine the LSB connector slip load which is required to obtain optimum response. As noted in Reference (13), and also supported by results generated during the current study but not presented herein, the optimum connector slip load is relatively independent of the seismic excitation itself. Thus, a single earthquake record suffices in this procedure to optimize the design of friction-jointed precast structures.

TABLE 3.1 - Properties of prototype walls.

Description			Value
(a) Panels and loading			
Panel thickness (mm)			200
Modulus of elasticity (MPa)			29.2×10^3
Poisson's ratio			0.15
Compressive strength (MPa)			34
Gravity load/story (kN)			490
Tributary story mass (kg)			128×10^3
(b) Type B horizontal joints			
Thickness (mm)			200
Modulus of elasticity (MPa)			13.8×10^3
Compressive strength (MPa)			14.5
Axial parameters:	k_1	(kN/mm/mm)	13.15
	k_2	(kN/mm/mm)	2.39
	k_3	(kN/mm/mm)	0.001
	k_t	(kN/mm/mm)	0.25
	u_1	(mm)	0.176
	u_2	(mm)	0.420
Shear parameters:	k_s	(kN/mm/mm)	5.75
	k_r		0.575
	r		0.15
	μ_f		0.40
(c) Vertical joint LSB connectors			
Axial stiffnesses:	k_c	(kN/mm)	1950
	k_t	(kN/mm)	490
Shear stiffnesses:	k_s	(kN/mm)	640
	k_b	(kN/mm)	320

Note: See Figs. 3.3 for definition of parameters related to joint behaviour.

TABLE 3.2 · Maximum responses of walls.

TYPE A

slip load (kN)	base shear (kN)	top disp. (mm)	panel stress (MPa)	LSB disp. (mm)
0	7980	72.8	36.4	28.8
40	6435	57.8	29.7	22.3
80	5721	47.1	25.2	17.5
160	5441	26.8	17.5	8.1
320	5704	18.1	16.9	2.7
640	6848	21.2	20.9	1.3

TYPE B

slip load (kN)	base shear (kN)	top disp. (mm)	panel stress (MPa)	LSB disp. (mm)	LSB tensile load (kN)	critical LSB work (kN·mm)
0	4179	103.2	14.8	38.9	250	0
40	3406	69.1	14.5	25.1	148	12210
80	3562	64.3	14.5	20.0	196	12680
80[1]	2477	39.1	12.0	2.2	247	2010
80[2]	4167	63.1	14.8	15.4	172	11700
160	4205	55.2	14.1	13.3	284	8920
160[1]	2206	28.9	11.5	0.2	260	0
320	4718	49.5	14.7	4.3	282	5280
320[1]	2265	33.7	11.6	0.3	271	0
640	5574	56.5	14.7	0.9	190	0

slip load (kN)	max. slip (mm)	total slip (mm)	gap opening (mm)	axial deformation (mm)
0	1.4	10.1	8.2	3.4
40	0.8	8.7	4.2	1.5
80	0.9	8.3	4.3	1.6
80[1]	10.9	60.9	0.5	0.5
80[2]	1.5	9.1	4.1	2.0
160	1.0	10.7	3.6	2.1
160[1]	7.3	59.2	0.2	0.4
320	1.2	12.2	5.7	3.7
320[1]	7.5	60.4	0.3	0.4
640	1.3	11.4	6.5	4.5

[1] unreinforced horizontal joints
[2] limited slip of 15 mm for LSB connectors

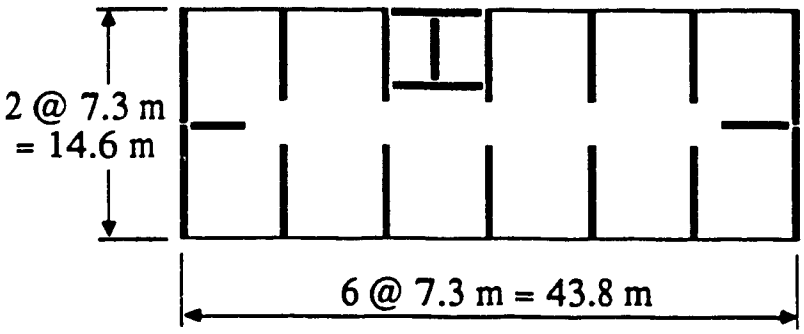

Figure 3.1(a) Floor plan of prototype structure.

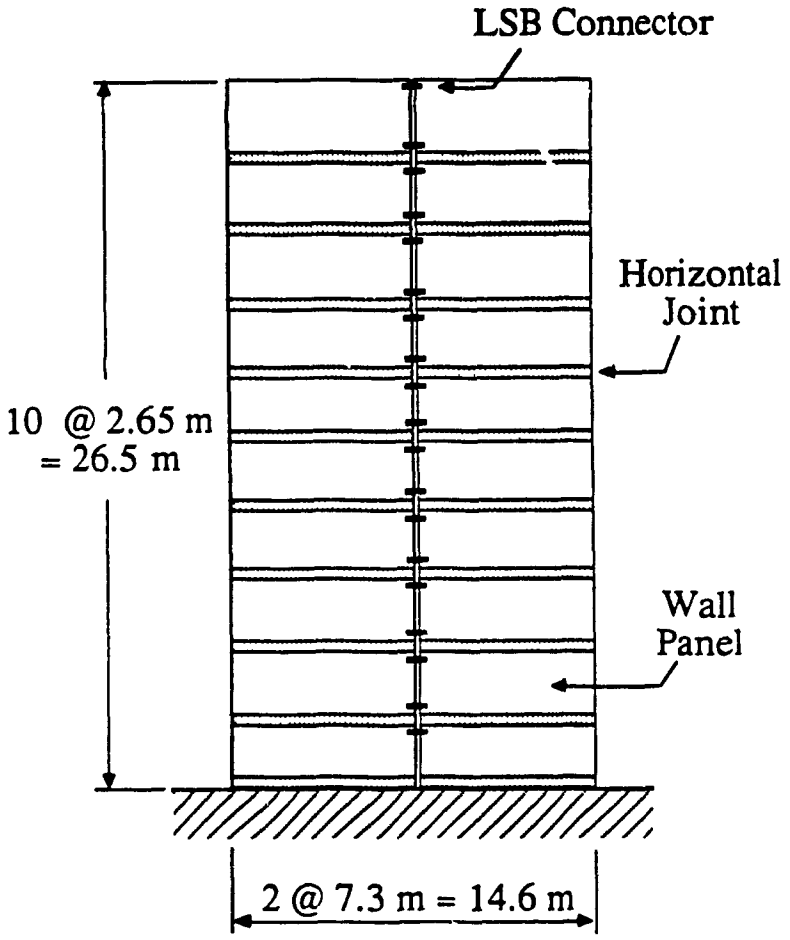

Figure 3.1(b) LSB Jointed End Wall

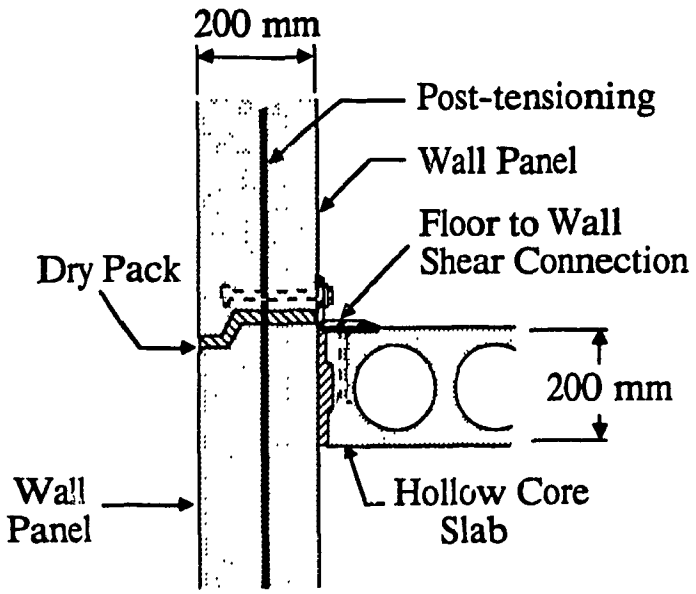

(a) Type A

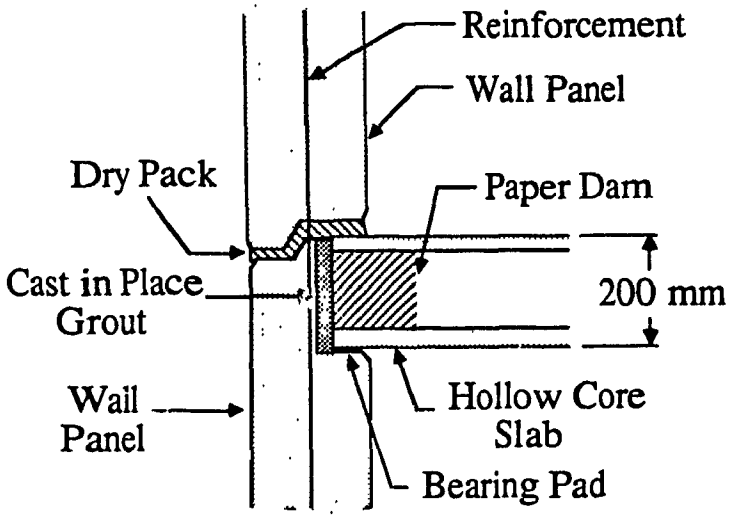

(b) Type B

Figure 3.2 Joint details; (a) horizontal joint for Type A wall; (b) horizontal joint for Type B wall.

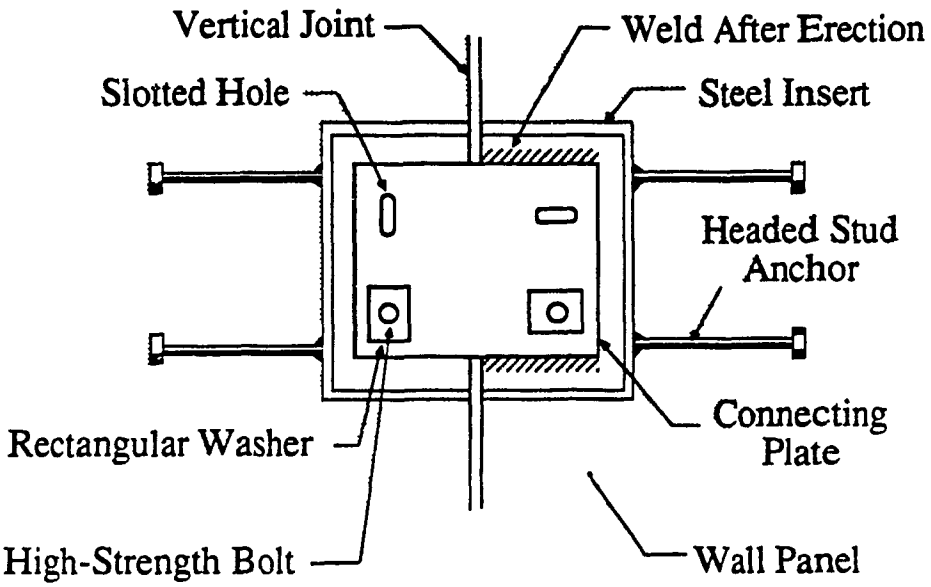

Figure 3.2 Joint details; (c) limited slip bolted (LSB) connector.

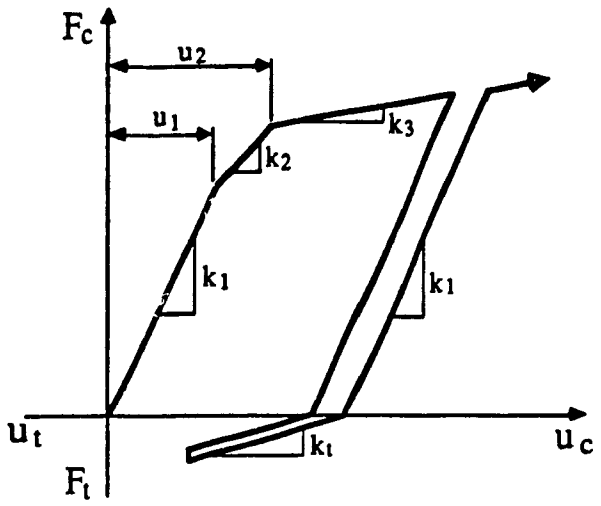

(a) Compression and Tension

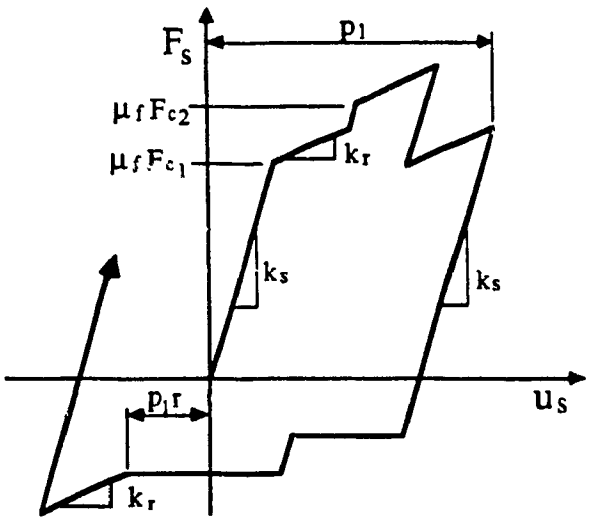

(b) Shear

Figure 3.3 **Force-deformation relations for joints; (a) horizontal joint axial behaviour; (b) horizontal joint shear behaviour**

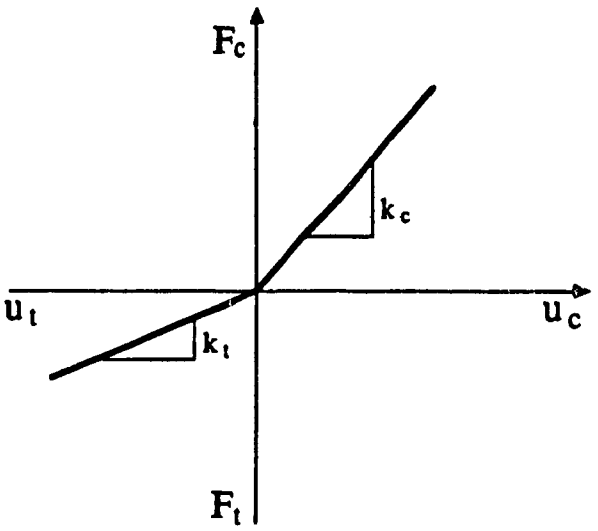

(c) Compression and Tension

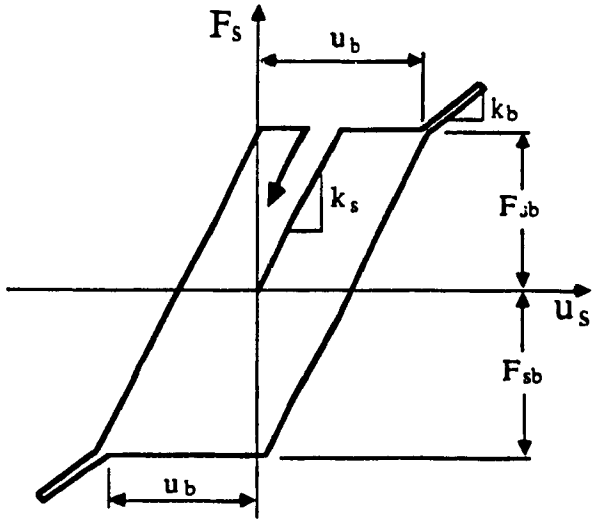

(d) Shear

Figure 3.3 Force-deformation relations for joints; (c) LSB connector axial behaviour; (d) LSB connector shear behaviour

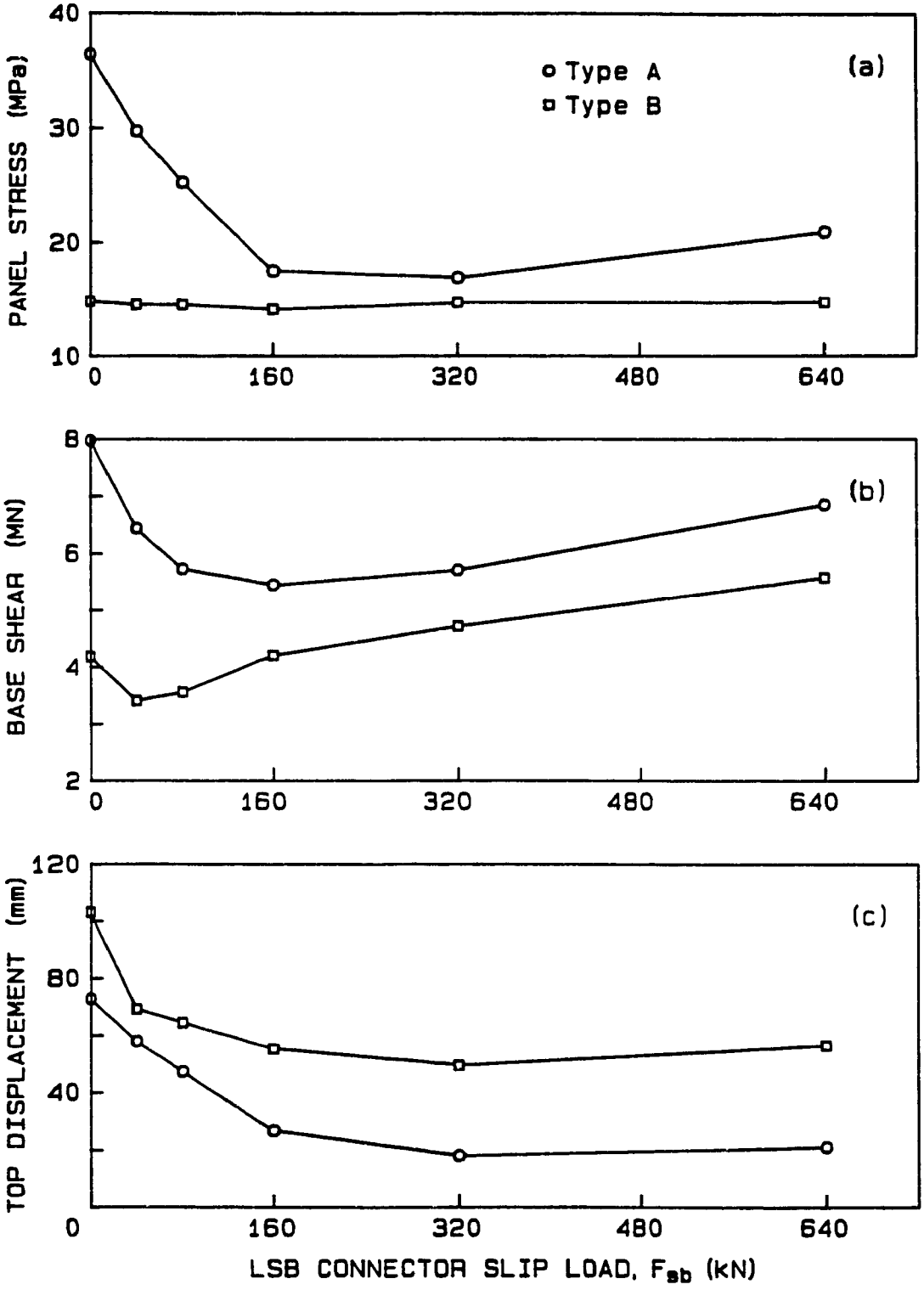

Figure 3.4 Optimum LSB connector slip load for Types A and B walls.

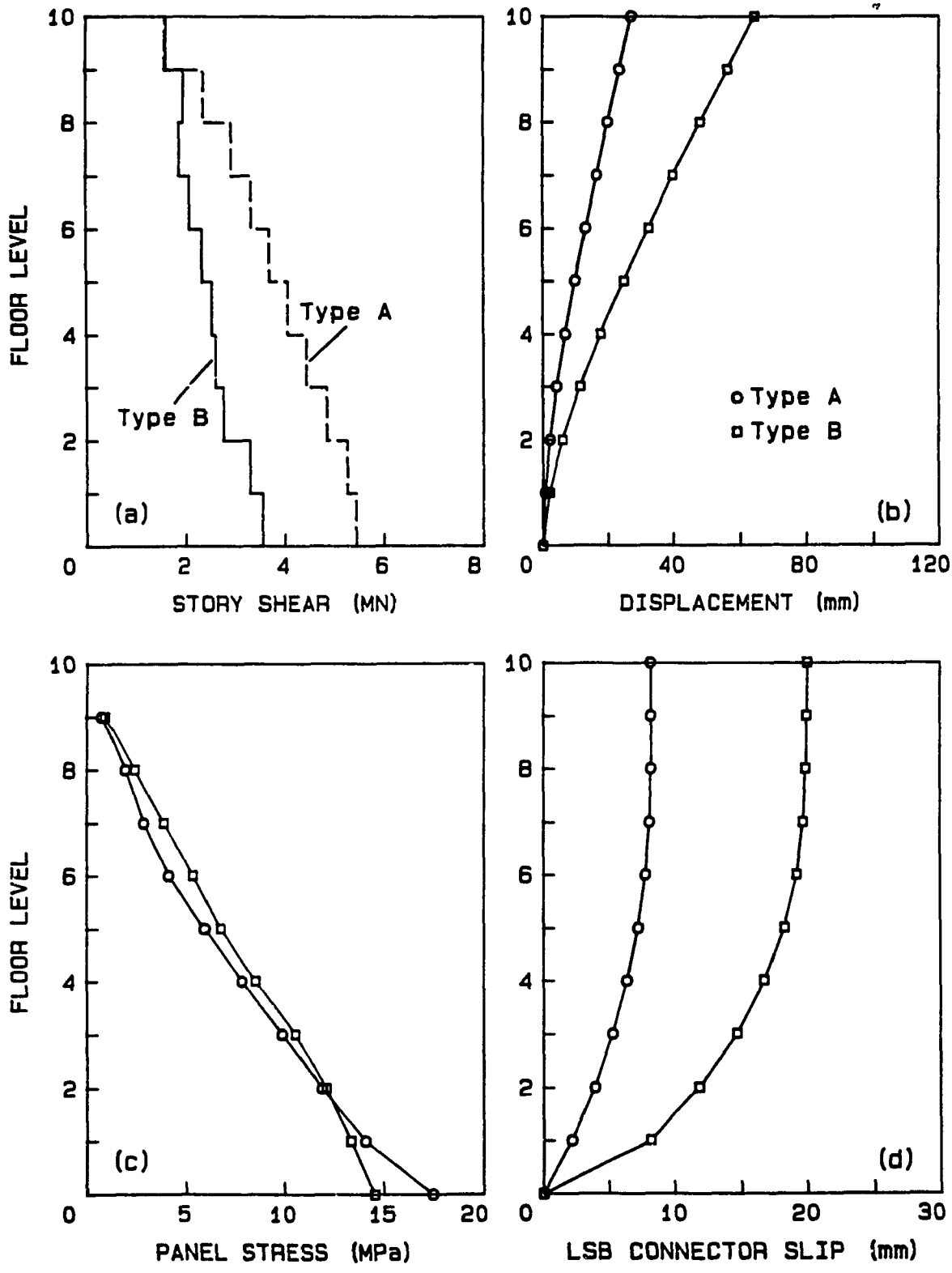

Figure 3.5 Comparison of maximum response envelopes for Types A (F_{sb} = 160 kN) and B (F_{sb} = 80 kN) walls at optimum LSB connector slip loads.

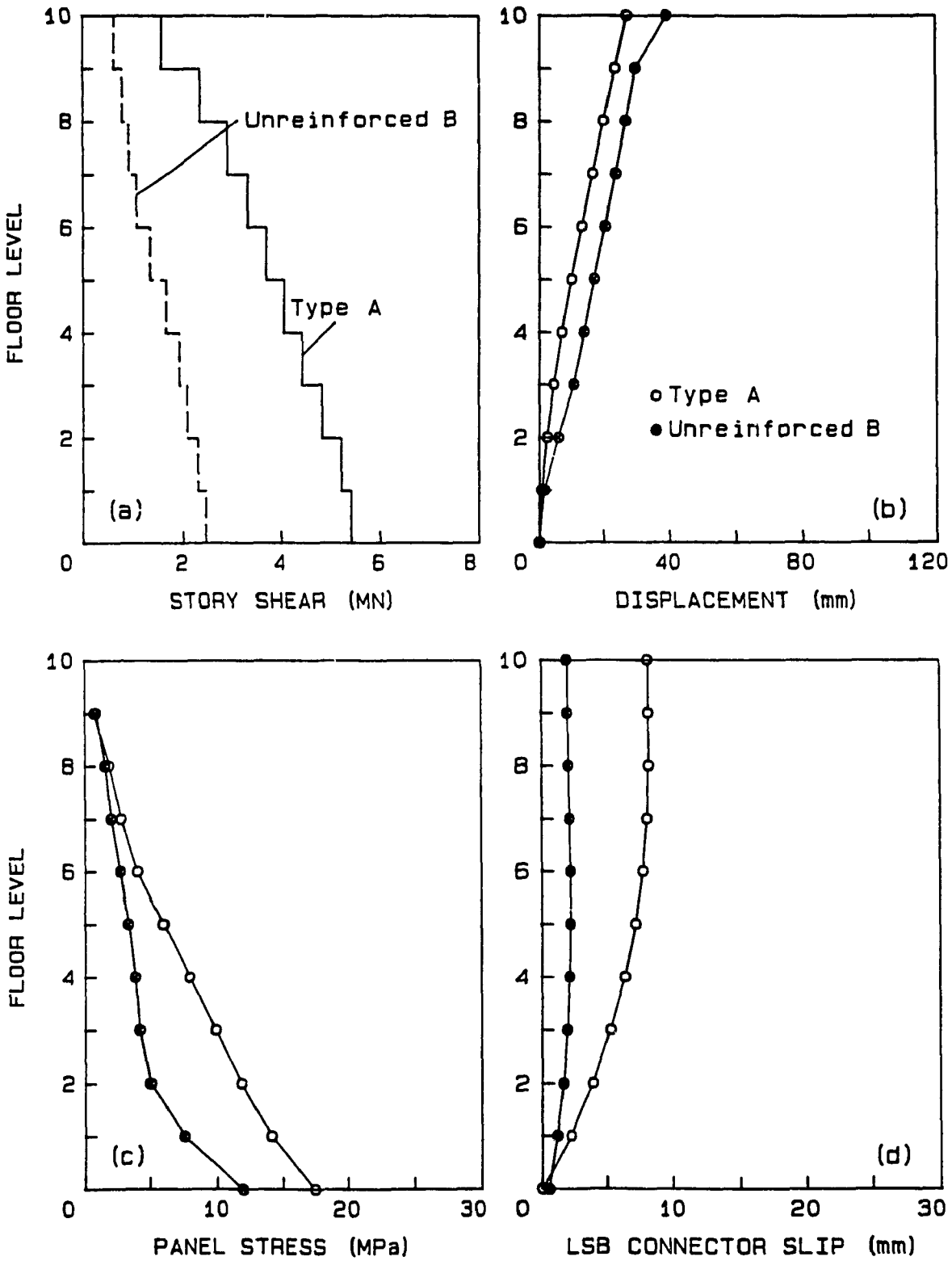

Figure 3.6 Comparison of maximum response envelopes for Types A (F_{sb} = 160 kN) and unreinforced Type B (F_{sb} = 80 kN) walls at optimum LSB connector slip loads.

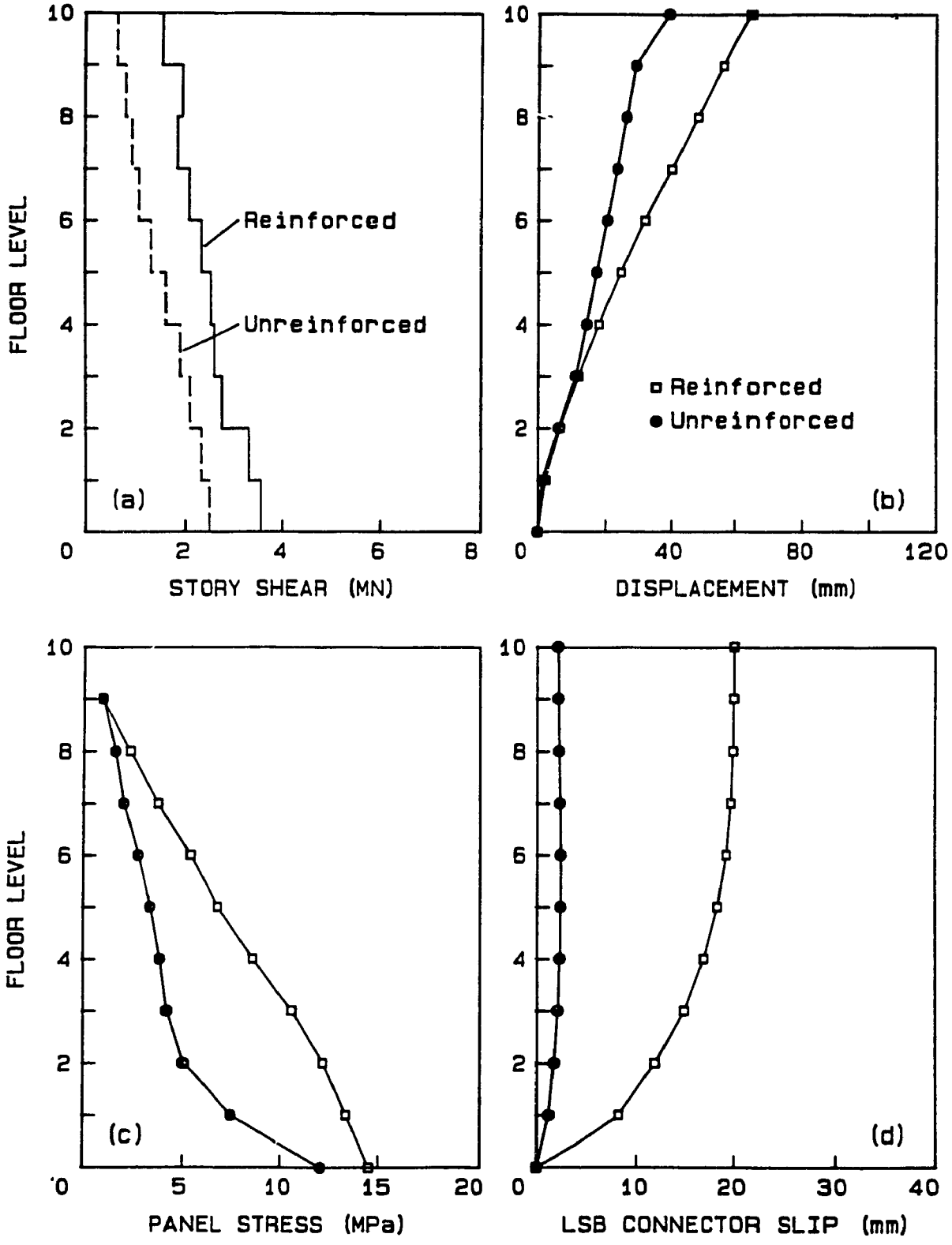

Figure 3.7 Effect of vertical reinforcement on response of Type B walls.

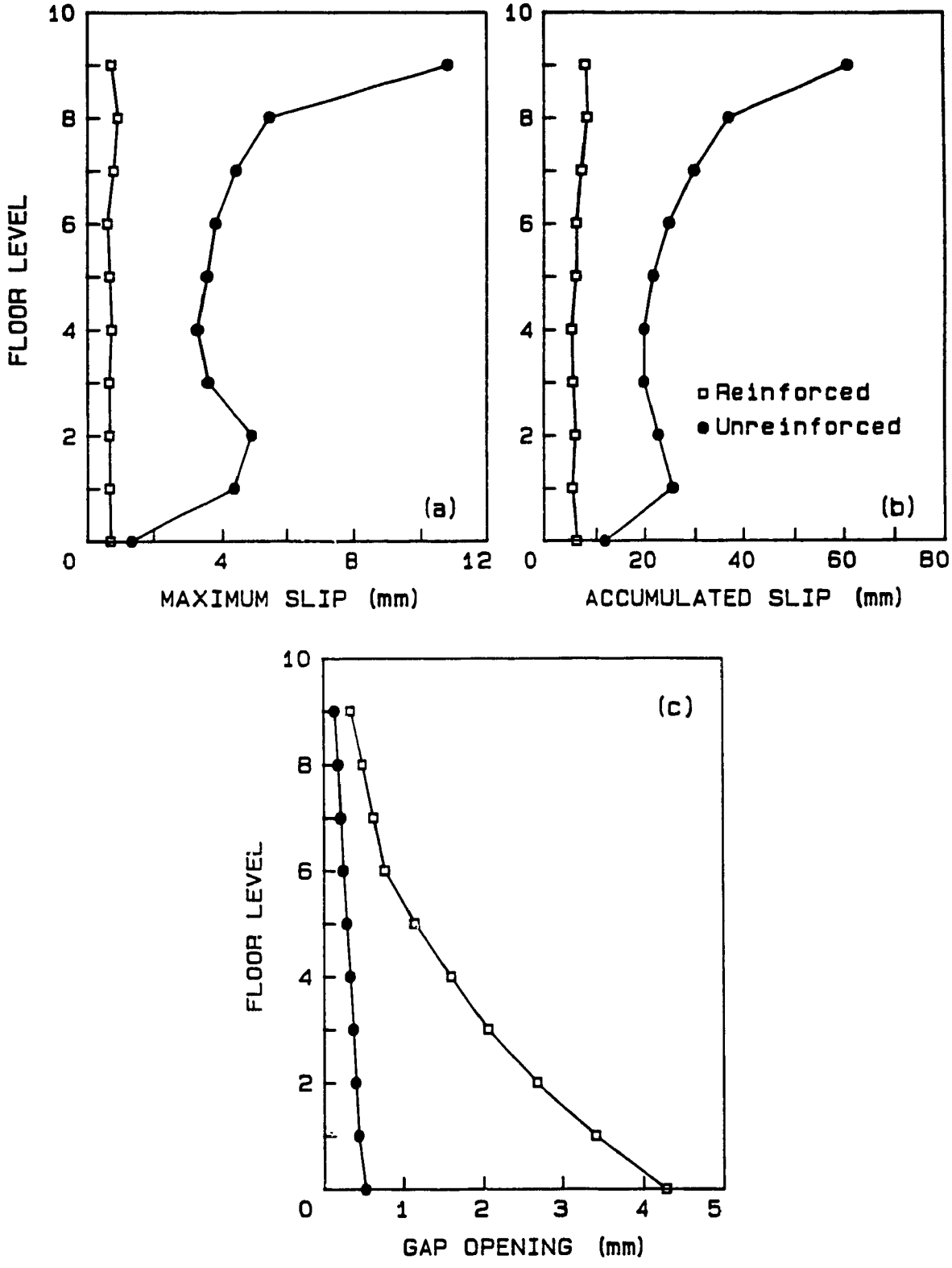

Figure 3.8 Effect of vertical reinforcement on deformation in Type B horizontal joints.

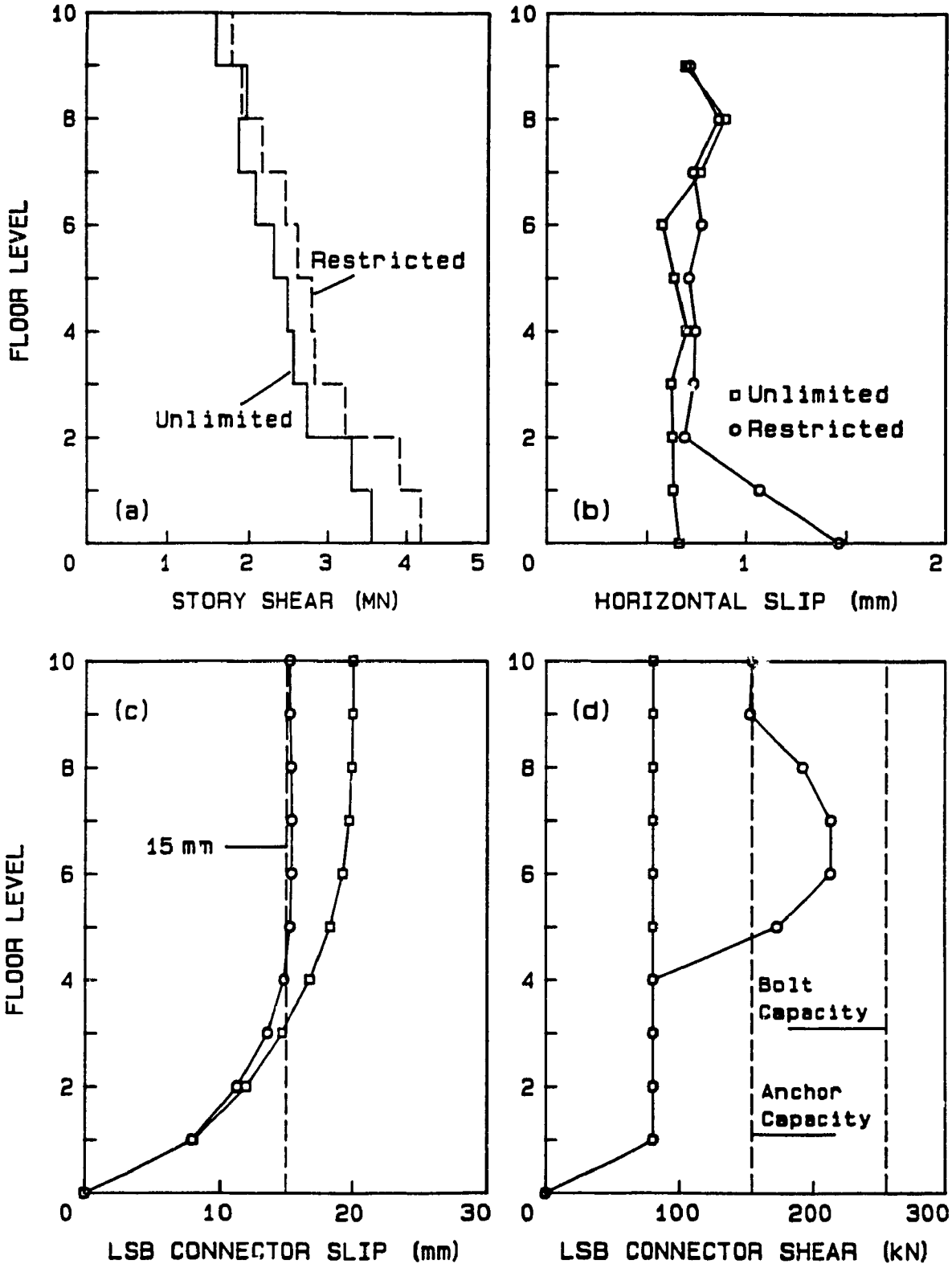

Figure 3.9 Effect of restricting LSB connector slip length on response of Type B walls.

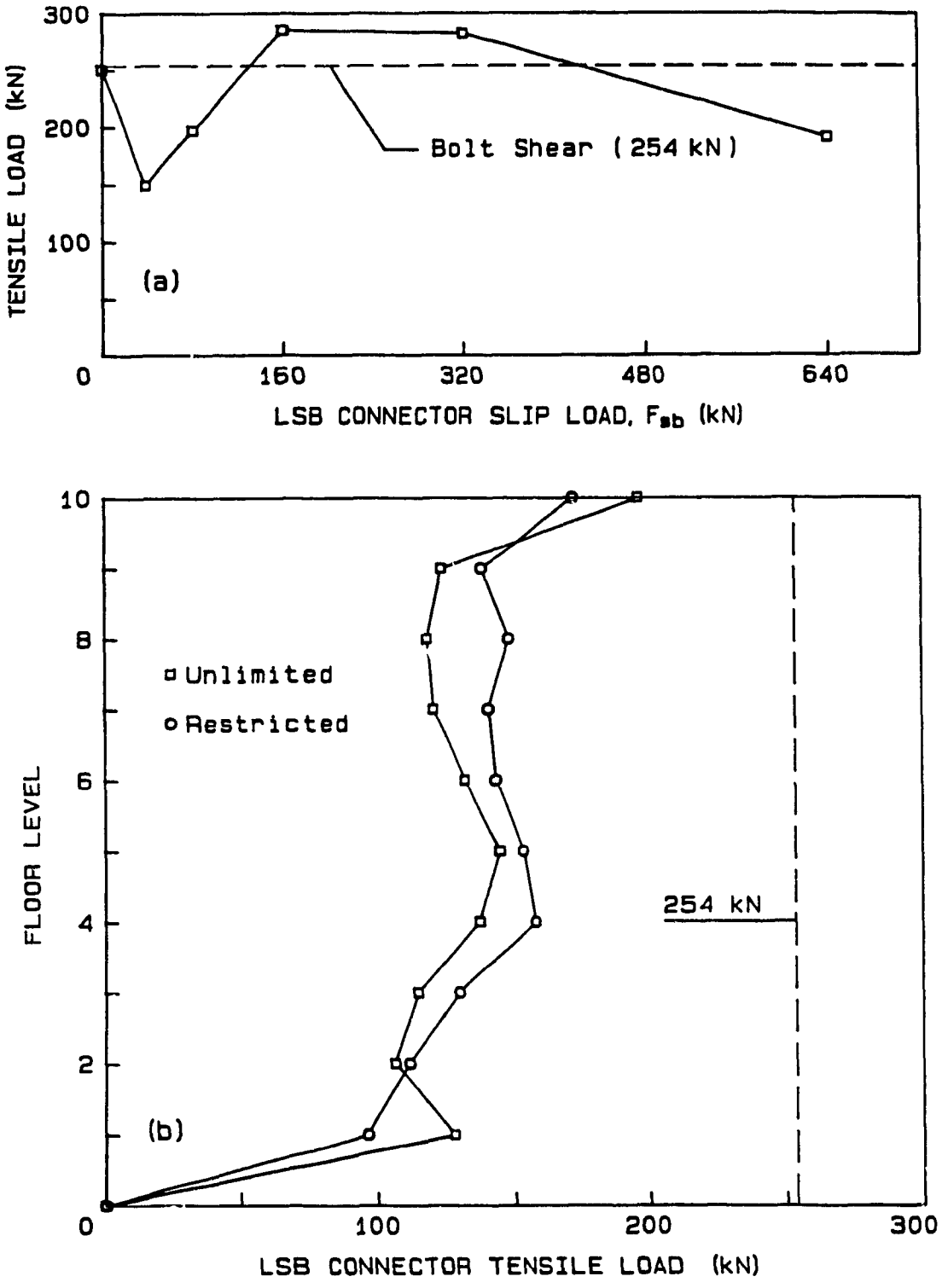

Figure 3.10 Tensile load on LSB connectors of Type B walls: (a) effect of slip load; (b) effect of restricted slip.

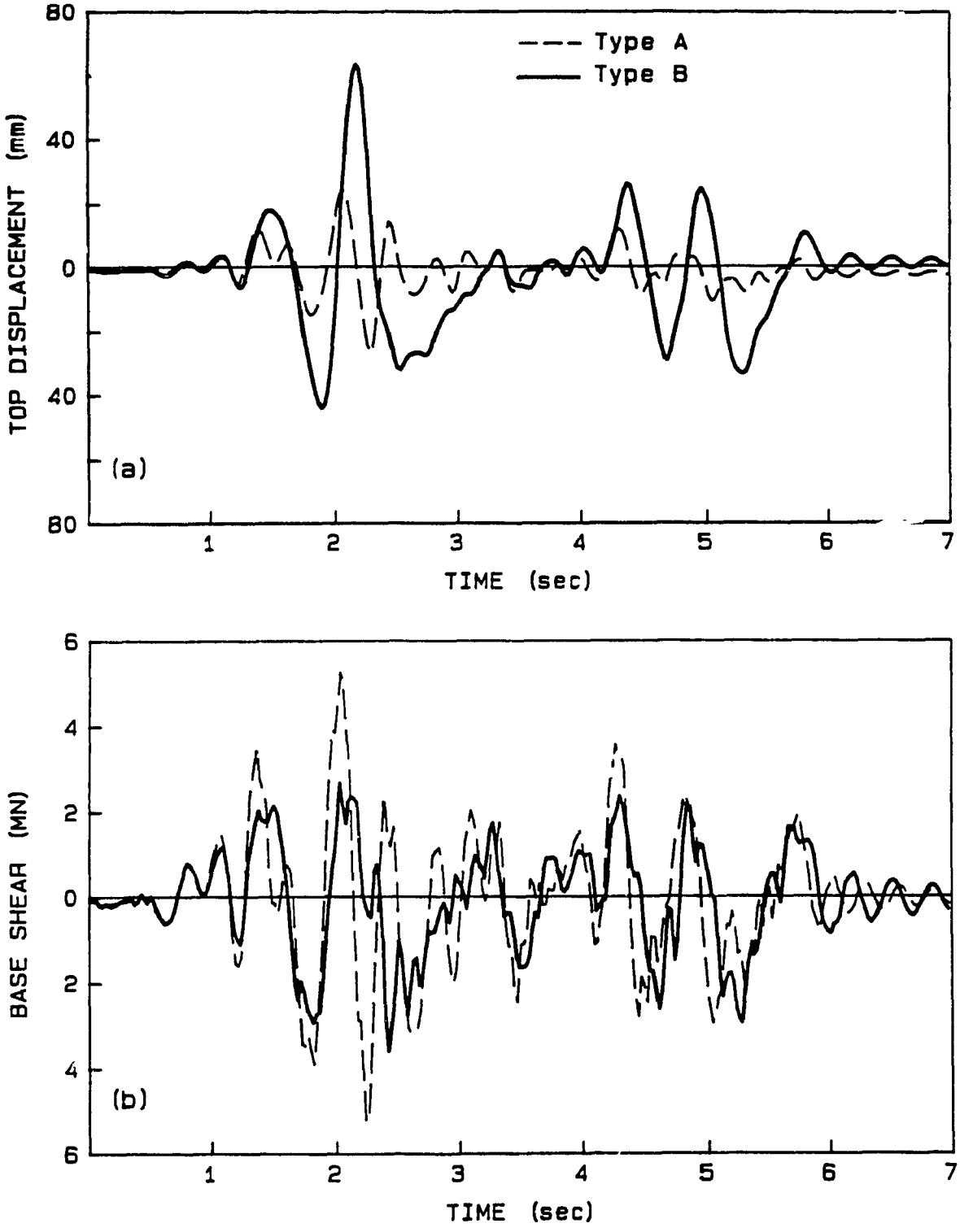

Figure 3.11 Top displacement and base shear time histories for Types A and B walls.

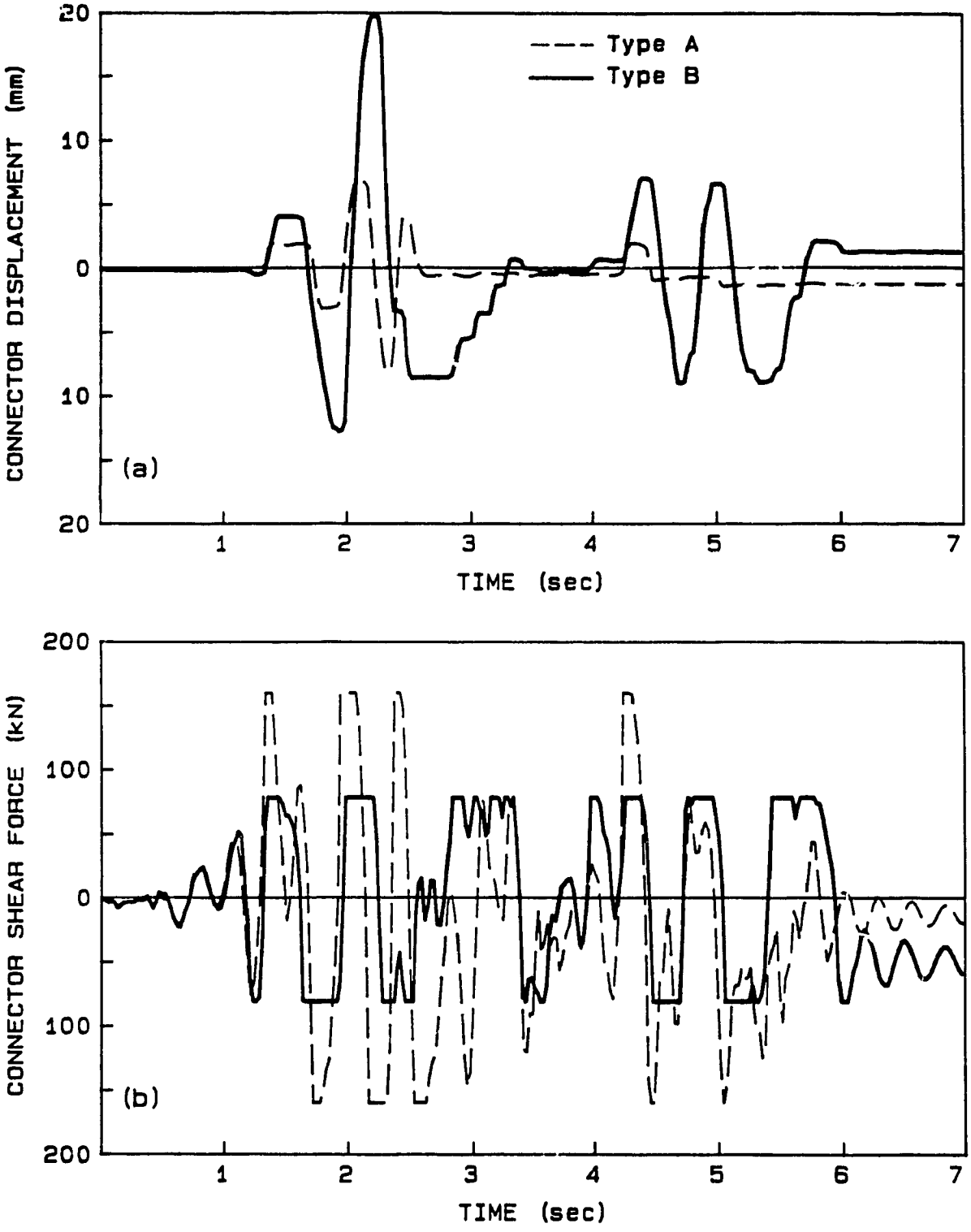

Figure 3.12 Top LSB connector time histories for Types A and B walls: (a) deformation; (b) shear force.

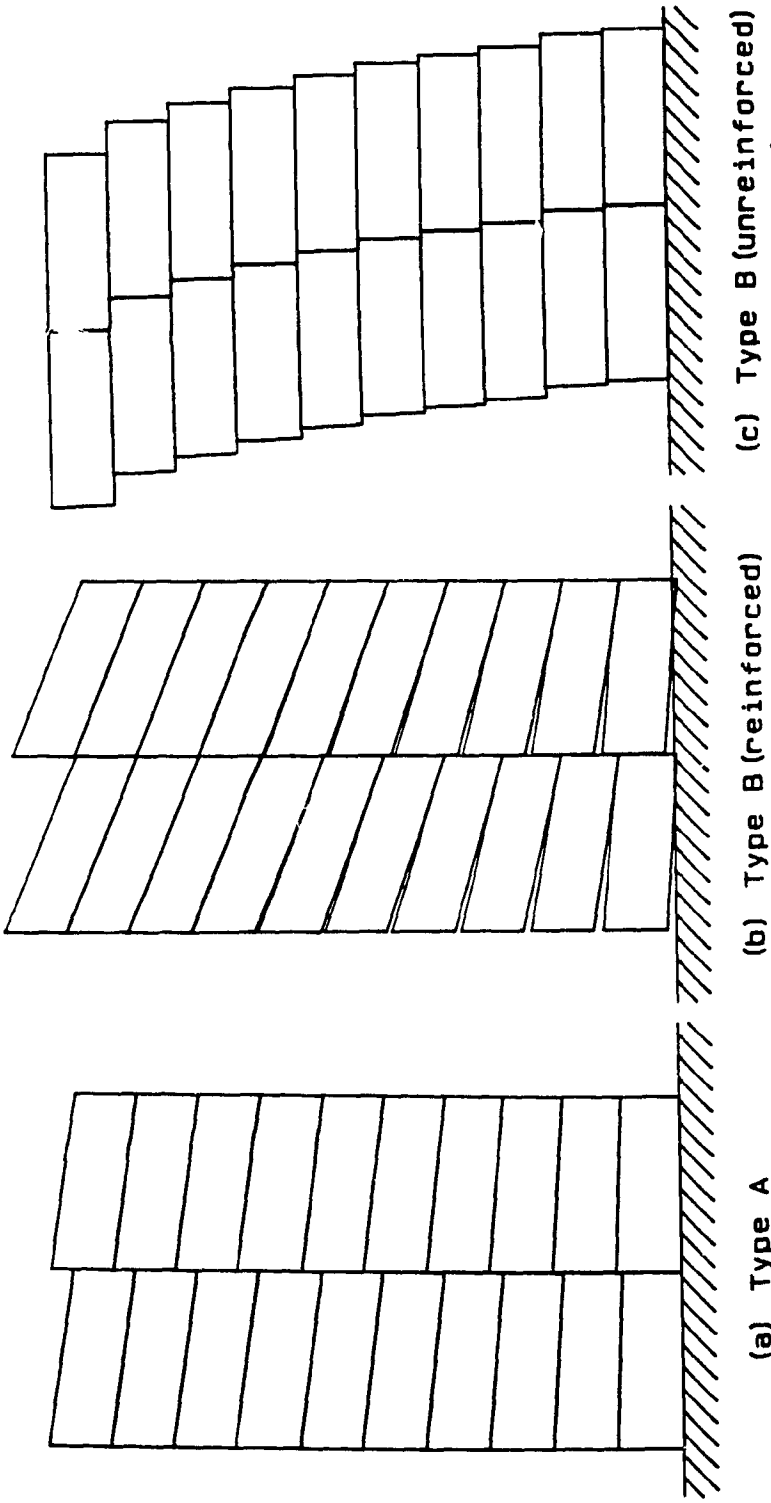

Figure 3.13 Deformed wall configurations at times of maximum displacement. X,Y deformation scales: (a) 25,125; (b) 5,125; (c) 125,25.

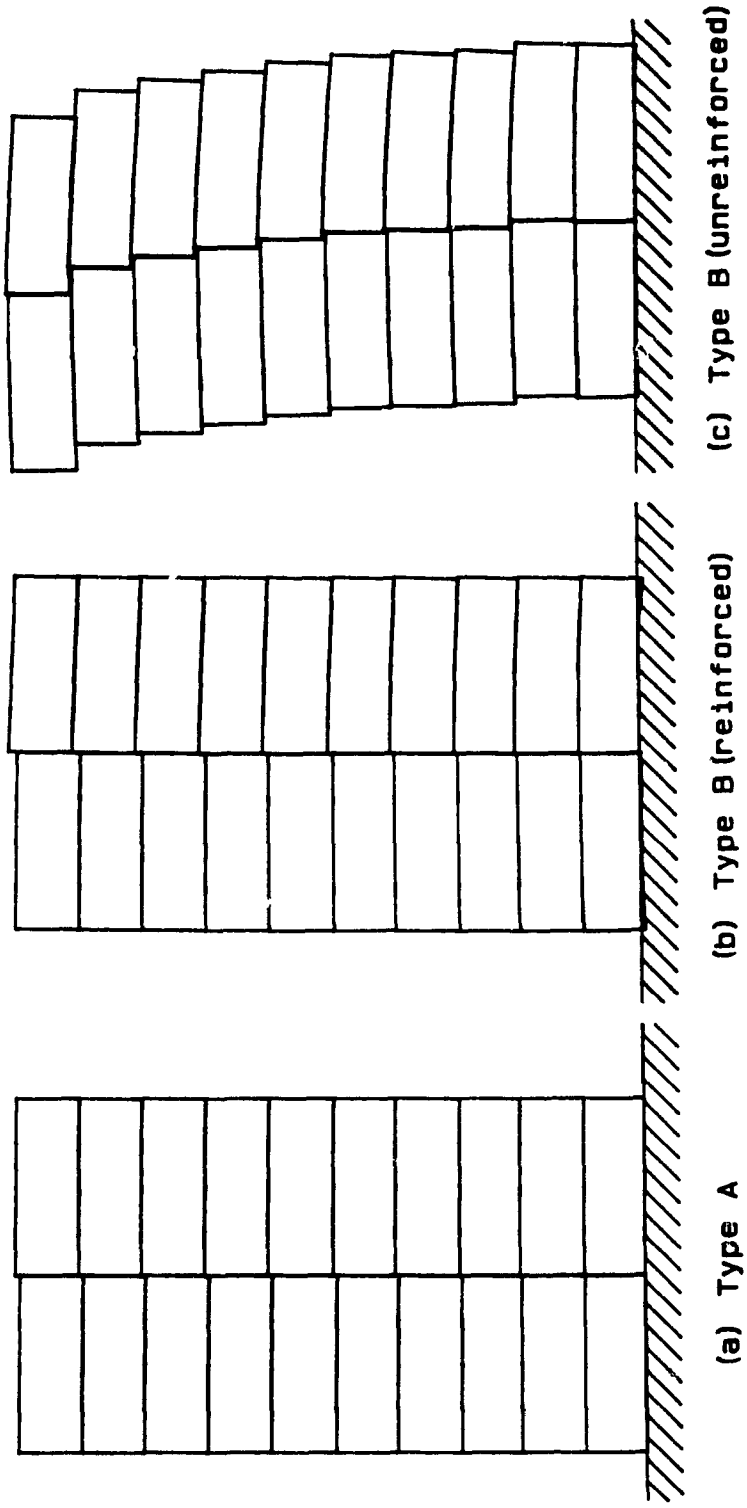

Figure 3.14 Deformed wall configurations at 0.75 seconds after termination of excitation. X,Y deformation scales: (a) 125, 250; (b) 125, 250; (c) 125, 250.

CHAPTER IV

CONTROLLING SEISMIC DAMAGE IN PRECAST LARGE PANEL STRUCTURES

4.1 INTRODUCTION

Failure of precast panel wall systems during severe earthquake excitation can be expected to occur as a result of damage to the interpanel joints, where locations of weakness exist due to reduced stiffness and strength in comparison to the panels[6,8,27]. As the development of overall ductility in precast systems is difficult, acceptable seismic response therefore depends on inelastic action in the joints.

Damage to the vertical joints during seismic activity, where shear deformation dominates[32], can be avoided by employing the limited slip bolted (LSB) mechanical connectors[13] of Chapter III. These connectors slip at the predetermined "slip load" F_{sb}, thus imposing a limit on the shear force attracted by them and allowing the connector anchorages to remain elastic. Hence, damage to the vertical joint is avoided. The resulting improvement to seismic response can be considerable due to the inherently efficient energy dissipating nature of these connectors, and optimal response is possible by adjusting, or 'tuning', the slip load F_{sb}.

Platform-type horizontal joints are commonly used in North America[40] and are analyzed as continuous, precracked planes[6]. Shear slip and rocking along the crack interface account for the inelastic action of the horizontal joints, and both analytical and experimental

studies on panelized structures have shown the extent to which seismic forces can cause large deformations in the horizontal joints[4,5,8,14,17]. Slip is associated with energy dissipation, whereas rocking, although by itself not a source of energy dissipation, can also reduce the level of seismic forces[8,14]. Hysteresis loops during slip (when the shear capacity of the joint is reached) have been shown in tests on European "Vranica" type horizontal joints to exhibit essentially elasto-plastic behaviour and thus an excellent energy dissipating capacity[27]. Tests on platform, or "American", type joints have also shown good energy dissipating potential[26,36]. These findings thus justify the idealized essentially elasto- plastic model adopted for shear behaviour of the horizontal joints and discussed in detail in Chapter III.

However, a tendency to exhibit less stability in the hysteresis behaviour has also been noted with increased cyclic loading at high slip, with accompanying degradation of the joint and subsequent loss of strength. As well, compressive deformation can be severe due to the effect of rocking, during which the horizontal joints alternately open and close. This potential for serious damage can thus undermine the structure's overall stability during earthquakes.

4.2 OUTLINE OF INVESTIGATION

Whereas the previous chapter examined the overall response of two different LSB jointed wall systems (Types A and B), this chapter focuses primarily upon horizontal joint response, and only for the Type B nonlinear behaving horizontally jointed wall. Optimum slip load and energy dissipation in the LSB connectors are considered, and

the associated structural integrity of the wall is examined. In particular, the level of damage to the horizontal joints is studied, and minimization of this damage is attempted through: (1) different schemes of vertical reinforcement, and (2) introduction of base isolation.

4.2.1 Prototype Structure

The prototype wall used is identical to the Type B model employed in Chapter III, part of a typical 10-story precast large panel (LP) building of the crosswall type. The 10-story coupled end shear wall includes continuous platform horizontal joints which allow both shear slip and gap opening, and LSB mechanical connectors along the vertical joint. Full details of the wall properties and loading can be found in Chapter III and Table 3.1.

4.2.2 Earthquake Excitation

Four different earthquake records are employed in the study. Only the first six seconds of these records are used, followed by one second of zero acceleration. The accelerograms are scaled to match the intensity of the 1940 El Centro NS record, intensity being defined as the area under the 5 per cent damped relative velocity response spectrum between periods of 0.1 and 3.0 seconds. Spectra are determined through the Fortran program SPECEQ[41] and computed for the full duration of the earthquake records.

The records consist of the 1940 El Centro NS, 1952 Taft N693E, 1949 Olympia N10W and the Newmark-Blume-Kapur artificially generated earthquake. Since the El Centro record is demonstrated to yield the

most severe structural response, it is used over the full range of slip loads. The Taft record is employed similarly, although producing far less severe response. The Olympia and the artificial input excitations are used only for the optimum slip load (F_{sb} = 80 kN). Fig. 4.1 shows these accelerograms (scaled), while Table 4.1 summarizes the details of each record.

4.3 OVERALL RESPONSE

4.3.1 Optimum Slip Load

Optimization of earthquake response in structures entails minimizing the difference between the seismic energy fed into and energy dissipated by the structure. For a given earthquake, input energy depends primarily upon the building's mass and fundamental period, while energy dissipation is largely controlled by the level of ductility or inelastic action in the structure.

The above energy dissipation is a major criterion in the seismic design of precast LP systems. It has been demonstrated that the vertical joints of LP walls can provide an ideal location for energy dissipation, where slip or yielding of the coupling elements can effectively reduce seismic forces; the limited slip bolted connectors employed herein are designed to slip at a predetermined slip load F_{sb} analogous to the yield level for non-slipping bolted mechanical connectors[11], or beam coupling elements[17]. This slip load can be adjusted for maximum energy dissipation and an optimum slip load exists whereby seismic response can thus be minimized. At a slip load of 640 kN, the wall acts as an elastically coupled shear wall, since the slip load is sufficiently high to prevent slip from occurring.

As demonstrated in Chapter III, an optimum slip load close to 80 kN was obtained for the prototype Type B wall when considering overall responses such as maximum wall stress, base shear and top displacement. Fig. 4.2 depicts these response parameters as a function of connector slip load F_{sb} including also results for the scaled 1952 Taft S69E record. The figure shows that although absolute response, or response of the LSB jointed shear wall relative to an isolated or elastically coupled shear wall, is highly dependent on the earthquake characteristics, both earthquake excitations suggest an optimum slip load of approximately 80 kN. Selection of a design slip load can thus be made based only on the characteristics of the structure and remains independent of the ground motion itself. Earlier studies on coupled walls, assuming elastic wall and horizontal joint behaviour, also confirmed an optimum vertical joint yield level[11] that was relatively independant of the seismic excitation.

Envelopes of maximum response at connector slip loads of 0, 80 and 640 kN, are shown in Figs. 4.3 and 4.4 for the El Centro and Taft input excitations, respectively. As both Figs. 4.3(a) and 4.3(b) as well as Figs. 4.4(a) and 4.4(b) show, the use of slipping vertical joint connectors (F_{sb} = 80 kN) incorporates the advantages of lower displacements at all levels as provided by the elastically coupled wall (F_{sb} = 640 kN), while at the same time exhibiting the decreased story shears that the isolated, uncoupled wall attracts (F_{sb} = 0 kN). Stresses in the wall panels are not noticeably different for the three slip loads for the El Centro excitation (Fig. 4.3(c)), but of note is that the ultimate strength in compression of the horizontal joints (f'_c = 14.5 MPa) is reached at the base for all three cases. For the Taft

earthquake, Fig. 4.4(c) shows greater reductions in maximum panel stress at the optimum slip load. The decreased severity of this record is reflected by the base stresses, where only at F_{sb} = 0 kN is the ultimate horizontal joint strength reached.

Fig. 4.5 plots peak response of the LSB connectors versus slip load F_{sb}, for the El Centro and Taft excitations. Fig. 4.5(a) shows LSB slip at optimum (F_{sb} = 80 kN) is 8 and 20 mm for Taft and El Centro, respectively. As noted in Chapter III, such slip must be accommodated in the bolt slot length as otherwise bearing of the bolts results in increased response.

Fig. 4.5(b) shows that maximum shear load on the connectors is limited to the capacity F_{sb}, so that elastic design of connector anchorages is possible by the priori knowledge of the maximum expected load. At F_{sb} = 640 kN, slip has not occurred in both cases, thus confirming elastic coupling of the wall at this connector capacity. Tensile forces in the connectors are presented in Fig. 4.5(c), which shows that minimum tensile force is incurred for F_{sb} close to 80 kN. At this slip load, the tension of 200 kN is adequately resisted by the connector tensile capacity of 254 kN (see Chapter III).

4.3.2 Energy Dissipation in the LSB Connectors

As noted in the preceding section, structural response can be optimized for all earthquake input by selecting an appropriate 'optimum' slip load, whereby overall structural responses such as panel stresses and story shears are minimized. A measure of such an optimum slip load can be obtained by considering the total amount of energy dissipated in the LSB connectors. The amount of seismic energy

dissipated in a single LSB connector is measured by the total area enclosed by the hysteretic loops tracing its behaviour in shear. Since such behaviour is elasto-plastic, this area is equal to the product of the connector slip load and accumulated slip travel.

Energy dissipation cannot occur in the connectors when F_{sb} = 0 kN, since no load is sustained. At the upper limit of slip load (640 kN in this study), energy dissipation is also zero, since vertical joint deformation remains elastic. Thus, the slip load producing maximum energy dissipation in the LSB connectors lies between the cases of uncoupled walls, and those that are elastically coupled.

Energy dissipated by the LSB connector having the maximum value out of all the connectors, or by the critical connector, is shown in Fig. 4.6(a) as a function of the connector slip load. Energy dissipation is observed to rise to a maximum at F_{sb} = 80 kN. Thus, the optimum slip load for structural response also exhibits the largest potential for energy dissipation in the critical connector. Figs. 4.6(b) and 4.6(c) show envelopes of energy dissipation at slip loads of 40, 80, 160 and 320 kN for El Centro and Taft, respectively, and reveal that the relationship between slip load and critical connector energy dissipation as disclosed in Fig. 4.6(a) holds true at all floor levels; thus, the total energy dissipated in the connectors is also maximum at F_{sb} = 80 kN. Although the maximum energy dissipation occurs in the topmost connector, at this slip load practically all the connectors contribute equally toward energy dissipation (levels 4-10). By contrast, the energy curves for high F_{sb} (F_{sb} = 320 kN) peak at the lower floors and thus imply reduced ability to improve seismic response.

4.3.3 Structural Integrity

Time histories of top lateral displacement of the wall are shown in Figs. 4.7 and 4.8 (El Centro and Taft, respectively), at slip loads of 0, 80, and 640 kN. Stable response over the seven seconds for each time history is demonstrated by the lack of perceptible drift from zero displacement. At F_{sb} = 0 kN, large and steady amplitudes of vibration begin at 1.8 and 3.8 seconds, corresponding respectively to the onset of large accelerations in the El Centro and Taft input records (see Figs. 4.1(a) and 4.1(b)), and continue at seven seconds, one second following termination of input excitation. Severity of response is considerably reduced for the optimum slip load F_{sb} = 80 kN for which response approaches that of elastically coupled walls, and return to zero displacement at seven seconds is observed.

Figs. 4.9 to 4.12 represent idealized deformed shapes of the wall, with the scale for deformation exaggerated for clarity. Depicted in Figs. 4.9 and 4.10, for the El Centro and Taft earthquake records respectively, are the wall configurations at times of maximum positive lateral displacement for slip loads of 0, 80 and 640 kN. The general shapes of the wall at slip loads of 0 and 80 kN show little difference both for the El Centro and Taft earthquake records, displaying large gap opening and vertical joint slip. Higher vertical joint slip for F_{sb} = 0 is apparent for both earthquake excitations. Also noteworthy is the significant reduction in gap opening at F_{sb} = 80 kN and employing the Taft earthquake record. At F_{sb} = 640 kN, full elastic coupling at the vertical joint prevents slip and wall behaviour resembles that of a single stack precast wall.

The deformed shapes of the wall at 6.75 seconds are seen in Figs. 4.11 and 4.12. For both F_{sb} = 80 and 640 kN, the wall returns nearly to its original undeformed shape. For the uncoupled wall (F_{sb} = 0 kN), Figs. 4.11(a) and 4.12(a) (for El Centro and Taft, respectively) do not suggest that the structure develops severe permanent deformation, but as shown in Figs. 4.7(a) and 4.8(a), only imply continued oscillation. In the cases of both the uncoupled and fully coupled walls, however, severe compressive deformation can be seen in the base horizontal joint. The El Centro excitation induces some permanent joint damage at the base even at the optimum slip load (Fig. 4.11(b)), whereas no damage is incurred for the Taft excitation (Fig. 4.12(b)). Thus, although integrity of the structure as a whole is observed to be generally excellent at optimum LSB connector slip load, the residual compressive deformation at the base horizontal joint warrants concern. The following sections address this aspect of horizontal joint integrity.

4.4 RESPONSE IN HORIZONTAL JOINTS

The role of horizontal joints in the seismic response of panelized structures has been previously investigated[4,5,8,14,17] and shown to be of considerable importance. The possibility of damage in these joints due to slip and rocking must be considered. Results presented herein for the horizontal joints are thus mainly concerned with the degree and significance of deformation (both shear and axial) in the joints. Joint influence on overall structural response has been previously studied in Chapter III.

4.4.1 Optimum Slip Load

Figs. 4.13(a) and 4.13(b) plot peak values of maximum slip and accumulated slip in the horizontal joints versus the LSB connector slip load for the El Centro and Taft earthquake records. Maximum joint gap opening (or uplift) and compressive axial deformation are shown in Figs. 4.13(c) and 4.13(d). As for the overall structural responses seen in Fig. 4.2, response parameters related to the horizontal joints shown here are also minimized at a slip load close to 80 kN and are independent of the input excitation employed.

For the El Centro excitation, Fig. 4.13(a) shows a maximum slip length of 0.9 mm for F_{sb} = 80 kN (0.6 mm with Taft), while the isolated wall (F_{sb} = 0 kN) shows the highest value at 1.4 mm (1.1 mm for Taft at F_{sb} = 320 kN). These values, however, do not suggest significant slip in the joints. Cyclic shear load tests on European 'Vranica' type unreinforced horizontal joints by Verbic[27] indicated elastic shear behaviour at deformation up to about one mm before the ultimate joint shear strength was reached. A displacement controlled loading phase followed, during which up to 20 mm of slip was observed with accompanying energy dissipating characteristics. Tests on unreinforced platform joints[36] with cyclically reversing shear loads at progressively increasing magnitude produced no evidence of energy dissipation after 5 cycles of load and 0.05 mm of deformation. Pinched hysteretic shear behaviour after 9 cycles and 0.25 mm deformation also did not suggest energy dissipation, but well defined energy dissipating characteristics appeared in the hysteresis loops at slip approaching 5 mm and approximately 11 total cycles of load. Vertical loading of the joints for both models was applied to include the

effects of both dead weight and overturning moment, and unlike the cases herein and in actual seismic response, kept constant during the test.

Horizontal joint slip in the present study, however, is 'localized' in nature and not 'global' as observed in the tests[27,36]. In the former case, slip is localized within a certain region of the horizontal joint, which for analytical purposes implies slip in one element while others, representing the same joint. remain elastic. Global slip is more important in terms of energy dissipation, since all points along the joint are in contact and have reached the shear strength[9]. The slip observed herein thus provides little, if any, energy absorption due to the combined effects of its low magnitude (Fig. 4.13(a)), and localized nature. Consequently, potential damage to the joint is limited since the amplitude of slip is relatively small and minimizes the detrimental effects that cyclic load reversals can have.

More important is the extent to which gap opening occurs. At all slip loads, substantial uplift is observed. With F_{sb} = 80 kN, however, reduction in gap opening and related axial deformation are significant as demonstrated in Figs. 4.13(c) and 4.13(d). For the more critical El Centro ground motion, values are 47 and 52 per cent less than for the isolated wall and 34 and 64 per cent less than for the elastically coupled wall, for gap opening and compressive deformation respectively. The similarity between the two figures shows the effect that large joint opening, indicative of rocking, has on compressive deformation. The ultimate compressive strength of the composite horizontal joints corresponds to a compressive deformation of 0.42 mm

(or 0.0021 strain for the 200 mm thick joints), and is seen to be exceeded for all slip loads and both earthquake records. However, subsequent crushing and degradation of the joint associated with strains beyond that at ultimate strength are much more pronounced for the isolated and fully coupled walls.

4.4.2 Envelopes of Joint Response

Envelopes of maximum horizontal joint response are presented in Figs. 4.14 and 4.15. Approximately uniform distributions of slip and accumulated slip over the wall height are indicated by Figs. 4.14(a) and 4.14(b) (El Centro) and by Figs. 4.15(a) and 4.15(b) (Taft). As noted previously, this slip is not particularly significant in terms of energy dissipation nor joint degradation, since the magnitude of slip is both low and 'localized' at the joint ends. Reduced accumulated slip for F_{sb} = 80 kN, however, is revealed by the data and, in particular, at the more critical lower levels. Note that, due to the effects of localized slip, the maximum and accumulated slip envelope values do not necessarily occur in the same regions at given joint levels.

Substantially lower magnitudes of gap opening at all levels are also noted for F_{sb} = 80 kN, as shown in Figs. 4.14(c) and 4.15(c). A nearly linear increase in gap opening is demonstrated at all slip loads from top to bottom. Associated rocking is thus much more severe at the lower joints, where accompanying normal joint forces are also notably greater. The result is that, at the lower levels, high concentration of compressive force develops at the joint ends.

The envelopes of maximum compressive deformation in the

horizontal joints of Figs. 4.14(d) and 4.15(d) indicate that, as a consequence, crushing occurs in the lower joints when normal strain in the joint exceeds that corresponding to the ultimate joint strength; however, it is noted that the LSB connector slip load of 80 kN significantly reduces response. For the Taft earthquake and F_{sb} = 80 kN, base deformation just exceeds deformation at maximum joint strength and thus does not immediately imply crushing failure. Tests have shown that strain in excess of 0.004 for equivalent low-strength concrete (14.5 MPa and ultimate strain of approximately 0.002) can be sustained prior to failure[42]. This corresponds to a deformation of about 0.8 mm for the joints employed in this study, implying a ductility factor of about 2. Tests[20] on platform joints have also suggested ductile characteristics, although strains beyond a ductility factor of one were not recorded due to potential instrumentation damage. For the other cases, including F_{sb} = 80 kN and El Centro, deformation at the base exceeds the ultimate deformation of 0.42 mm by a factor of at least 4, and thus strongly indicates joint failure. At F_{sb} = 0 kN, the ultimate deformation of 0.42 mm is exceeded up to level 2 for El Centro and to level 1 for Taft.

4.4.3 Time Histories of Slip and Axial Deformation

Figs. 4.16 and 4.17 show time histories of localized horizontal joint shear slip for F_{sb} = 0, 80 and 640 kN, and for the El Centro and Taft input excitations. The results are presented for local slip at the far left edge of the base horizontal joint; similar behaviour can be observed at corresponding edges of other floor levels, as evidenced by the envelopes of maximum and accumulated slip in Figs. 4.14 and

4.15.

These figures demonstrate an essentially monotonic increase in slip with time although, with the exception of F_{sb} = 80 kN and El Centro, all the cases exhibit at least one reversal in slip magnitude. For optimum F_{sb}, maximum slip coincides with the onset of increased seismic intensity (Figs. 4.1(a) and 4.1(b)), but thereafter shows only minor fluctuation. A characteristic reduction in slip action is displayed for F_{sb} = 80 kN. Lack of major reversals in slip direction for all cases confirms that shear degradation is not significant. As noted also in studies by Scanlon and Kianoush[17], the benefit of providing reinforcement in the joint is that shear slip is kept low; rocking (or gap opening), on the other hand, is intensified.

This dominance of rocking action over shear slip can be seen in Figs. 4.18 and 4.19 which depict time histories of axial deformation at the left edge of the base horizontal joint. The diagrams reveal that the compressive deformation is substantially greater for both uncoupled, simple walls and the elastically coupled walls. In these, large compressive deformation is the result primarily of a high degree of rocking. The latter is typified by the oscillating nature of the curves, varying between tension (positive deformation) and compression (negative deformation). Axial or compressive deformation, however, either reaches or exceeds the value (0.42 mm) corresponding to ultimate joint strength at all slip loads. Although performance in the horizontal joints with optimized LSB connectors is noticeably improved, corner crushing at the base is nevertheless still encountered and may promote structural instability. Proposals to redress this potential danger are examined in the following section.

4.5 MINIMIZING DAMAGE IN HORIZONTAL JOINTS

It was previously seen that seismic performance of the present coupled shear wall is optimized at a slip load of 80 kN. However, the problem of damage due to compressive failure in the lowermost joints was demonstrated to accompany this otherwise enhanced performance. Of concern also is the possibility of reinforcement yielding as a result of excessive gap opening. Thus, further optimization of the prototype structure to reduce the potential for damage, in particular at the lower joints, is attempted. This consists of different forms of reinforcement to enhance vertical continuity as well as modification of the lowermost joint in order to introduce base isolation.

4.5.1 Effect of LSB Slip Load

Figs. 4.20 and 4.21 plot envelopes of maximum gap opening and compressive deformation across the base horizontal joint for both the El Centro and Taft excitations at vertical connector slip loads of 0, 80, and 640 kN (note that at 7.30 m of the wall base the vertical joint is represented by a dashed line). Both Figs. 4.20(a) and 4.21(a) highlight the distinct nature of isolated uncoupled versus fully coupled wall behaviour. Independent action of the two wall halves is shown for F_{sb} = 0 kN, revealing large maximum gap opening not only at the extreme outer joint edges, but also at the vertical joint line (7.30 m), while for F_{sb} = 640 kN the envelope curve resembles that for a single stack LP wall, with minimum gap opening at the vertical joint edge. LSB coupled shear walls (F_{sb} = 80 kN) yield the lowest peak magnitude of gap opening and also generally lower magnitudes

across the joint.

Gap opening in the horizontal joints has thus far been discussed mainly as related to its influence on the anticipated compressive deformation. However, with the provision of vertical reinforcement across the joints, large gap opening becomes important in itself. Stretching of the steel reinforcing bars beyond their yield point can occur when the magnitude of joint opening becomes large. Yield stress f_y = 450 MPa for the reinforcing steel allows a maximum elastic strain of 0.0023. Assuming an unbonded length[31] of 800 mm allows a maximum deformation of 1.8 mm prior to yield. Figs. 4.14(c) and 4.15(c) indicate that vertical reinforcement remains elastic for the Taft excitation but is expected to have yielded up to level 2 for the El Centro motion (F_{sb} = 80 kN).

In this study, however, all reinforcement is assumed to remain elastic; hence, further reference to the problem of yielding of the reinforcing bars is therefore related to minimization of gap opening, with attempts made to restrict the deformation in the steel to the elastic range.

Figs. 4.20(b) and 4.21(b) confirm the severity of compressive deformation at the outer joint edges and, for F_{sb} = 0 kN, at the vertical joi' also (7.30 m of wall base). At joint locations other than the wall edges, the figures show that for F_{sb} = 80 kN deformations are below the failure level.

Fig. 4.22 shows response envelopes across the base horizontal joint for the four earthquake excitations described earlier (Figs. 4.1(a) to 4.1(d)). Demonstrated is the fact that, despite scaling each earthquake acceleration record to match the intensity of El

Centro, base response still varies substantially between the four cases. Response is most severe for the El Centro excitation, while the Olympia record yields the least magnitude of gap opening and axial compressive deformation. More importantly, Fig. 4.22(a) shows that, with the exception of the El Centro excitation, gap opening is under 1.8 mm across the base, while Fig. 4.22(b) reveals compressive deformation at the base at or below 0.42 mm. Thus, if the exclusion of the El Centro record is justified due to its apparent severity, joint response at the base using the optimum slip load of 80 kN may be deemed acceptable, both in terms of reinforcement yielding and joint compressive crushing. Attempts to reduce response for the El Centro excitation follows.

4.5.2 Effect of Different Vertical Reinforcement

Thus far, vertical continuity for the structure has been provided by steel reinforcing bars. The total area of steel employed was equal to 0.5% of the gross cross-sectional area of the horizontal joint, distributed evenly across the joint. CPCA provisions for the seismic design of ductile flexural walls[30] require an amount of distributed reinforcing steel equal to at least 0.25 per cent of the joint area, and thus the 0.5 per cent employed is well above code minimum.

The concentrated reinforcement, in addition to the distributed steel, consists of an amount of steel equal to 0.5% of the joint area of one wall (width = 7300 mm) placed at each wall end region (near 0 and 7.3 m, and 7.3 and 14.6 m of the shear wall). This also is more than double the 0.2 per cent minimum that CPCA seismic provisions require for concentrated reinforcement in regions of plastic hinging,

or 0.1 per cent for other regions. The assumption is made that this additional steel has no influence on shear behaviour of the horizontal joints, but only serves to increase the tensile stiffness across the joints. Post-tensioning is studied separately, by placing ungrouted bars (anchored only at the base and roof) through the wall at the same locations. A total of four post-tensioning tendons is thus employed, each with a diameter of 31.8 mm and ultimate strength of 1035 MPa. A post-tensioning force of 492 kN per bar, or 60 per cent of the bar strength, is used.

Fig. 4.23 shows the effect of vertical continuity on base joint response. Presented are results for extra (concentrated) edge reinforcement and provision of post-tensioning bars along the panel edges. The results are for the more severe El Centro earthquake and a slip load of F_{sb} = 80 kN. Fig. 4.23(a) shows that significant reduction in maximum gap opening at the base occurs with added edge reinforcement, displaying a peak magnitude of 1.7 mm as compared to 4.3 mm with only distributed steel. Post-tensioning, on the other hand, has almost no effect on gap opening at the base. Results not shown, however, reveal reductions in gap opening from levels 4 and above with zero gap opening at the uppermost levels using post-tensioning, indicating that such vertical continuity is effective at the upper floor levels only. Compressive base deformation, shown in Fig. 4 23(b), shows little change both with the addition of edge reinforcement and post-tensioning. Edge deformation remains well above the axial deformation at ultimate joint strength and, thus, the problem of base edge crushing is not alleviated through the additional vertical reinforcement examined.

Larger bars of 38.1 mm diameter and an increased post-tensioning force of 1000 kN per bar (85 per cent strength) also did not eliminate the problem of gap opening in the lower joints, although gap opening was entirely eliminated at the top three joints. Bars of high stiffness, or an equivalent diameter of 61.8 mm, and post-tensioning force of 800 kN were then placed 5 per wall and anchored every second floor, for a total of 10 bars across the wall. This scheme showed slight improvement in gap opening of the lower joints, but still not sufficient to reduce maximum gap opening to less than the elastic limit of 1.8 mm. Maximum base gap opening reduced 12 per cent to 3.8 mm from 4.3 mm, while gap opening was eliminated at joint levels 3, 5, 6, 7, 8 and 9. Thus, even with relatively high area or post-tensioning force of the bars, gap opening at the base is not eliminated nor reduced to less than 1.8 mm. The fact that the tensile stiffness across the horizontal joints is significantly higher for additional edge reinforcement than with post-tensioning bars suggests that gap opening can be eliminated through proper detailing to allow for high stiffness at the joint edges.

Thus, while vertical steel remains elastic with the addition of edge reinforcement, corner crushing of the lowermost joint cannot be avoided for the apparently severe effects of the El Centro excitation. For this earthquake, the prototype structure equipped with tuned LSB connectors enjoys the benefits of no damage in the vertical joint as well as controlled slip action in the horizontal joints below the level to invite degradation in stiffness and strength; only crushing limited to the edges of the base horizontal joint is to be expected.

4.5.3 Effect of Base Isolation

To eliminate even the above remaining corner crushing at the base of the optimized LSB connected prototype structure, the properties of the lowermost joint were modified to simulate the effects of base isolation. This innovative concept of seismic design involves isolating the structure from the ground, thus limiting transmission of earthquake motions through the building. Seismic isolation has been reported to offer a desirable alternative to conventional methods of seismic design for precast structures[43], and studies[44,45,46] have confirmed the significant reduction in forces that this method produces. For the wall employed herein, steel friction slip plates were employed at the base, and base isolation was modelled by the removal of reinforcement at the base joint and the reduction of μ_f from 0.4 to 0.2. In addition to allowing unlimited base slip, the effect of limiting slip through the use of shear keys was studied. A limited slip distance of 20 mm was used in the latter case, with a stiffness in shear equal to approximately double that of the initial stiffness once joint slip reached 20 mm. Distributed reinforcement of 0.5 per cent was otherwise assumed at all other joint levels and vertical joint coupling by LSB connectors (F_{sb} = 80 kN) was maintained.

Further details for the actual construction of the base to allow for such properties was not pursued further, but rather the results of having such base isolating features was focused upon. Fig. 4.24 shows the effect of base isolation on base joint response. It is clear that both maximum gap opening and compressive deformation are greatly reduced, to levels which do not suggest either reinforcement

yielding nor joint crushing. Thus, although deformation remains relatively high at the joint ends, the magnitudes have been reduced to readily acceptable levels. Moreover, while unlimited slip produces optimum response, base response is not much different if slip is restricted to 20 mm.

Fig. 4.25 plots associated envelopes of overall response over the wall height. Optimum results with full base isolation are confirmed here; base shear is reduced from 3562 kN to under 1000 kN and maximum panel stress from 14.6 MPa to 7.5 MPa. The drawback with allowing unlimited base slip, however, is that the wall does not return to its original position following ground motion. Fig. 4.25(b) reveals that the lateral floor displacements are virtually identical over the height of the structure and only the 40 mm base slip needs to be considered in design. This slip is, however, essentially permanent and remains after termination of the seismic excitation.

To avoid the expected problems associated with such large permanent base slip, shear keys or stops may be employed to limit slip. A limit of 20 mm is imposed on base slip. Compared to the standard base, the maximum base shear increases only slightly to 3880 kN from 3560 kN, while maximum panel stress reduces from 14.5 to 10.5 MPa. On the other hand, a slip limit of 10 mm (not shown) produced an unacceptably high base shear of 6500 kN. Fig. 4.25(b) shows that the maximum base slip of 20 mm is accompanied by a maximum top lateral displacement of 42 mm, representing a relative 22 mm wall displacement. The corresponding LSB slip of Fig. 4.25(d) is reduced dramatically as base isolation now constitutes the principal mechanism of seismic energy dissipation and the LSB connectors tend to act as

non-slipping connections.

Envelopes of maximum horizontal joint response over the wall height are shown in Fig. 4.26. Figs. 4.26(a) and 4.26(b) indicate significantly reduced slip action due to base isolation from levels 2 upwards, but increased maximum and accumulated slip at level 1. The high level of slip at the base joint associated with base isolation also suggested considerable cyclic action, as accumulated slip of 209 mm and 246 mm accompany the maximum slip lengths of 20 and 40 mm, respectively. A reduction in deformation similar to that for the base joint noted in Fig. 4.24 is observed at other levels also. Figs. 4.26(c) and 4.26(d) show that maximum gap opening is under 1.6 mm and compressive deformation less than 0.42 mm at all levels.

Thus, the base joint designed for a coefficient of friction of 0.2 and a slip allowance of 20 mm is very effective in providing a damage free precast structure. It should be noted, however, that while small (less than one mm), gap opening may be considered an undesirable feature in seismic response. The latter restriction will thus limit the range of application of base isolation to structures lower than the 10 stories of the present wall.

4.6 CONCLUSIONS

Seismic performance of a 10-story LP shear wall equipped with LSB vertical connectors and nonlinear behaving horizontal joints (Type B wall from Chapter III) has been studied, in particular with respect to minimization of damage in the horizontal joints. Based upon the results obtained, the following observations are noted:

1. A slip load of 80 kN minimizes seismic response; this optimum

slip load is independant of ground motion type for equal intensities. However, additional data not presented also showed that the relative variation in response with slip load is unchanged even at different intensities (see Appendix Fig. K). 'Tuning' of buildings for optimal behaviour by adjustment of the connectors slip load thus involves consideration only of the building's properties.

2. Energy dissipation in the LSB connectors is maximized over the entire height of the wall at F_{sb} = 80 kN. As well, at this optimum slip load, nearly all the connectors contribute equally toward energy dissipation. By contrast, at higher slip loads, the contribution of the upper connectors is minimal.

3. Seismic behaviour of the prototype structure is characterized by panel rocking and vertical joint shear slip. While the latter is noted to improve response through energy dissipation, rocking causes both compressive stress concentrations and large gap opening in the horizontal joints. The result is crushing of the lowermost joint edges as well as stretching and yielding of the reinforcing bars. Although this problem is not eliminated at optimum slip load, minimization of joint deformations at F_{sb} = 80 kN is observed.

4. The problem of joint crushing and reinforcement yielding is restricted to the case of the El Centro excitation, despite the fact that the other earthquake excitations employed are scaled to match its intensity.

5. Slip of the reinforced horizontal joints is localized in nature, and low magnitudes of slip combined with essentially monotonic slip increase over time excludes both the possibility of energy dissipation and degradation due to shear slip in the joint.

6. For the El Centro excitation, joint crushing is observed at the base joint even for optimum slip load, showing a compressive deformation ductility factor of up to 4 at the base edges. Yielding of the reinforcement due to excessive gap pening occurs up to level 3. Neither of these damaging aspects in the horizontal joints, however, incurs instability toward overall wall response.

7. Provision of concentrated edge reinforcement serves to reduce gap opening in the lower joints to levels commensurate with elastic behaviour of the reinforcing steel. However, post-tensioned vertical bars reduce gap opening only at the upper joints, and gap opening in the lowermost joints remains generally unchanged.

8. Base isolation introduces a different mechanism of energy dissipation to the wall, namely that of shear slip of the base horizontal joint instead of LSB slip. Allowing unlimited slip at the base by reducing μ_f to 0.2 and no reinforcement allows considerable improvement in structural response, in terms of story shear, panel stress and joint deformation. Horizontal joint deformations are reduced to levels which do not invite crushing nor reinforcement yielding.

9. Problems with accompanying a base slip of 41 mm with full base isolation can be prevented through the use of stops or shear keys at the base. A predetermined limit of 20 mm does not show as great improvement in response as that with unlimited slip, but nevertheless eliminates damage to the horizontal joints and still shows substantial reductions in overall responses such as story shear and panel stress. Both forms of base isolation, however, removes the need for LSB connectors to dissipate energy and thus their effectiveness.

TABLE 4.1 · Earthquake records

	Description	(A)	(B)	(C)	(D)
(1)	1940 El Centro (N-S)	0.30	2.22	0.32	1.00
		-0.32	2.01		
(2)	1952 Taft (S69E)	0.32	3.68	0.32	2.11
		-0.28	4.90		
(3)	Newmark-Blume-Kapur Artificial	0.22	1.67	0.30	0.30
		-0.30	3.42		
(4)	1949 Olympia (N10W)	0.26	1.07	0.33	2.00
		-0.33	1.36		

(A) maximum acceleration (positive and negative) as ratio of gravity in scaled input record
(B) corresponding times (sec) of maximum accelerations
(C) maximum absolute acceleration from (A)
(D) factor applied to earthquake acceleration record to yield intensity of El Centro record. Intensity defined as area under the 5 per cent damped relative velocity response spectrum, between periods of 0.1 and 3.0 seconds.

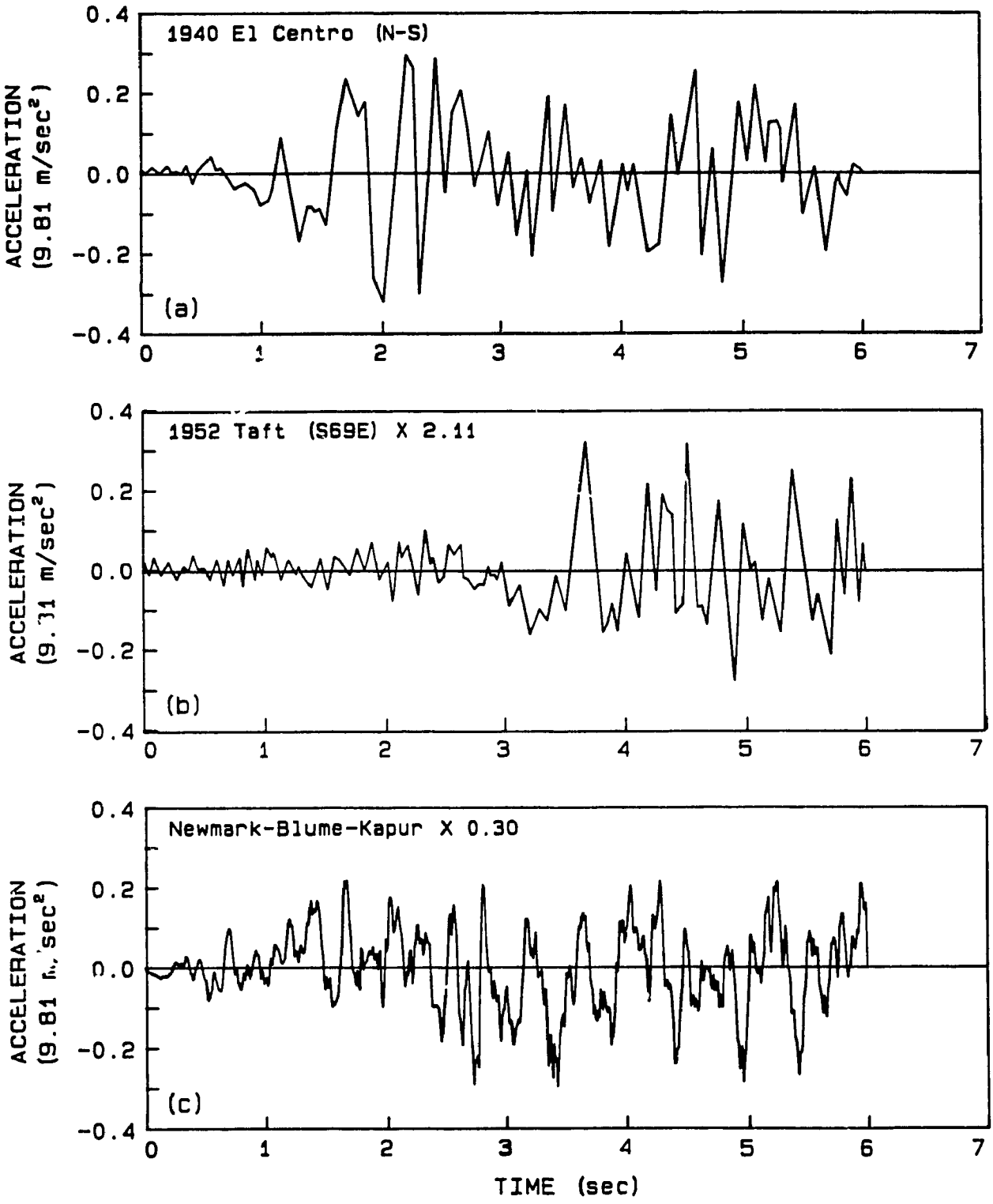

Figure 4.1 Earthquake excitations used for study, scaled to El Centro intensity.

Continued

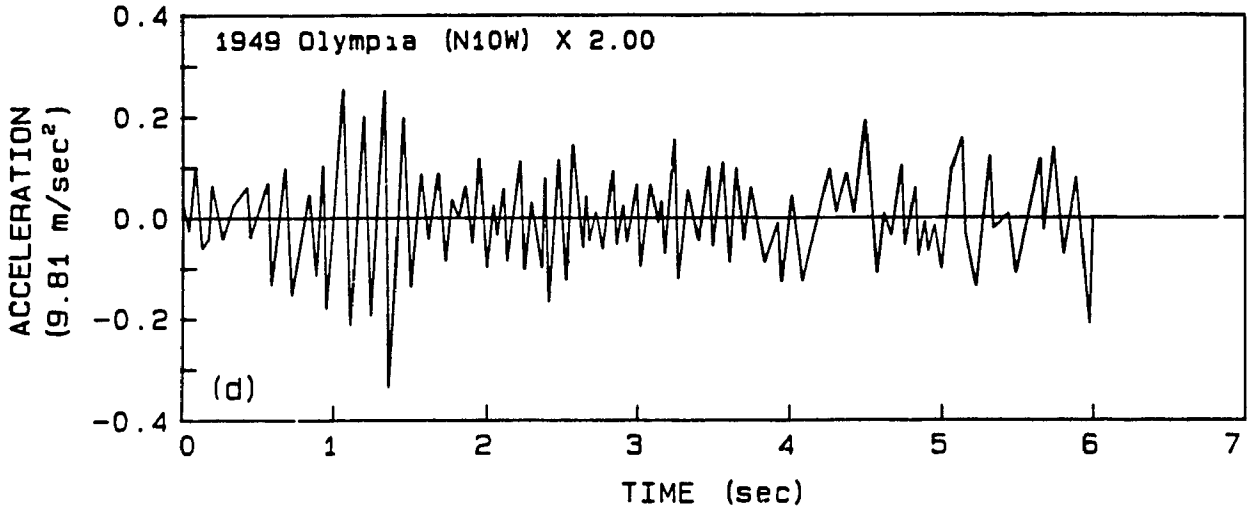

Figure 4.1 (Continued)

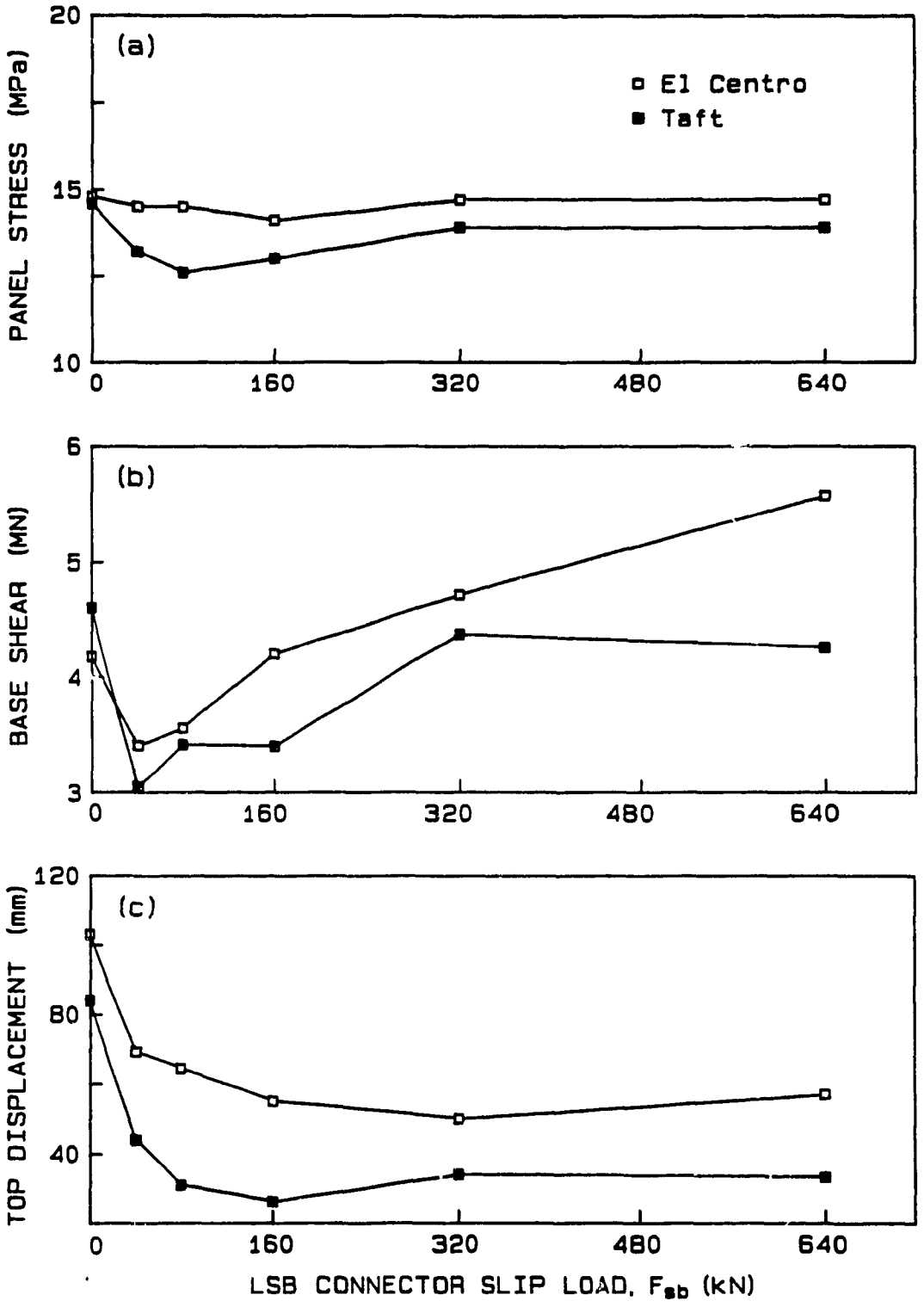

Figure 4.2 Effect of LSB connector slip load on overall response for El Centro and Taft excitations.

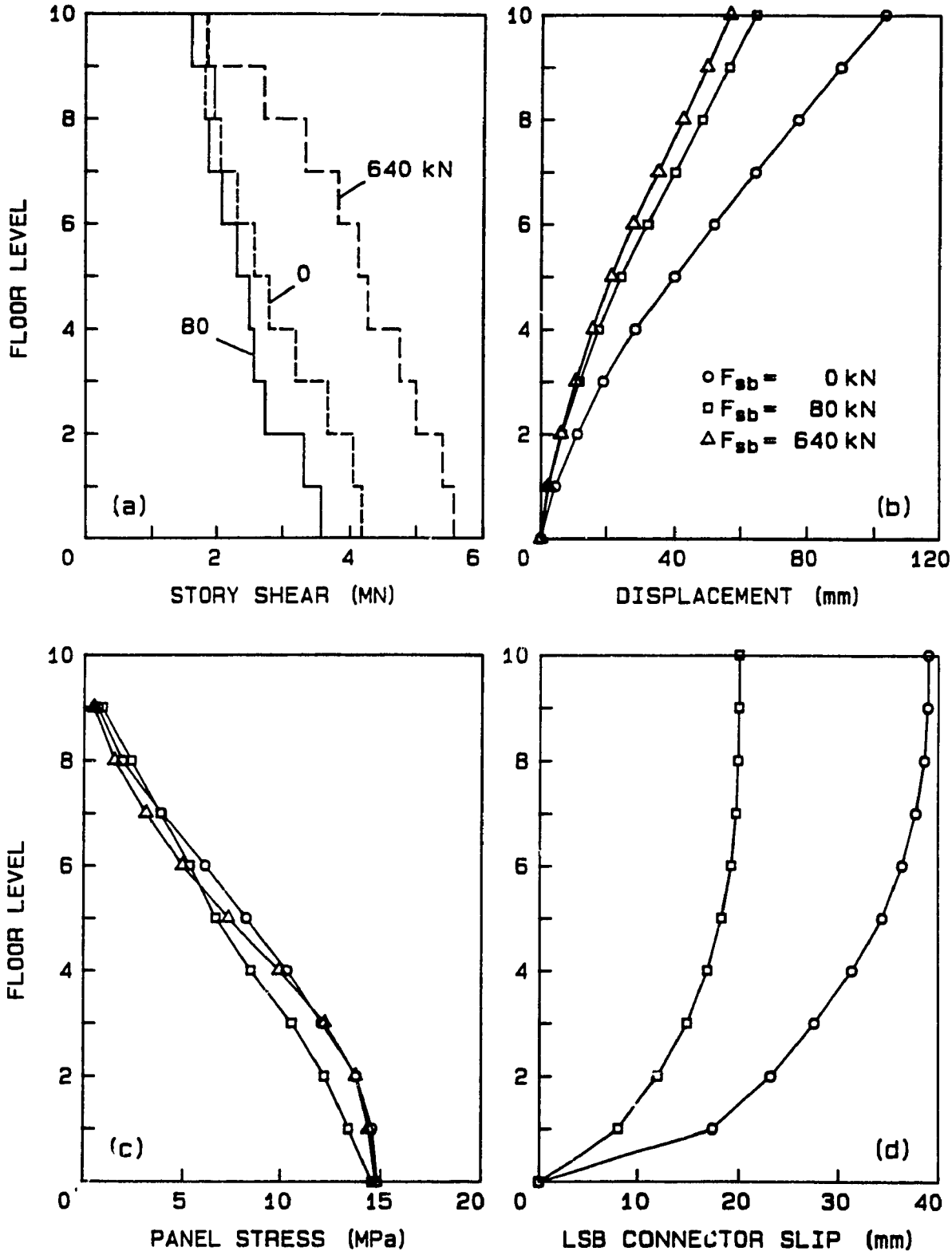

Figure 4.3 Comparison of envelopes of maximum overall response for slip loads of 0, 80 and 640 kN and El Centro excitation.

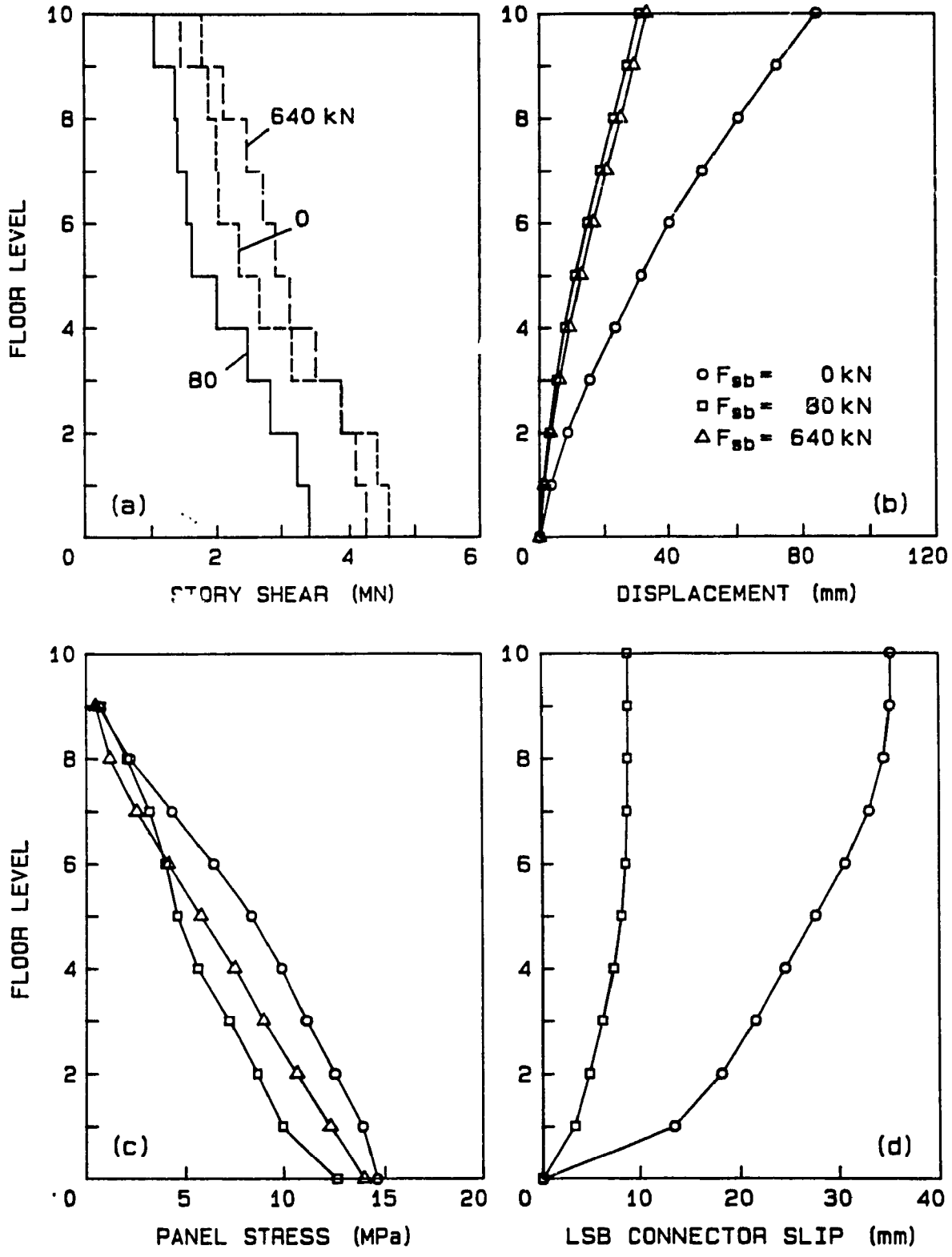

Figure 4.4 Comparison of envelopes of maximum overall response for slip loads of 0, 80 and 640 kN and Taft excitation.

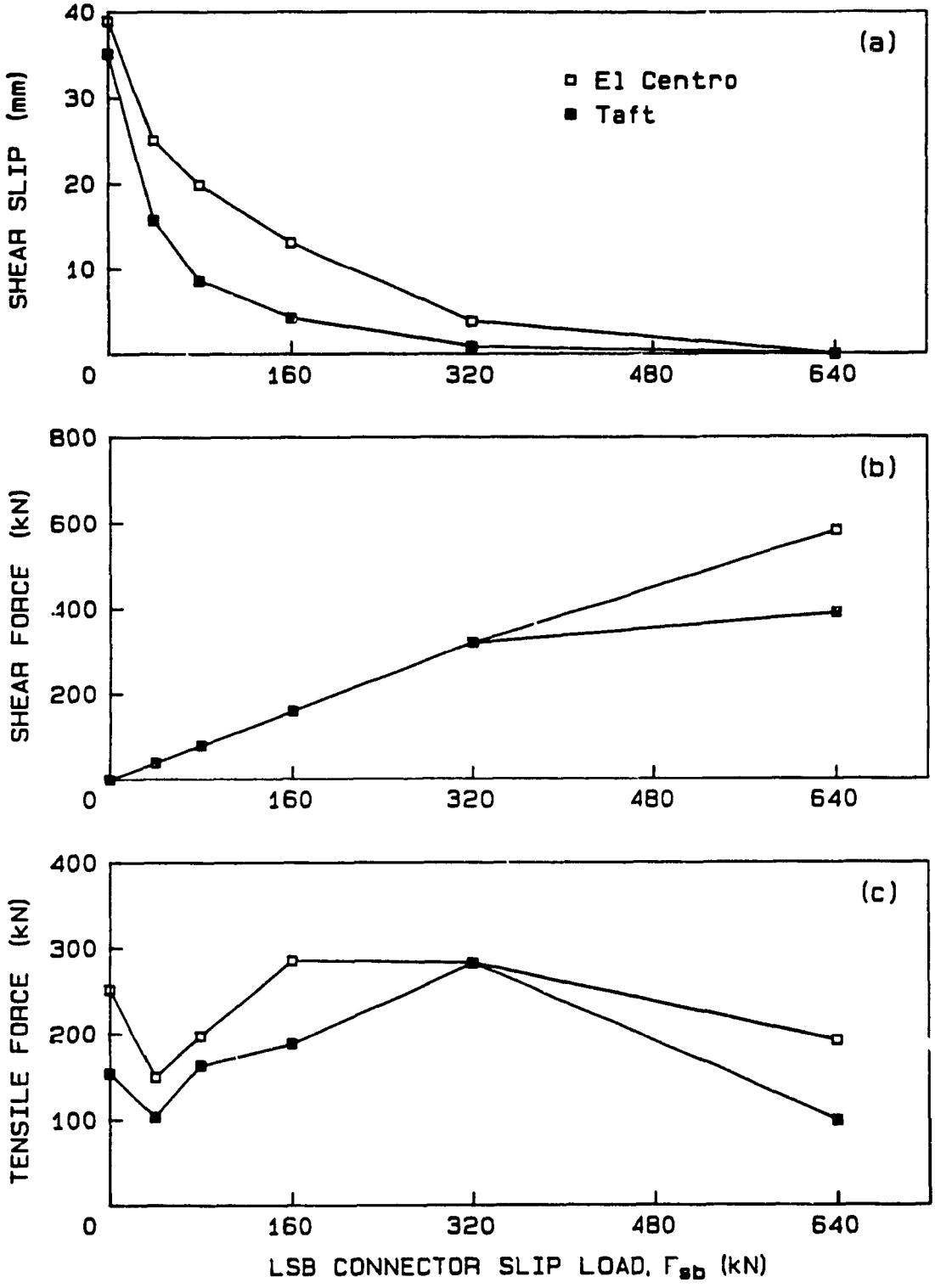

Figure 4.5 Effect of LSB connector slip load on connector response for El Centro and Taft excitations.

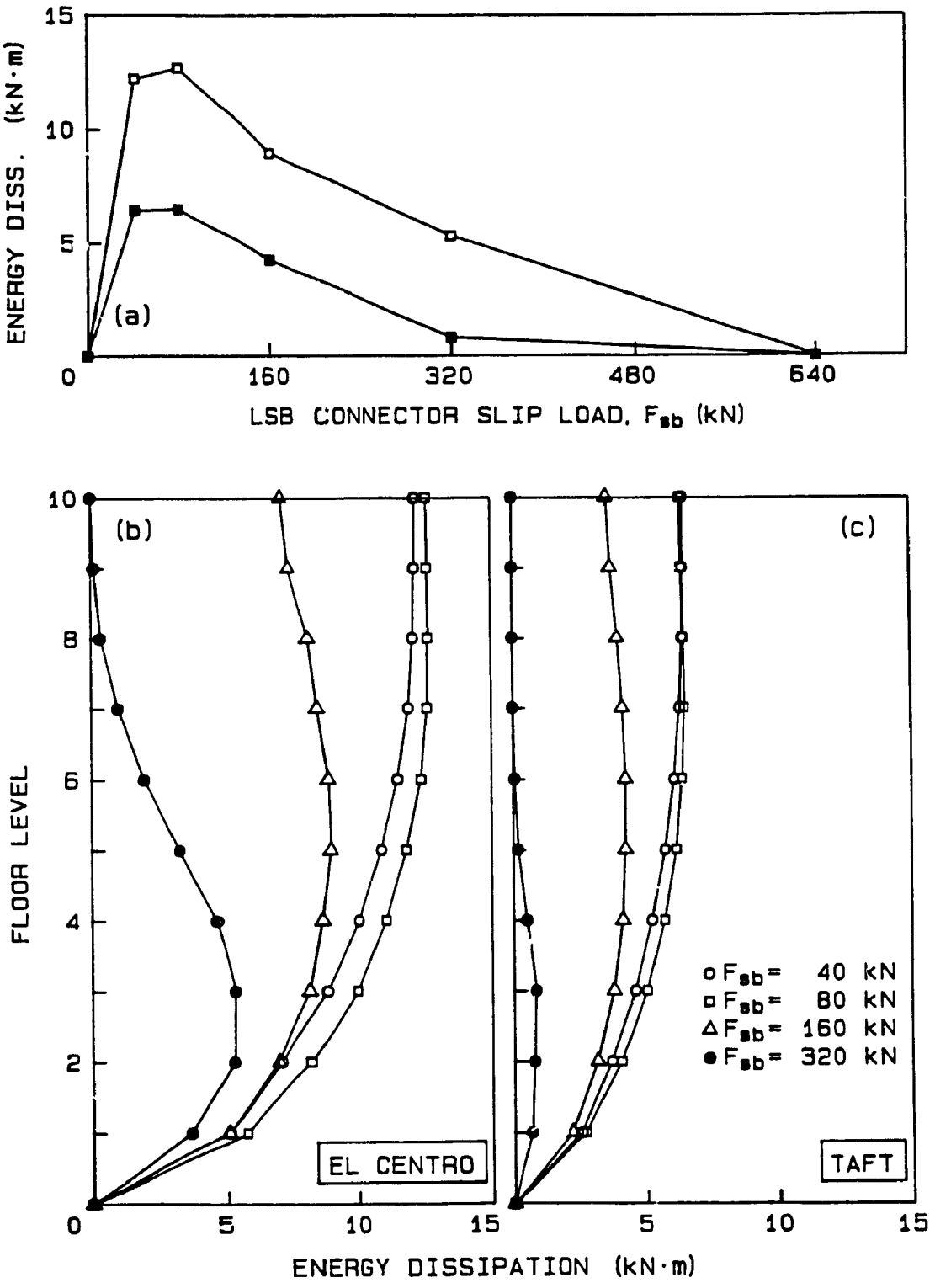

Figure 4.6 Energy dissipation in LSB connectors for El Centro and Taft excitations: (a) effect of LSB connector slip load on critical connector energy dissipation; (b) and (c) envelopes of energy dissipation for slip loads of 40, 80, 160 and 320 kN.

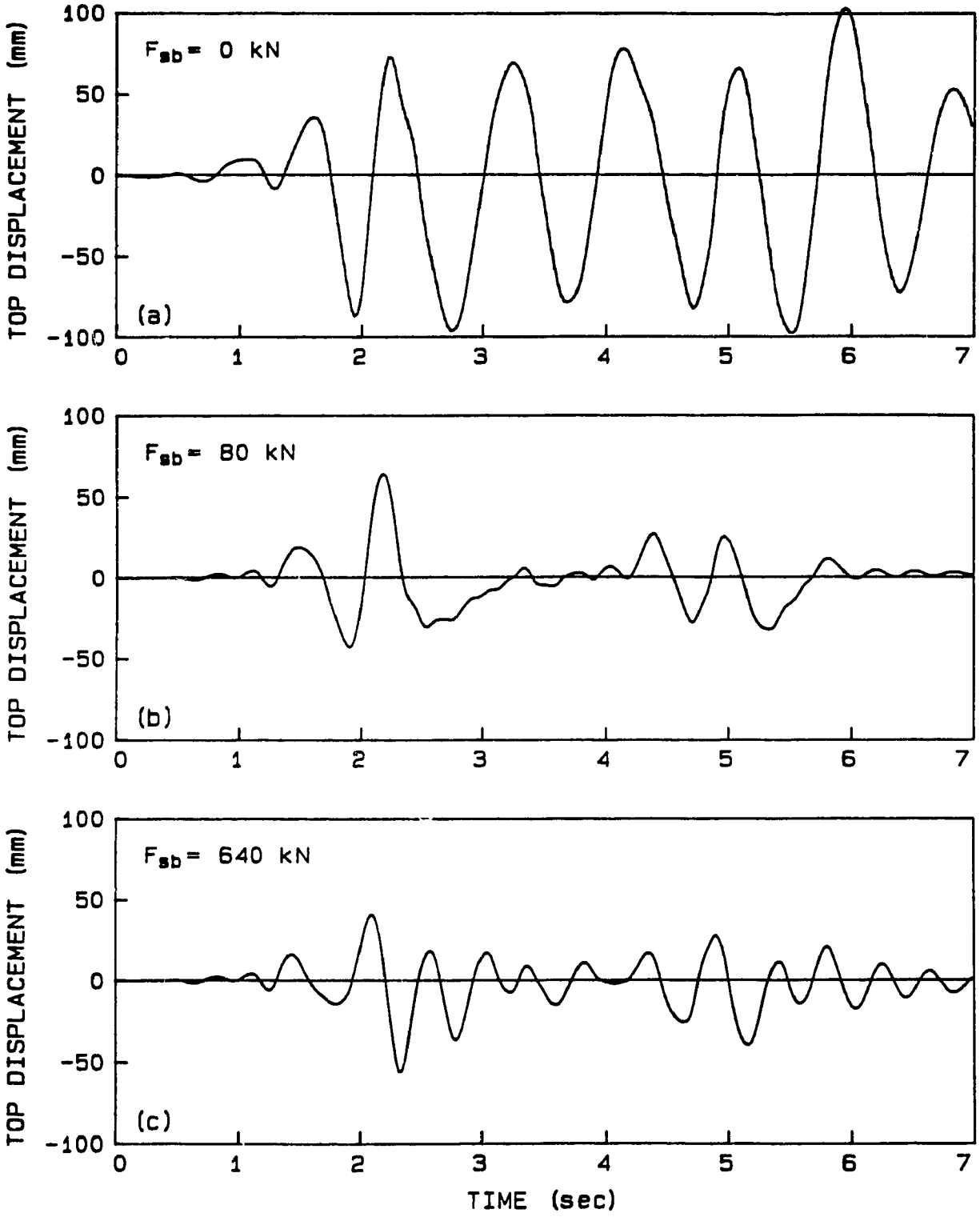

Figure 4.7 Top displacement time histories for slip loads of 0, 80 and 640 kN and El Centro excitation.

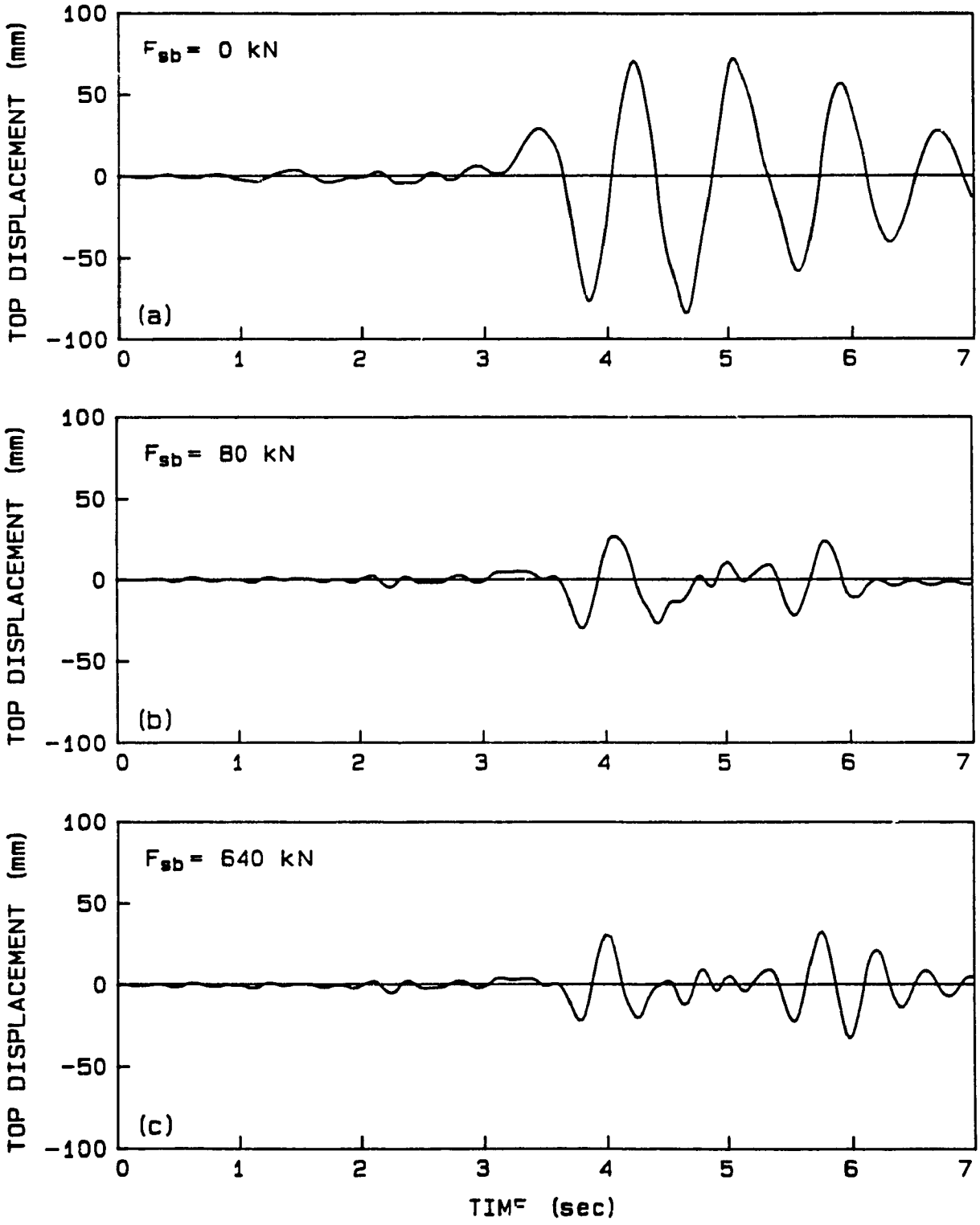

Figure 4.8 Top displacement time histories for slip loads of 0, 80 and 640 kN and Taft excitation.

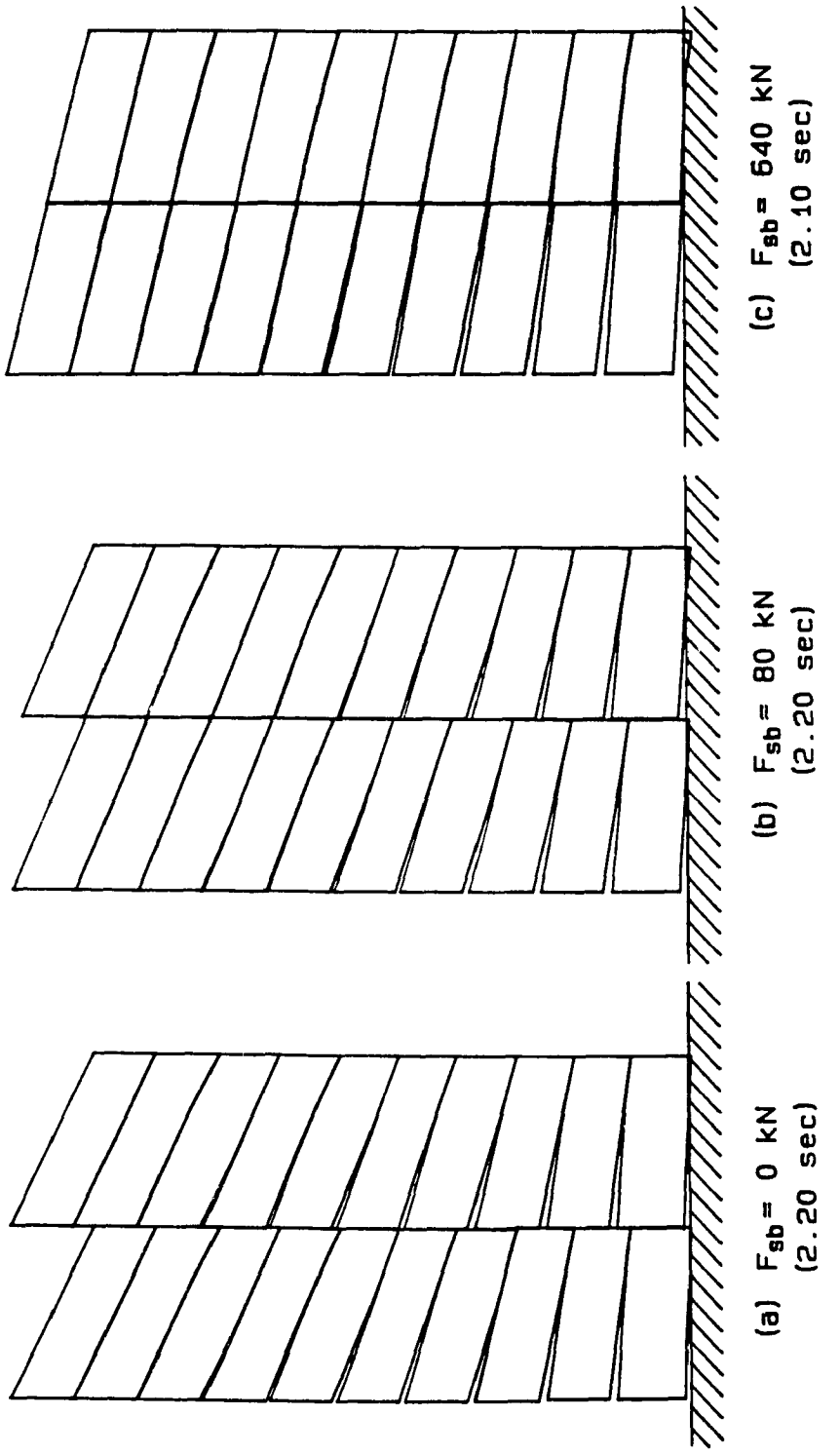

Figure 4.9 Deformed wall configurations at times of maximum positive displacement for slip loads of 0, 80 and 640 kN and El Centro excitation. X,Y deformation scales: (a) 5,125; (b) 5,125; (c) 5,125.

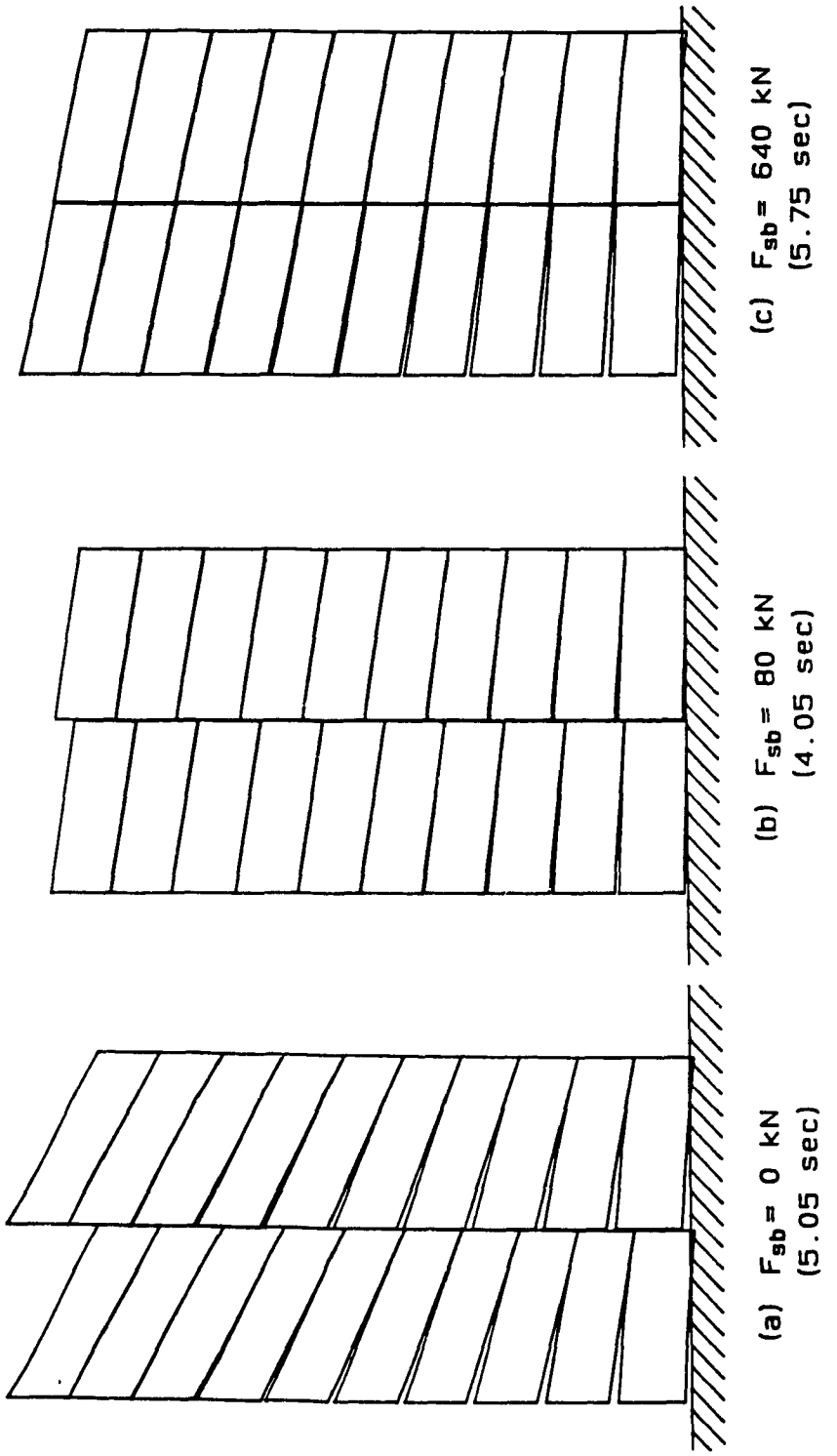

Figure 4.10 Deformed wall configurations at times of maximum positive displacement for slip loads of 0, 80 and 640 kN and Taft excitation. X,Y deformation scales: (a) 5,125; (b) 5,125; (c) 5,125.

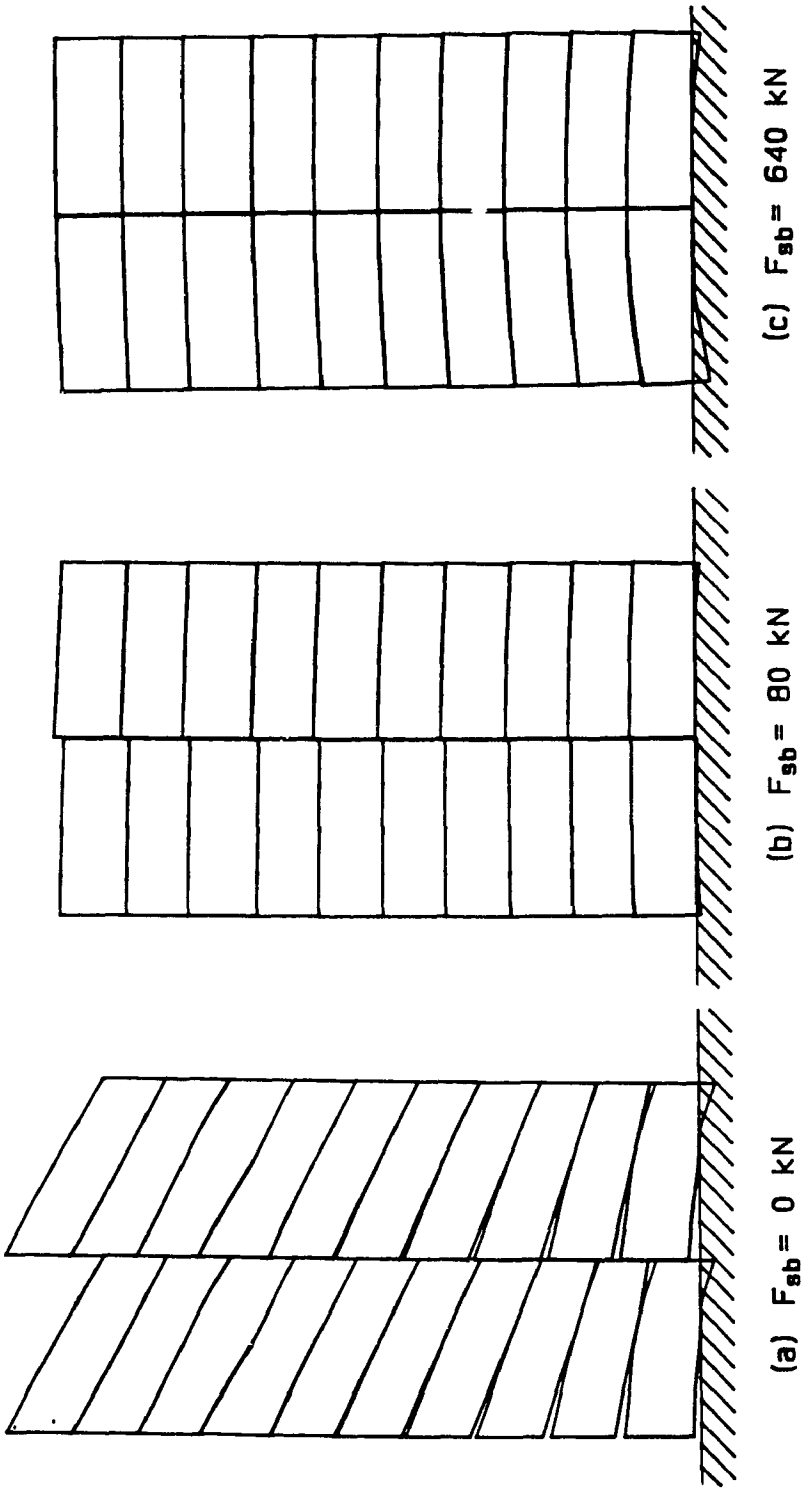

Figure 4.11 Deformed wall configurations at 0.75 seconds after termination of excitation for slip loads of 0, 80 and 640 kN and El Centro excitation. X,Y deformation scales: (a) 10,250; (b) 125,250; (c) 125,250.

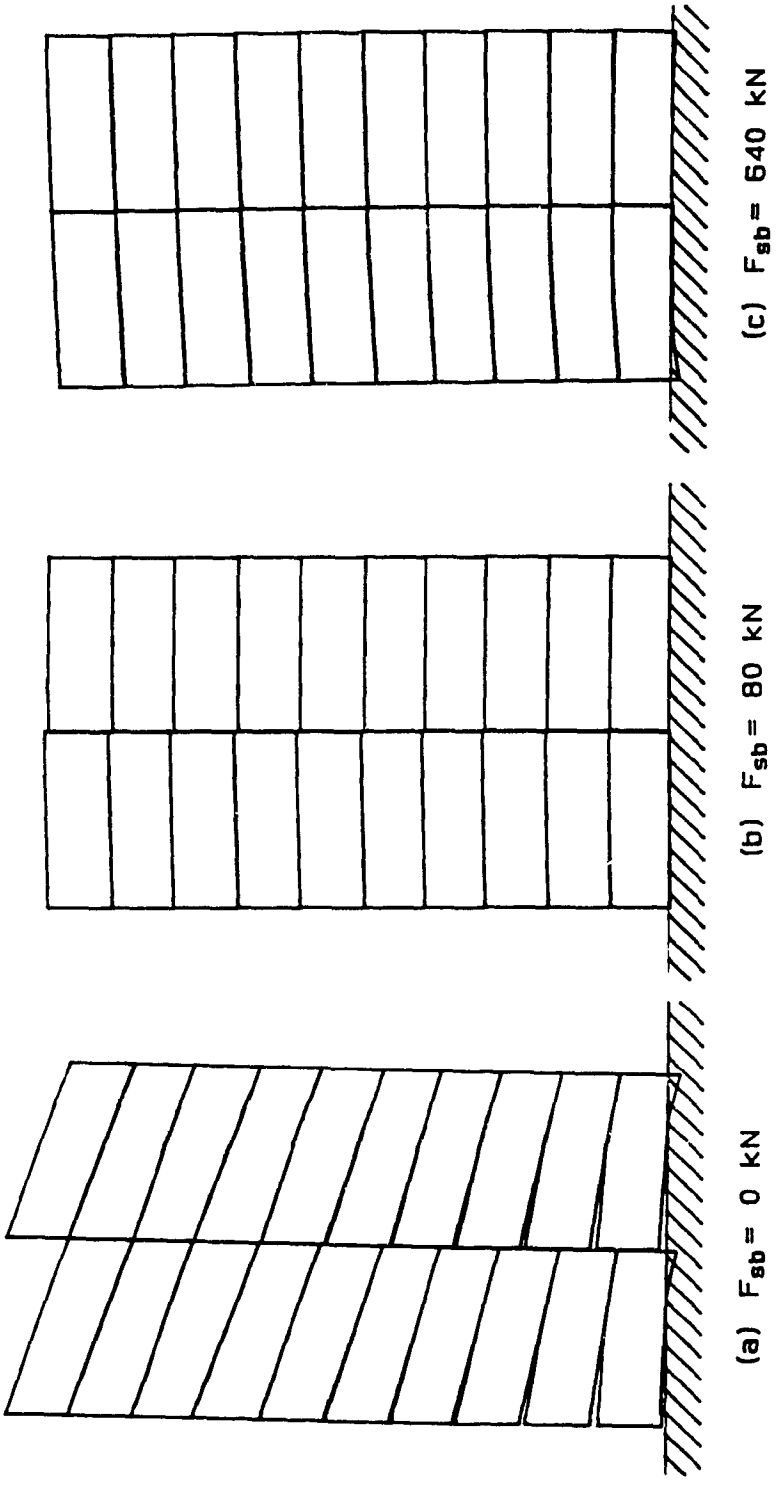

Figure 4.12 Deformed wall configurations at 0.75 seconds after termination of excitation for slip loads of 0, 80 and 640 kN and Taft excitation. X,Y deformation scales: (a) 10,250; (b) 125,250; (c) 125,250.

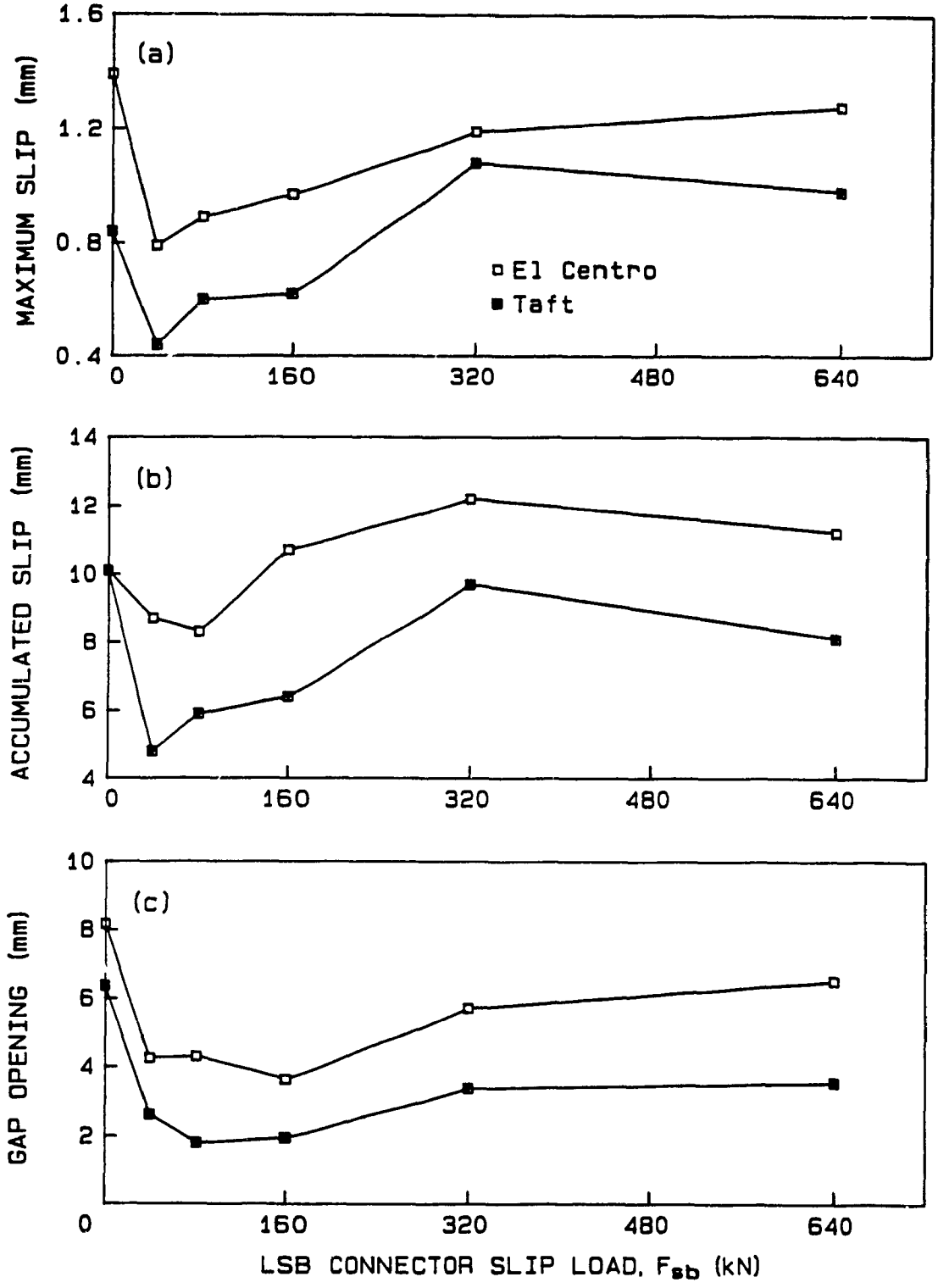

Figure 4.13 Effect of LSB connector slip load on horizontal joint response for El Centro and Taft excitations.

Continued

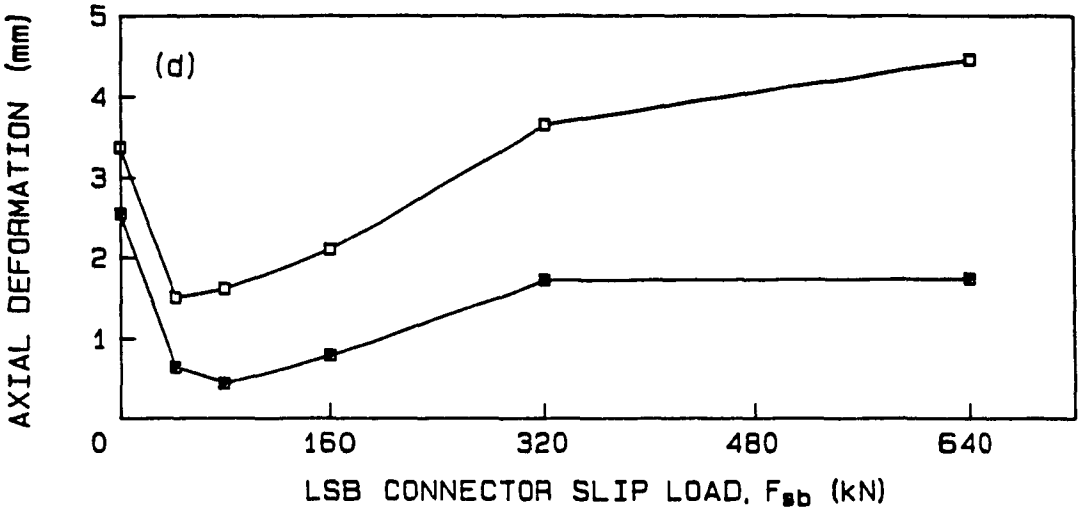

Figure 4.13 (Continued)

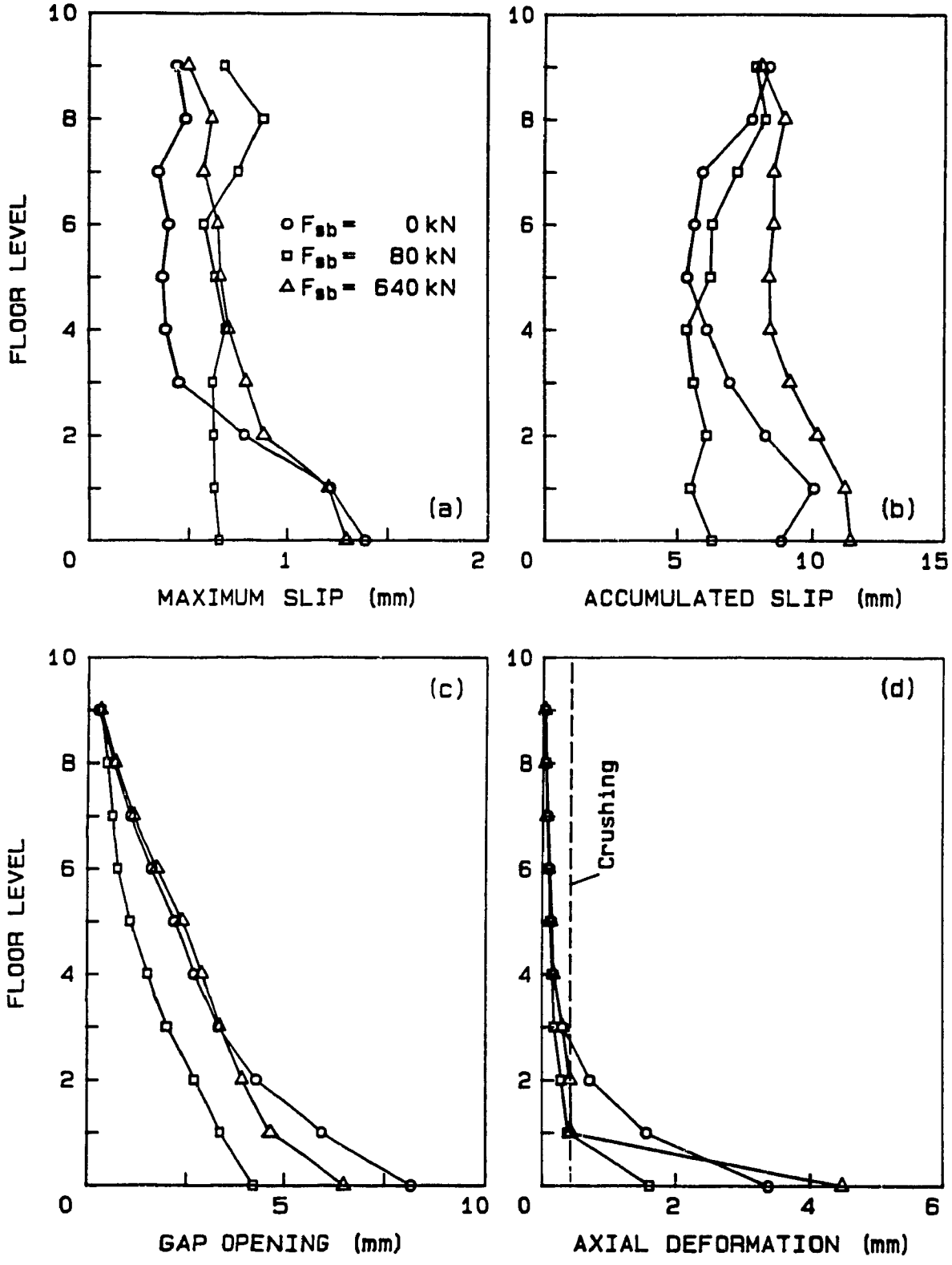

Figure 4.14 Comparison of envelopes of maximum horizontal joint response for slip loads of 0, 80 and 640 kN and El Centro excitation.

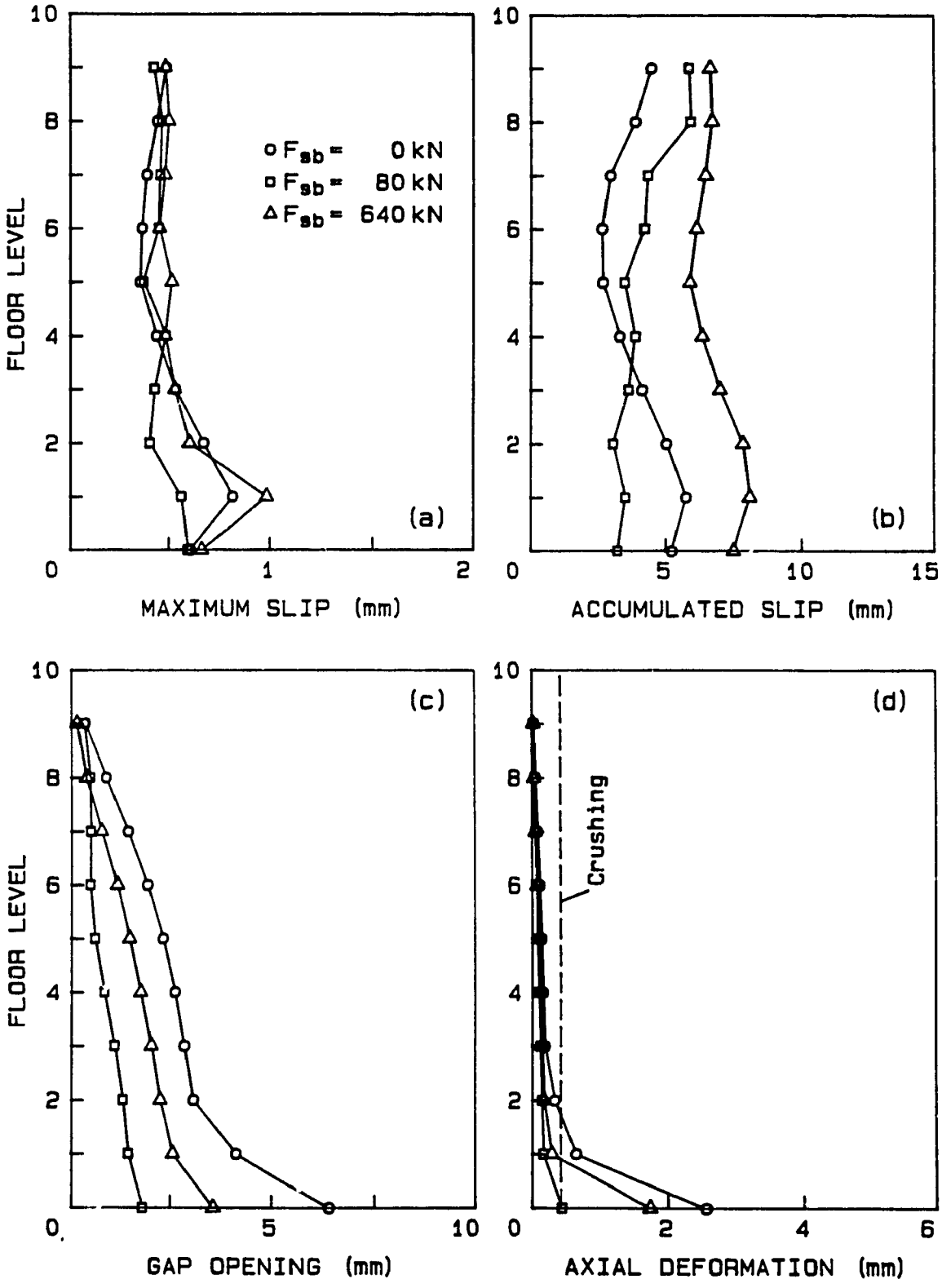

Figure 4.15 Comparison of envelopes of maximum horizontal joint response for slip loads of 0, 80 and 640 kN and Taft excitation.

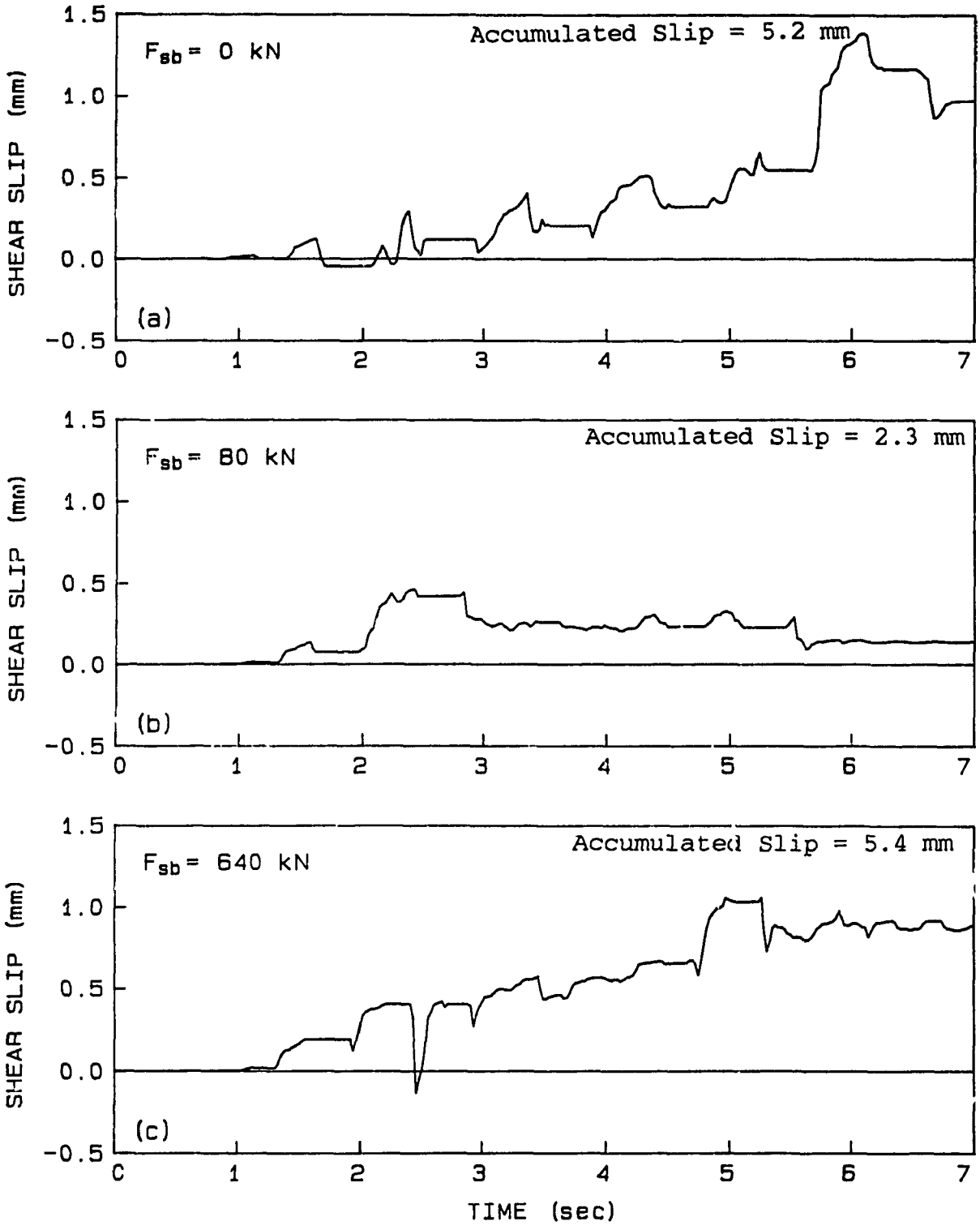

Figure 4.16 Time histories of localized horizontal joint shear slip at left edge of base for slip loads of 0, 80 and 640 kN and El Centro excitation.

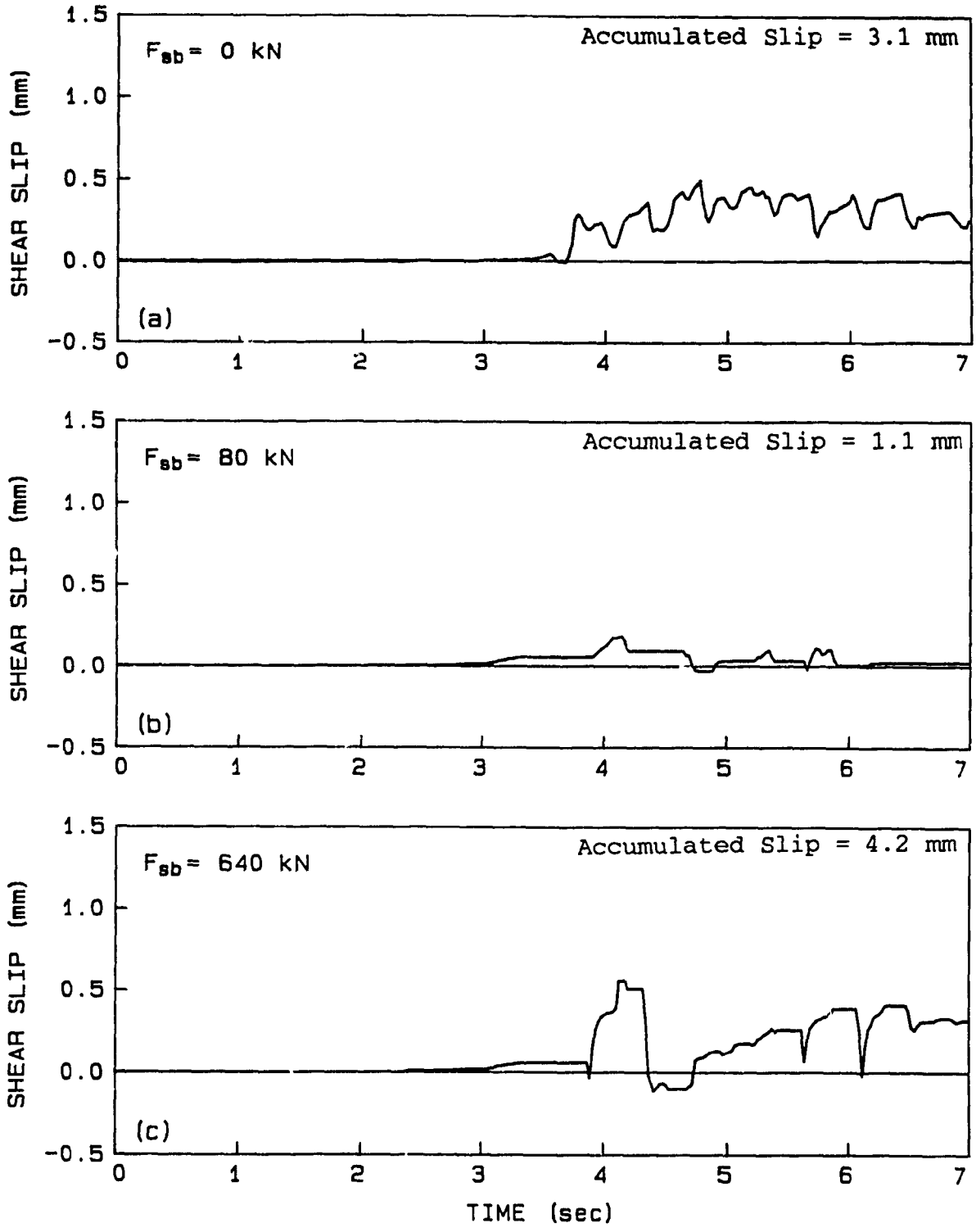

Figure 4.17 Time histories of localized horizontal joint shear slip at left edge of base for slip loads of 0, 80 and 640 kN and Taft excitation.

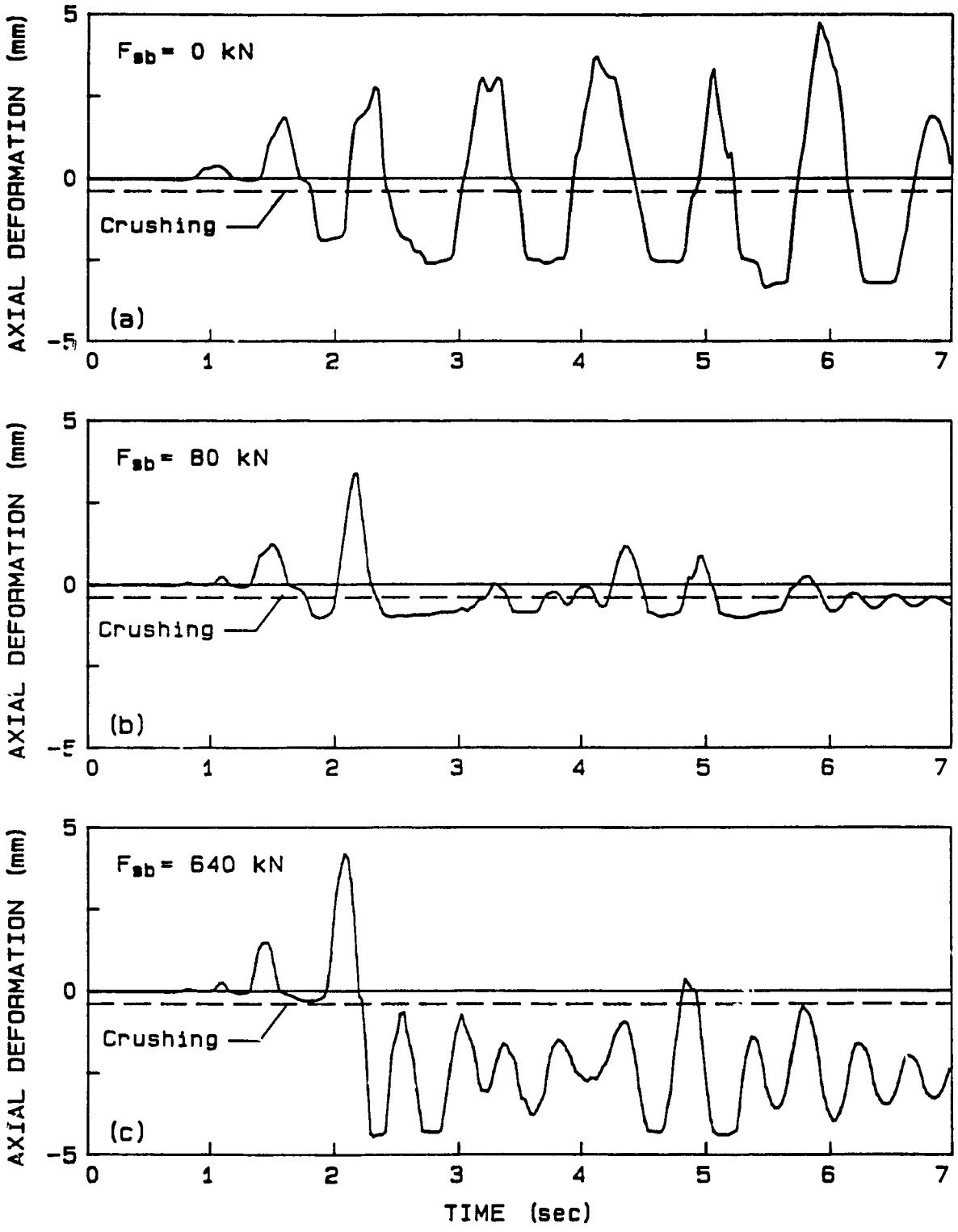

Figure 4.18 Time histories of horizontal joint axial deformation at left edge of base for slip loads of 0, 80 and 640 kN and El Centro excitation.

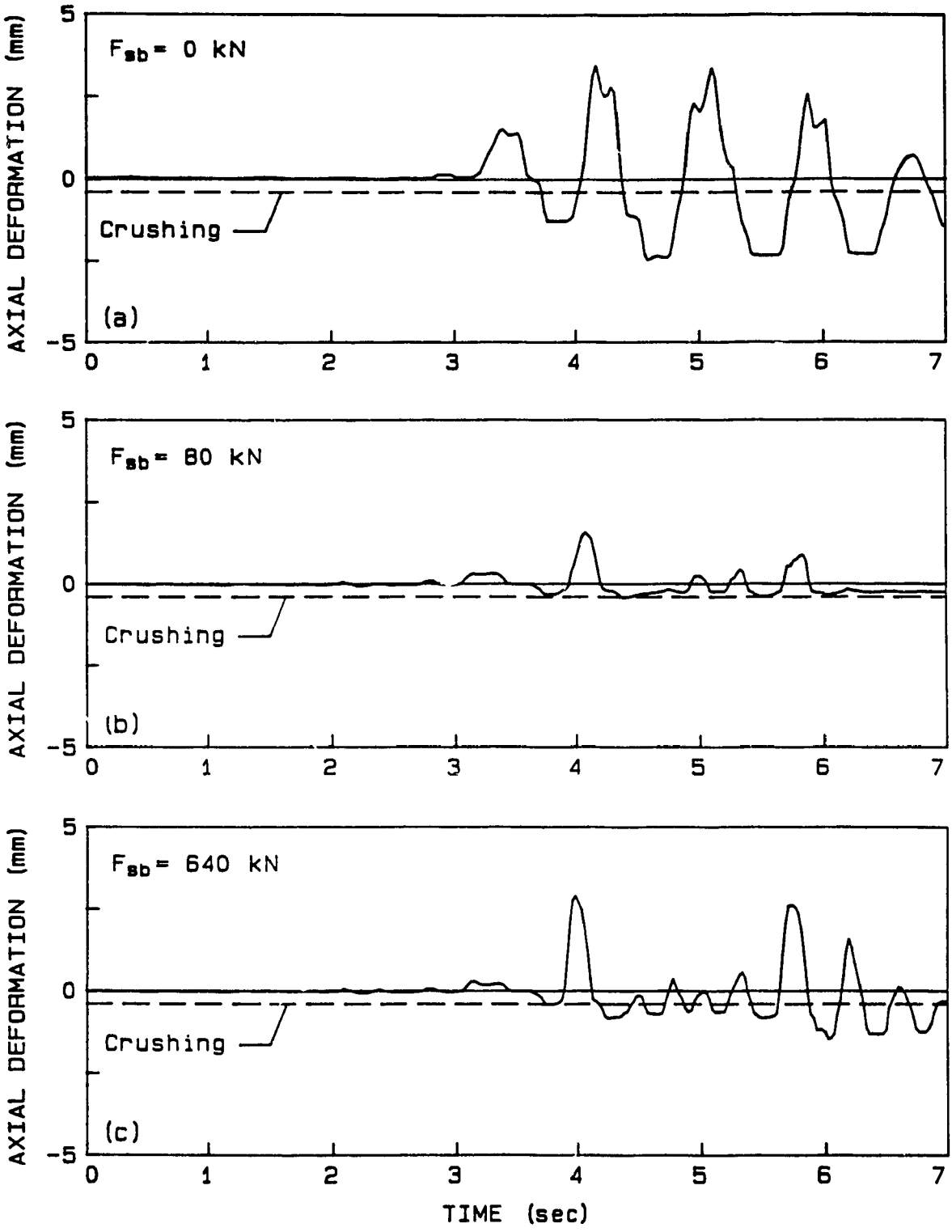

Figure 4.19 Time histories of horizontal joint axial deformation at left edge of base for slip loads of 0, 80 and 640 kN and Taft excitation.

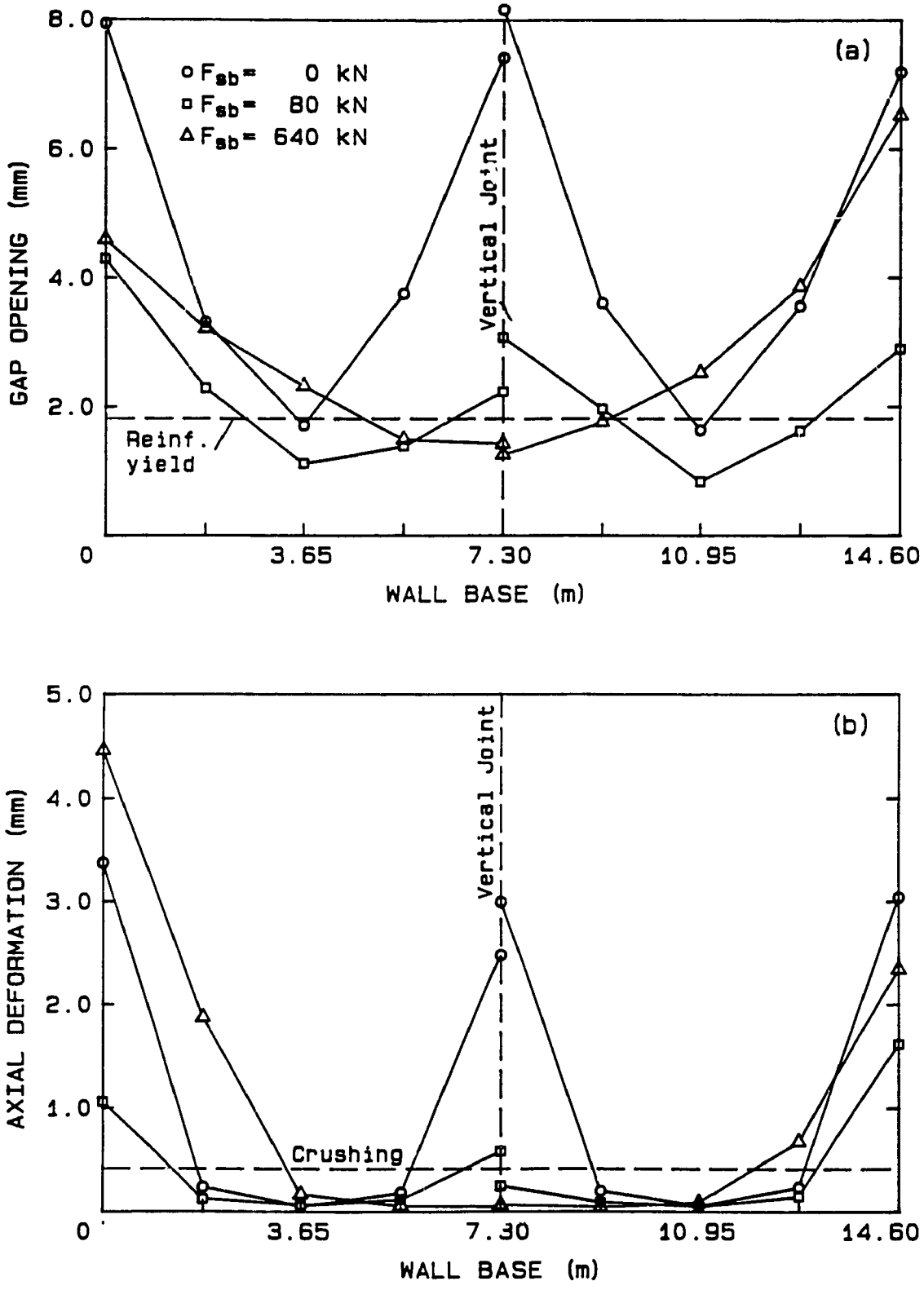

Figure 4.20 Horizontal joint response envelopes across base for slip loads of 0, 80 and 640 kN and El Centro excitation.

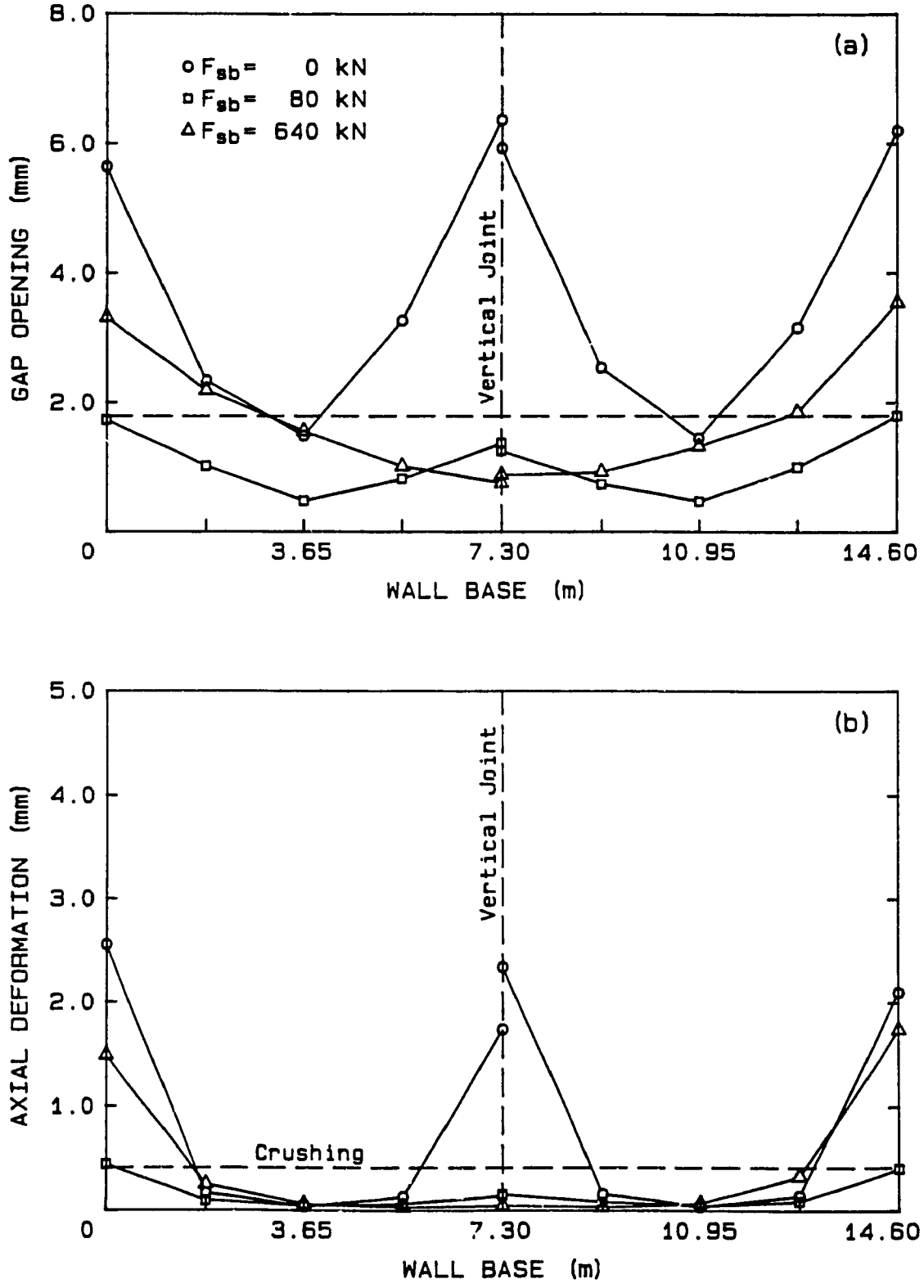

Figure 4.21 Horizontal joint response envelopes across base for slip loads of 0, 80 and 640 kN and Taft excitation.

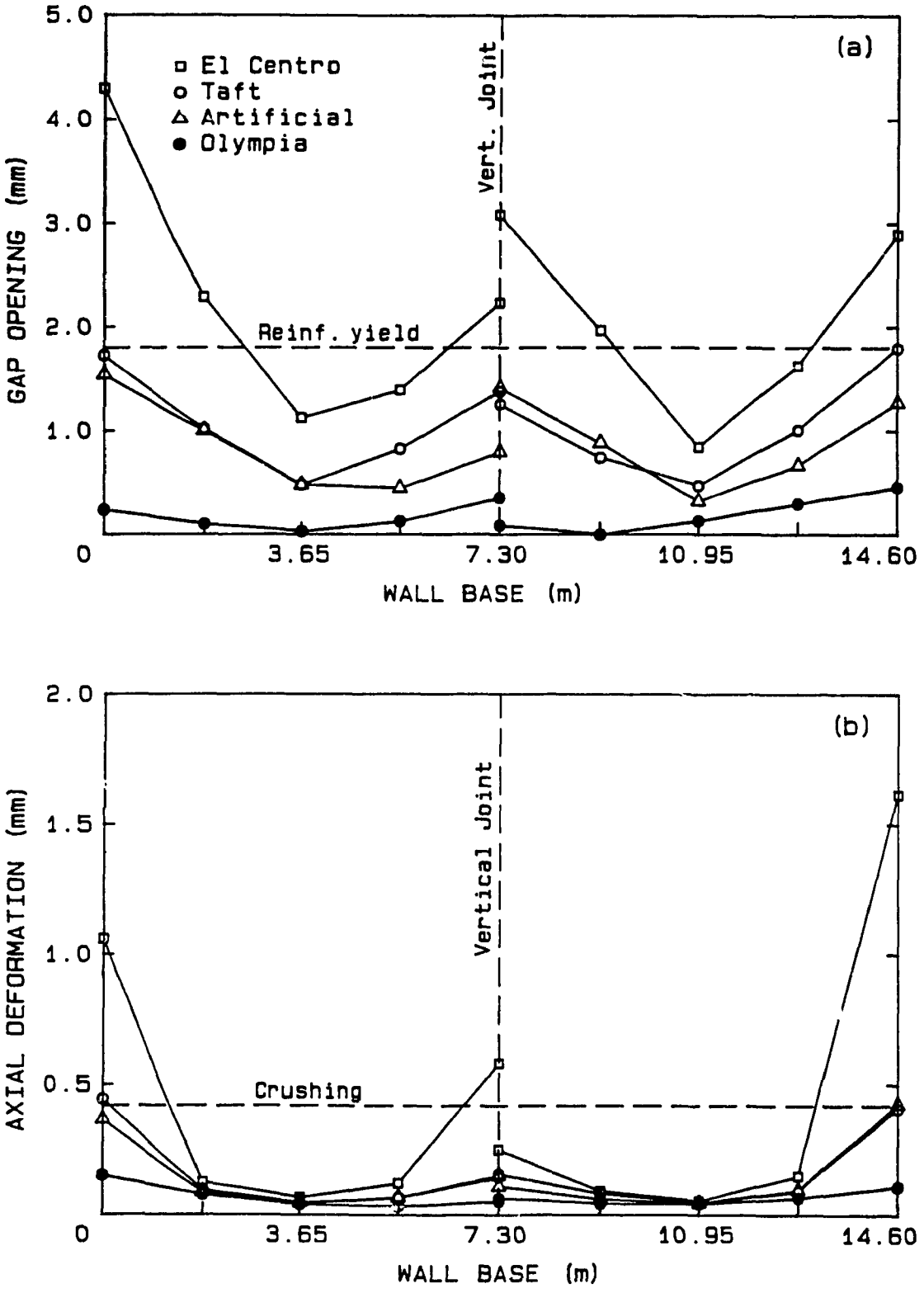

Figure 4.22 Effect of earthquake excitation on horizontal joint response envelopes across base at optimum LSB connector slip load.

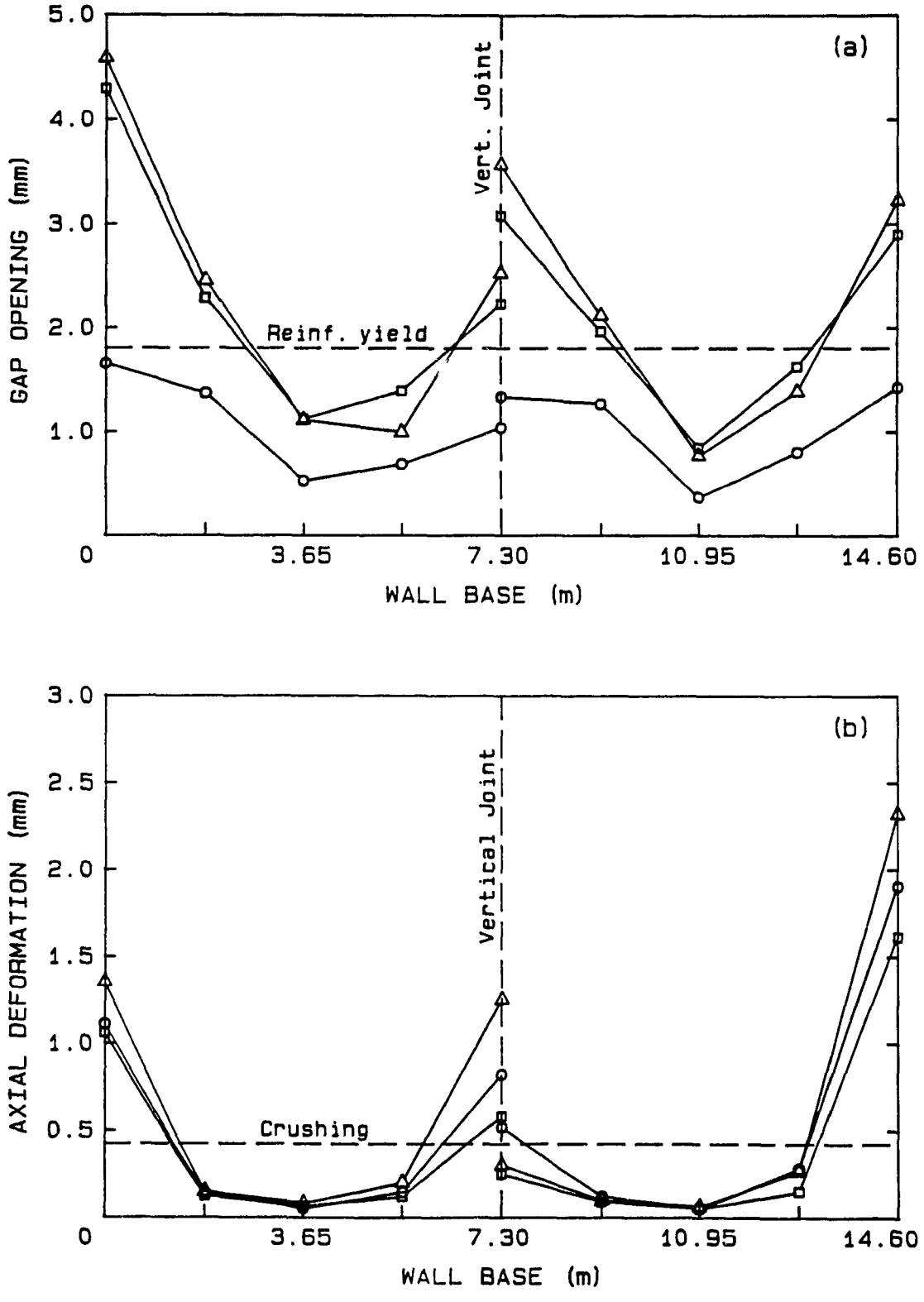

Figure [illegible] Effect of vertical reinforcement on horizontal joint response envelopes across base at optimum LSB connector slip load and El Centro excitation.

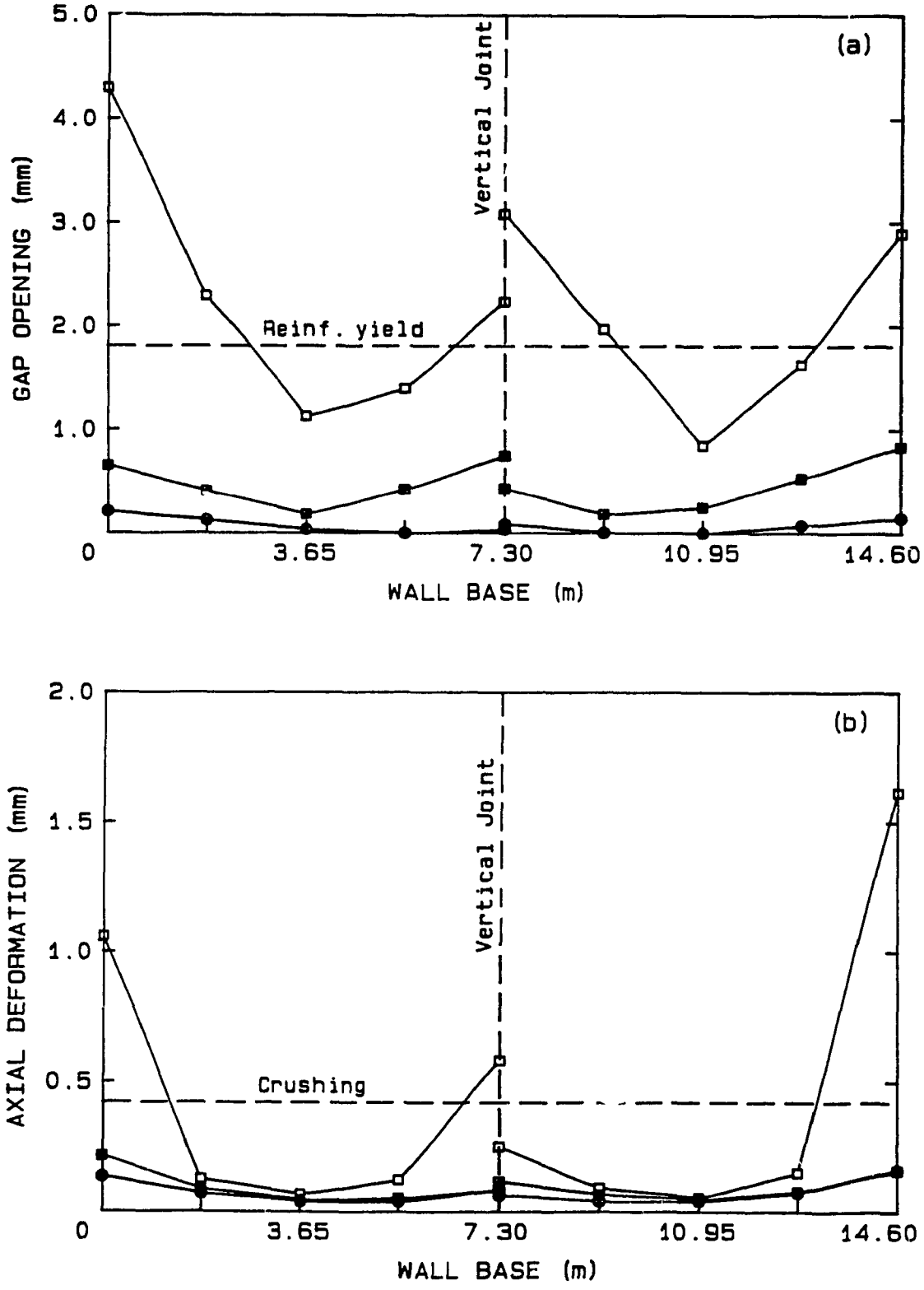

Figure 4.24 Effect of base isolation on horizontal joint response envelopes across base at optimum LSB connector slip load and El Centro excitation.

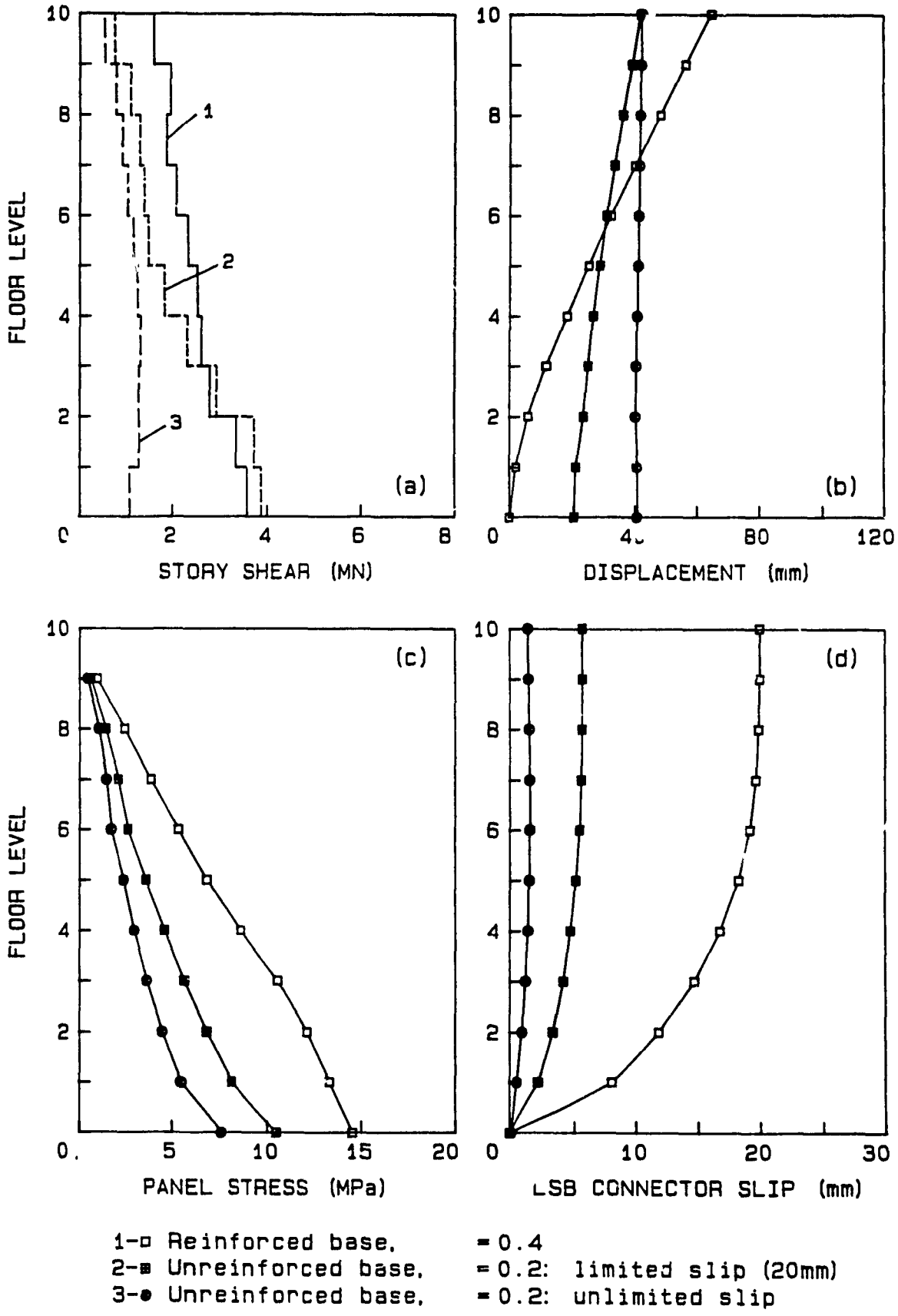

Figure 4.25 Effect of base isolation on envelopes of maximum overall response at optimum LSB connector slip load and El Centro excitation.

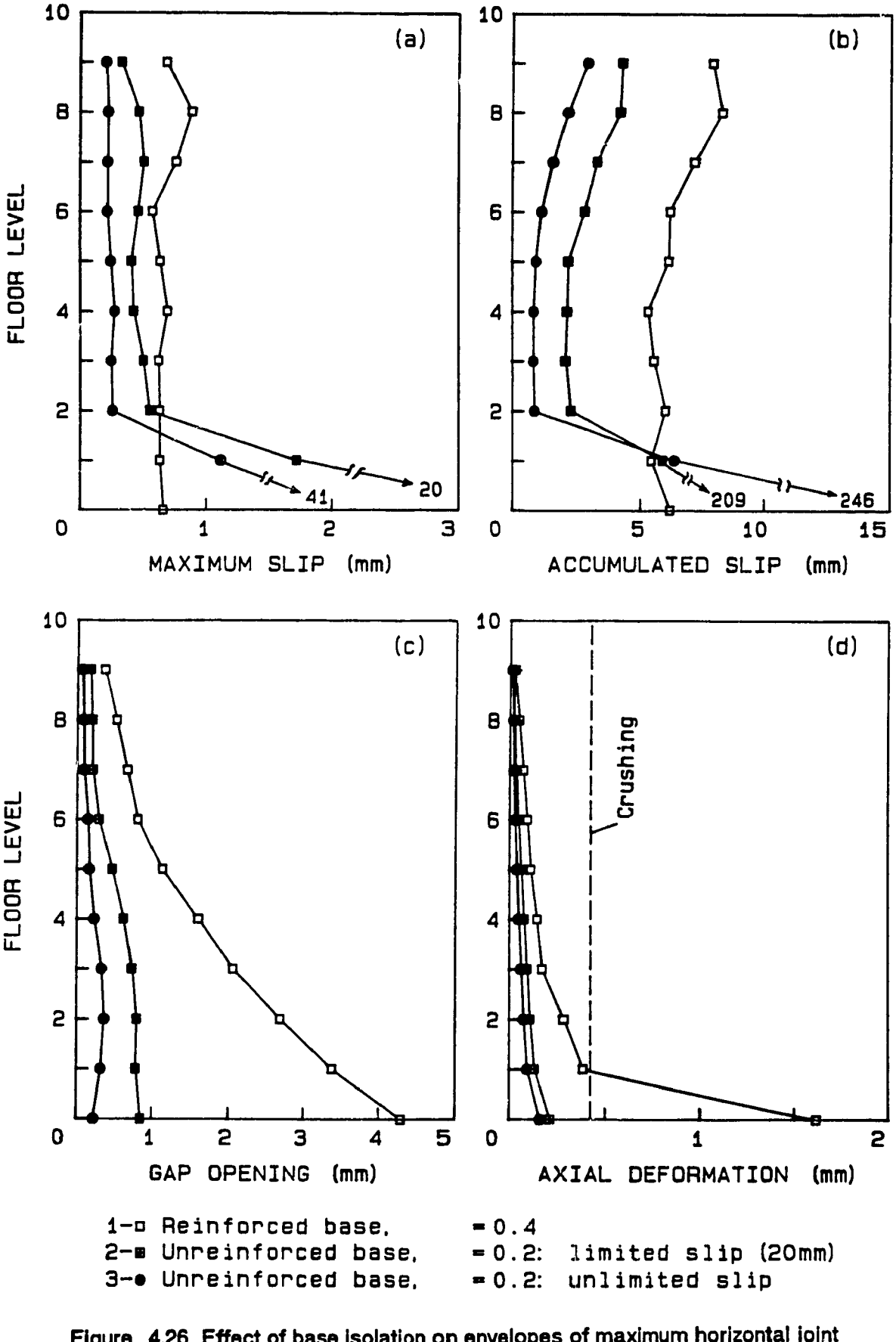

Figure 4.26 Effect of base isolation on envelopes of maximum horizontal joint response at optimum LSB connector slip load and El Centro excitation.

CHAPTER V

SUMMARY AND CONCLUSIONS

Nonlinear time-history dynamic analyses have been conducted to study the seismic performance of large precast panel shear walls. In particular, the nonlinear behaviour of horizontal and vertical joints has been examined. A finite element procedure was employed. Individual precast panels were modelled by 4-node plane stress rectangular elements with linear elastic behaviour, while horizontal and vertical joints were represented by discrete orthogonal spring elements with nonlinear inelastic behaviour. Transverse and vertical ties were modelled by elastic, uniaxial truss or bar elements.

A parametric investigation was performed on a 12-story multi-panel wall with unreinforced, wet platform horizontal joints and welded headed stud mechanical vertical joint connectors. The influence of horizontal joint coefficient of friction μ_f, post-tensioned vertical ties, connector shear strength and hysteretic behaviour, and distributed vertical reinforcement through the horizontal joints was studied. The following observations were made concerning response to seismic loading:

(1) Increased slip action of the horizontal joints was observed when low μ_f was employed; however, maximum slip length increased with higher μ_f. Improved response at low μ_f indicated the energy dissipating nature

horizontal joint slip. Vertical joint yielding was minimized at low μ_f.

(2) Horizontal tie forces designed according to PCA recommendations exceeded the elastic strength at the upper levels. However, vertical continuity in the form of both vertical post-tensioned ties and reinforcement reduced the forces to the elastic range. Integrity of the wall, particularly at the upper levels, was substantially improved.

(3) Inelastic action in the vertical joints with low connector strength F_y, as compared to the horizontal joints seen with low μ_f, resulted in far greater improvements in response. Low F_y, however, resulted in ductility demand exceeding the expected capacity of 36.

(4) An optimum design involving vertical continuity with either post-tensioning or reinforcement, and low connector yield levels to confine inelastic action largely to the vertical joints, was noted.

Seismic analyses were also carried out on a 10-story coupled shear wall with limited slip bolted (LSB) connectors along the vertical joint. These previously proposed mechanical friction-type connectors were designed to slip at a predetermined slip load F_{sb}, thus alleviating potential problems due to material yielding and excessive ductility demand. Results were studied for walls with continuous behaviour assuming strong horizontal joints (Type A) and walls having nonlinear behaving reinforced platform horizontal joints (Type B). An evaluation of the optimum slip load and integrity of the walls was

performed. Based on the results, the following observations and conclusions were made:

(1) A well-defined optimum slip load of F_{sb} = 160 kN was shown for Type A walls, while Type B walls had a less well defined slip load dependant on the particular response parameter. However, the structure could still be "tuned" to provide overall optimum response at a connector slip load less than for Type A joints (F_{sb} = 80 kN).

(2) Unreinforced Type B horizontal joints reduced the level of forces in the structure considerably, but was accompanied by relatively high maximum and accumulated slip.

(3) Inadequate length of the slotted bolt holes resulting in bearing of the bolts against the connector plates had no major effects on overall response in general. However, dramatic increases in the load on the LSB connectors were shown. Yielding of the connector anchorages was indicated, although failure of the LSB connector bolts was not anticipated. Based on the results, anchorage and bolt-shear capacities should be designed for approximately three times the optimum slip load F_{sb} to prevent these modes of failure if the required slot length is not provided.

(4) Both Types A and B walls exhibit excellent performance in terms of structural integrity, returning essentially to the undeformed configuration after the end of the earthquake. Reinforced Type B walls showed pronounced rocking during the earthquake, and some permanent, but not large, deformation along the vertical joint. Unreinforced

Type B walls, however, showed insignificant participation of the vertical joint while large and primarily non-corrective horizontal shear slip was noted.

Further study was conducted only for the Type B wall with reinforced platform horizontal joints. In particular, the level of damage incurred to the horizontal joints was accessed. The following was noted:

(1) The optimum slip load F_{sb} = 80 kN was independant of ground motion record, and maximized energy dissipation of the connectors over the entire wall height. Nearly all connectors contributed equally toward energy dissipation, while at higher slip loads, the contribution of the upper connectors was minimal.

(2) Rocking and vertical joint slip characterized behaviour of the wall. While rocking had beneficial aspects with respect to seismic response, resulting stress concentrations at the joint edges caused localized crushing of the horizontal joints. Large gap opening also resulted in reinforcement yielding. At F_{sb} = 80 kN, joint deformation was minimized but did not eliminate the preceding problems. Crushing was , however, confined to the base and limited to the edges, while yielding occured only up to level 3.

(3) Shear slip in the horizontal joints was localized in nature, and exhibited an essentially monotonic increase over time. Combined with the relatively low magnitudes of maximum slip, the possibility of

damage due to cyclic shear degradation was excluded.

(4) Reinforcement yielding was eliminated with concentrated edge reinforcement. Post-tensioned vertical ties eliminated gap opening at the upper levels, but did not reduce the level of gap opening at the lower joints below the yield displacement of the steel reinforcement. Localized base crushing was not removed by either form of vertical continuity.

(5) Base isolation allowed controlled energy dissipation at the base horizontal joint which significantly reduced the magnitude of forces in the structure. Both base crushing and reinforcement yielding was eliminated. A limit of 20 mm on the length of base slip increased the magnitude of story shears, but countered the potential problem that unlimited base slip may have. Damage to the horizontal joints was still prevented, and substantial reductions in structural response noted. However, base isolation eliminated the need for the LSB connectors to dissipate energy and thus their effectiveness.

REFERENCES

1. MacLeod, I.A., "Large Panel Structures" Handbook of Concrete Engineering 2nd Edition edited by Mark Fintel, Van Nostrand Reinhold Company Inc., New York 1985, pp. 514-535.

2. Fintel, M., "Performance of Precast Concrete Structures During Rumanian Earthquake of March 4, 1977" PCI Journal V.22, No.2, March-April 1977, pp. 10-15.

3. Tuchman,J. and Ichniowski,T., "Precast Frame Buildings Hit Heavily in Armenia" ENR (Engineering News-Record) January 12, 1989, pp. 11-13.

4. Oliva, M.G. and Shahrooz, B.M., "Shaking Table Tests of Wet Jointed Precast Panel Walls" Proceedings of the Eighth World Conference on Earthquake Engineering, California V.6 1984, pp. 717-724.

5. Harris, H.G. and Caccese, V., "Seismic Behaviour of Precast Concrete Large Panel Buildings Using a Small Shaking Table" Proceedings of the Eighth World Conference on Earthquake Engineering, California V.6 1984, pp. 757-764.

6. Becker, J.M. and Llorente, C., "The Seismic Response of Simple Precast Concrete Panel Walls" Proceedings of the 2nd U.S. National Conference on Earthquake Engineering, Stanford, California, August 1979, pp. 423-432.

7. Zhang, L. and Na, X., "Study of Seismic Behaviour of Precast Concrete Large Panel Buildings" Proceedings, Fifth Canadian Conference on Earthquake Engineering, Ottawa, 1987, pp. 875-880.

8. Becker, J.M., Llorente C. and Mueller, P. "Seismic Response of Precast Concrete Walls" Earthquake Engineering and Structural Dynamics, V.8, No.6, November-December 1980, pp.545-564.

9. Becker, J.M., Roesset, J.M., Llorente, C. and Lanham, K. "The Seismic Response of Precast Concrete Panel Buildings Considering Connection Behaviour" Proceedings, Sixth European Conference on Earthquake Engineering, Dubrovnik, Yugoslavia, V2. 1978, pp. 257-264.

10. Mueller, P. and Becker, J.M. "Seismic Characteristics of Composite Precast Walls", Proceedings, Third Canadian Conference on Earthquake Engineering, Montreal, Canada June, 1979 pp. 1169 - 1199.

11. Mueller, P. and Becker, J.M. "Seismic Behaviour of Precast Walls Coupled Through Vertical Connections" Proceedings of the Seventh World Conference on Earthquake Engineering, Istanbul,Turkey, V.7 September 1980 pp. 23-30.

12. Mueller, P., "Behavioural Characteristics of Precast Walls" Proceedings, Workshop on Design of Prefabricated Concrete Buildings for Earthquake Loads, ATC-8, Applied Technology Council, Berkeley, California, 1981, pp. 277-308.

13. Pall, A.S., Marsh, C. and Fazio, P., "Friction Joints for Seismic Control of Large Panel Structures" PCI Journal V.25, No.6, November-December 1980, pp. 38-61.

14. Shricker, V. and Powell, G.H., "Inelastic Seismic Analysis of Large Panel Buildings' Report No. EERC 80-38, Earthquake Engineering Research Center, University of California, Berkeley, 1980, 282 pp.

15. Kianoush, M.R. and Scanlon, A., "Seismic Response of Large Panel Coupled Wall Systems" Proceedings, Fifth Canadian Conference on Earthquake Engineering , Ottawa 1987, pp. 251-256.

16. Kianoush, M.R. and Scanlon, A., "Inelastic Seismic Response of Precast Concrete Large Panel Coupled Shear Wall Systems" Report No. 134 Department of Civil Engineering, University of Alberta 1986, 300 pp.

17. Scanlon, A., and Kianoush, R., "Behaviour of Large Panel Precast Coupled Wall Systems Subjected to Earthquake Loading" PCI Journal V.33, No. 5, September-October 1988, pp. 124-151.

18. Pekau, O.A., Zielinski, Z.A., and Lee, A.W.K., "Precast Shearwalls Subjected to Local Panel Collapse" ACI Journal V.82, No.3, May-June, 1985, pp. 324-330.

19. Pekau, O.A., Zielinski, Z.A., Lee, A.W.K. and Hum, D., " Dynamic Effects of Panel Failure in Precast Concrete Shearwalls" ACI Journal, V.85, No.3 May-June 1988, pp.277-285.

20. Harris, H.G. and Iyengar, S., "Full Scale Tests on Horizontal Joints of Large Panel Structures", PCI Journal V.25, No.2, March-April 1980, pp. 72-92.

21. Canadian Prestressed Concrete Institute, Metric Design Manual: Precast and Prestressed Concrete, Ottawa, 1982.

22. Spencer, R.A., and Neille, D.S., "Cyclic Tests of Welded Headed Stud Connections" PCI Journal V.21, No.3, May-June 1976, pp. 70-83.

23. Ollgard, J.G., Slutter, R.G., and Fisher, J.W., "Shear Strength of Connectors in Lightweight and Normal-Weight Concrete", Engineering Journal, V.3, No.2, April, 1971, pp. 55-64.

24. 'Design and Construction of Large-Panel Concrete Structures" PCA Report No.2, 1976, 133 pp. and PCA Report No.4, 1977, 156 pp.

25. Desayi, P., and Krishan, S., "Equation for the Stress-Strain Curve of Concrete" ACI Journal, Proceedings V.61, No.3, March 1964, pp. 345-350.

26. Mattock, Alan H., "Shear Transfer Under Cyclically Reversing Loading Across an Interface Between Concretes Cast at Different Times" Report No. SM 77-1 Department of Civil Engineering, University of Washington, Seattle, June 1977, 86 pp.

27. Verbic, B. and Terzic, N., "Behaviour of Panel Connections of Multi-Story Large Panel Buildings Under Cyclic Loading" Proceedings, Sixth European Conference on Earthquake Engineering Dubrovnik, Yugoslavia, 1978 V3. pp. 215-22.

28. MacGregor, J.G., "The Shear Strength of Reinforced Concrete Members" ASCE-ACI Task Committee 426 on Shear and Diagonal Tension of the Committee on Masonry and Reinforced Concrete of the Structural Division, ASCE Journal of Structural Division, 1973, pp. 1091-1187.

29. Paulay, T., Park, R. and Phillips, M.H., "Horizontal Construction Joints in Cast in Place Concrete" ACI, Special Publication No. SP-42, Detroit, 1974.

30. Concrete Design Handbook, CSA Standard CAN3-A23.3-M84 Canadian Portland Cement Association, Ottawa 1985.

31. Cheema, T.S. and Klingner, R.E., "Tensile Anchorage Behaviour of Deformed Reinforcement in Grouted Concrete Masonry", ACI Journal V.82, No.3, May-June 1985, pp. 372-380.

32. Pekau, O.A., "Influence of Vertical Joints on the Earthquake Response of Precast Panel Walls" Building and Environment, V.16, No.2, 1981, pp. 153-162.

33. Takeda, T., Sozen, M.A., and Nielson, N.N., "Reinforced Concrete Response to Simulated Earthquakes" Journal of Structural Division, ASCE, V.96, Part 2, December 1970, pp. 2557-2574.

34. Mondkar, D. and Powell, G., "ANSR-I: General Purpose Computer Program for Analysis of Non-Linear Structural Response" Report No. EERC 75-37, Earthquake Engineering Research Center, University of California, Berkeley 1975, 150 pp.

35. Bathe, K.J., Wilson, E.L. and Peterson, E.F., "SAP IV: A Structural Analysis Program for Static and Dynamic Response of Linear Systems" Report No. EERC 73-11, Earthquake Engineering Research Center, University of California, Berkeley, 1973.

36. Harris, H.G. and Abboud, B.E., "Cyclic Shear Behaviour of Horizontal Joints in Precast Concrete Large Panel Buildings" Proceedings of a Workshop on Design of Prefabricated Concrete Buildings for Earthquake Loads, Applied Technological Council, 1981, pp. 403-438.

37. Handbook of Steel Construction, Canadian Institute of Steel Construction, Willowdale, Ontario, 1986.

38. Mattock, A.H., "The Shear Transfer Behaviour of Cracked Monolithic Concrete Subjected to Cyclically Reversing Shear", Report No. SM 74-4, Department of Civil Engineering, University of Washington, Seattle, 1974.

39. ASCE, "Tall Building Criteria and Loading", Monograph on Planning and Design of Tall Buildings, Vol. 1B, 1980, pp. 251-386.

40. Martin, L.D. and Korkosz, W.J., Connections for Precast Prestressed Concrete Buildings Including Earthquake Resistance, Prestressed Concrete Institute, Illinois, 1982.

41. Nigam, N.C. and Jennings, P.C. "SPECEQ: Generation of Response Spectra Digitized at Equal Time Intervals" NISEE/Computer Applications, University of California, Berkeley, 1968.

42. Freedman, S. "Properties of materials for Reinforced Concrete" Handbook of Concrete Engineering 2nd Edition edited by Mark Fintel, Van Nostrand Reinhold Company Inc., New York 1985 pp. 169 - 251.

43. Mayes, R.L., Buckle, I.G. and Jones, L.R., "Seismic Isolation - A Solution to the Earthquake Problems of the Precast Concrete Industry" PCI Journal V.33, No.3, May-June 1988 pp. 25-57.

44. Mostaghel, N. and Khodaverdian, M. "Dynamics of Resilient-Friction Base Isolator (R-FBI)" Earthquake Engineering and Structural Dynamics V.15, No. 3, April 1987, pp. 379 - 390.

45. Lee, D.M. and Medland, I.C. "Base Isolation for Earthquake Protection of Multi-Storey Shear Structures" Earthquake Engineering and Structural Dynamics V.7, No.6, November-December 1979, pp. 555 - 568.

46. Eisenberger, M. and Rutenberg, A. "Seismic Base Isolation of Asymmetric Buildings" Eng. Structures V.8, No.1, January 1986, pp. 2 - 8.

47. National Building Code of Canada, National Research Council of Canada, Ottawa, 1985

APPENDIX A

LOADING

A.1 Loading for 12-story multi-panel shear wall

Assume a dead load P = 3.8 kPa (80 psf) acting on all floors. From Fig. 2.1(b), the tributary area acting on an interior wall is thus:

$$A_t = (11 + 2.44 / 2) \text{ X } 8.46 = 103.4 \text{ m}^2$$

Thus, the weight due to load P per floor is given by:

$$W_f = 3.8 \text{ X } 103.4 = 396 \text{ kN}$$

From Table 2.1(a), the weight per panel is:

$$2400 \text{ X } 2.97 \text{ X } 3.67 \text{ X } 0.2 = 5232 \text{ kg} = 51.3 \text{ kN}$$

Thus, the weight due to the panels' self-weight is given by:

$$W_p = 3 \text{ X } 51.3 = 154 \text{ kN}$$

The distributed gravity loads acting on the shear wall (with a total width of 3 X 3.67 = 11.01 m) is thus:

$$w_f = 396 / 11.01 = 36.0 \text{ kN/m}$$
$$w_p = 154 / 11.01 = 14.0 \text{ kN/m}$$

And the mass per story is given by

$$M = (396 + 154) \text{ X } 1000 / 9.81 = 56\,000 \text{ kg}$$

A2. Loading for 10-story LSB coupled shear wall

Assume a dead load P = 6.0 kPa (125 psf) acting on all floors.From Fig. 3.1(a), the tributary area acting on an exterior wall is thus:

$$A_t = 2 \text{ X } 7.3 \text{ X } (7.3 / 2) = 53.3 \text{ m}^2$$

Thus, the load due to load P per floor is given by:

$$W_f = 6.0 \text{ X } 53.3 = 320 \text{ kN}$$

The weight per panel is:

W_p = 2400 X (2.65 · 0.20) X 7.3 X 0.2 = 8590 kg = 85 kN

Thus, the weight due to the panels' self-weight is given by:

W_p = 2 X 85 = 170 kN

The total gravity load per story is thus:

W_t = 320 + 170 = 490 kN

For the building, the weight per story due to P = 6.0 kPa is:

6.0 X (6 X 7.3 X 2 X 7.3) = 3837 kN

Assuming that the contribution of the panels is equivalent to 14 panels per story, the weight per story due to the panels is:

14 X 85 = 1190 kN

Thus, the total weight / mass per floor = 3837 + 1190 = 5027 kN = 512000 kg

Assuming that each end wall possesses 1 / 4 of the building's total lateral stiffness, the tributary lateral story mass for the end walls is thus

512000 / 4 = 128 000 kg

APPENDIX B

PLATFORM HORIZONTAL JOINTS

Calculations for horizontal joint properties are identical for both the 12-story and 10-story walls; thus, presented are calculations for the 12-story wall's horizontal joints only.

B.1 Horizontal joint axial behaviour

Composite joint strength can be approximated by CPCI design formula[21]:

$$\frac{\phi P_{nj}}{l} = \phi f'_{cj} t_g \sqrt{\frac{t}{t_g}}$$

where t = effective wall width = 200 mm
t_g = width of grout joint = 100 mm
ϕ = 0.70
f'_{cj} = strength of grout joint = 29 MPa

Thus:

$$\frac{\phi P_{nj}}{l} = 0.7 \text{ X } 29 \text{ X } 100 \sqrt{\frac{200}{100}} = 2870 \text{ N/mm}$$

f'_c = 2870 / 200 = 14.4 MPa

From Ref.(25), the equation for the stress-strain curve of concrete is given by:

$$f = \frac{E\varepsilon}{1+(\frac{\varepsilon}{\varepsilon_0})^2} \qquad (1)$$

For the horizontal joints other than the base, we have:

E = 13 800 MPa (assume half grout E)
f'c = 14.5 MPa

By setting ε to equal ε_o in Eq.(1), we thus set ε_o = 0.002101, and by substitution:

$$f = \frac{13.8\,\varepsilon}{1 + (\frac{\varepsilon}{0.002101})^2} \quad kN/mm^2 \qquad (2)$$

For the joints, t = 200 mm and h = 250 mm. Thus, for one panel width (3670 mm):

$u = 250\ \varepsilon$

$u_2 = 250 \times 0.002101 = 0.525$ mm (deformation at f'_c)

$A_j = 3670 \times 200 = 734\,000$ mm^2 (cross-sectional joint area)

The force-displacement relation of the joint is thus:

$$F = \frac{40517\,u}{1 + (\frac{u}{0.525})^2} \qquad (3)$$

A trilinear approximation of Eq.(3) gives (see Fig. 2.5(a)):

k_1 = 38600 kN/mm = 38600 / 3670 = 10.52 kN/mm/mm

k_2 = 7000 kN/mm = 7000/3670 = 1.91 kN/mm

u_1 = 0.220 mm

u_2 = 0.525 mm

B.2 Horizontal Joint Shear Behaviour

A Poisson's ratio of $\nu = 0.2$ for the joints gives a modulus of rigidity G:

$$G = \frac{E}{2(1+\nu)} = \frac{13.8}{2(1+0.2)} = 5.75 \text{ kN/mm}^2$$

The shear stiffness k_s of the horizontal joints is thus:

$$k_s = \frac{G A_j}{h} = \frac{5.75 \text{ X } 734000}{250} = 16882 \text{ kN/mm}$$

k_s = 16882 / 3670 = 4.6 kN/mm/mm

Note that at the base joint, calculations for both the axial and shear properties are based on E = 27600 MPa and f'_c = 29 MPa.

APPENDIX C

HORIZONTAL JOINT REINFORCEMENT

Vertical reinforcement in the horizontal joints assumed to contribute toward tensile stiffness depending on amount of reinforcement; shear stiffness contribution assumed to be constant within range of per cent steel used. Calculations for tensile stiffness are the same for both 12-story and 10-story walls, and thus only calculations for the 12-story wall are shown.

With 0.5 per cent distributed reinforcement, the area of steel per floor is:

$$A_s = 0.005 \text{ X } (3 \text{ X } 3670 \text{ X } 200) = 11010 \text{ mm}^2$$

From Ref.(31), the stiffness k_b of a No. 8 bar (area 507 mm^2) with intermediate embedment in masonry was approximately:

K_b = 2000 kips/in = 350 kN/mm

k_b = 350 / 507 = 0.69 kN/mm per mm^2 of steel

Assuming that the reinforcement passes through the joint (h = 250 mm) without any bonding, the stiffness k_j between panels is thus:

$$k_j = \frac{E_s A_s}{h} = \frac{200 \text{ X } 1}{250} = 0.8 \text{ kN/mm per mm}^2 \text{ of steel}$$

The equivalent stiffness k_e across the joint is thus given by:

$$k_e = \frac{1}{\frac{1}{0.69} + \frac{1}{0.80} + \frac{1}{0.69}} = 0.25 \text{ kN/mm per mm}^2 \text{ of steel}$$

K_e = 0.25 kN/mm/mm^2 X 11010 mm^2 = 2755 kN/mm

k_e = 2755 / (3 X 3670) = 0.25 kN/mm/mm

As well, at the base, properties are assumed to be the same.

APPENDIX D

12-STORY WALL: VERTICAL CONNECTORS

D.1 Compressive behaviour

Bottom 1 / 10 of vertical joints between panels are grouted, with axial compressive stiffness of grout assumed half that of the horizontal joints. The equivalent stiffness of the bottom vertical joint connectors, and adjusting for a 20 mm grout thickness, is thus:

k_c = 0.5 X 10.52 = 5.26 kN/mm/mm

k_c = 5.26 X (250 / 20) = 65.75 kN/mm/mm

K_c = 65.75 X (2970 / 10) = 19530 kN/mm

The ungrouted axial compressive stiffness of the top connectors can be assumed to be 1 / 10 of that for the grouted connectors, or:

K_c = 19530 / 10 = 1953 kN/mm

D.2 Tensile behaviour

Tensile stiffness is based on the stiffness of horizontal, or transverse, ties. It is given that the tensile force F_x in the horizontal tie at a particular story is expressed as[24]:

$$F_x = \frac{\alpha_x W l_d^2}{2 h_s}$$

where

α_x is a coefficient depending on the particular building height and cantilever height

W is the design floor load equal to D + 0.5 L

l_d is the unsupported length of the cantilever

h_s is the constant story height

Thus, assuming L = 16 kN/m and hence W = 58 kN/m:

$$F_x = \alpha_x \left[\frac{58 \times 10^{-3} \times 3670^2}{2 \times 2970} \right] = 132\,\alpha_x$$

From the design chart in the reference[24], α_x = 1.00 at roof level is maximum, and the required tie strnegth there is thus:

F_x = 132 X 1.00 = 132 kN at roof level

For floor level 11, where α_x = 0.45, the required ties force is :

F_x = 132 X 0.45 = 60 kN

..and since α_x decreases downward, ties chosen elsewhere based on requirements at floor level 11 would be satisfactory. As well, a recommended minimum tie strength of 80 kN is indicated by Ref.(24). Accordingly, the unstressed prestressing strands selected for use as horizontal ties[21] are:

Roof Level: 12.7 mm diameter strand; A_s = 99 mm^2; F_y = 147 kN
Levels 1-11: 9.5 mm diameter strand; A_s = 52 mm^2; F_y = 80 kN

The tensile stiffness k_t of the ties to be used in the analysis is based on a debonding length of 60 tie diameters

$$k_t = \frac{A_s E_s}{60\,d}$$

For d = 12.7 mm,

$$k_t = \frac{99 \times 200}{60 \times 12.7} = 24.4 \text{ kN/mm}$$

For d = 9.5 mm

$$k_t = \frac{52 \times 200}{60 \times 9.5} = 18.2 \text{ kN/mm}$$

Note that at the floor levels, this tensile stiffness is divided between the two connectors, or k_t = 9.1 kN/mm.

D.3 Vertical connector shear behaviour

From an empirical formula[23], the strength Q_u of shear connectors is given by:

$$Q_u = \frac{1}{2} A_s \sqrt{f_c E_c}$$

where for the design connectors (12.7 mm studs)

$$Q_u = \frac{1}{2}(0.196)\sqrt{4.2 \text{ X } 4000} = 12.7 \text{ kips} = 56.5 \text{ kN}$$

or for two studs, the connector shear strength is:

$$F_y = 2 \text{ X } 56.5 = 113 \text{ kN}$$

Also, as given by the formula[23]:

$$\frac{Q}{Q_u} = (1 - e^{-18u})^{2/5}$$

and assuming 99.99 per cent of the strength Q_u is reached, the maximum deformation u_{max} of the connectors is about 11.7 mm. Also, from Ref.(22), we have u_{max} = 12.8 mm and an elastic limit of 0.36 mm.

Thus, the maximum ductility demand is given by:

$$\mu_{max} = 12.8 / 0.36 = 36$$

and this limit is assumed for other connector sizes. Thus, for connectors of size 2 X 12.7 mm, we can choose:

F_y = 104 kN
u_y = 0.36 mm
μ_{max} = 36

Ref.(21) also gives design formulae for the strength of shear connectors, and produce similar results.

APPENDIX E

10-STORY WALL: LSB CONNECTORS

The shear strength of the connector is based on the following formulae[37]:

$$B_r = \phi\ t\ n\ e\ F_u \ < \ 3\ \phi\ t\ d\ n\ F_u \qquad (1)$$

$$V_r = 0.6\ \phi\ n\ m\ A_b\ F_u \qquad (2)$$

... where, assuming A325 M22 bolts for the LSB connectors:

B_r = factored bearing resistance of connector plate
V_r = factored shear resistance of connector bolt (s)
ϕ = 0.67
t = plate thickness = 20 mm
d = bolt diameter = 22 mm
n = number of bolts
e = end distance = 30 mm
m = number of shear planes
A_b = cross sectional bolt area = 380 mm^2
F_u = specified tensile plate strength = 450 MPa (1)
= specified tensile bolt strength = 830 MPa (2)

From Eq.(1),

B_r = 0.67 X 20 X 2 X 30 X 450 = 360 kN
< 3 X 0.67 X 20 X 22 X 2 X 450 = 800 kN OK

From Eq.(2),

V_r = 0.6 X 0.67 X 2 X 1 X 380 X 830 = 254 kN

Thus, if the bolts are in bearing, the strength is governed by V_r = 254 kN.

However, the connector anchorage can also yield. The strength of the studs (assuming 19.1 mm diameter headed studs) is given by[21]:

$$\phi\ V_c = \phi\ m\ A_s\ F_y \qquad (3)$$

where

ϕ = 0.7
m = 1.0
A_s = cross sectional area of stud = 287 mm^2
F_y = yield strength of stud = 400 MPa

Thus:

$$\phi V_c = 0.7 \text{ X } 1.0 \text{ X } 287 \text{ X } 400 = 80 \text{ kN}$$

And for 2 stud anchors per LSB connector, the anchorage shear strength = 160 kN.

The pullout capacity of the studs is given by[21]:

$$\phi P_c = \phi A_o (0.33 \lambda \sqrt{f'_c})$$

where

ϕ = 0.7
A_o = area of assumed failure surface
λ = 1.0
f'_c = strength of panel concrete = 34 MPa

A_o can be conservatively assumed to be a 45° truncated cone, so that

$$A_o = \sqrt{2} \; l_e \pi (l_e + d_h)$$

where

l_e = stud length = 155 mm
d_h = stud head diameter = 32 mm

A_o = 1.41 X 155 π (155 + 32) = 124000 mm^2

$$\phi P_c = 0.7 \text{ X } 124000 \text{ X } 0.33 \text{ X } \sqrt{34} = 163 \text{ kN}$$

And for two studs, the pullout strength = 2 X 163 = 325 kN. However, since the bearing resistance of the plate is governed by the bolt shearing strength of 254 kN, the pullout strength is in fact only 254 kN.

APPENDIX F

VERTICAL TIES

Selection of vertical ties are based on PCA[24] minimum design recommendations. Calculations shown are for the 12-story wall. The horizontal shear force at each floor level is given as:

$$V_x = \frac{\beta_x W l_d^2}{2 h_s}$$

where

β_x is a coefficient depending on the particular building height and cantilever depth

The other variables are the same as those described in Appendix D.2. Thus,

$$V_x = \beta_x \left[\frac{58 \times 10^{-3} \times 3670^2}{2 \times 2970}\right] = 132\,\beta_x$$

In addition, the vertical ties must also act as tensile ties to resist any tensile forces induced by the cantilever suspension mechanism. Thus, by using two ties per panel, the required tensile force per tie is calculated as:

$$\text{Tensile force per tie} = V_x / 2 + W\, l_d / 2$$

The highest tensile force requirement occurs at the first level, where $\beta_x = 1.45$ is maximum. Hence, the required strength per tie is:

$$T = \frac{1.45 \times 132}{2} + \frac{58 \times 10^{-3} \times 3670}{2} = 200\ \text{kN}$$

Thus, we choose high strength steel bars of diameter 17.5 mm, A_s = 240 mm^2 and f_{pu} = 1035 MPa. Taking a post-tensioning force equal to 60 per cent of the tie strength:

F_y = design strength = 0.9 X 1035 X 240 / 1000 = 224 kN

PT = post-tensioning force = 0.6 X 224 = 135 kN

APPENDIX G

NBCC 1985 WIND ANALYSIS OF 10-STORY SHEAR WALL

G.1 Equivalent lateral forces:

Specified loadin due to wind loads were determined from Section 4.1.8 of the NBCC (1985)[47]:

$$p = q\, C_e\, C_g\, C_p$$

p = specified external pressure, kPa
q = reference velocity pressure, kPa = CV^2
C_e = exposure factor = $(h/10)^{1/5}$ but > 0.90
C_g = gust factor = 2.0
C_p = external pressure coefficient = 1.8

The refererence velocity pressure is found from a conversion factor C and the basic wind velocity V. Here, V is assumed to equal 30 m/s (note: V = 24 m/s in Montreal). Thus:

$$q = CV^2 = 650 \times 10^{-6} \times 30^2 = 0.585 \text{ kPa}$$
$$p = 0.585 \times C_e \times 2.0 \times 1.8 = 2.106\, C_e$$

The equivalent lateral forces due to the wind pressure is found by the area exposed to the wind. This area can be found considering a story height h = 2.65 m and bay width of 7.3 m for the building plan (see Fig. 3.1). Thus:

$A = 7.3 / 2 \times 2.65 / 2 = 4.836 \text{ m}^2$ (level 1 and 10)
$A = 7.3 / 2 \times 2.65 = 9.673 \text{ m}^2$ (levels 2-9)

Thus, the following table is constructed, showing the equivalent static lateral forces F to be applied:

Table G.1

Level	Ce	F (kN)
1	0.90	9.17
2	0.91	18.33
3	0.96	19.56
4	1.01	20.57
5	1.06	21.59
6	1.10	22.41
7	1.13	23.02
8	1.16	23.63
9	1.19	24.24
10	1.22	12.43

G.2 Results of analyses:

Figs. G.1(a) and G.1(b) show response of the 10-story wall under the NBCC equivalent static wind loading. A top displacement of only 0.48 mm is shown in Fig. G.1(a), compared to over 60 mm when the time-history dynamic analyses of Chapter III was employed. This low top displacement reflects other overall responses as well, including low base shear (sum of lateral forces shown in Table G.1, or 195 kN) and wall stresses. Both horizontal joint slip and gap openining do not occur, while the LSB connectors remain well below the slip load of 80 kN, as demonstrated in Fig. G.1(b).

Thus, under normal service loads due to wind, slip of the LSB connectors does not occur; integrity of the wall is excellent, with no slip or gap opening of the horizontal joints as well.

APPENDIX H

NBCC 1985 SEISMIC ANALYSIS OF 10-STORY SHEAR WALL

H.1 Equivalent lateral forces

Specified loading due to earthquake motion were determined from Section 4.1.9 of the NBCC (1985)[47]. Equivalent lateral forces were obtained using the minimum lateral seismic force V at the base of the structure, where:

$$V = v\ S\ K\ I\ F\ W$$

v	=	zonal velocity ratio	=	0.40
S	=	seismic response factor	=	0.41
K	=	ductility factor	=	1.3
I	=	importance factor	=	1.0
F	=	foundation factor	=	1.0
W	=	dead load + 25 per cent of snow load	=	4920 kN

The zonal velocity ratio v = 0.4 was selected based upon the assumption that the structure is situated in a velocity-related seismic zone 6, the highest specified in the NBCC. S = 0.41 was calculated assuming an acceleration to velocity zone ratio $Z_a / Z_v = 1$ and a fundamental period of 0.31 sec. A snow load of 80 kN was assumed to act on the roof. The base shear is thus:

$$V = 0.4 \times 0.41 \times 1.3 \times 1.0 \times 1.0 \times 4920 = 1050 \text{ kN}$$

The lateral forces were distributed to the floor levels according to:

$$F_x = \frac{(V - F_t) W_x h_x}{\sum_{i=1}^{n} W_i h_i}$$

W_x = 490 kN (also at roof)

$(V - F_t)$ = 1050 kN

h_x = 2.65 i m, where i = story level

$\Sigma W_i h_i$ = 490 X 2.65 (1 + 2 + 3 + ... 10) = 71418 kN·m

Substituting, F_x = 19.1 i kN, where i = story level. The distribution of lateral forces is shown in Fig. H.1. An equivalent distributed triangular load is shown in Fig. H.2, which can be used for simple hand calculations of forces (where w = 2V / L).

H.2 Results:

Envelopes of static response are shown in Figs. H.3(a) to H.3(d) for equivalent NBCC seismic lateral forces. The story shear envelope can be easily derived from the lateral loads shown in Fig. H.1(a), incurring a maximum base shear of 1050 kN. The lateral displacement curve shown in Fig. H.3(a) shows a maximum top displacement of 3.9 mm, and a profile characteristic of laterally loaded coupled walls; that is, flexural dominance in the lower stories, but a shear configuration for the upper levels. Panel stresses shown in Fig. H.3(b) reveal stresses in the panels well belowe the 14.5 MPa strength of the horizontal joints; a maximum stress of 4.2 MPa is found at the base .

As for joint behaviour, little deformation is noted. Shear slip of the horizontal joints is non-existant, while gap opening is limited to the lowest four joints, to a maximum of only 0.17 mm at the base (Fig. H.3(c)). However, more significantly, shear slip occurs in the vertical LSB connectors, as indicated in Fig. H.3(d). A maximum slip of 0.21 mm occurs at level 4.

Comparison between response herein using the static method of the NBCC and that from Chapters III and IV employing a full dynamic time-history analysis of the wall reveals considerable differences. In the latter case, overall responses are dramatically higher, and joint action much more significant. Thus, design of LP walls using the NBCC method can underestimate forces and response by a wide margin.

A check of static response can be checked by simple hand calculations based on the loading shown in Fig. H.2, and assuming monolithic cantilever action. The equation for top lateral displacement is given by:

$$\partial_t = \frac{11}{120}\frac{w L^4}{E I}$$

Thus, with a wall thickness of t = 200 mm and E = 29200 MPa:

$$\partial_t = \frac{11}{120}\frac{79.25 \text{ X } 26.5^4}{27600 \text{ X } 1000 \text{ X } (0.2 \text{ X } 14.6^3/12)} = 0.0025 \text{ m} = 2.5 \text{ mm}$$

This is 35 per cent less than the 3.9 mm obtained with the static computer analysis. Panel stresses are maximum at the wall base; stresses are due to the wall weight (σ_a) and moment caused by the lateral loading w (σ_m). Thus, assuming cantilever action:

$$\sigma_a = \frac{W}{A} = \frac{4900}{0.2 \text{ X } 14.6} = 1678 = 1.68 \text{ MPa}$$

$$\sigma_m = \frac{My}{I} = \frac{(1050 \text{ X } 2/3 \text{ X } 26.5) \text{ X } 7.3}{0.2 \text{ X } 14.6^3/12} = 2611 = 2.61 \text{ MPa}$$

And thus:

σ_1 = -1.68 + 2.61 = 0.93 MPa (tension)
σ_2 = -1.68 - 2.61 = -4.29 MPa (compression)

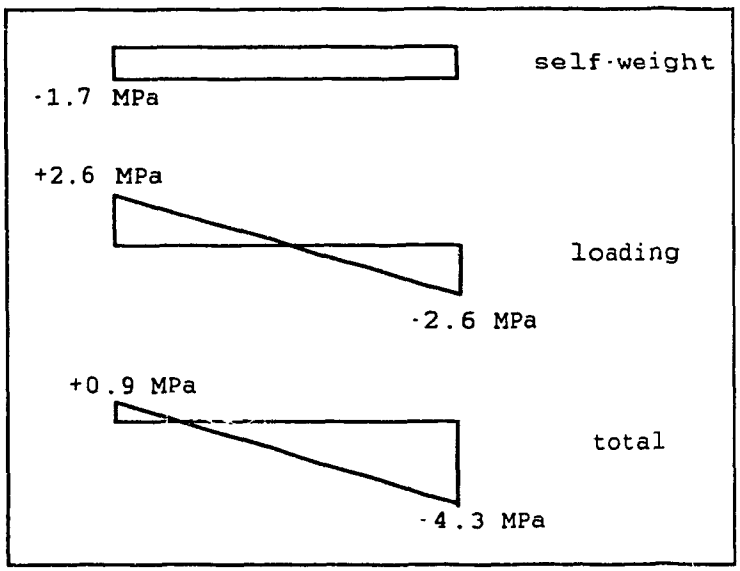

Note that the maximum compressive stress of 4.3 MPa obtained here compares well with the maximum of 4.2 MPa found with computer analysis.

APPENDIX I

TEST OF JOINT ELEMENT SHEAR BEHAVIOUR

To test for proper behaviour of the orthogonal joint spring elements in shear, a simple 2-node model was created, consisting of two elements placed in parallel and sharing the same nodes. The models are schematically illustrated in Figs. I.1(a) and I.2(b), for the horizontal and vertical joint elements respectively.

Element 1 was the test element where correct hysteretic behaviour was checked, while Element 2 was used as a non-yielding element. The models were subjected to the initial 1.5 seconds of the Newmark-Blume-Kapur acceleration record (Fig. 4.1(c)), scaled by a factor of 0.9. As shown, this input excitation was applied horizontally for the horizontal joint elements, while the vertical joint elements were subjected to vertical accelerations. Node 1 was fixed, while Node 2 was free to translate and rotate; an arbitrary mass was assigned to node 2. Both Elements 1 and 2 were assigned identical properties, except that Element 2 was prevented from yielding. No damping was assumed.

It should be noted that the properties and loading employed herein were selected to produce the best behaviour for illustrative purposes, and can be adjusted to study response more carefully. No significance is attached to the units used; however, they are indicated for clarity. Three cases of shear behaviour are detailed: (1) reinforced horizontal joint shear behaviour (2) vertical joint elasto-plastic shear behaviour; and (3) vertical joint stiffness degrading shear behaviour.

The properties assigned to the elements are summarized:

k_a = 10000 kN/mm
M = 1.0 $kN \cdot s^2$ / mm
F = 1000 kN

(1) Horizontal Joint Shear Behaviour (Reinforced)

k_s = 200 kN/mm
m_f = 0.40 (for Element 2, m_f = 9999)
r = 0.5
k_r / k_s = 0.10

(2) Vertical Joint Shear Behaviour (Elasto-plastic)

k_s = 200 kN/mm
u_y = 1.0 mm
F_y = 200 kN (for Element 2, u_y = 100 , F_y = 20000)

(3) Vertical Joint Shear Behaviour (Stiffness Degrading)

k_s = 200 kN/mm
u_y = 1.0 mm
F_y = 200 kN (for Element 2, u_y = 100 , F_y = 20000)
α = 0.5

Fig. I.2(a) shows the hysteretic shear behaviour of Element 1 for case (1). Confirmation of the behaviour as described in Chapter II is shown. Note that the axial load for the model is constant, so that the shear resistance $\mu_f F_c$ of the element (in this case, 0.4 X 1000 / 2 = 200 kN) is invariant.

The shear behaviour of vertical joint Element 1 assuming elasto-plastic elements is detailed in Fig. I.2(b), while that for degrading behaviour is illustrated in Fig. I.2(c). Except for Fig. I.2(c) , adjustments are made to the figures to allow for following of the hysteretic loops.

In a similar manner, tests of axial behaviour of the elements are conducted.

APPENDIX J

TEST OF FINITE ELEMENT MESH

A 1 X 3 finite element mesh was employed for the panels of the 12-story shear wall of Chapter II, while a 1 X 4 mesh was used for the panels of the 10-story shear wall of Chapters III and IV. Length to width aspect ratios for the individual finite elements were 2.4 and 1.3 for the 12-story and 10-story walls respectively. Since the mesh for the 12-story model was coarser and elements possessed higher aspect ratios, a check for numerical convergence was conducted on the 12-story wall using a finer mesh size and an aspect ratio closer to one (see Fig. J.1).

A mesh size of 4 X 3 was used for the panels of the 12-story wall, each finite element having an aspect ratio of 1.7. Loading was similar to the model employed in Chapter 3. Figs. J.2(a) to J.2(c) show that the coarser mesh employed in the study introduces very small differences in response from the finer mesh. Time history of top displacement is almost identical over the 5 seconds of analysis, while both story shear and gap opening envelopes reveal little differences over the wall height.

APPENDIX K

EFFECT OF DIFFERENT EARTHQUAKE INTENSITY ON OPTIMUM SLIP LOAD

Fig. K.1 shows that the relative response between different slip loads is generally unchanged even at different earthquake intensities.

APPENDIX L

GROUTED VERTICAL TIES

To model vertical ties grouted along its length, but with an unbonded length through the horizontal joints, ten truss elements connected from floor to floor were used to model each tie. This ensures panel movement at any level due to slip or uplift would affect the ties correctly, whereas simply connecting a single truss element from bottom to top ignores the effects panel slip or uplift concentrated in the mid-stories may have on the ties. By grouting, the effective stiffness of the ties is changed.

32 mm (1.25 in) diamteter ties were employed, with varying assumed stiffnesses by adjustment of the element area. A post-tensioning force of 490 kN per tie (60 per cent of tie strength) was provided, and 10 ties (5 per panel stack) used. The effect of grouted ties is to increase the effective stiffness across each horizontal joint considerably, and thus reduce gap opening. Fig. L.1 plots envelopes of gap opening across the base, for different effective unbonded lengths of the ties.

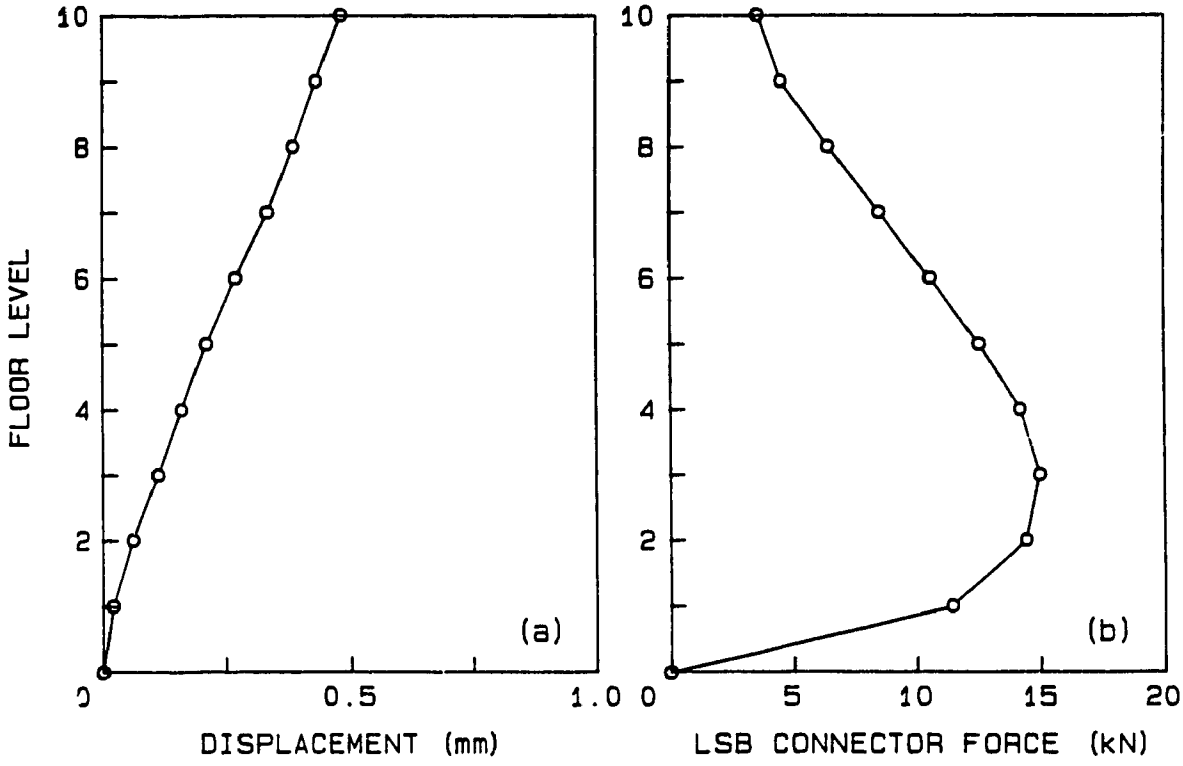

Figure G.1 Static response envelopes for NBCC wind loading.

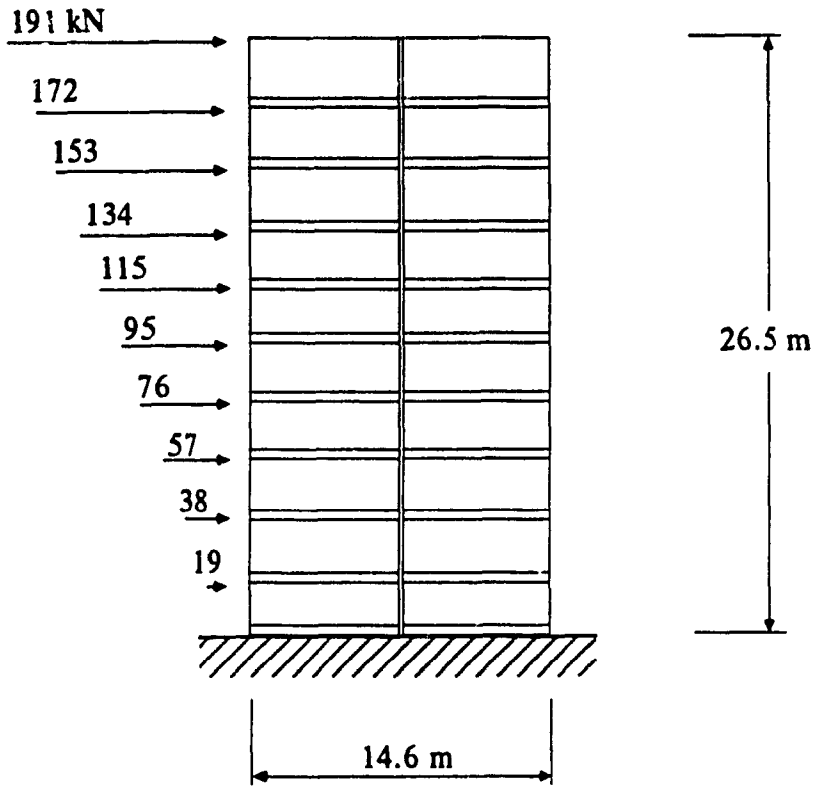

Figure H.1 Equivalent static lateral loading for NBCC seismic analyses.

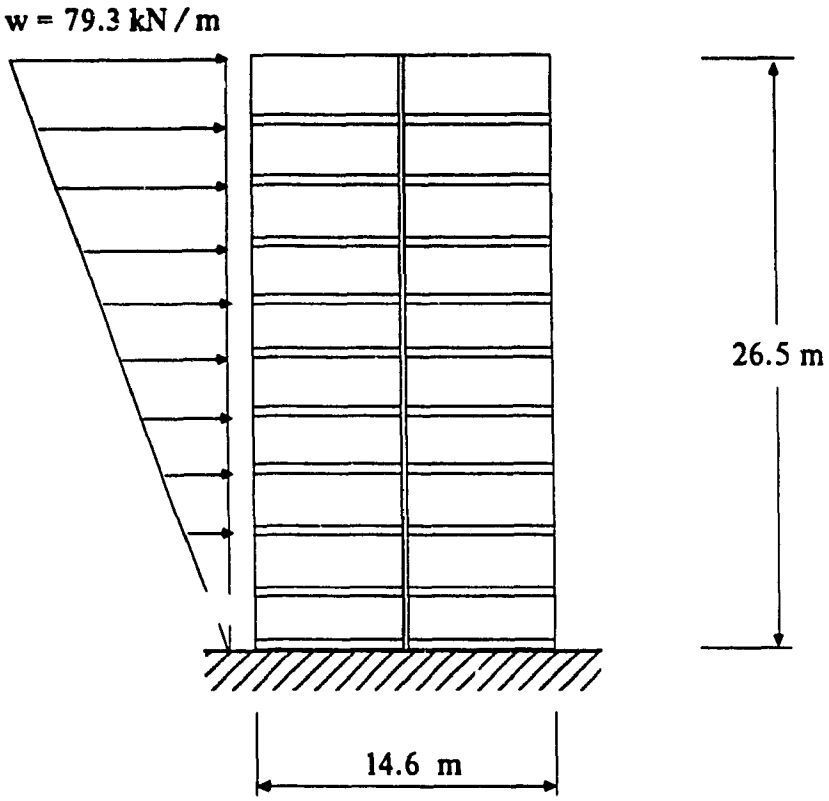

Figure H.2 Distributed triangular static loading from NBCC seismic forces.

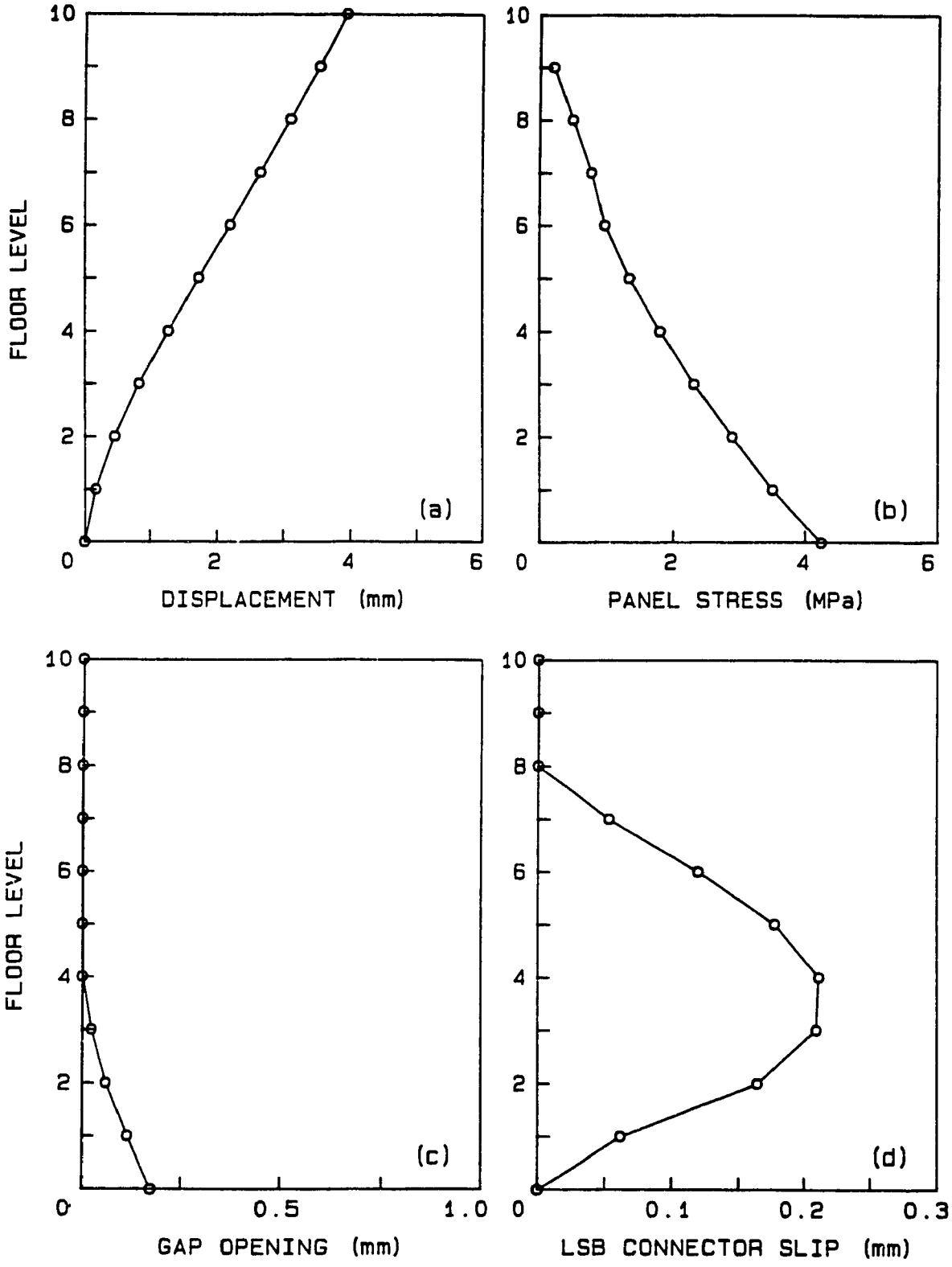

Figure H.3 Static response envelopes for NBCC seismic forces.

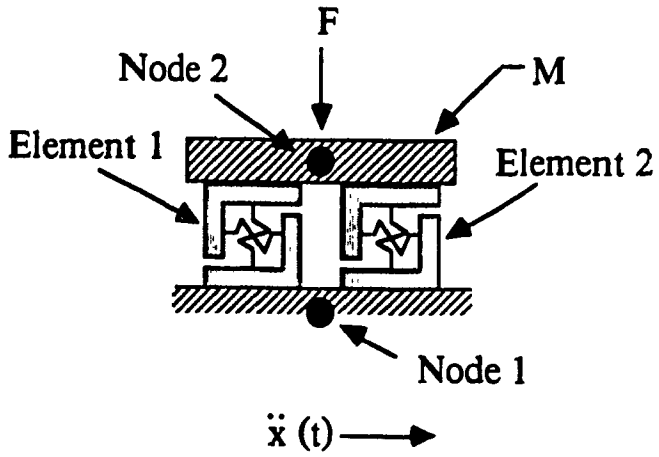

(a) 2-Node Model for Horizontal Joint Elements

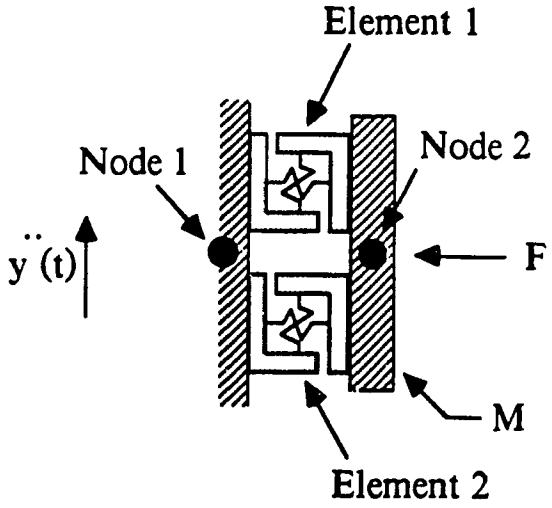

(b) 2-Node Model for Vertical Joint Elements

Figure I.1 2-node models for joint element testing.

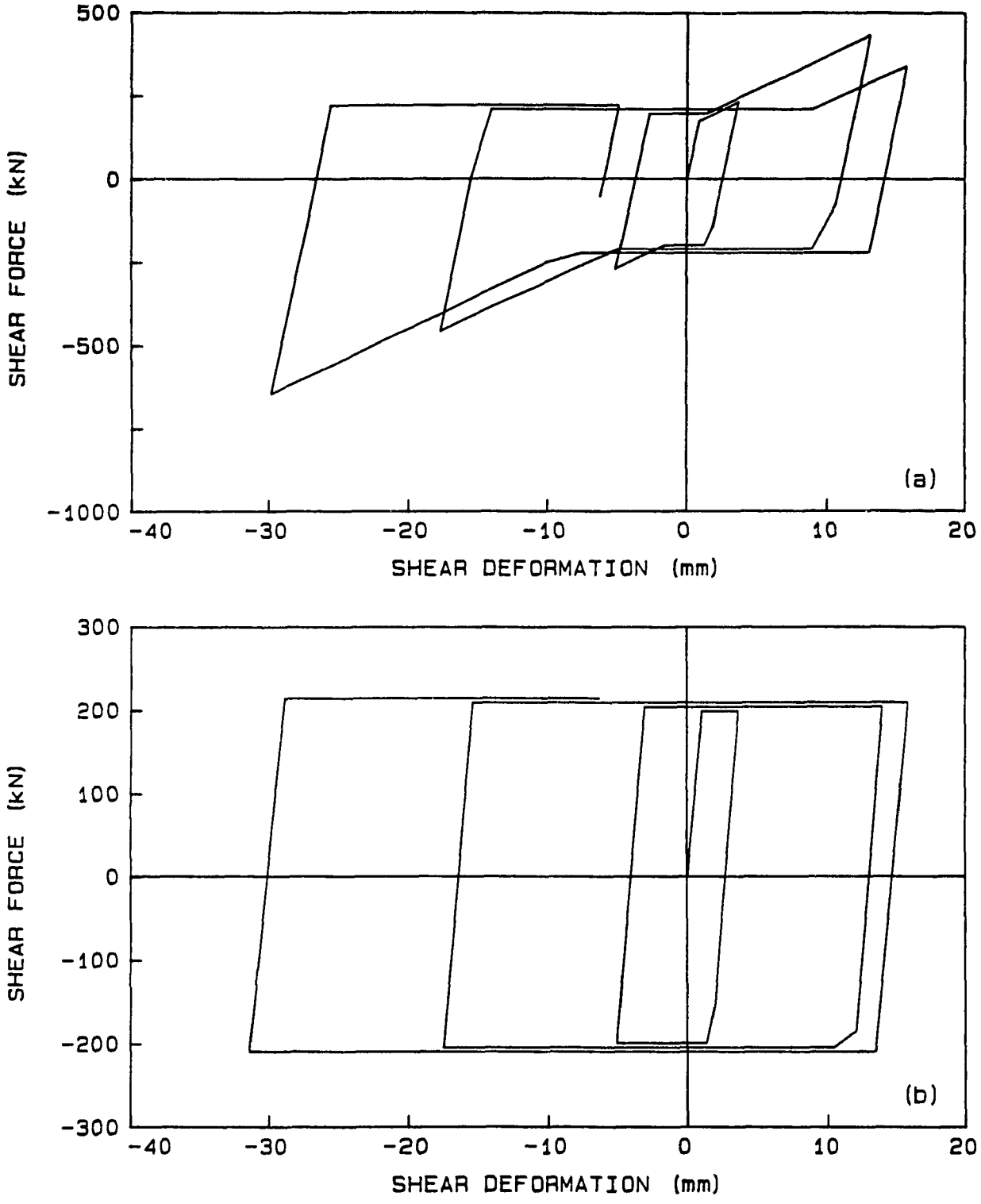

Figure I.2 Hysteretic shear behaviour of joint elements: (a) reinforced horizontal joint element; (b) elasto-plastic vertical joint element

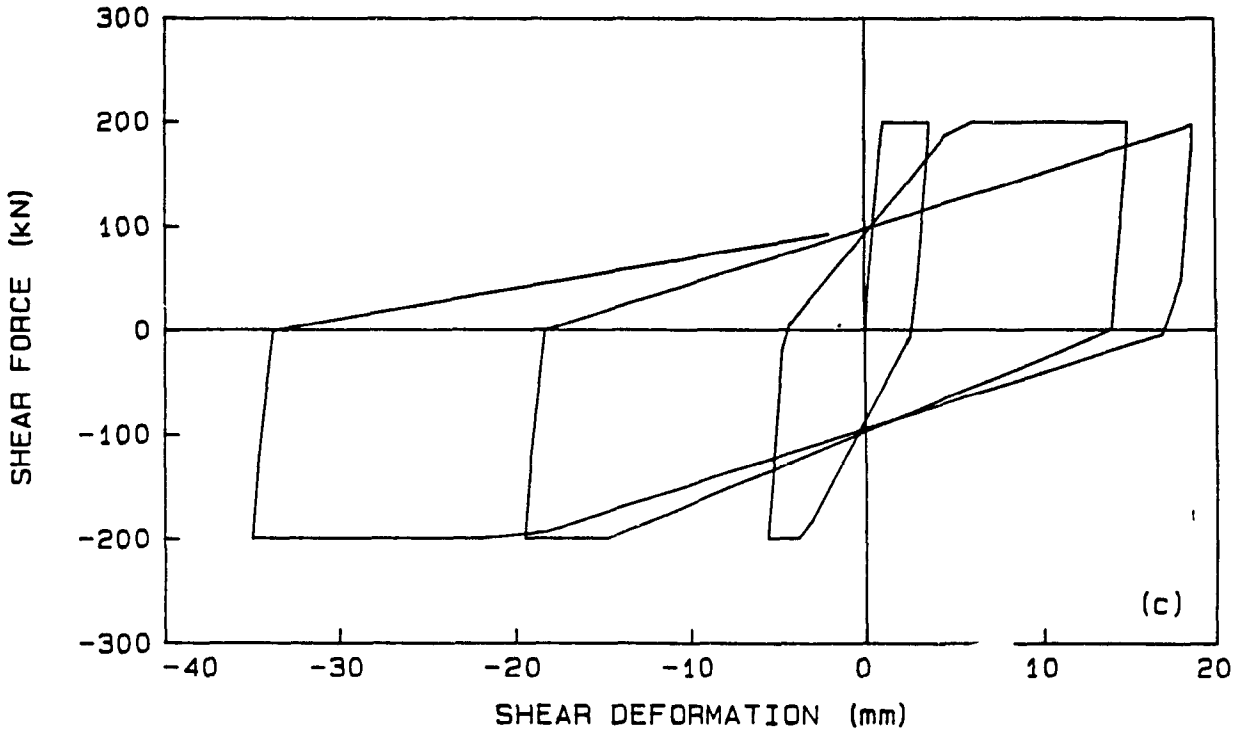

Figure I.2 Hysteretic shear behaviour of joint elements: (c) stiffness degrading vertical joint element

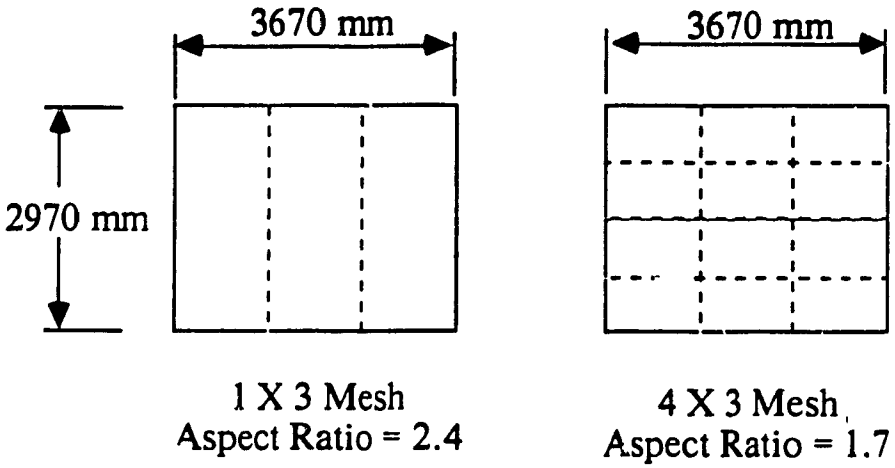

Figure J.1 Comparison of finite element meshes used for panel elements: 12-story multi-panel wall.

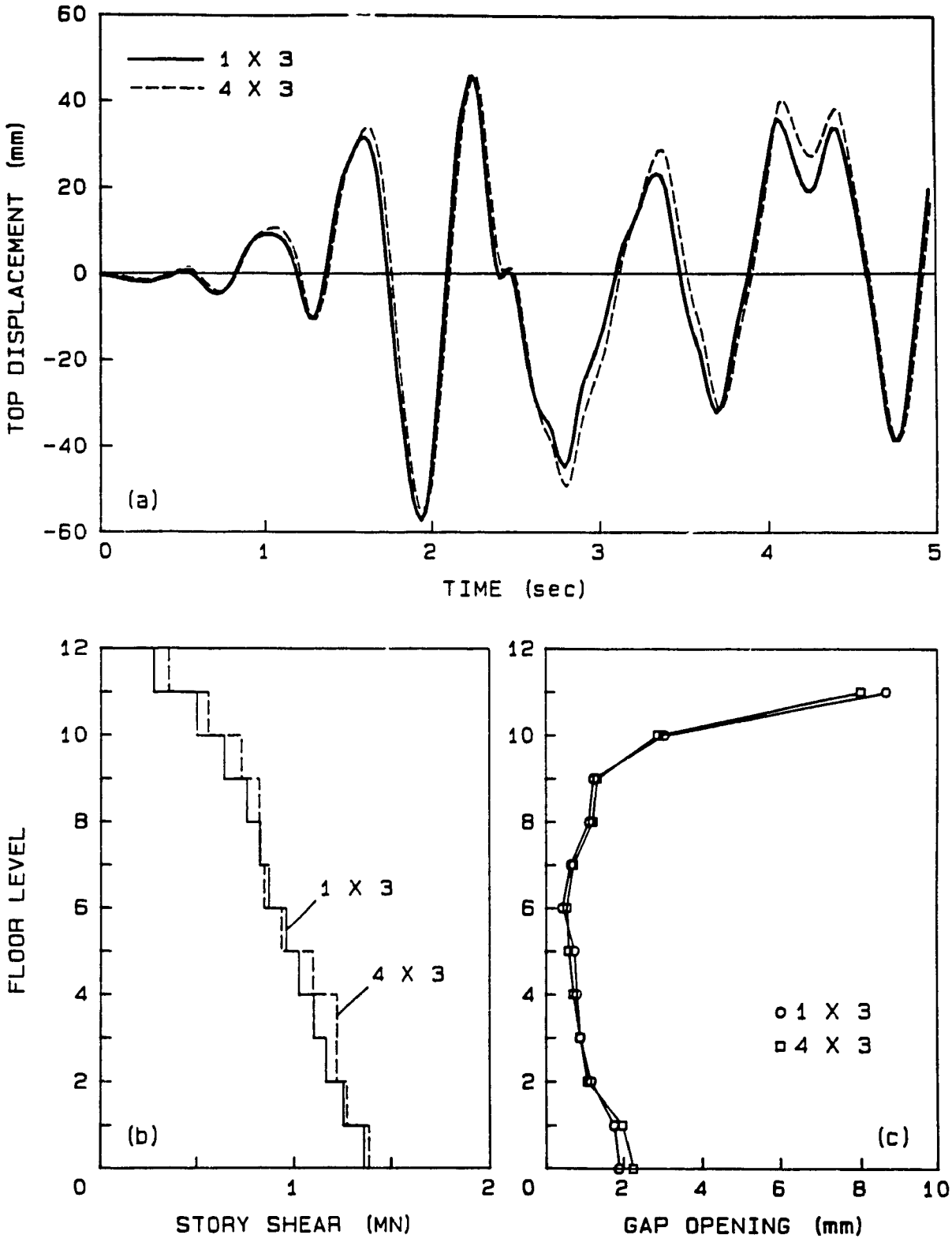

Figure J.2 Comparison of results between 1 X 3 coarse and 4 X 3 fine panel mesh: 12-story multi-panel wall.

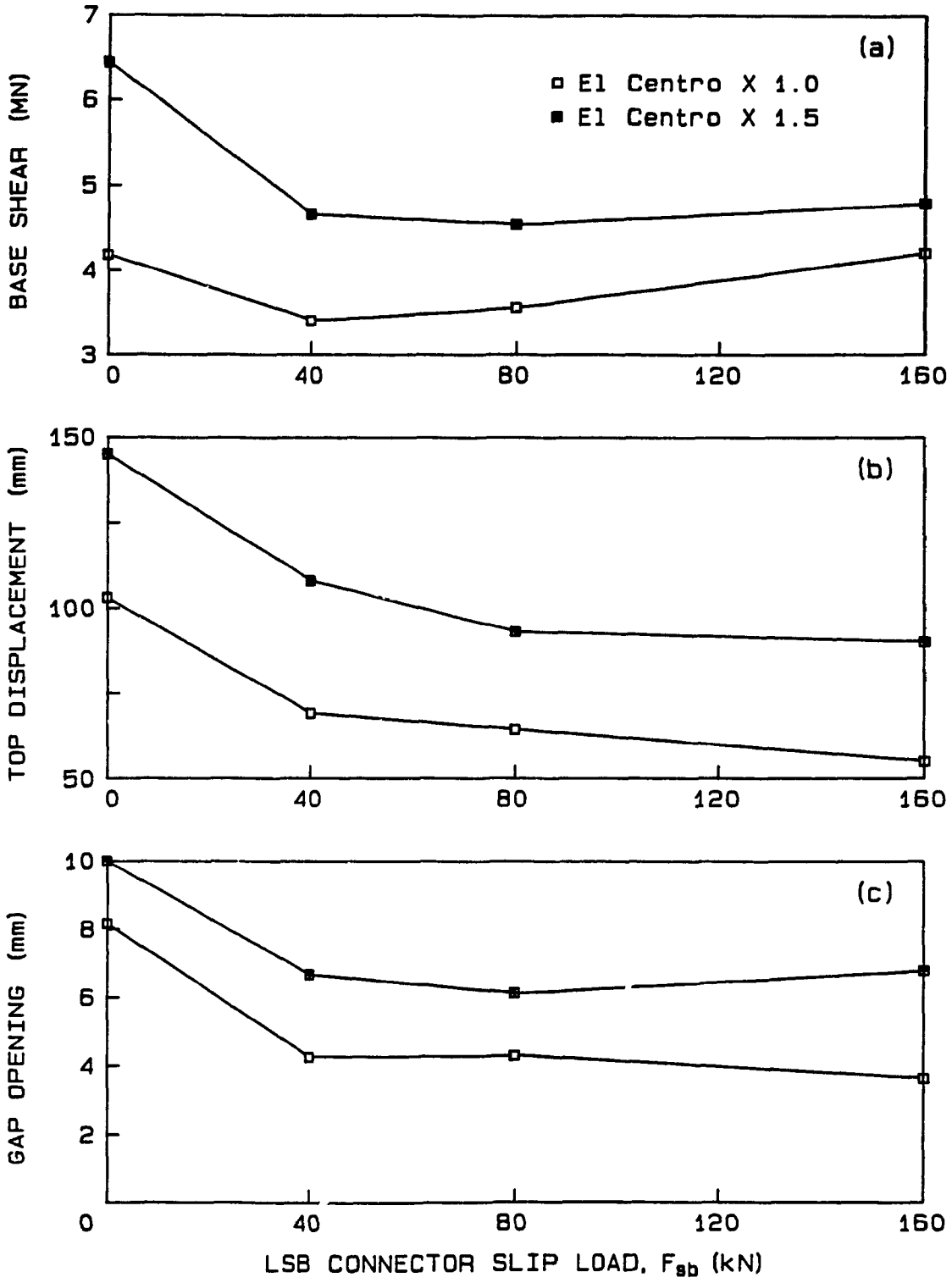

Figure K.1 Comparison of Response for Different Intensities of El Centro

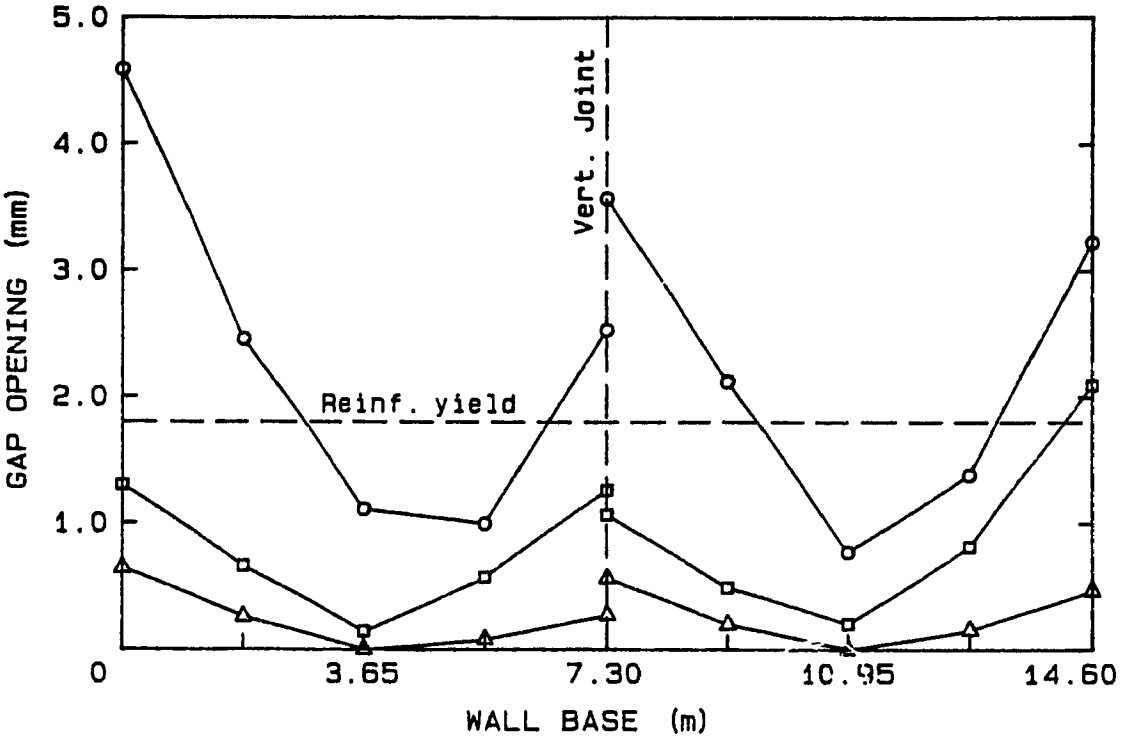

o 4 ungrouted post-tensioned ties, post-tensioning force = 490 kN

□ 10 grouted post-tensioned ties, post-tensioning force = 490 kN
Unbonded length = 1050 mm

△ 10 grouted post-tensioned ties, post-tensioning force = 490 kN
Unbonded length = 450 mm

Properties of Vertical Ties:	Nominal Diameter = 32 mm
	Nominal Area = 804 mm2
	fpu = 1030 MPa

Figure L.1 Envelopes of Gap Opening Across Base for Grouted and Ungrouted Ties